4th Micro and Nano Flows Conference

MNF2014

7-10 September 2014

University College London, UK

www.mnf2014.com

MICRO AND NANO FLOWS 2014

MNF2014

ISBN: 9781908549167

Conference and Organising Committee

Conference Committee

Chair:	**T.G. Karayiannis** *Brunel University, UK*
	J. Brandner *Karlsruhe Inst. of Technology, Germany*
	M.W. Collins *Brunel University, UK*
	S. Garimella *Georgia Institute of Technology, USA*
	D. Papageorgiou *Imperial College, UK*
	A. Redaelli *Politecnico di Milano, Italy*
	Y. Takata *Kyushu University, Japan*
	J. Xu *North China Electric Power University, China*
Scientific Secretary	**C.S. König** *Brunel University, UK*

Local Organising Committee

Chair:	**S. Balabani** *University College London, UK*
Co-Chair:	**P. Angeli** *University College London, UK*
	A. Gavriilidis *University College London, UK*
	S. Kuhn *University College London, UK*
	R. Shipley *University College London, UK*
	M. Tiwari *University College London, UK*


Brunel
UNIVERSITY
LONDON


HEXAG
HEAT EXCHANGER ACTION GROUP


ASME
PRESS


heat transfer society


LCN
LONDON CENTRE FOR
NANOTECHNOLOGY


Process Intensification Network


energy
INSTITUTE


Institution of
MECHANICAL
ENGINEERS


UCL ENGINEERING
Change the world


UCL


IPEM

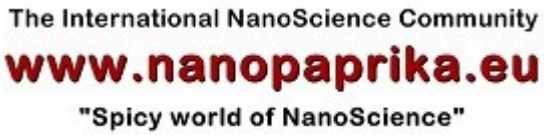
The International NanoScience Community
www.nanopaprika.eu
"Spicy world of NanoScience"


UIT
Unione Italiana
Termofluidodinamica

Programme Guide

	Sunday, 7th September 2014
18:00-19:30	**Welcome Reception and Registration** **Room: Roberts Foyer G02**

	Monday, 8th September 2014			
from 8:00	**Registration –Roberts Foyer G02**			
09:30-9.45	**Welcome address- Profs Michael Arthur (UCL's President and Provost) & Tassos Karayiannis (Chair)** Room: **Darwin B40 LT**			
09:45-10:30	**Plenary Paper:** **Advances and challenges in computational research of micro and nano flows (id 214)** **Professor Dimitris Drikakis** Room: **Darwin B40 LT** Chair: **T. G. Karayiannis**			
10:30-11:00	**Coffee/Tea Roberts Foyer G02**			
	MINISYMPOSIUM I **Mathematical modelling of multiphase microflows**	**Single Phase 1** **Experimental**	**Multiphase 1** **Boiling 1**	**Nanofluids 1**
11:00-13:00	Session 1 Room: **Darwin B40 LT**	Session 1 Room: **Roberts G06**	Session 1 Room: **Roberts 106**	Session1 Room: **Roberts G08**
	Chair: **D. Papageorgiou & D. Drikakis**	Chair: **K. A. Mouza & R. Osellame**	Chair: **D. Del Col & P. Angeli**	Chair: **G. Tang & A. Gavriilidis**
	Paper: **Particle self-diffusiophoresis near solid walls and interfaces (id 231)** Authors : D. Crowdy	Paper: **Electrodiffusion Method of Near-Wall Flow Diagnostics in Microfluidic Systems (id 145)** Authors : J. Tihon , V. Penkavova, P. Stanovsky, J. Vejrazka	Paper: **Effect of Surfactant on Flow Boiling Heat Transfer of Ethylene Glycol/Water Mixtures in A Mini-tube (id 21)** Authors : Z. Feng, Z. Wu, W. Li, B. Sunden	Paper: **Thermal conductivity of nanofluids in nanochannels (id 188)** Authors: M. Frank, N. Asproulis , D. Drikakis
	Paper: **Stretching of a capillary bridge featuring a particle-laden interface: particle sedimentation in the interface (id 232)** Authors : L. Botto	Paper: **Experimental and Numerical Analysis of Single Phase Flow in a micro T-junction (id 121)** Authors : P. Vocale , G. Puccetti, B. Pulvirenti , G. Morini	Paper: **The Leidenfrost Phenomenon on Structured Surfaces (id 69)** Authors : G. R. Duursma, R. A.P. Kennedy, K. Sefiane	Paper: **Experimental and numerical investigation on forced convection in circular tubes with nanofluids (id 158)** Authors: L. Colla , L. Fedele , O. Manca , L. Marinelli , S. Nardini
	Paper: **Macroscopic effects of microscopic roughness in suspensions (id 233)** Authors: H. J. Wilson	Paper: **Characterization of fluid flow in a microchannel with a flow disturbing step (id 19)** Authors : I. A. Stogiannis, A D. Passos , A. A. Mouza , S V. Paras, V. Penkavova , J. Tihon	Paper: **Comparative study of heat transfer and pressure drop during flow boiling and flow condensation in minichannels (id 85)** Authors : D. Mikielewicz, R.Andrzejczyk , B.Jakubowska, J.Mikielewicz	Paper: **Experimental evaluation of heat transfer coefficient for nanofluids (id 12)** Authors: C. Menale, F. D'annibale, A. Mariani, R. Bubbico
	Paper: **Fluctuating force-coupling method for interacting colloids (id 234)** Authors: E.E. Keaveny	Paper: **Fluid drag-reducing effect and mechanism of superhydrophobic surfaces with micro-nano textures (59)** Authors: J. Zhang, Z. Yao, P. Hao, H. Tian, N. Jiang	Paper: **Pool Boiling Enhanced by Electric Field Distribution in Micro Sized Space (id 88)** Authors : I. Kano	Paper: **Nanofluid flow and heat transfer in channel entrance region (id 23)** Authors: J. T. C. Liu, G. Puliti
	Paper: **Dynamic unbinding transitions and deposition patterns in dragged meniscus problems (id 235)** Authors: M. Galvagno, D.Tseluiko, U. Thiele	Paper: **Gas recognition based on the physicochemical parameters determined by monitoring diffusion rates in microfluidic channels (49)** Authors: A. Hooshyar Zare , V.Ghafarinia , S. Erfantalab , F. Hossein-Babaei	Paper: **Flow Boiling Heat Transfer of Refrigerant R-134a in Copper Microchannel Heat Sink (id 111)** Authors: V.V. Kuznetsov* , A. S. Shamirzaev	Paper: **Study on Thermal Conductivity of Gas Phase in Nano-porous Aerogel (id 65)** Authors: C. Bi, G.Tang, Q. Sheng, B. Fu

	Paper: **Asymptotic analysis of evaporating droplets (id 236)** Authors: N. Savva , A. Rednikov, P Colinet		Paper: **Flow Boiling in Rectangular Microchannels: 1-D Modelling of the Influence of Inlet Resistance on Flow Reversal (id 179)** Authors: Sateesh Gedupudi, David B.R. Kenning, Tassos G. Karayiannis	Paper: **Three-dimensional multi-level heat transfer model of silica aerogel (id 107)** Authors: He Liu, Zeng Y. Li, Xin P. Zhao And Wen Q. Tao
	Paper: **A particle flow specific boundary element formulation for microfluidic applications (id 206)** Authors: B. Baranoglu, B.Çetin		Paper: **Flow Patterns and Comparison with Correlations for Vertical Flow Boiling of R245fa in Small to Micro Tubes (id 170)** Authors: T. G. Karayiannis, E. A. Pike-Wilson , L. Chen, M. Mahmoud, Y. Tian	Paper: **Effect of nanomaterial properties on thermal conductivity heat transfer fluids and nanomaterial suspension (id 182)** Authors: R. S. Khedkar, S. S. Sonawane, K. L. Wasewar
	Paper: **Absolute and Convective Instabilities in Non-local Active-Dissipative Equations Arising in the Modelling of Thin Liquid Films (id 7)** Authors: D Tseluiko, M. G. Blyth, D. T. Papageorgiou			
13:00-14:00	**Lunch Roberts Foyer G02**			
14:00-14:30	**Keynote paper:** **Blood flow in silico: from single cell to blood rheology** **Professor Gerhard Gompper** Room: **Roberts G06** Chair: **C. Koenig**			
	Biomedical 1 **Blood flow/RBC transport**	**Single phase 2** **Heat transfer 1**	**Multiphase 2** **Evaporation and Condensation**	
14:30-15:45	Session 2 Room: **Roberts G08**	Session 2 Room: **Roberts 106**	Session 2 Room: **Roberts G06**	
	Chair: **K. Tatsumi & S. Balabani**	Chair: **J. Brandner & V. Kuznetsov**	Chair: **D. Mikielewicz & M. Mamoud**	
	Paper: **Microconfined flow behavior of red blood cells by image analysis techniques (id 52)** Authors: G. Tomaiuolo, L. Lanotte , A. Cassinese , S. Guido	Paper: **Experimental Apparatus for the Study of micro Heat Exchangers with Inlet Temperatures between -200 and 200 °C and Elevated Pressures (id 198)** Authors : A. Parahovnik, N. Tzabar, G. Yossifon	Paper: **Preliminary measurements of heat transfer during condensation in microchannels (id 2)** Authors : H. S. Wang, J. Sun, L. Ruan, J. W. Rose	
	Paper: **Multiphase measurement of blood flow in a microchannel (id 192)** Authors : J. M. Sherwood, D. Holmes, Efstathios Kaliviotis , S. Balabani	Paper: **The Influence of Geometry on the Thermal Performance of Microchannels in Laminar Flow with Viscous Dissipation (id 163)** Authors : M. Lorenzini ,N. Suzzi	Paper: **Experimental Study of Slug Flow for Condensation in a Square Cross-Section Micro-Channel at Low Mass Velocities (id 136)** Authors : G. El Achkar, M. Miscevic, P.Lavieille	
	Paper: **Microfluidic interactions between red blood cells and drug carriers by image analysis techniques (id 77)** Authors: R. D'apolito, F. Taraballi, S. Minardi , X. Liu , S. Caserta, A. Cevenini, E. Tasciotti , G. Tomaiuolo, S. Guido	Paper: **Heat transfer enhancement with gas-to-gas micro heat exchangers (id 173)** Authors : I. Gerken, J. J. Brandne, R. Dittmeyer	Paper: **Measurement and Modeling of Void Fraction in High Pressure Condensing Flows through Microchannels (id 201)** Authors : B. Keinath, S. Garimella	
	Paper: **Off-plane motion of an oblate capsule in a simple shear flow (id 13)** Authors: A-V Salsac, C. Dupont, F. Delahaye , D. Barthes-Biese	Paper: **Heat transfer characteristics of hybrid microjet – microchannel cooling module (id 71)** Authors: T. Muszynski , R. Andrzejczyk	Paper: **Explosive Vaporization of Water and Isopropyl Alcohol on a Flat Microheater (id 118)** Authors : V.V. Kuznetsov, I. A. Kozulin	
			Paper: **Flow measurement using micro-PIV within evaporating sessile drops of self-rewetting mixtures (id 28)** Authors: J. R.E. Christy, K. Sefiane , J. C. Ebeling , T. Seewald , S. Harman	
15:45-16:15	**Coffee/Tea Roberts Foyer G02**			

	Biomedical 2 **Blood flow modelling**	Single Phase 3 **Modelling 1-CFD and moment method**	Multiphase 3 **Boiling 2**
16:15-18:15	Session 3 Room: **Roberts G08**	Session 3 Room: **Roberts 106**	Session 3 Room: **Roberts G06**
	Chair: **A. Barakat & J. Sherwood**	Chair: **J. Reese & S. Paras**	Chair: **J. Xu & D.Poulikakos**
	Paper: **Margination of Micro- and Nano-Particles in Blood Flow and its Effect on the Efficiency of Drug Delivery (id 156)** Authors: K. Muller , D. A. Fedosov, G. Gompper	Paper: **Cylindrical Couette Flow in the Transition Regime by the Method of Moments (id 11)** Authors : X-J. Gu , D. R. Emerson	Paper: **Flow boiling heat transfer of a non-azeotropic mixture inside a single microchannel (id 160)** Authors : D. Del Col *, M. Azzolin, S. Bortolin
	Paper: **Deformability of red blood cells affects their velocity in deterministic lateral displacement devices (id 53)** Authors : T. Krüger, D. Holmes, P. V. Coveney	Paper: **Aerodynamic behavior of the bridge of a capacitive RF MEMS switch (id 148)** Authors: D. Isvoranu, S. Sorohan, G. Ciuprina	Paper: **A numerical study of bubble growing during saturated and sub-cooled flow boiling in micro channels (id 50)** Authors : Q. Liu, B. Palm
	Paper: **An investigation on the rheodynamics of human red blood cells using high performance computations (id 189)** Authors: D. Xu , A. Munjiza , E. Avital , C. Ji , E. Kaliviotis , J. Williams	Paper: **Simulation of Gas Micro Flows based on Finite Element and Finite Volume Method (id 197)** Authors : A. Westerkamp, J. Bünger, M. Torrilhon	Paper: **On the effect of the dynamic contact angle of a vapor embryo interface trapped in a nucleation site (id 199)** Authors : L. Léal, M. Miscevic, P. Lavieille, F. Topin, Lounès Tadrist
	Paper: **Behaviour of the von Willebrand Factor in Blood Flow (id 178)** Authors: K. Muller , D. A. Fedosov , G. Gompper	Paper: **Microfluidic multiscale model of transport phenomena for engineering and interdisciplinary education applied to elements of a Stirling engine (id 26)** Authors : M. Krol	Paper: **Variation of Important Non-Dimensional Numbers During Bubble Growth at Nucleation Site in Microchannels (id 83)** Authors: S. T. Kadam , R. Kumar
	Paper: **Local Regulation of Arterial Tone: an Insight into Wall Dynamics Using Mathematical Models (id 78)** Authors: E. Boileau, D. Parthimos, P. Nithiarasu	Paper: **Laminar Fluid Flow in Microchannels with Complex Shape (id 47)** Authors: M. B. Atmanskikh, O. V. Rusakova, P. Zubkov	Paper: **Single Phase Flow Pressure Drop and Heat Transfer in a Rectangular Metallic Microchannel (id 169)** Authors: A. M. Sahar , M. R. Ozdemir, M. M. Mahmoud, J. Wissink , T. G.Karayiannis
	Paper: **A model of oxygen dynamics in the cerebral microvasculature and the effects of morphology on flow and metabolism (ID 116)** Authors: C. S. Park, S. J. Payne	Paper: **Numerical Simulation of Microflows with Moment Method (id 186)** Authors: Z. Cai	Paper: **Comparison of heat transfer characteristics in surface cooling with boiling microjets of water, ethanol and HFE7100 (id 86)** Authors: D. Mikielewicz , T. Muszynski
	Paper: **A CFD and FEM Approach to a Multicompartmental Poroelastic Model for CSF Production and Circulation with Applications in Hydrocephalus Treatment and Cerebral Oedema (id 138)** Authors: J. C. Vardakis , D. Chou , B. J. Tully & Y. Ventikos	Paper: **Grad's moment equations for binary gas-mixture of hard spheres (id 184)** Authors: V. K. Gupta, N. Sarna , M. Torrilhon	
18:15	**End of Sessions**		

Tuesday, 9th September 2014

from 8:00	**Registration –Roberts Foyer G02**		
09:15-09:45	**Keynote paper:** **Optimization of magnetic actuation protocol to enhance mass transfer in solid/liquid microfluidic systems** **Professor Evgeny Rebrov** Room: **Roberts G06** Chair: **P. Angeli**		
09:45-11:00	**Expert session- part 1** Room: **Roberts G06** Chair**: M. Oshima & C. Koenig**		
	Paper: **New look into medicine and biology with thermoacoustic and optoacoustic tomography (id 220)** Authors: V. Ntziachristos Paper: **Optical sensing of miRNA activity in cells (id 219)** Authors: Z. Medarova Paper: **Optical assessment of gel-like mechanical and structural properties of surface layers: single particle tracking and molecular rotors (id 221)** Authors: A. Marki & A. R. Pries Paper: **Towards the identification of spatially resolved mechanical properties in tissues and materials: State of the art, current challenges and opportunities in the field of flow measurements (id 222)** Authors: P. D. Ruiz Paper: **Optical coherence tomography – variations on a theme (id 230) -POSTER** Authors: J. A. T. Halls, N. Fomin, C. A. Greated, C. S. Koenig, M. Collins		
11:00-11:30	**Coffee/Tea Roberts Foyer G02**		
11:30-12:45	**Expert session- part 2** Room: **Roberts G06** Chair: **M. Oshima & C. Koenig**		
	Paper: **Monolithic optofluidic chips: from optical manipulation of single cells to quantum sensing of fluids (id 224)** Authors: R. Osellame Paper: **Plasmonic droplets for high throughput sensing (id 226)** Authors: J. B. Edel Paper: **Optical coherence tomography measurements of biological fluid flows with picolitre spatial localisation (id 227)** Authors: S. J. Matcher Paper: **Imaging flows using CMOS sensors (id 228)** Authors: S. P. Morgan, D. He, S. Shen, B. R. Hayes-Gill Paper: **Continuous and Simultaneous Measurement of Micro Multiphase Flow using confocal Micro-Particle Image Velocimetry (Micro-PIV) (id 229)** Authors: M. Oshima & M. Oishi		
12:45-13:45	**Lunch Roberts Foyer G02**		
13:45-14:15	**Keynote paper:** **Unified modeling suite for two-phase flow, convective boiling and condensation in macro- and micro-channels (id 217)** **Professor J. Thome** Room: **Roberts G06** Chair: **T. G. Karayiannis**		
14:15-16:00	**MINISYMPOSIUM II** **(Lab on a Chip)**	**Single Phase 4** **Modelling 2-DS, MC, LBM**	**Multiphase 4** **Liquid-liquid, Droplets 1**
	Session 2 Room: **Roberts G06**	Session 2 Room: **Roberts G08**	Session 2 Room: **Roberts 106**
	Chair: **A. Radaelli & C. Koenig**	Chair: **D. Valougeorgis & G. Gompper**	Chair: **E. Rebrov & D. Wen**
	Paper: **Droplet Microfluidics for High Throughput Biological Analysis (id 209)** Authors : H. Andersson-Svahn	Paper: **Kinetic calculation of rarefied gaseous flows in long tapered rectangular microchannels (id 36)** Authors: L. Szalmas	Paper: **Two-phase aqueous-ionic liquid flows in small channels of different diameter (id 172/240)** Authors: D. Tsaoulidis, Q. Li, M. Chinaud, P. Angeli

	Paper: **Sample Preparation for Point of Care Molecular Diagnostics (id 211)** Authors: W. Balachandran, R. McKay, P. Crow, B. Manoharanehru	Paper: **A New Heterogeneous Multiscale Technique for Microscale Gas Flows (id 31)** Authors: S. Y. Docherty, M. K. Borg, D. A. Lockerby, J. M. Reese	Paper: **From Core-Shell Drops to Drops with Ultra-thin Shells via Non-confined Microfluidics (id 154)** Authors: A. Chaurasia, D. Josephides, S. Sajjadi
	Paper: **Microfluidic Platform for Adherent Single Cell High-Throughput Screening (id 104)** Authors: P. Occhetta, C. Malloggi, A. Gazaneo, M. Licini, A. Redaelli, G. Candiani, M. Rasponi	Paper: **Non-equilibrium gas flow and heat transfer in a bottom heated square microcavity (id 17)** Authors: G. Tatsios, M. H. Vargas, S. K. Stefanov, D. Valougeorgis	Paper: **Electrophoretic manipulation of multiple-emulsion droplets (id 117)** Authors: A. M. Schoeler, D. N. Josephides, A. S. Chaurasia, S. Sajjadi, P. Mesquida
	Paper: **Design of an air-flow microchamber for microparticles detection (id 103)** Authors: E. Bianchi & F. Nason, M. Carminati, L. Redala, L. Cortelezzi, G. Ferrari, M. Sampietro, G. Dubini	Paper: **Microchannel fluid flow and heat transfer by lattice boltzmann method (id 74)** Authors: R. Zarita, M Hachemi	Paper: **Flow pattern in inner cores of double emulsion droplets (id 200)** Authors: S. Ma, J.M. Sherwood, W.T.S. Huck, S. Balabani
	Paper: **A Passive Micromixer for Bioanalytical Applications (id 152)** Authors: I. K. Kefala, V. E. Papadopoulos, G. Kokkoris, G. Karpou, D. Moschou, G. Papadakis and A. Tserepi	Paper: **Non-classical Thermal Physics in Force-driven Micro-channel Gas Flows (id 57)** Authors: R. S. Myong	Paper: **Droplet Initiated Rupture of High Viscosity Jets to Create Uniform Emulsions (id 159)** Authors: D. Josephides, S. Sajjadi
	Paper: **Lab-on-Chip for testing Myelotoxic effect of drugs and chemicals (id 114)** Authors: M. Rasponi, A. Gazaneo, A. Bonomi, P. Occhetta, L. Cavicchini, V. Cocce, G. B. Fiore, A. Pessina, A. Redaelli	Paper: **Numerical study for magnetic fluid by lattice Boltzmann method (id 48)** Authors: W. Zhou, Y. Yan	
	Paper: **Modeling of on-chip (bio)particle separation and counting using 3D electrode structures (id 66)** Authors: B. Cetin, S. Zeinali		
16:00-16:30	**Coffee/Tea Roberts Foyer G02**		
	Biomedical 3 **Blood flow and applications**	**Single phase 5** **Modelling 3-Molecular dynamics 1**	**Multiphase 5** **Liquid-liquid, Droplets 2**
16:30-18:00	Session 3 Room: **Roberts G06**	Session 3 Room: **Roberts G08**	Session 3 Room: **Roberts 106**
	Chair: **T. Yamaguchi & T. Krüger**	Chair: **J. Zhang & D. Fedosov**	Chair: **A-V. Salsac & D. Tsaoulidis**
	Paper: **Characterisation of the Mechanobiology of Stents In-Vitro (id 193)** Authors: L. Boldock, C. Poitevin, H. L. Casbolt, S. Hsiao, P. C. Evans, C. M. Perrault	Paper: **A Molecular Dynamics Study of Proton Hopping in Nafion Membrane (id 34)** Authors: T. Mabuchi and T. Tokumasu	Paper: **Microfluidic droplet control by photothermal interfacial flow (id 203)** Authors: M. Muto, M. Motosuke
	Paper: **Optimization of Drug-Eluting Stents (id 171)** Authors : F. Bozsak, J. Chomaz, A. Bakarat	Paper: **Transport properties and structure of fluids in hydrophobic/hydrophilic nanochannels (id 30)** Authors : F. Sofos, T. Karakasidis, A. E. Giannakopoulos and A. Liakopoulos	Paper: **Mechanical characterisation of cross-linked albumin capsule membranes (id 20)** Authors: P. Gires, A. V. Salsac, E. Leclerc, F. Edwards-Levy, D. Barthes-Biesel
	Paper: **Dielectrophoretic Manipulation of Particles and Lymphocytes Using Rail-type Electrodes (id 237)** Authors : K. Tatsumi, H. Okui, K. Kawano, K. Nakabe		Paper: **Prediction of the liquid film characteristics in open inclined microchannels (id 14)** Authors: A. D. Anastasiou, A. Gavriilidis, A. A. Mouza
18:00	**End of Sessions**		
19.30	**Conference Dinner - Thames Cruise on Symphony**		

Wednesday, 10th September 2011

from 8:00	**Registration**		
09:30-10:00	**Keynote paper:** **Microfluidics for energy applications** **Professor D. Sinton** Room: **Roberts G06** Chair: **S. Balabani**		
10:00-11:15	**Biomedical 4** **Applications & Biotechnology 1**	**Single Phase 6** **Heat transfer 2**	**Multiphase 6** **Solid-liquid**
	Session 1 Room: **Roberts G06**	Session 1 Room: **Roberts G08**	Session 1 Room: **Roberts 106**
	Chair: **D. Sinton & S. Oshita**	Chair: **A. Cioncolini & M. Tiwari**	Chair: **Y. Yan & K. Tatsumi**
	Paper: **Effective Transport Template for Particle Separation In Microfluidic Bumper Arrays (id 134)** Authors: S. Cerbelli, F. Garofalo and M.Giona	Paper: **Optimal microscale water cooled heat sinks for targeted alleviation of hotspot in microprocessors (id 39)** Authors: C. S. Sharma, M. K. Tiwari, D. Poulikakos	Paper: **Synthesis of Silver Nanoparticles using Non-Fouling Microfluidic Devices with Fast Mixing (id 131)** Authors : R. Baber, L. Mazzei, N. T. K. Thanh, A. Gavriilidis
	Paper: **Experimental Investigation on the Behavior of Artificial Magnetic Cilia (id 80)** Authors: A. Marucci, G. P. Romano	Paper: **Numerical Studies on Geometric Features of Microchannel Heat Sink with Pin Fins (id 180)** Authors: J. Zhao, S. Huang, L.g Gong	Paper: **Novel microgels fabricated on microfluidic devices (id 142)** Authors: B. Lu, M. D. Tarn, T. K. Georgiou, N. Pamme
	Paper: **The study of the influence of morphology anisotropy of clusters of superparamagnetic nanoparticle on magnetic hysteresis by Monte Carlo simulations (id 45)** Authors : R. Fu, C. Roberts, Y. Yan	Paper: **Influence of metallic porous microlayer on pressure drop and heat transfer of stainless steel plate heat exchanger (id 87)** Authors: J. Wajs, D. Mikielewicz	Paper: **Pore-Scale Study on Two-phase Flow in Porous Media (id 129)** Authors: Z. Liu, H. Wu
	Paper: **Electromagnetic Actuated Stirring in Microbioreactors Enabling Easier Multiplexing & Flexible Device Design (id 132)** Authors: M. J. Davies, I. Munro, C. K.L. Tan, M. C. Tracey, N. Szita	Paper: **Temperature Stabilisation in Fischer Tropsch Reactors using Phase Change Material (id 82)** Authors: A. O. Odunsi, T. S. O'donovan, D. A. Reay	Paper: **Photothermal Conversion Efficiencies of Silver Nanoparticle Dispersions (id 161)** Authors: D. Wen, H. Zhang, H-J. Chen, G.Lin
11:15-11:45	**Coffee/Tea Roberts Foyer G02**		
11:45-13:00	**Biomedical 5** **Biotechnology 2**	**Single phase 7** **Modelling 4- Molecular Dynamics 2**	**Multiphase 7** **Liquid-liquid, droplets & gas- liquid**
	Session 2 Room: **Roberts G06**	Session 2 Room: **Roberts G08**	Session 2 Room: **Roberts 106**
	Chair: **G. Dubini & C. A. Cortes-Quiroz**	Chair: **Y. Ventikos & B. Cetin**	Chair: **J. Coupland & S. Kuhn**
	Paper: **Continuous Flow vs. Static Chamber µPCR Devices on Flexible Polymeric Substrates (id 153)** Authors: V. E. Papadopoulos, I. N. Kefala, G. Kokkoris, A. Tserepi	Paper: **Fluid transport properties under confined conditions (id 15)** Authors: V. Rudyak, A. Belkin, D. Ivanov	Paper: **Magnetic actuation of microparticles for mass transfer enhancement (id 79)** Authors: P. A. Lisk, E. Bonnot, Md. Taifur Rahman, F. Aiouache, R. Bowman, R. Pollard, E. Rebrov
	Paper: **Analysis and design optimization of an integrated micropump-micromixer operated for bio-MEMS applications (id 162)** Authors: C. A. Cortes-Quiroz, A. Azarbadegan, I. D. Johnston, M. C. Tracey	Paper: **Temperature Distribution in the Force-driven Poiseuille Flow by Molecular Dynamics (id 58)** Authors: R. Ranjith, J. H. Park, R. S. Myong	Paper: **Microdevices for Continuous Sized Based Sorting by AC Dielectrophoresis (id 106)** Authors: E. Altinagac , Y. Genc, H. Kizil, L. Trabzon, A. Beskok
	Paper: **Constant depth microfluidic networks based on a generalised Murray's law for Newtonian and power-law fluids (id 42)** Authors: K. Zografos, R. W. Barber, D. R. Emerson and M. S. N. Oliveira	Paper: **Nanoscale Prediction of Graphite Surface Erosion by Highly Energetic Gas - Molecular Dynamics Simulation (id 139)** Authors: R. Murugesan, N. Chandrasekaran, J. H. Park	Paper: **A Model for Uphill Droplet Motion (id 140)** Authors: F. M. Mancio Reis, P. Lavieille, M.Miscevic

	Paper: **Reactive oxygen species by water containing nanobubbles and its role in the improvement of barley seed germination (id 70)** Authors: S. Liu, S. Oshita, Y. Makino		Paper: **Co-current horizontal flow of a Newtonian and a non-Newtonian fluid in a microchannel (id 213)** Authors: E.P. Roumpea, A. D. Passos, A.A. Mouza, S. V. Paras
	Paper: **Corner Accumulation Behavior of Spermatozoa in Microchannels (id 181)** Authors: R. Nosrati, P. J. Graham, D. Sinton		Paper: **Absorption of spherical bubbles in a square microchannel (id 130)** Authors: D. Mikaelian, B. Haut, L. De Canniere, B. Scheid
13:00-13:45	**Lunch Roberts Foyer G02**		
13:45-14:15	**Keynote paper** **Advances in hybrid molecular/continuum methods for micro and nano flows** **Professor Jason Reese** Room: **Roberts G06** Chair: C. Koenig		
	Nanofluids 2	**Single Phase 8** **Lab on a chip**	**Multiphase 8** **Gas-liquid, Bubbles**
14:15-15:45	Session 3 Room: **Roberts G08**	Session 3 Room: **Roberts 106**	Session 3 Room: **Roberts G06**
	Chair: **Y. Yan & Y. Sui**	Chair: **D. Emerson & V. Rudyak**	Chair: **B. Scheid & J. Christy**
	Paper: **Dependence of nanofluid viscosity on nanoparticle size and material (id 25)** Authors: V. Ya. Rudyak, S. l. Krasnolutskii, D.A. Ivanov	Paper: **Similarities in Dielectrophoretic and Electrophoretic Traps (id 93)** Authors: N. Chandrasekaran, R. Murugesan, J. H. Park	Paper: **A novel micro separator using the capillary separation effect with locally populated micro pin fin structure (id 100)** Authors: B. An, J.g Xu, D. Sun
	Paper: **The gas leakage dynamic flow in nanoporous silica aerogel under different pressure difference (id 108)** Authors: X. P. Zhao, Z. Y. Li, H. Liu, W. Q. Tao	Paper: **Electrohydrodynamically Induced Mixing and Pumping of Multifluid Systems in Microchannels (id 10)** Authors: R. Cimpeanu, D. T. Papageorgiou	Paper: **Measurement of Cavitation in a Sliding Bearing using Digital Holography (id 207)** Authors: T. Tang, L. Arevalo, J. M. Coupland
	Paper: **Thermal Conductivity and Rheology Behavior of Aqueous Nanofluids Containing Alumina and Carbon Nanotubes (id 9)** Authors: Z. Wu, Z. Feng, L. Wadso, B. Sunden	Paper: **Ion drag EHD micropump with single walled carbon nanotube (SWCNT) electrodes (id 37)** Authors: Md. Kamrul Russel, P. Ravi Selvaganapathy, C. Y. Ching	Paper: **A Hydrodynamic Study of Benzyl Alcohol Oxidation in a Micro-Packed Bed Reactor (id 149)** Authors: N. Al-Rifai, M. Morad, G.Leivadarou, E. Cao, G. Brett, G. J. Hutchings, A. Gavriilidis
	Paper: **Experimental Investigation on Performance of Silver nanofluid in Absorber/Receiver of parabolic Trough Collector (id 208)** Authors: D. R Waghole, R .M. Warkhedkar, V.S.Kulkarni	Paper: **Development of interconnected silicon micro-evaporators for the on-detector electronics cooling of the future ITS detector in the ALICE experiment at LHC (id 165)** Authors : A. Francescon, G. Romagnoli, A. Mapelli, P. Petagna, C. Gargiulo, L. Musa, J. R. Thome, D. Del Col	Paper: **Scalability of mass transfer in Taylor flow in capillaries (id 76)** Authors : V. Nappo, S. Kuhn
	Paper: **An experimental study of dynamic flow of nanofluid with different concentrations (id 43)** Authors: J. Hong, P. Glover, Y. Yan	Paper: **Investigation of laser induced phosphorescence and fluorescence of acetone at low pressure for molecular tagging velocimetry in gas microflows (id 115)** Authors: H Si Hadj Mohand , F. Samouda, C. Barrot , S. Colin ,A. Frezzotti	Paper: **Three-dimensional simulation of cavitating flow in real journal bearing geometry (id 29)** Authors: M. Schmidt, P. Reinke, M. Nobis, M. Riedel
15:45	**Conference closure & farewell coffees**		
16:00-18:00	**Visits to the London Centre of Nanotechnology**		

Abstracts

4th Micro and Nano Flows Conference
UCL, London, UK, 7-10 September 2014

New measurements of heat transfer during condensation in microchannels

Hua Sheng WANG [1,*], Jie SUN [1,2], John W. ROSE [1,*]

* Corresponding author: Tel.: ++44 (0)2078825275; Fax: ++44 (0)2078825356; Email: j.w.rose@qmul.ac.uk
1 School of Engineering and Materials Science, Queen Mary, University of London, UK
2 Institute of Engineering Thermophysics, the Chinese Academy of Sciences, China

Keywords: Heat transfer, Condensation, Microchannel

ABSTRACT

In almost all experimental investigations of heat transfer during condensation in microchannels the vapour-side heat transfer coefficient has been obtained from overall (vapour-to-coolant) measurements by subtraction of resistances or Wilson plot methods. Measurements of this type are susceptible to large uncertainty. In two recent (Purdue University (2012) and Rensselaer Polytechnic Institute (2012) and one earlier investigation (Kyushu University (2002)) attempts have been made to measure local channel surface temperature and local heat flux along the channel. The fluids used were R134a (RPI and Kyushu) and FC72 (Purdue). A wholly theoretical study of Wang and Rose (2005, 2011), based only on the Nusselt approximations and with no empirical input, includes the transverse surface tension driven flow towards the corners of noncircular channels. The theory predicts the distribution along a channel of local heat flux and local quality, for given vapour mass flux and variation along the channel of vapour-surface temperature difference. The theory agrees closely with the detailed experimental data (see Fig. 1). It is shown that surface tension plays a vital role in the condensation process.

To provide more data, in particular using a fluid with a significantly different surface tension (water), a new experiment has been designed which should provide data of unsurpassed accuracy. 98 thermocouples are very accurately located at different depths below the surface of 6 parallel channels (1.5 mm x 1.0 mm) and at 7 positions along the flow path (total length 500 mm) (see Fig. 2). The temperature measurements throughout the condenser block are used in an inverse solution to determine the distribution along the channels of local surface temperature and local heat flux. Provisional results for condensation of steam are given in the paper and implications for theory are discussed.

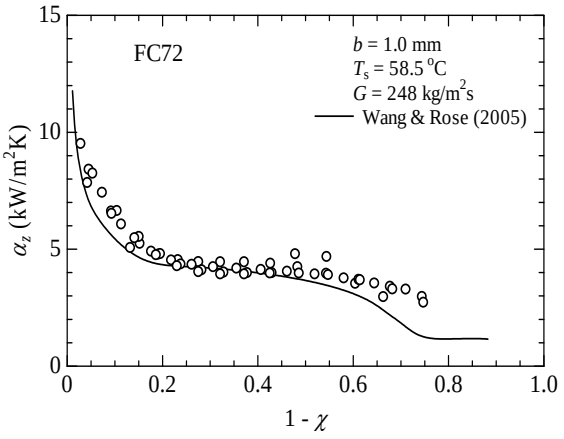

Fig. 1 Comparison of theory with measurements of of Kim and Mudawar (2012). α_z denotes local heat-transfer coefficient, χ denotes vapour quality

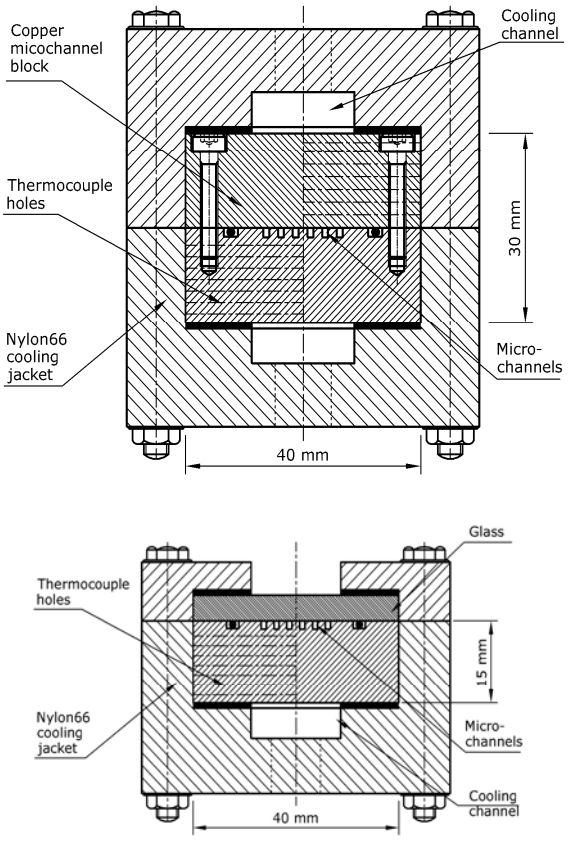

Fig. 2 Section though test block and cooling jacket for heat-transfer measurements and visual observation

4th Micro and Nano Flows Conference
UCL, London, UK, 7-10 September 2014

Absolute and Convective Instabilities in Non-local Active-Dissipative Equations Arising in the Modelling of Thin Liquid Films

Dmitri TSELUIKO [1,*], Mark G. BLYTH [2], Demetrios T. PAPAGEORGIOU [3]

* Corresponding author: Tel.: ++44 (0)1509 223190; Fax: ++44 (0)1509 223969; Email: d.tseluiko@lboro.ac.uk
1 Department of Mathematical Sciences, Loughborough University, UK
2 School of Mathematics, University of East Anglia, UK
3 Department of Mathematics and Department of Chemical Engineering, Imperial College London, UK

Keywords: Absolute/Convective Instability, Thin Films, Boundary Integral Methods, Non-local Equations

Absolute and convective instabilities in non-local systems that arise in the modelling of thin-film flows in the presence of various external effects and complexities are discussed. The particular emphasis is on the analysis of thin-film flows over flat or corrugated walls in the presence of an applied electric field. Electrified liquid films arise, for example, in coating processes where liquid films are deposited onto a target surfaces with a view to producing an evenly coating layer. In practice, the target surface, or substrate, may be irregular in shape and feature corrugations or indentations. This may lead to non-uniformities in the thickness of the coating layer. Attempts to mitigate film-surface irregularities can be made using, for example, electric fields. We analyse the stability of such thin-film flows and show that if the amplitude of the wall corrugations and/or the strength of the applied electric field is increased the convectively unstable flow undergoes a transition to an absolutely unstable flow. The theoretical predictions are supported by time-dependent simulations.

4th Micro and Nano Flows Conference
UCL, London, UK, 7-10 September 2014

Thermal Conductivity and Rheology Behavior of Aqueous Nanofluids Containing Alumina and Carbon Nanotubes

Zan WU [1,*], Zhaozan FENG [2], Lars WADSO [3], Bengt SUNDEN [1]

* Corresponding author: Tel.: +46 46 2228604; Fax: +46 46 2224717; Email: zan.wu@energy.lth.se
[1] Department of Energy Sciences, Lund University, Lund, Sweden
[2] Department of Energy Engineering, Zhejiang University, Hangzhou, China
[3] Division of Building Materials, Lund University, Lund, Sweden

Keywords: Nanofluid, Thermal conductivity, Viscosity, Carbon nanotube, Agglomeration, Interfacial thermal resistance

Abstract

In this study, thermal conductivity and rheology behavior of aqueous alumina and multi-walled carbon nanotube (MWCNT) nanofluids were measured and compared with several analytical models. Both thermal conductivity and viscosity of the two nanofluids increase with increasing volume fraction. The experimental thermal conductivity data for the two nanofluids are located near the lower Hashin-Shtrikman bound and far away from the upper Hashin-Shtrikman bound. Therefore there is still enough room for thermal conductivity enhancement. Further conductivity enhancement of the nanofluids can be achieved by manipulating particle or agglomeration distribution and morphology. The structure-property relationship was checked for the nanofluids. Possible agglomeration size and interfacial thermal resistance were obtained and partially validated. Based on the Chen et al. model, a revised model was developed by incorporating the effects of interfacial thermal resistance into the Hamilton-Crosser model. The revised model can accurately reproduce the experimental data based on the agglomeration size extracted from the rheology analysis. In addition, thermal conductivity change of the alumina/water nanofluid with elapsed time was also investigated. The average thermal conductivity decreases with elapsed time. Besides, thermal conductivity measurements were conducted for nanofluid mixtures of alumina/water and MWCNT/water nanofluids.

4th Micro and Nano Flows Conference
UCL, London, UK, 7-10 September 2014

Electrohydrodynamically Induced Pumping and Mixing of Multifluid Systems in Microchannels

Radu CIMPEANU [1], Demetrios T. PAPAGEORGIOU [1,*]

* Corresponding author: Tel.: ++44 (0)2075 948369; Fax: ++44 (0)2075 948517; Email: d.papageorgiou@imperial.ac.uk
1: Department of Mathematics, Imperial College London, UK

Keywords: Stability, Electrohydrodynamics, Microfluidics, Mixing

We investigate electrostatic stabilization mechanisms acting on stratified flows. Prescribing a difference in voltage potential to generate uniform horizontal electric fields has already been shown to suppress the Rayleigh-Taylor instability in cases where heavier fluid lies above lighter fluid [a]. From a different perspective, vertical electric fields can be used to generate interfacial dynamics in stably stratified systems for flows between horizontally aligned parallel solid walls. We aim to model efficient electrohydrodynamic control procedures in small scale confined geometries that induce time dependent flows without requiring an imposed velocity field or moving parts.

Using linear stability theory, we identify the most unstable wavenumbers for a given microscale geometry to deduce electric fields strengths that can be utilized to produce a required wave pattern. We perform comprehensive parameter studies in order to gain more knowledge about the sensitivity of the system. Starting from simple mechanisms, such as uniform field on-off protocols, we present promising results in this context. Two-dimensional computations using the volume-of-fluid (VOF) method are conducted to fully validate the linear stability theory. We then numerically examine practical optimization possibilities in the nonlinear regime, for example distributions of field strengths and time intervals between on and off positions.

In this study we also propose a mechanism for inducing pumping by generating a traveling wave voltage distribution on one or both of the electrodes. This is a good model of what could be achieved by a distribution of strip electrodes on the substrate followed by an appropriate sequential on-off voltage protocol along the substrate. The technique only requires the manipulation of the imposed electric field. We will show via extensive numerical simulations that this pumping phenomenon is a result of an externally induced nonlinear traveling wave that forms at the fluid-fluid interface. The generated flux allows for further improvement of the microfluidic mixing process and has numerous other relevant ramifications.

The analytical and numerical tools constructed give us the possibility to discuss competitive alternatives in a broad spectrum of applications, from microfluidic mixing to electrostatically induced soft lithography.

[a] CIMPEANU, R., PAPAGEORGIOU, D.T. & PETROPOULOS P.G., On the control and suppression of Rayleigh-Taylor instability using electric fields. Phys. Fluids, 2013, under review.

4th Micro and Nano Flows Conference
UCL, London, UK, 7-10 September 2014

Cylindrical Couette Flow in the Transition Regime by the Method of Moments

Xiao-Jun Gu*, David R. Emerson

* Corresponding author: Tel.: ++44 (0)1925 603663; Fax: ++44 (0)1925 603634; Email: xiaojun.gu@stfc.ac.uk
Scientific Computing Department, STFC Daresbury Laboratory, Warrington, WA4 4AD, UK

Keywords: Micro Flow, Moment method, cylindrical Couette flow

Gas flows in micro-electro-mechanical systems (MEMS) suffer from rarefied effects since the gas molecules collide with solid walls more often than among themselves to reach to the equilibrium state. As a result, the traditional hydro-thermal-dynamic model, the Navier-Stokes-Fourier (NSF) equations, fail to capture many nonequilibrium phenomena associated with rarefaction. The extent of the rarefaction is measured by the Knudsen number, *Kn*, the ratio of the molecular mean free path, λ, to the characteristic length of the geometry. When $Kn < 0.1$, i.e. in the slip regime, the NSF equations coupled with appropriate velocity-slip and temperature-jump wall boundary conditions may predict certain main features of the flow. When the Knudsen number is > 0.1, in the transition regime, usually kinetic theory is required to study the flow details. The Boltzmann equation and the direct simulation Monte Carlo (DSMC) are the main kinetic methods to simulate nonequilibrium gas flow. However, they are computationally expensive, particularly for flows at low speed in the early transition regime. Despite great efforts being made to overcome the numerical difficulties and computing costs, solutions using the Boltzmann equation or DSMC are still too difficult to be widely used in practical engineering applications. Alternative approaches have been developed to alleviate the difficulties in kinetic theory but are accurate enough for engineering design.

Extending hydro-thermal-dynamics into the transition regime is one of the most promising approaches [1]. The method of moments, which was originally proposed by Grad as an approximate solution procedure to the Boltzmann equation, is currently being used to bridge the gap between the hydro-thermal-dynamics and kinetic theory. In this approach, the Boltzmann equation is satisfied in a certain average sense rather than at the molecular distribution function level. How far the hydro-thermal-dynamics should be extended, i.e. how many moments should be used, largely depend on the flow regime. It was found [2, 3] that the regularized 13 moment equations (R13) are not adequate enough to capture the Knudsen layer in Kramers' problem and the regularized 26 moment equations (R26) are required to accurately reproduce the velocity defect found with kinetic data. However, both the R13 and R26 equation models can capture many nonequilibrium phenomena produced by kinetic theory, such as the tangential heat flux in planar Couette flow and the bimodal temperature profile in planar force-driven Poiseuille flow in the early transition regime [4]. In the present study, we investigate the effect of streamline curvature on the accuracy of the results obtained by the moment method.

One of the simplest situations involving curvature is the problem of shear flow between two concentric, rotating cylinders of infinite length, i.e. cylindrical Couette flow. It has been studied by various methods in different regimes. For many low speed flows, it should be sufficient to use a linearized set of moment equations. In the present study, both the linearized R13 (LR13) and R26 (LR26) equations are used to study the behavior of cylindrical Couette flow in the early transition regime. The predicted results from the moment equations are compared with kinetic data for a range of Knudsen number, which is defined as the ratio of the mean free path to the gap between the two cylinders. Illustrated in figure 1 are the velocity profiles of $Kn=0.5$ obtained from hydro-thermal-dynamic models of different sophistication and the accommodation coefficient, α, at the cylinder walls is 1.0 and 0.05 respectively. In comparison with the DSMC data [5], the accuracy of each model is clearly shown in the figure. In addition, the curvature effect on the velocity, shear stress and heat flux are analysed in the present study.

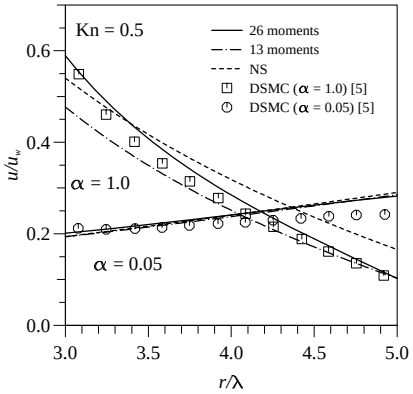

Figure 1. Angular gas velocity against radial distance of the cylindrical Couette flow. Inner cylinder radius $R_1=3\lambda$ with a wall velocity u_w. Stationary outer cylinder radius $R_2=5\lambda$. Accommodation coefficient α=1.0 and 0.05, respectively.

References

[1] Struchtrup, H., Macroscopic transport equations for rarefied gas flows. Springer, Berlin (2005).
[2] Young, J. B., Int. J. of Heat and Mass Transfer 54:2902, 2011.
[3] Gu, X. J. and Emerson, D. R., Phys. Rev. E 51, 016313, 2009.
[4] Gu, X. J. and Emerson, D. R., J. Fluids Mech. 636:117, 2009.
[5] Tibbs, K. W., Baras, F. and Garcia A. L., Phys. Rev. E 56:2282, 1997.

4th Micro and Nano Flows Conference
UCL, London, UK, 7-10 September 2014

Experimental evaluation of heat transfer coefficient for nanofluids

Carla MENALE [1,*], Francesco D'ANNIBALE [2], Andrea MARIANI [2], Roberto BUBBICO [1]

* Corresponding author: Tel.:0630486467; Email: carla.menale@enea.it
1 Department of Chemical Engineering, Sapienza University of Rome, Rome, Italy
2 ENEA Laboratory of Thermal Fluid Dynamics, Rome, Italy

Keywords: Nanofluids, Heat transfer, Base fluid, Laminar, Turbolent

Historical attempts to achieve higher heat transfer rates, adding particles in the order of millimeters or even micrometers, have encountered problems. Suspensions with millimeter or micrometer-sized particles are known to cause severe problems in heat transfer equipment. In more recent years the international research community has shown significant interest in investigating nanofluids to be used as heat transfer fluids or coolants.
The purpose of this work is to make heat transfer experimental tests on nanofluids.
The tested nanofluids are:

- TiO_2-9wt% supplied by ItN Nanovation AG (a German company specialized in nanoparticles and nanofluids production)
- Al_2O_3-9wt% supplied by ItN
- ZrO_2-9wt% supplied by ItN
- Base fluid of ZrO_2-9wt% supplied by ItN
- SiC-3wt% supplied by the ENEA Technical Unit for Development of Applications of Radiations
- Al_2O_3-3wt% supplied by ItN
- Al_2O_3-9wt% supplied by ITN, added with malic acid
- Al_2O_3-9wt% supplied by ITN, added with acetic acid
- Al_2O_3-20wt% in water-ethylene glycol (50-50), supplied by ITN, with pH=6, (lowered with acetic acid)
- Al_2O_3-9wt% in water-antifrogen N (50-50), supplied by ITN

The HETNA experimental facility (Hydraulic Experiments on Thermomechanics of Nanofluids) has been designed to produce experimental comparison of the difference in the behavior of nanofluid and base fluid without nanoparticles, using two parallel identical loops. The diagram of each of the two loops is shown in Figure 1.

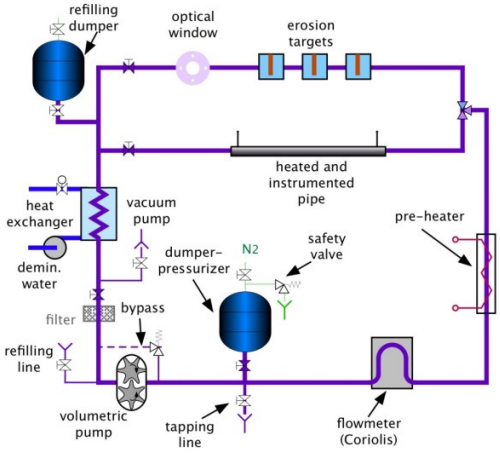

Figure 1: Schematic diagram of each of the two identical loops.

The precision is higher because the control system maintains the two loops under identical conditions, so that small variations during the long-term tests can be considered negligible for the comparison. The first phase of the rig operation consists of filling both loops with the base fluid, followed by initial calibration tests. Then one of the loops is filled with the nanofluid for the real experiments.
The convective heat transfer is evaluated in a circular pipe (I.D. 4mm) heated with uniform heat flux (from 20 to 240 kW/m^2) and flow regimes from laminar to turbulent. Tests have been performed to compare the heat transfer of nanofluids and the corresponding base fluid at the same velocity (from 0.7 to 1.6 m/s) or Reynolds number (from 300 to 6000), and they have also been compared with values calculated from some of the most widely used correlations.
The evaluation of the heat transfer performance of the nanofluid, with respect to its base fluid, depends on the parameter used as a reference. If the fluid velocity is used, the nanofluid heat transfer coefficient is generally less than for the basic fluid. Using the Reynolds number as a reference parameter, the nanofluid heat transfer coefficient turns out to be higher than the basic fluid. This is generally due to the higher viscosity of the nanofluid (the presence of nanoparticles increases the fluid viscosity with respect to the basic fluid), which for the same Reynolds number calls for a higher velocity (with the increase in the nanofluid density much smaller than in the viscosity), thus allowing a better heat transfer performance. Needless to say, due to the higher velocity, for the same Reynolds number, pressure drops associated with nanofluids are higher than those typical of the basic fluid (generally also affected by the presence of nanoparticles, tending to further increase pressure losses).
Experimental data, show that nanofluid heat transfer coefficients do not appear to have an anomalous increase, and differences appear to be only due to different flow conditions that fluids are working under. A confirmation of this result can be given by the comparison of nanofluids heat transfer coefficient with predictions obtained using correlations developed for pure fluids. As these correlations account for fluid physical properties; we can conclude that nanofluids behave like a homogeneous fluid with physical properties accounting for the presence of nanoparticles, without any evidence of anomalies that might be linked to solid nanoparticles. Therefore, the possible heat transfer enhancement using nanofluids depends on the parameters that more affect convective heat transfer (k, ρ, μ, cp), in turn affected by the type, size, shape, and volume of nanoparticle (initial values and values of agglomeration that may occur in the nanofluid after its preparation), as well as from surfactants used to stabilize the nanofluid.

4th Micro and Nano Flows Conference
UCL, London, UK, 7-10 September 2014

Off-plane motion of an oblate capsule in a simple shear flow.

Anne-Virginie SALSAC [1,*], Claire DUPONT [2], Fabien DELAHAYE [1], Dominique BARTHES-BIESEL [1]

* Corresponding author: Tel.: +33 (0)3 44 23 73 38; Email: a.salsac@utc.fr
1 Biomechanics and Bioengineering Laboratory (UMR CNRS 7338), Université de Technologie de Compiègne, France
2 Solids Mechanics Laboratory (UMR CNRS 7649), Ecole Polytechnique, France

Keywords: oblate capsule, fluid-structure interaction, finite element method, boundary integral method, shear flow

1 Introduction

Microcapsules consist of a liquid internal medium enclosed within a thin elastic membrane. The dynamics of a spheroidal capsule in simple shear flow has recently received great attention [1,2,3], owing to its relevance to model a red blood cell (RBC). Most studies have modeled the motion of a capsule with its revolution axis in the shear plane, which is a special case, as it is an equilibrium configuration in Stokes flow conditions. It has been shown that the capsule motion depends on the capillary number *Ca*, ratio of the viscous to elastic forces. At low *Ca*, the capsule has a tumbling motion and rotates like a solid particle. As *Ca* is increased, the capsule experiences a transition and takes a swinging motion where it oscillates about the straining direction, while the capsule membrane tank-treads around the deformed shape (fluid-like motion). As *Ca* is further increased, the oscillation amplitude decreases and a tank-treading motion is recovered.

We have recently studied the motion of an initially off-plane *prolate* capsule in shear flow and shown that tumbling is mechanically unstable as the capsule revolution axis moves to become normal to the shear plane (rolling regime) [2]. At high *Ca*, the swinging regime is stable. In the intermediate range of capillary numbers, the capsule precesses around the vorticity axis. We have shown that the stable equilibrium states do not depend on the initial orientation of the capsule revolution axis.

Dupire et al. [4] found experimentally that a RBC orbit is unstable in simple shear flow near the tumbling-to-swinging transition. This shows that the dynamics of *oblate* capsules is still not well understood, particularly at low *Ca*. The present objective is to investigate the influence of the capillary number, viscosity ratio and initial orientation on the equilibrium configurations of an oblate capsule.

2 Method

We consider an oblate capsule (with long-to-short axis ratio equal to 0.5) with different inner-to-outer viscosity ratio λ, suspended in a simple shear flow. The capsule wall is described as an elastic suface obeying a strain-hardening Skalak type law [5]. The capsule revolution axis is initially positioned with an angle ζ_0 with respect to the vorticity axis.

To solve the fluid-structure interaction problem, we use a numerical model, coupling a finite element method for the capsule deformation with a boundary integral method for the internal and external flows [2,3]. Knowing the initial position of the capsule membrane, we compute the stretch ratios and tension tensor using the membrane constitutive law. The membrane equilibrium equation is solved using a finite element method to deduce the load on the membrane. The velocity of the membrane nodes is obtained from the boundary integral formulation. The new position of the capsule membrane points is calculated integrating the velocity with an explicit second-order Runge-Kutta scheme.

3 Results and discussion

The capsule equilibrium motion is found to be independent of the capsule initial inclination ζ_0 and to depend only on *Ca* and λ.

For viscosity ratios $\lambda \leq 1$ and low *Ca* ($Ca \leq 0.02$), the oblate capsule rotates around the vorticity axis and eventually places its revolution axis in the shear plane. The tumbling motion observed when the revolution axis is initially in the shear plane is recovered and is therefore mechanically stable. As *Ca* is increased ($0.05 < Ca \leq 0.9$), the oblate capsule places its smallest and longest deformed axes in the shear plane and assumes a swinging motion, which is stable only until $Ca \sim 0.9$. Above this threshold, the capsule takes a rolling motion with its revolution axis normal to the shear plane.

For $\lambda > 1$, the swinging motion is no longer observed. Only two stable configurations are found: tumbling at low *Ca* and rolling at higher *Ca*. The value of *Ca* at which the transition occurs depends on λ.

The numerical model indicates that a capsule initially placed off the shear plane takes a very long time to reach the stable equilibrium state. But in experiments such as [4], it is only possible to visualize the motion of artificial capsules or RBC over short times. Thus, it is probable that in vitro observations correspond to transitory capsule configurations rather than the stable states.

References

[1] Sui Y, Low H, Chew Y, Roy P. 2008. Tank-treading, swinging, and tumbling of liquid filled elastic capsules in shear flow. PRE. 77, 016310.

[2] Walter J, Salsac A-V, Barthès-Biesel D. 2011. Ellipsoidal capsules in simple shear flow: prolate versus oblate initial shapes. J Fluid Mech. 676, 318-347.

[3] Dupont C, Salsac A-V, Barthès-Biesel D. 2013. Off plane motion of a prolate capsule in shear flow. J Fluid Mech. 721, 180-198.

[4] Dupire J, Socol M, Viallat A. 2012. Full dynamics of a red blood cell in shear flow. PNAS. 109, 81-88.

[5] Barthès-Biesel D, Diaz A, Dhenin E. 2012, Effect of constitutive laws for two-dimensional membranes on flow-induced capsule deformation J. Fluid Mech. 460, 211-222.

4th Micro and Nano Flows Conference
UCL, London, UK, 7-10 September 2014

Prediction of the liquid film characteristics in open inclined microchannels.

Antonios D. Anastasiou [1], Asterios Gavriilidis[2], Aikaterini A. Mouza[1*]

* Corresponding author: Tel.:+30 2310 994161; Fax:+30 2310 996209; Email: mouza@auth.gr
[1] Department of Chemical Engineering, Aristotle University of Thessaloniki, Greece
[2] Department of Chemical Engineering, University College London, UK

Keywords: Microreactor, Falling Film, μ-PIV, Film Thickness

Falling film microreactors (*FFMR*) are important gas-liquid microdevices, in which extended specific surfaces (up to 20,000 m^2/m^3) can be obtained while the formed liquid film remains stable over a wide range of gas and liquid flow rates ***[1]***. The advantages offered by these devices, i.e. enhanced heat and mass transfer capabilities, attracted the interest of many researchers and as a result various papers concerning the design and operation of *FFMRs* have been published during the last decade.

In the majority of these works i.e. ***[2]*** the film thickness was estimated by well-known macroscale correlations of the. However, it has been proven that these correlations are not valid in the microscale ***[3]***. Thus, there is a need to formulate new correlations, which are valid in the microscale and can be used for the design of *FFMR*s.

Important parameters for designing *FFMR*s are the thickness (H) of the liquid film and the shape of the interface, which determines the gas-liquid interfacial area. In a previous work ***[4]*** we have proposed correlations for estimating the film thickness (H) (***eq.1***) and for calculating the shape of the interface (***eq.2***).

$$H/W_o = C\cdot(Re^a Ca^b Fr^d)^f \qquad (1)$$

where *Re, Fr* and *Ca* are the *Reynolds, Froude* and *Capillary* number respectively, while *a, b, C, d* and *f* are equation constants.

$$Y/(H_f - H) = K + A(W/W_O) + B(W/W_O)^2 \qquad (2)$$

Equation (***2***) express the local height of the meniscus (***Y***) as a function of the distance from the wall (**W**). The parameters H, H_f and W_o are defined in ***Figure 1***, whereas the constants ***A, B, K*** are simple functions of the geometrical characteristics of the microchannel and the liquid film, i.e. H_f, H and Wo ***[4]***.

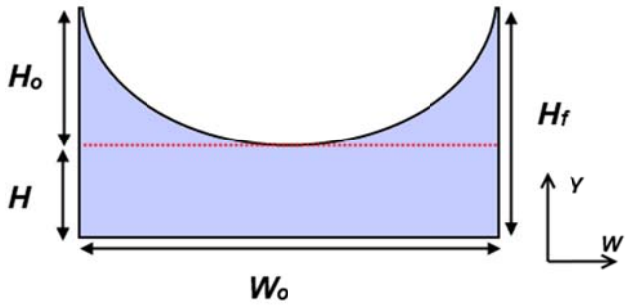

Figure 1: Geometrical characteristics of the liquid film.

The aforementioned correlations are based on data originated from *PMMA* μ-channels with various widths using various fluids. The aim of the present work is to check their validity using other microchannel materials.

Initial experiments are conducted in three microchannels with widths (W_o) *1200, 600* and *300* μm engraved on brass. Pure water as well as aqueous solutions of glycerol and butanol are used. During the experiments the geometrical characteristics of the liquid film are determined by a *μ-PIV* system using a previously published technique ***[3]***. By comparing these results with data ***[4]*** concerning a test section made of *PMMA,* it is found that ***eq. 1*** can predict well the film thickness, provided that the constant **C** is properly adjusted (***Figure 2***). More experiments are currently in progress using more microchannel materials in order to check the validity of these correlations.

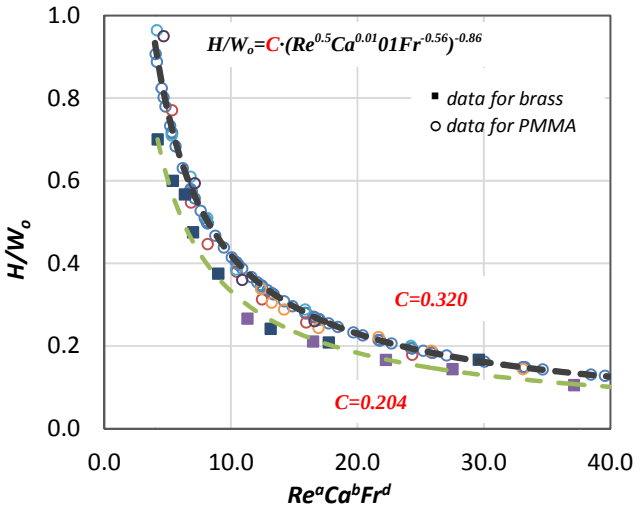

Figure 2: Comparison between film thickness data for microchannels made of *PMMA* and brass.

References

1. Ziegenbalg, D., Löb, P., Al-Rawashdeh, M. M., Kralisch, D., Hessel, V. & Schönfeld, F. 2010. Chemical Engineering Science, **65**, 3557-3566.
2. Kane, A., Monnier, H., Tondeur, D. & Falk, L. 2011. Capability of a falling film microstructured contactor for the separation of binary mixtures. Chemical Engineering Journal, **167**, 455-467.
3. Anastasiou, A.D., Makatsoris, C., Gavriilidis, A. & Mouza, A.A. 2013. Application of μ-PIV for investigating liquid film characteristics in an open inclined microchannels. Experimental Thermal and Fluid Science, **44**, 90-99.
4. Anastasiou, A.D., Gavriilidis, A. & Mouza, A.A. 2013. Study of the hydrodynamic characteristics of a free flowing liquid film in open inclined microchannels. Chemical Engineering Science, **101**, 744-754.

4th Micro and Nano Flows Conference
UCL, London, UK, 7-10 September 2014

Fluid transport properties under confined conditions

Valery RUDYAK*, Alexander BELKIN, Denis IVANOV

* Corresponding author: Tel.: +7(383)2668014; Email: valery.rudyak@mail.ru
Novosibirsk State University of Architecture and Civil Engineering, 630008, Novosibirsk, Russia

Keywords: Micro Flow, transport coefficients, nonequilibrium statistical mechanics, molecular dynamics

Extensive studies of liquid and gas microflows have been motivated by the emergence of a large number of microelectromechanical systems (MEMS) and nanotechnology. Their performance is largely determined by transport processes in the fluid. Thus, mixing in micromixers is due to diffusion processes, and the energy expended in pumping the fluid depends on the fluid viscosity. However, the transport properties in confined spaces differ significantly from bulk transport properties. Diffusion becomes anisotropic (Rudyak et al., 2011), the viscosity increases (Karnidakis et al., 2011).

An important factor that determines transport processes in confined spaces is the interaction of fluid molecules with the molecules of the surface. In a nanochannel with a characteristic diameter of the order of ten nanometers, it is meaningless to speak of the viscosity or thermal conductivity of the fluid individually. It is necessary to consider these properties for the entire system consisting of the fluid and the walls of the nanochannel. Of course, the experimental study of these properties is not easy. Moreover, it is first necessary to develop an adequate theory that, in particular, will help interpret experimental data. The aim of the present work is to develop such a theory. It is constructed using methods of nonequilibrium statistical mechanics (Rudyak, Belkin, 1995); the relations obtained are analyzed by molecular dynamics simulation.

The "fluid–channel wall" system is regarded as a two-phase medium, in which each phase has a particular velocity and temperature. Its dynamics is described by an N -particle distribution function F_N which satisfies the Liouville equation

$$\partial F_N / \partial t + L_N F_N = 0 ,$$

where L_N is the Liouville operator. The state of the system is defined by the partial values of the density , momentum, and energy. These quantities are the averages of the corresponding dynamic variables. Subjecting these variables to the Liouville operator, we obtain the transport equation for them.

To close the transport equations, a nonequilibrium ensemble is needed. According to the hypothesis of the possibility of reducing the level of description of the system, the ensemble is sought in the form of the sum of quasi-equilibrium and dissipative parts

$$F_N = F_{N0} + F_{N1} .$$

The quasi-equilibrium function F_{N0} is derived from the conditions of extremum of information entropy, and F_{N1} is determined using a variant of the projection operator method (Rudyak, Belkin, 1995).

The quantities (the stress tensor, heat flux vector, etc.) included in the transport equation are expressed in terms of correlation functions of microscopic fluxes. These functions are calculated by molecular dynamics simulation. Intermolecular interactions and the interaction between the fluid molecules and the surface are described using the parameters of the potentials of real substances.

The results obtained show that the transfer equations describing transport processes in confined spaces should contain not only the stress tensor and the heat flux vector, but also the interfacial forces responsible for the transfer of momentum and heat due to the interaction with the wall surfaces.

The stress tensor and the heat flux vector fluid can be expressed tin terms of the effective viscosity and thermal conductivity. However, the constitutive relations contain additive terms that correspond to the fluid–fluid and fluid–surface interactions. Thus, not only do the fluid transport coefficients in nanochannels differ from the bulk transport coefficients, but also they are not determined only by the parameters of the fluid. Studying the transfer of momentum and energy of fluids, it is necessary to introduce the viscosity and thermal conductivity of the fluid–surface system.

This work was supported in part by the Russian Foundation for Basic Researches (grant No. 13-01-00052-a) and by the FSP "Scientific and scientific-pedagogical personnel of innovative Russia in 2009-2013" of the Ministry of Education and Science of the Russian Federation (project No. 14.B37.21.1639)

References

Rudyak, V.Ya., Belkin, A.A., Egorov, V.V., Ivanov D.A. About fluids structure in microchannels. Int. J. of Multiphysics, 2011, 5(2), 145-155.

Karnidakis G., Beskok A., Aluru N. Microflows and nanoflows – Interdisciplinary Applied Math. Springer Science+Business Media, Inc., 2005.

Rudyak V.Ya., Belkin A.A. Statistical hydromechanics of multiphase systems. J. Aerosol Sci., 1995, 25, S19.

4th Micro and Nano Flows Conference
UCL, London, UK, 7-10 September 2014

Non-equilibrium gas flow and heat transfer in a bottom heated square microcavity

Giorgos TATSIOS [1], Manuel H. VARGAS [1], Stefan K. STEFANOV [2], Dimitris VALOUGEORGIS [1,*]

* Corresponding author: Tel.: ++30 24210 74058; Fax: ++30 24210 74085; Email: diva@uth.gr
1 Department of Mechanical Engineering, University of Thessaly, Greece
2 Institute of Mechanics, Bulgarian Academy of Sciences, Sofia, Bulgaria

Keywords: Kinetic Theory, Rarefied Gas Dynamics, Thermal Creep, Knudsen Number, GASMEMS.

Efficient flow and heat transfer modeling in vacuum packaged MEMS is of major importance in order to ensure design optimization and operation performance. A packaged device is commonly modeled as four plates forming a square cavity, the bottom of which represents the hot chip and is maintained at high temperature, while the other three plates are maintained at room temperature. A rarefied gas is enclosed in the cavity. This flow configuration has attracted considerable attention and has been tackled by the DSMC, the R13 and the unified gas kinetic methods. It has been found that the flow along the walls does not necessarily go from the cold towards the hot region (typical thermal creep flow) but in the opposite direction as well [1,2]. It has been seen that the detailed structure of the flow domain and the strength of the unexpected vortices are depending on the Knudsen number (Kn) and the temperature ratio of the temperature of the three isothermal walls over the heated bottom temperature, denoted by T2 and T1 respectively.

In the present work this flow configuration is examined via a deterministic approach by the direct solution of the nonlinear Shakhov kinetic model equation, which is discretized based on a second order finite volume scheme in the physical space and the discrete velocity method in the molecular velocity space. Simulations are performed for Kn=0.1, 1, 10 and T2/T1=0.1, 0.5, 0.9. At the walls purely diffuse Maxwell boundary conditions are considered. For the case of T2/T1=0.1 and various Knudsen numbers simulations have been also performed by the DSMC method and very good agreement between the deterministic and stochastic results has been obtained.

Typical results are shown in Figure 1, where temperature contours and streamlines are plotted for a square cavity, with T2/T1=0.1 and Kn=10. The flow is symmetric along the vertical axis at x=0. The temperature τ is monotonically reduced from the bottom (y=0) towards the top (y=1) of the cavity. The two vortices in the bottom rotate due to thermal transpiration as expected and the flow along the lateral walls is from the cold towards the hot region. It is seen however, that the two vortices at the top rotate counter-wise and the flow along the lateral walls is from the hot towards the cold region. In very small Knudsen numbers only the two bottom vortices are present covering the whole flow field. As the Knudsen number increases these vortices are squeezed and the two top vortices start to appear. At moderate and large Knudsen numbers they are well developed. This behavior is typical in all temperature ratios although the exact flow pattern varies. Also, the flow rate of the vortices is reduced as the temperature difference is reduced. In this work a detailed description of the flow properties and characteristics on these parameters is provided in a wide range of the Knudsen number for small, moderate and large temperature differences.

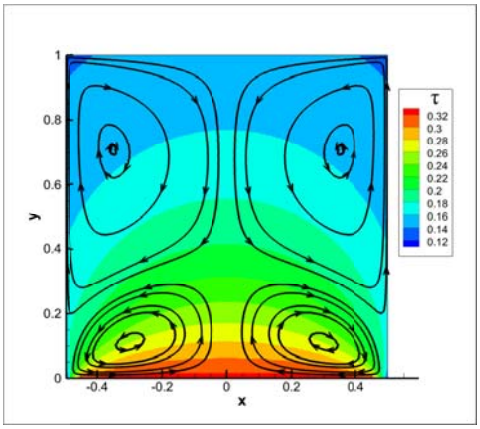

Figure 1: Streamlines and temperature contours for flow in a bottom heated microcavity with T2/T1=0.1 and Kn=10.

To further analyze the flow patterns the distribution function is decomposed into one part which is due to the free motion of the particles coming directly from the boundaries and into another part which is due to particle collisions. The contribution of each part of the solution is separately examined and a physical interpretation of the flow configuration, including the hot-to-cold flow close to the side walls, in the whole range of the Knudsen number is provided.

Acknowledgments
This research obtained financial support from the Association EURATOM/Hellenic Republic and the European Community's Seventh Framework programme (FP7/2007-2013) under GA 215504.

References

1. Rana, A., Torrilhon, M., Struchtrup, H. 2012. Heat transfer in micro devices packaged in partial vacuum, Journal of Physics: Conference Series, 362, 012034.
2. Huang, J., Xu, K., Yu, K., 2013. A Unified Gas-Kinetic Scheme for Continuum and Rarefied Flows III: Microflow simulations. Commun. Comput. Phys., 14 (5), 1147-1173.

4th Micro and Nano Flows Conference
UCL, London, UK, 7-10 September 2014

Characterization of fluid flow in a microchannel with a flow disturbing step

Ioannis A. STOGIANNIS[1], Agathoklis D. PASSOS[1], Aikaterini A. MOUZA[1], Spiros V. PARAS[1*], Vera PENKAVOVA[2], Jaroslav TIHON[2]

* Corresponding author: Tel.: ++30 2310 996174; Email: paras@auth.gr
[1] Chemical Engineering Department, Aristotle University of Thessaloniki, GR
[2] Institute of Chemical Process Fundamentals, Academy of Sciences of the Czech Republic, CZ

Keywords: Microchannels, Electrodiffusion technique, CFD

Microfluidics has been identified as one of the most promising fields in modern process engineering. Additionally, microfluidics is one of the key components used in order to realize *lab-on-a-chip* systems. The main advantages of microsystems are the high surface-to-volume ratios leading to more compact equipment, the increased efficiency and operability especially in heat transfer applications and the enhancement of fluid mixing.

In the micro-scale, mixing can be induced by active or passive methods. In passive micromixers there is no need for external energy and mixing performance is enhanced by complex designs of the microchannel geometry that modify the flow path and increase contact time between fluids. A typical modification of the channel wall is an orthogonal barrier, effectively creating a step in the fluid flow path that promotes mixing. Although flow over a step has been extensively studied in the macroscale, to the authors' best knowledge limited research have been done in the microscale.

The scope of this work is to characterize the flow around a flow disturbing step aiming to investigate the effect of key design characteristics on the length of the recirculation zones (*reattachment length*). This parameter has been identified as the most important in applications of microchannels like fluid mixing and heat transfer enhancement. In the macroscale it has been found that the reattachment length depends primarily on the geometrical characteristics of the channel and the fluid Reynolds number[1].

We identify the ***recirculation zones*** using two techniques, i.e.:

- The *electrodiffusion technique*, that uses gold microelectrodes flush-mounted on the wall, is usually implemented to measure local values of wall shear stress (*WSS*)[2]. On the active surface of the electrode a fast electrochemical reaction takes place and the current is measured under diffusion-limited conditions. *Lévêque's* formula is then applied to determine the mean *WSS*.
- The μ-Particle Image Velocimetry (μ-*PIV*), a common non-intrusive technique for measuring 2D velocity fields in μ-channels with high spatial resolution. In this case the *WSS* is estimated using methods based on curve fitting on the measured velocity data.

Experiments were conducted in a microchannel (***Fig. 1a***) made by micro-milling a *PMMA* plate. Gold electrodes, realized by a novel technique based on sacrificed substrate, are implemented on the channel wall. An *UV* lithography technique was used in order to build μ-structures on the μ-channel later filled with gold using galvanic deposition[3].

To assess the effect of different geometrical characteristics of the step on the extent of the recirculation zones, the expensive and time consuming experiments were replaced by CFD simulations. The *CFD* code employed was validated using experimental data obtained by both the aforementioned techniques. Three dimensionless groups (***Fig. 1b***) are introduced and used as design variables for the *CFD* simulations, namely:

- The step aspect ratio (l/d) defined as the length of the step (l) divided by its height (d).
- The step height to channel height ratio (d/H) that expresses the blockage ratio of the step in the channel.
- The *Reynolds* number using as characteristic length the step height (d).

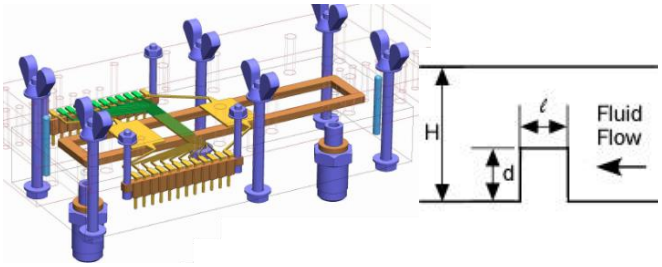

Figure 1: *a) 3D reconstruction of the microchannel with electrodiffusion microsensors, b) geometrical parameters of the μ-channel.*

During the post-processing, using a custom software routine, it is possible to calculate the reattachment lengths of the recirculation zones shown in ***Fig. 2***.

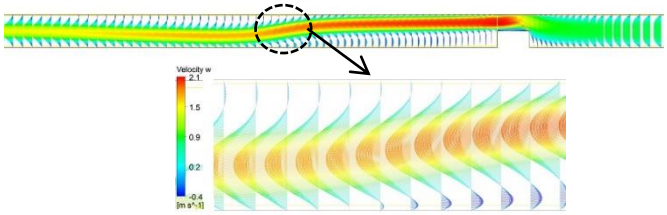

Figure 2: *Typical velocity field over a step with two recirculation zones.*

Preliminary results show that the extent of the reattachment length is significantly affected by the set of design variables used. The study, which is still in progress, is expected to give useful insights concerning the design of μ-channels with flow disturbing steps.

References

1. Tihon, J., J. Legrand, and P. Legentilhomme, *Exp. Fluids*, 2001. **31**(5): p. 484-493.
2. Hanratty, T.J. and J.A. Campbell, *Measurement of wall shear stress*, in *Fluid mechanics measurements*, J. Goldstein, Editor. 1996, Taylor & Francis: Washington, DC. p. 575-648.
3. Schrott, W., M. Svoboda, Z. Slouka, and D. Snita, *Microelectron Eng*, 2009. **86**(4-6): p. 1340-1342.

4th Micro and Nano Flows Conference
UCL, London, UK, 7-10 September 2014

Mechanical characterisation of reticulated albumin capsule membranes

Pierre-Yves Gires [1], Anne-Virginie Salsac [1,*], Eric Leclerc [1], Florence Edwards-Lévy [2], Dominique Barthès-Biesel [1]
* Corresponding author: Email: anne-virginie.salsac@utc.fr
1 Laboratoire de Biomécanique et de Bioingénierie (UMR CNRS 7338), Université de Technologie de Compiègne, Compiègne
2 Institut de Chimie Moléculaire de Reims (UMR CNRS 7312), Université de Reims Champagne-Ardenne, Reims

Keywords: Microfluidic, Capsule, Membrane, Mechanical properties

1 Introduction

Capsules are microscopic droplets surrounded by a membrane with shear resistant properties. In many applications, there is the need to quantify the capsule mechanical behaviour in order to tune the membrane composition adequately. But characterising micrometric size deformable particles is a challenge. A microfluidic technique has been designed to enable the measurement in batch of the capsule deformation under a prescribed flow. The technique presents the advantage over others, such as micropipette aspiration, to be easily applicable to a capsule population. It is based on the observation of the motion and deformation of capsules flowing in a transparent capillary tube with comparable transverse dimension as the particles. We present results on reticulated human serum albumin (HSA) capsules, with a mean diameter of 150µm, and investigate the effect of the HSA concentration.

2 Material and methods

2.1. Experimental procedure

The experimental procedure is similar to the one described in Chu et al. (2011). The capsules are prepared using an interfacial cross-linking method, from an emulsion of droplets of aqueous solutions of HSA suspended in an organic phase containing a cross-linking agent. Four concentrations of HSA are considered: 15%, 20%, 25% and 30% w/v. The capsules are transferred in glycerol and injected into a cylindrical glass microchannel (radius 75µm, length 1.5cm) using a syringe pump. Videos of the capsule in the middle region of the tube are recorded with a high-speed camera mounted on a microscope at a controlled temperature. After a selection procedure detailed further, the contour of each capsule is extracted manually and its velocity is measured (in the range 0.1-7cm/s).

2.2. Model

The capsules are assumed to be spherical at rest with a membrane made of a bi-dimensional strain-softening neo-Hookean material, with shear modulus G_s. The internal liquid is incompressible and Newtonian with viscosity μ. The capsule is suspended into another Newtonian liquid with viscosity μ and forced to flow in a small capillary tube. Inertia is negligible. When a steady state exists, the velocity and deformed shape of a capsule only depend on the size ratio a/R between the capsule and channel radii and the capillary number $\mu U/G_s$ where U is the mean unperturbed velocity of the external liquid. A possible pre-inflation factor α is considered, defined as the ratio between the inflated and initial radii of the capsule.

2.3. Numerical database

As described in Chu et al. (2011) and references therein, the fluid-structure interactions of the capsule flowing in the microchannel are solved by the mean of a boundary integral formulation, with the membrane stresses calculated by a finite element method. The resulting database contains geometric characteristics of the capsule deformation (e.g. axial and total transverse lengths) and velocity as functions of a/R, Ca and α. Two values of pre-inflation are considered: $\alpha = 0\%$ and 1.5%.

2.4. Inverse analysis

Only symmetrical capsules with a size ratio and rear concavity within the database range are kept in the analysis. For each analysed capsule ($a/R \in [0.75,1.02]$), we determine the ensemble of geometric and dynamic parameters *(a/R, Ca)* that fit the measured deformations. The mean G_s and standard deviation σ are calculated for each capsule. Then for a given capsule population, we determine the mean value $\langle G_s \rangle$ and the global standard deviation $\langle \sigma \rangle$ of the G_s distribution.

3 Results

3.1. Results from the inverse analysis

All the capsule profiles can only be fitted with the neo-Hookean model in the case of a 1.5% pre-inflation ratio, which indicates that the capsules are slightly pre-stressed.

For some capsules, σ / G_s may be as large as 0.9, which is not meaningful. This occurs for instance for weakly deformed capsules, for which the deformation is close to the experimental uncertainties. To get significant results, we then consider only capsules with $\sigma / G_s < 1/3$.

3.2. Effect of HSA concentration

As shown in the table below, the shear modulus increases significantly with the HSA concentration.

HSA concentration	15%	20%	25%	30%
$\langle G_s \rangle$; $\langle \sigma \rangle$(mN/m)	47; 17	49; 14	102; 30	369; 130

This increase could be due to a thickening of the membrane or to a tightening of its molecular structure. This issue could be resolved by measuring the number of chemical bonds between the proteins, for example by means of the method of Andry et al. (1996).

4 Conclusion

The microfluidic method thus allows to characterise capsules with a cross-linked HSA membrane prepared under different physico-chemical conditions.

Bibliography

M.-C. Andry, F. Edwards-Levy, M.-C. Levy. *Int. J. Pharm.* 128 (1996): 197-202.
T.-X. Chu, A.-V. Salsac, E. Leclerc, D. Barthès-Biesel, H. Wurtz, F. Edwards-Lévy*J. Colloid Interface Sc.* 355 (2011): 81-88.

4th Micro and Nano Flows Conference
UCL, London, UK, 7-10 September 2014

Effect of Surfactant on Flow Boiling Heat Tranfer of Ethylene Glycol/Water Mixtures in A Mini-tube

Zhaozan FENG [1], Zan WU [2,*], Wei LI [1], Bengt SUNDEN [2]

* Corresponding author: Tel.: +46 46 2228604; Fax: +46 46 2224717; Email: zan.wu@energy.lth.se
[1] Department of Energy Engineering, Zhejiang University, Hangzhou, China
[2] Department of Energy Sciences, Lund University, Lund, Sweden

Keywords: Nanofluid, Surfactant, Ethylene glycol/water mixture, Flow boiling, Mini-tube

Abstract: In this study, the effect of adding a surfactant (sodium dodeobcylbenzene sulfonate, SDBS) to ethylene glycol/water mixtures boiling in a vertical mini-tube was studied. Experiments were done using solutions containing 300 ppm by weight of surfactant and the results were compared with those for pure mixture. Local heat transfer coefficient was measured and found to be dependent on the mass quality. Addition of surfactant significantly enhanced the evaporation of saturated liquid, so that the difference between outlet fluid temperature and outlet bubble point temperature of SDBS solutions was much higher than that of ethylene glycol/water mixture. Though the surfactant intensifies the vaporization process, it does not necessarily enhance the heat transfer coefficient. The heat transfer coefficients at two different mass fluxes were compared, and the result could be explained based on the local flow pattern and heat transfer mechanism. After a critical quality, higher quality will deteriorate the heat transfer due to intermittent dryout, therefore adding surfactant to generate more vapor may have a negative effect on the heat transfer of flow boiling in a mini-tube, which is contrast to the experience of enhancing nucleate pool boiling heat transfer with trace surfactant.

4th Micro and Nano Flows Conference
UCL, London, UK, 7-10 September 2014

Nanofluid Flow and Heat Transfer in Channel Entrance Region

Joseph T. C. Liu [1,*]

* Corresponding author: Tel.: +1 4018632654; Fax: +1 4018639028; Email: joseph_liu@brown.edu
1 School of Engineering and the Center for Fluid Mechanics, Brown University, USA

Keywords: Nanofluid Flow, Heat Transfer, Channel Leading Edge

The present work uses the continuum description of nanofluid flow to study the flow, heat and mass transfer in the entrance and developing region of channels or tubes, where the viscous and heat conduction layers are thin and much more intense than fully developed flow.. Instead of supplementing the formulation with thermodynamic properties based on mixture calculations, use id made of recent molecular dynamical computations of such properties. The density-heat capacity factor, which is important in addition to enhanced thermal conductivity to heat transfer, is significantly higher than that obtained from mixture calculations. This has enormous consequences to heat transfer and attempts are made on this basis to interpret some of the anomalous laminar heat transfer rates observed in experiments.

1 Introduction

The purpose of the present contribution is to incorporate the recent results molecular dynamics computations of nanofluid thermodynamic properties (Puliti & Paolucci, 2012) in the continuum formulation of the dynamics and thermodynamics of nanofluid flow. The formulation is applied to the entrance region of channels and tubes where the transport layers are thin and where unusual high heat transfer rates have been observed (Wen & Ding 2004; Jung, et al., 2009) even for small volume fractions of the nanoparticles.

2. Description of the formulation and results

Buongirno (2006) gave significant impetus to the continuum description of nanofluid flow by generalizing the multiphase flow description, applied by Pfautsch (2008) to boundary layers. It was pointed out in Liu (2012) that the density-heat capacity relation is an inertia effect that could also contribute to heat transfer rate enhancement, in addition to the enhanced thermal conductivity of nanofluids. However, the density-heat capacity obtained from a mixture calculation fall short in explaining the heat transfer enhancement (Liu 2012). Puliti (2012) also criticized the shortcomings of the mixtures results and found that density-heat capacity product could be nearly twice that from ideal mixture results. This would an enormous implication in explaining the relative heat transfer enhancement.

The continuum formulation is specialized to that for the entrance region of nanofluid flow into channels and tubes, where the transport layers are so thin that a "plug flow" approximation suffices with the convection velocity given by the channel entrance velocity. In this case, the viscous, heat conduction and mass transfer layers are simplified into a the Rayleigh-Stokes form of coupled "heat equations". The problem is further simplified by noticing that the experimentally observed heat transfer enhancement occurs even at very low nanoparticle volume concentrations of a few percent, which allows a perturbation procedure about a pure fluid, in ascending powers of the volume fraction. In this case, the nanofluid problem becomes first order in the volume fraction, while "forced" by the solutions of the zeroth order which are the Rayleigh-Stokes solutions in terms error functions for the momentum, heat and mass transfer problems. Analytical solutions for the first order problems result. Puliti (2012) computed properties of nanofluid composed of nano sized gold particles, though different from the ususal experimental nanoparticles of metal oxides, it is possible to compare the nanofluid results in terms of heat transfer enhancement over that of a clean fluid, much in the same way results of metal oxides were compared.

References

Buongiorno, J., 2006 Convective transport in nanofluids. ASME J. Heat Transfer 128, 2 40-250. (doi:10.1115/1.2150834)

Jung, J.-Y., Oh, H.-S., Kwak, H.-Y., 2009 Forced convective heat transfer of nanofluids to microchannels. Int. J. Heat Mass Transfer 52, 466-472.

Liu, J.T.C., 2012 On the anomalous laminar heat transfer intensification in developing region of nanofluid flow in channels or tubes.. Pro. R. Soc. A 468, 2383-2398. (doi:10.1098/repa.2011.0671)..

Pfautsch, E., 2008 Forved convection in nanofluids over a flat plate. M.Sc. Thesis,, U. Missouri.

Puliti, G., Paolucci, S., 2012 Thermodynamic properties of gold-water nanofluids using molecular dynamics. J. Nanopart Res. 14:1296 (10.1007/s11051-012-1296-4)..

Wen, D., Ding, Y., 2004 Experimental investigation into convective heat transfer of nanofluids at the entrance region under laminar flow conditions. Int. J. Heat Mass Transfer 47, 5181-5188. (doi:10.1016/j.ijheatmasstransfer.2004.07.012).

4th Micro and Nano Flows Conference
UCL, London, UK, 7-10 September 2014

Dependence of nanofluid viscosity on nanoparticle size and material

Valery Ya. RUDYAK*, Sergey L. KRASNOLUTSKII, Denis A. IVANOV

* Corresponding author: Tel.: +79139137970; Fax: +7(383)2664083; Email: Valery.Rudyak@mail.ru
The Novosibirsk State University of Architecture and Civil Engineering, Russian Federation

Keywords: Nanofluids; Nanoparticles; Viscosity; Molecular Dynamics; Effect of Nanoparticles Size

Nanofluids are two-phase systems consisting of a carrier medium (liquid or gas) and nanoparticles. They are successfully used or are planned be to used in various chemical plant and reactors, to cool various devices, design new systems for production and transport of thermal energy, in biotechnologies, MEMS, and nanotechnologies for various purposes, in medicine, etc. Since almost all applications of nanofluids are associated with channel flows, viscosity is a determining factor in their application. It has been firmly established that the viscosity of nanofluids is much greater than the viscosity of conventional disperse liquids at equal volume concentrations of dispersed particles and is not described by any of the classical theories of the viscosity of such liquids (Einstein, Batchelor, Mooney, Akrivos and Chang, Krieger and others) (see reviews [1–3] and papers [4, 5]).

In recent studies it has been shown that the viscosity of nanofluids at a given concentration of nanoparticles increases with decreasing size, but contrary data have also been reported [1, 3]. Thus, the question of how the viscosity of nanofluids depends on particle size is still relevant.

In the kinetic theory of gas nanosuspensions, it has also been established that the viscosity of gas nanosuspensions also depends on nanoparticle material [3]. Obtaining systematic data that would allow an unambiguous answer to the question of the dependence of the viscosity of nanofluids on nanoparticle material is the second objective of this work.

Obtaining experimental data on the viscosity of nanofluids is complicated by several factors: the difficulty of producing monodispersed suspensions, various methodological problems of accurately measuring particle size and concentration, the uniformity of their distributions, the formation of agglomerates of particles, etc. An "ideal" experiment can be performed using the method of molecular dynamics (MD) simulations. Therefore in this study, the method of molecular dynamics was used. The simulation was performed using a cubic cell with periodic boundary conditions. The interaction between the molecules of the carrier fluid was described by the 6-12 Lennard-Jones (LD) potential. The interaction of the carrier-fluid molecules with nanoparticles was described by the RK potential [6]. The RKI was used as the nanoparticle interaction potential [7]. The evolution of the system was calculated by integrating the Newton equations.

The carrier fluid was argon. The simulation was performed for spherical nanoparticles of lithium and aluminum with a diameter of 1, 2, and 4 nm. The number of argon molecules in the cell was 7000–15000. The number of nanoparticles in the cell was varied from 1 to 64, and the volume fraction of nanoparticles from 1% to 12%.

For Li–Ar nanofluid (argon based nanofluid with lithium nanoparticles), it was found that the effective viscosity decreases steadily with increasing diameter of the nanoparticles.

To obtain the dependence of the viscosity of a nanofluid on nanoparticle material, we performed calculated for nanofluids with lithium and aluminum nanoparticles with a diameter of 2 nm in argon for volume concentrations of nanoparticles of 1–10%. As a result, the viscosity of the nanofluid with aluminum nanoparticles was found to be significantly lower than the viscosity the nanofluid with lithium nanoparticles at a given volume fraction of nanoparticles.

This work was partially supported by the Russian Foundation for Basic Research (Grant No. 13-01-00052) and the Federal Target Program "Research and scientific-pedagogical personnel of innovative Russia" (contract No, 14.V37.21.1639).

References

1. Mahbubul I.M., Saidur R., Amalina M.A. Latest developments on the viscosity of nanofluids. *International J. Heat and Mass Transfer*. 2012. Vol. 55. P. 874–885.

2. Hosseini S.Sh., Shahrjerdi A., Vazifeshenas Y. A review of relations for physical properties of nanofluids, *Australian J. Basic and Applied Sciences*. 2011. Vol. 5. No. 10. P. 417–435.

3. Rudyak V.Ya. Viscosity of nanofluids. Why it is not described by the classical theories. *Advances in Nanoparticles*. 2013. Vol. 2. P. 266–279.

4. Rudyak V.Ya., Dimov S.V., Kuznetsov V.V. On the dependence of the viscosity coefficient of nanofluids on particle size and temperature. *Technical Phys. Letters*. 2013. V. 39, No. 9. P. 779–782.

5. Rudyak V.Ya., Dimov S.V., Kuznetsov V.V., Bardakhanov S.P. Measurement of the viscosity coefficient of an ethylene glycol–based nanofluid with silicon dioxide particles. *Doklady Physics*. 2013. Vol. 58, No. 5. P. 173–176.

6. Rudyak V.Ya., Krasnolutskii S.L. The interaction potential of dispersed particles with carrier gas molecules. *Proc. 21st Int. Symp. on RGD*. Toulouse, Gépadués-Éditions, 1999. V. 1. P. 263–270.

7. Rudyak V.Ya., Krasnolutskii S.L., Ivanov D.A. The interaction potential of nanoparticles. *Doklady Physics*. 2012. Vol. 57. Iss. 1. P. 33–35.

4th Micro and Nano Flows Conference
UCL, London, UK, 7-10 September 2014

Microfluidic multiscale model of transport phenomena for Engineering and interdisciplinary education Applied to elements of a Stirling engine

Michael KROL *1

* Tel. ++491715775570; Email: michael_krol48@yahoo.com
1: Chemical Engineering Institute, c/o M. Kraume,
Berlin University of Technology, Germany

Keywords: singlephase, multiphase flows, pumps, turbines, thermodynamics

Microfluidic model [12 – **19**, 20] based on elementary mathematical tools **[10, 20]** and basic corpuscular physics [2, 3] is applied to rotating flow configuration simulating the Stirling engine [3]**.** However, mathematical simplicity of the model facilitates its manifold applications not only in micro and standard macro, single- and multiphase flows in engineering but in biology, medicine and interdisciplinary sciences as well. As **Dynamics of disperse systems** [14 - 20] it promotes the **common physical background** of multiple, apparently unrelated phenomena **[1-6, 12–20]**.

Main features of the method [12 – 20] compared with [1, 5] are:

- **no differential notation where possible**, aiming at conditions in defined volumes (particles) or on surfaces instead of imaginary conditions at points. Physical quantities are determined at required scale by choice of the reference volumes/surfaces and use of the mean value theorem (MVT) of integral calculus [10] where required. Compared with methods based on Navier-Stokes equations the method is applicable to discrete particles, saves one integration step and facilitates the analysis considerably.
- **Newton's second law is explicit equation of motion instead of** Navier-Stokes eqs. [4], Bernoulli eq. etc. [20]. Newton's law and conservation laws are applied to non-relativistic motion of particle systems in the range from individual particles, atoms, molecules or even electrons [3], over to macroscopic particle sets in solid or flowing systems of traditional mechanics [1, 5], up to celestial bodies of classical astro-physics [6]. Newton 's law used as equation of motion reads [12 - 20]:

$$\underline{F} = \frac{d}{dt}\int_V \rho \underline{v}\, dV \qquad (1)$$

Equation (1) defines gravity, similarly as electrostatic forces in micro or macroscopic systems [3, 6, 14 - 20] in terms of enforced changes of the state of motion. Pressure or friction forces in macroscopic systems are derived as results of averaged multiple molecular interactions [14, 20]. Conservation laws are written as [1, 14 - 20] e.g.:

$$\frac{d}{dt}\int_V \rho \underline{v}\, dV = \frac{\partial}{\partial t}\int_V \rho \underline{v}\, dV + \int_A \rho \underline{v}\ \underline{v} \bullet \underline{dA} \qquad (2)$$

The outlined microfluidic model was used to analyse motions of individual atoms (molecules) [19, 20] and to derive all definitions and equations of standard **continuum fluid mechanics and multiphase flows** such as: pressures, temperature, viscosity, heat conduction coefficients, Bernoulli equation, Navier-Stokes equations [14 - 20], diffusion coefficients [12, 11], flows through porous media or in fluidized beds [13, 14, 16 - 20] or in machines [16, 17, 20]. It allows analysis of approximations in Navier-Stokes equations [4, 20] as well as in other standard definitions and equations [20].and may be applied to motions of matter in micro- or macroscopic systems..

Current work concerns the title, subatomic applications, unsteady flows, non-Newtonian effects due to "viscous heating" [17, 20] etc.

[1] Hughes, W.F.; Brighton, J.A.; Fluid Dynamics; Schaum´s Outline Series in Engineering; McGraw-Hill Book Co.; 1967
[2] Reif, F.; Statistical Physics; McGraw-Hill Book Company; 1967
[3] Resnick, R; Halliday, D.; Physics; J. Wiley and Sons, Inc.; 1966
[4] Fefferman; Ch.; L.; Existence and smoothness of the Navier-Stokes equation; Princeton; NJ 08544-1000; 2000
[5] Hirsh, C.; Numerical Computation of Internal and External Flows; Elsevier; 2007
[6] Hoyle; F; Astronomy and Cosmology; Freeman and Co.; 1975
[10] Marsden,J.E.; Tromba, A.J.; Vector Calculus; Freeman and Co.; 1976
[11] Krol, M.; Experimentelle Untersuchung der Partikelbewegung bei hohen Feststoffkonzentrationen in turbulenten Mehrphasenströmungen; Phd. Thesis; University of Kaiserslautern; 1984
[12] Krol, M.; Prediction of relative particle fluid displacements in flowing suspensions at medium particle volume fractions by means of a simple stochastic model; 4th Miami Int. Conf. on: Multiphase Transport and Particulate Phenomena; Miami, USA; 1986; Multi-Phase Transport and Particulate Phenomena; Vol. 4; Hemisphere Publishing Corporation and Springer Publishing House (1988).
[13] Krol, M.: Pressure drop in porous media at arbitrary Reynolds numbers; European Aerosol Conference; Helsinki; Sept. 1995;
[14] Krol, M.: Fluiddynamik – Dynamik disperser Systeme; 1997/98
[15] Król, M.: Equation of Motion of a compressible Fluid derived from the Kinetic Theory of Gases and Newton's Second Law; Reports of the Polish Academy of Sciences; IMP PAN Rep. No. 3195/2003 and IMP PAN Rep. No. 3197/2003
[16] Król, M.; Physics of solids, liquids and gases; Lectures (GSW); Poland; 2005 - 2010
[17] Krol, M.; Physikalische Grundlagen der Ein- und Mehrphasen-Strömungen; Lectures at Technical University of Berlin; Germany 2006 - 2013
[18] Krol, M.: Momentum Exchange as common physical background of a transparent and physically coherent description of Transport Phenomena; Begell House Inc. Proceedings of the International Symposium "Turbulence, Heat and Mass Transfer 6";2009.
[19] Krol, M.; Significance of the microfluidic concepts for the improvement of macroscopic models of transport phenomena; paper with appendix submitted to the 3rd Micro and Nano Flows Conference, Thessaloniki, Greece; 2011. By courtesy of Brunel University, UK in internet under: michael_krol48
[20] Krol, M.; http://bookboon.com/de/studium/ingenieurwesen/ dynamik-disperser-systeme; 2012

4th Micro and Nano Flows Conference
UCL, London, UK, 7-10 September 2014

Flow measurement using micro-PIV within evaporating sessile drops of self-rewetting mixtures

Khellil Sefiane[1]*, John R.E. Christy[1], Johan C. Ebeling[1], Tobias Seewald[1], Souad Harmand[2]
* Corresponding author: Tel.: ++44 (0)131 6504873; Fax: ++44 (0)131 6506551; Email: ksefiane@ed.ac.uk
1 School of Engineering, The University of Edinburgh, King's Buildings, Edinburgh, EH9 3JL, UK
2 ENSIAME, Université de Valenciennes, France

Keywords: Evaporation, Marangoni, micro-PIV, Flow.

Recently interest has arisen in the use of so-called self-rewetting mixtures for micro-scale heat transfer systems. Such fluids, in which the surface tension can increase with increasing temperature, are expected to offer superior performance by extending the region of operation before dry-out of the heated surface sets in. Whilst improved performance has been shown in some practical situations using these fluids, it is not entirely clear as to the mechanism of such improvements.

We have studied the flow within evaporating sessile drops of 1-pentanol-water mixtures using micro-PIV and have observed three stages in the evaporation process. During the first stage there appears to be a single toroidal vortex with flow inwards along the base of the drop. The vortex only occupies the central region of the drop and appears to pulsate, reducing in size during evaporation, Figure 1. This is followed by a second transition stage to a third stage in which the flow is directed radially outward, as observed by us for pure water droplet evaporation and in the latter stages of ethanol/water drop evaporation. Temperature measurements, using IR thermography suggest that the initial stage of evaporation may be controlled by thermal Marangoni effects as opposed to the concentration driven Marangoni flows postulated for ethanol-water mixtures.

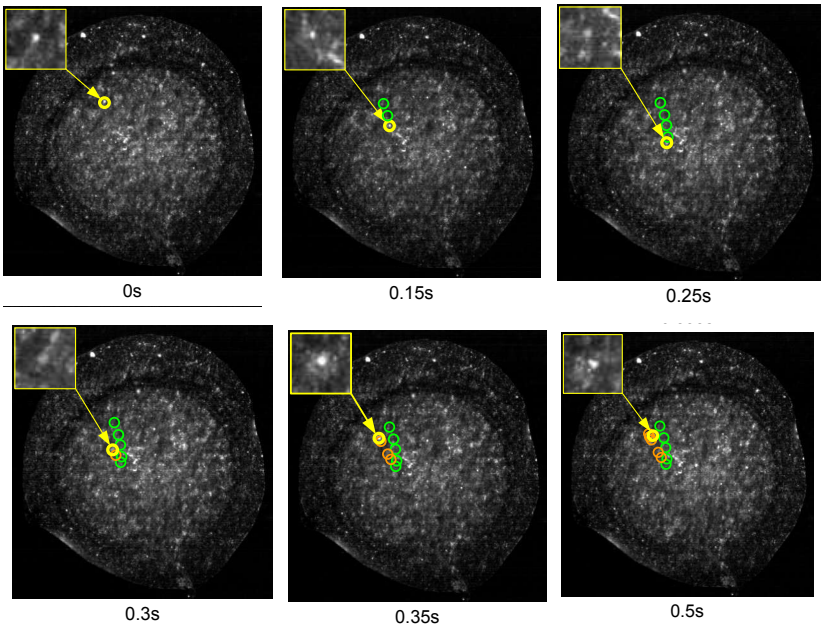

Figure 1. *The track of one particle for one rotation within the vortex*

4th Micro and Nano Flows Conference
UCL, London, UK, 7-10 September 2014

Three-dimensional simulation of cavitating flow in real journal bearing geometry

Marcus SCHMIDT [1,*], Peter REINKE [1], Matthias NOBIS [1], Marco RIEDEL [1]

* Corresponding author: Tel.: ++49 (0)375 536 3893; Fax: ++49 (0)375 536 3393; Email: marcus.schmidt@fh-zwickau.de
[1] Institut für Kraftfahrzeugtechnik, Westsächsische Hochschule Zwickau, GERMANY

Keywords: Micro Flow, Journal Bearing, Cavitation, CFD

Hydrodynamic journal bearings are commonly used in many technical applications because they provide low friction and minimal wear. In general, flow simulation during the engineering design process is carried out by means of the Reynolds equation. The Reynolds equation is a non-linear two-dimensional differential equation, which is based on the pressure and the gap between shaft and bushing in relation to bearing clearance, eccentricity, bushing deformation and load. If this flow model is integrated in a FEM-model of the entire engine is becomes a fast and very efficient tool for the development engineer for defining main bearing properties. However, due its two-dimensional nature it must fail where the lubricant flow inside the bearing becomes three-dimensional e.g., in the vicinity of feed holes or grooves. Moreover, in flow regions where the pressure drops locally below the vapor pressure of the lubricant gas bubbles are generated which in turn change the flow field forming three-dimensional structures. These complex and fully three-dimensional 2-phase flows can only be described with appropriate numerical models based on the Navier-Stokes equations including a cavitation model. The work on hand presents the numerical approach and the cavitation model based on the Rayleigh-Plesset equation. Moreover, a bearing flow experiment was designed and constructed with the goal to validate numerical results. The experimental set-up is a model of a real bearing at a 3:1 scale constructed in translucent acrylic plastic. Reynolds and mechanical similarity rules are observed. The scaled experiment allows measurements of velocity profiles inside the fluid film across the gap between rotor and housing. The measurements were carried out by means of Laser Doppler Velocimetry (LDV).
Finally, the validated 3D simulation model is applied on a real bearing, which was subject to an experimental investigation targeting cavitation. The numerical results include images of complex three-dimensional flow structures, vortices and vapor distributions. These three-dimensional results are compared with conventional 2D-data based on the Reynolds equation. In the test case the two-dimensional approach gives wrong information in 2 out of 6 critical regions pertaining cavitation failing in both, over- and under-prediction of cavitation. Whereas, the results computed with the three-dimensional model show excellent agreement with the experimental data. In summary, a new numerical model expands the scope for the numerical simulation of the lubricant flow in hydrodynamic journal bearings and improves the prediction of cavitation.

4th Micro and Nano Flows Conference
UCL, London, UK, 7-10 September 2014

Transport properties of fluids in hydrophobic/hydrophilic nanochannels

Filippos SOFOS, Theodoros E. KARAKASIDIS*, Antonios E. GIANNAKOPOULOS and Antonios LIAKOPOULOS

* Corresponding author: Tel.: +302421074163; Fax: +302421074125; Email: thkarak @uth.gr
Department of Civil Engineering, School of Engineering, University of Thessaly, Volos, GR

Keywords: Nano flows, Diffusion Coefficient, Shear Viscosity, Wettability

When downsizing towards the nanoscale, system dimensions have been found to affect channel flows mainly because of the presence of the walls that interact strongly with fluid particles. Parameters which are not taken into account at the classical theory continuum theory at the macroscale, should be taken into account at the nano or even micro-scale where the surface to volume ratio increases significantly. Such property is the wall/fluid interaction which determines the wetting (hydrophilic behavior) or not (hydrophobic behavior) of a surface.

1 Introduction

During the past decades, terms like super- or ultra- hydrophobic surfaces have been incorporated in order to describe hydrophobic surfaces, those where the contact angle between the fluid and the surface is greater than 150^o (Tsai et al. 2009).

Slip length is a quantity used to quantify hydrophobicity at the micro- or nano-scale. Both experiment and theoretical approaches have revealed that in channel flows past a microchannel with hydrophobic walls, due to reduction in the surface contact area between the flowing liquid and the solid wall, dramatic decrease in the overall flow resistance was observed (Neto et al. 2005). A popular simulation method for nanofluidics which is based on Newton's equations of motion and calculates interactions in the atomic/molecular level is Molecular Dynamics (MD) (Sofos et al. 2013).

2 Molecular Dynamics Method

In this work, we employ MD in order to carry out simulations for flat-wall nanochannels, which correspond to macroscopic Poiseuille flow. The system is periodic along the *x*- and *y*- directions, while the distance between the two plates is h=6.3nm. Atomic interactions between fluid particles are described by Lennard-Jones 12-6 type potentials $u^{LJ}(r_{ij}) = 4\varepsilon((\sigma / r_{ij})^{12} - (\sigma / r_{ij})^{6}$.

A qualitative wall wettability parameter representing hydrophobic or hydrophilic behavior is $\varepsilon_w/\varepsilon_f$ (*w*: wall, *f*: fluid). Assigning a value $\varepsilon_w/\varepsilon_f \geq 1$ represents an hydrophilic wall, while $\varepsilon_w/\varepsilon_f < 1$ represents an hydrophobic one. In order to qualify for wall wettability effects on flow, we consider values in the range $0.2 < \varepsilon_w/\varepsilon_f < 5.0$.

3 Simulation Results

Starting from a strongly hydrophobic wall ($\varepsilon_w/\varepsilon_f = 0.2$) we observe that fluid atoms are not attracted by the wall, but, as the hydrophobic character of the surface decreases and hydrophilicity increases, more fluid atoms are located closer to the wall as we can see from the radial distribution function calculated. For the most hydrophilic walls studied ($\varepsilon_w/\varepsilon_f = 2.0$ and 5.0) fluid atoms are located closer to the wall, presenting strong inhomogeneity.

Transport properties, such as the diffusion coefficient and shear viscosity, are very important in the understanding of mass and energy flow in channel flows. Based on relations from statistical thermodynamics (Sofos et al. 2009; Giannakopoulos et al. 2012) we calculated diffusion coefficient and shear viscosity values in layers along the nanochannel. The diffusion coefficient is affected by wall wettability in the two layers adjacent to the wall, attaining smaller than bulk values for small hydrophobicity ratios, and, in parallel, increasing average value as hydrophilicity increases. In the strongly hydrophobic channel ($\varepsilon_w/\varepsilon_f = 0.2$), diffusion coefficient values near the wall are greater than the bulk and even the inner channel values are affected (smaller than the bulk).

On the other hand, we observe that shear viscosity presents inverse behavior to diffusion coefficient. The adjacent to the wall layer is of great importance now, regarding minimization of the flow resistance. Minimum shear viscosity is calculated near the wall for the hydrophobic channels, while shear viscosity values are greater than the bulk past an hydrophilic wall.

4 Conclusion

Summarizing, in this work it was found that the effect of parameters that are taken into account only at the nanoscale, such as wall hydrophobicity or hydrophilicity, can significantly affect the flow and should be incorporated in theoretical studies and technological applications, for the design of smart surfaces, elimination of friction and lubrication, drug delivery and more.

Acknowledgement

Project implemented under the "ARISTEIA II" Action of the "OPERATIONAL PROGRAMME EDUCATION AND LIFELONG LEARNING", co-founded by ESF and National Resources.

References

Giannakopoulos, A.E., Sofos, F., Karakasidis, T.E., Liakopoulos, A., Int. J. Heat Mass Trans. 55, 5087 (2012).

Neto, C., Evans, D.R., Bonaccurso, E., Butt, H.-J., Craig, V.S.J., Rep. Prog. Phys. 68, 2859 (2005).

Sofos, F., Karakasidis, T.E., Liakopoulos, A., Int. J. Heat Mass Trans. 52, 735 (2009).

Sofos, F., Karakasidis, T.E., Liakopoulos, A., J. Comp. Theor. Nanosci. 10, 1 (2013)

Tsai, P., Peters, A.M., Pirat, C., Wessling, M.M., Lammertink, R.G.H., Lohse, D., Phys. Fluids 21, 112002 (2009).

4th Micro and Nano Flows Conference
UCL, London, UK, 7-10 September 2014

A New Heterogeneous Multiscale Technique for Microscale Gas Flows

Stephanie Y. DOCHERTY [1,*], Matthew K. BORG [1], Duncan A. LOCKERBY [2], Jason M. REESE [3]

* Corresponding author: Email: stephanie.docherty@strath.ac.uk
1 Department of Mechanical and Aerospace Engineering, University of Strathclyde, UK
2 School of Engineering, University of Warwick, UK
3 School of Engineering, University of Edinburgh, UK

Keywords: Multiscale Simulation, Hybrid, DSMC, Field-wise Coupling, Rarefied Gas Dynamics

While the conventional hydrodynamic equations are generally excellent for modelling the majority of fluid flow problems, the presence of localised regions of thermodynamic non-equilibrium can result in some degree of inaccuracy. Such regions appear, for example, when there are large gradients in fluid properties, or when surface effects become dominant (as in micro- or nanoflows). Although molecular simulation tools can provide an accurate modelling alternative in these cases, they are much too computationally expensive for resolving engineering spatial and temporal scales. Combining the computational efficiency of continuum methods with the accuracy of molecular treatments, multiscale 'hybrid' techniques have been a focus of intensive research over the past decade.

In this paper we report a new hybrid method for dilute gas flows that couples a continuum-fluid description to the direct simulation Monte Carlo (DSMC) method. To date, the development of continuum/DSMC hybrids has focused mainly on domain-decomposition techniques such as those considered by Hash and Hassan (1996). However, a fundamental disadvantage of domain-decomposition is that, to see any increase in efficiency over a pure DSMC simulation, the non-equilibrium flow must be confined to 'near-wall' regions. We therefore use a heterogeneous multiscale framework, which overcomes this limitation by adopting a micro-resolution approach that can be employed anywhere in domain; near walls, or in the bulk of the flow. A continuum-fluid model is applied across the entire domain, while the molecular solver (i.e. DSMC in our case) is applied in spatially-distributed micro regions. Our method is a version of the field-wise coupling (HMM-FWC) approach originally developed by Borg et al. (2013) for dense fluids: rather than providing a correction to a node on the continuum mesh, each micro element provides a correction to a continuum sub-region, the dimensions of which are identical to the micro element itself. This HMM-FWC is suitable for flow problems with varying degrees of scale-separation, and the location of the micro elements is not restricted by the nodes of the computational mesh.

In our hybrid, the coupling itself is performed through the computed momentum- and/or heat-fluxes. The method is demonstrated for test cases of micro Fourier and micro Couette flow, over a range of conditions. Our results show that the hybrid method can deal with both missing constitutive and boundary information, while remaining simple enough for validation against an equivalent full-scale DSMC simulation.

References

Hash, D.B., Hassan, H.A., 1996. Assessment of schemes for coupling Monte Carlo and Navier-Stokes solution methods. J. Thermophys Heat Transfer. 10, 242–249.

Borg, M. K., Lockerby, D. A., Reese, J. M., 2013. Fluid simulations with atomistic resolution: a hybrid multiscale method with field-wise coupling. J. Comput. Phys. 255, 149 – 165.

4th Micro and Nano Flows Conference
UCL, London, UK, 7-10 September 2014

A Molecular Dynamics Study of Proton Hopping in Nafion Membrane

Takuya MABUCHI [1,*] and Takashi TOKUMASU [2]

* Corresponding author: Tel.: +81 (0)22 2175292; Fax: +81 (0)22 2175239; Email: mabuchi@nanoint.ifs.tohoku.ac.jp
1 Graduate School of Engineering, Tohoku University, JAPAN
2 Institute of Fluid Science, Tohoku University, JAPAN

Keywords: Membranes, Fuel Cells, Proton Transport, Water Clusters

Polymer electrolyte fuel cells (PEFCs) are highly expected as a next-generation power supply system due to the purity of its exhaust gas, its high power density and high efficiency. The heart of PEFCs is polymer electrolyte membrane (PEM) that separated the reactant gases and conducts protons. Perfluorosulfonic acid Membranes, such as Nafion developed by DuPont, are the most widely used for PEM. In the nanoscopic structure of the membrane, ion clusters are formed by water molecules gathered vicinity of sulfonate groups which are hydrophilic parts of Nafion membrane, and protons transport inside of these water aggregations. The molecular level structure and transport mechanism of protons are important factors contributing to dynamic properties of protons in the membrane. Thus, it is critical to understand an important link between Nafion membrane nanostructure and the dynamics of water molecules and hydronium ions to enhance proton transport. In Nafion membranes, it is considered that proton hopping takes place although the water dynamic property in the bulk aqueous solution is inhibited by a lack of bulklike water structure at low water contents. However, the correlation between the Grotthuss mechanism and Vehicular mechanism components of proton diffusion in Nafion is yet to be clearly understood.

In this study, a revised empirical valence bond (EVB) model has been developed based on the previous study of EVB model reported by Walbran et al. [1] and in order to improve the description of proton mobility in both aqueous and Nafion environments. The new EVB model shows a larger proton diffusion coefficient, which is 0.69 ± 0.005 Å^2/ps and is within ~27% of the experimental value of 0.94 ± 0.01 Å^2/ps [2], than previous models of multistate EVB [3, 4] in the bulk water system. The calculated result of MSDs of the hydronium ion and water molecules in bulk aqueous solution are shown in Fig. 1. The result of hopping rate considered both the forward-hop to the new donor and backward-hop to the last donor also indicates a larger value of 0.46 ps^{-1} compared with the value of 0.16 ps^{-1} in the previous work [4]. In addition, we have applied the new EVB model to Nafion system and performed an atomistic analysis of the transport of hydronium ions and water molecules in the nanostructure of hydrated Nafion membrane by systematically changing the hydration level. After annealing procedure, the simulated density agreement with experiment is within 5.7 % for various water contents and the trends that density decreases with increasing hydration level are reproduced. A snapshot of water aggregation in Nafion membrane in our simulation is shown in Fig. 2. It is found that a large contribution of the Grotthuss mechanism for the diffusion of hydronium ions has been found at high water contents and this testifies the important impact of the diffusion with the Grotthuss mechanism in the membrane as well as in the bulk aqueous solutions.

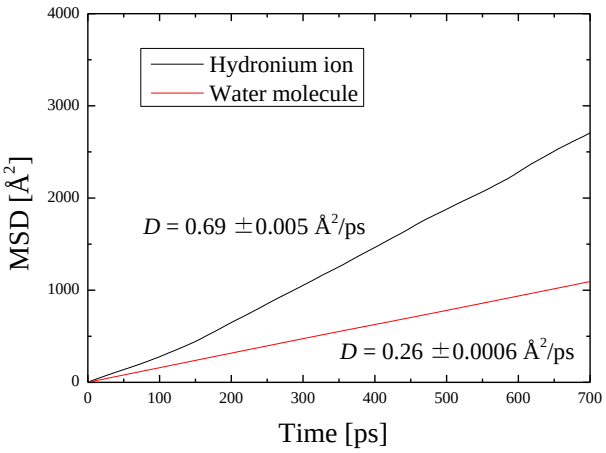

Fig. 1 MSDs of the hydronium ion and water molecules in bulk aqueous solution.

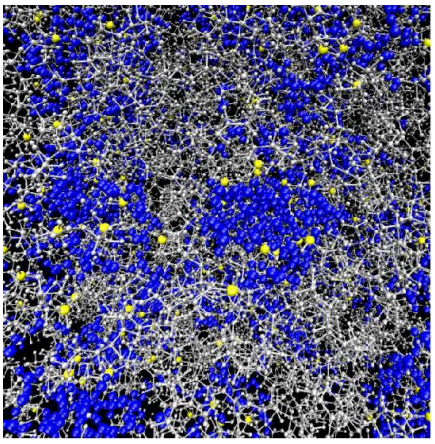

Fig. 2 Snapshot of water aggregations (in blue) and S of sulfonate groups (in yellow) in Nafion membrane at λ = 6.

References

[1] S. Walbran, A. A. Kornyshev, *J. Chem. Phys.* **2001**, *114*, 10039.
[2] N. K. Roberts, H. L. Northey, *Journal of the Chemical Society-Faraday Transactions I* **1974**, *70*, 253.
[3] K. Park, W. Lin, F. Paesani, *J. Phys. Chem. B* **2012**, *116*, 343.
[4] Y. J. Wu, H. N. Chen, F. Wang, F. Paesani, G. A. Voth, *J. Phys. Chem. B* **2008**, *112*, 467.

4th Micro and Nano Flows Conference
UCL, London, UK, 7-10 September 2014

Kinetic calculation of rarefied gaseous flows in long tapered rectangular microchannels

Lajos SZALMAS [1,*]

* Corresponding author: Tel.: ++49 (0)421 218 63495; Email: lszalmas@gmail.com
1 Center for Environmental Research and Sustainable Technology (UFT), University of Bremen, Germany

Keywords: Rarefied Gas Flows, Tapered Microchannels, Kinetic Calculation, BGK equation

Gaseous flows in microsystems have attracted considerable attention in fluid dynamic communities over the last few years. When the size of the device is in the range of microns, the molecular mean free path becomes comparable with the device size, and the details of the molecular interactions need to be taken into account. The proper description of such microflows requires the consideration of the velocity distribution function of the molecules and kinetic equations. The scope of the present paper is to discuss the determination of the behavior of pressure driven rarefied gas flows in microchannels at the kinetic level. As a new application of the methodology, preliminary results are presented for pressure driven flows of single gases through long rectangular tapered microchannels, which have constant widths but varying depths along the axis of the channel. The kinetic calculation is based on the solution of the linearized Bhatnagar-Gross-Krook (BGK) equation and refers to the determination of the mass flow rate through the channel and the axial distribution of the pressure. The BGK equation is solved by the discrete velocity method. It is shown that the mass flow rate exhibits the diodicity effect, which means that the flow rate depends on the orientation of the channel. If the gas flows from the larger cross section towards the smaller one, the flow rate is larger than in the opposite situation. The pressure profile strongly varies near the small cross section, and it has a quite different character than in the case of channels with uniform cross sections. The tapered microchannel might be useful for separating the different gaseous components in engineering applications.

4th Micro and Nano Flows Conference
UCL, London, UK, 7-10 September 2014

Ion drag EHD micropump with single walled carbon nanotube (SWCNT) electrodes

Md. Kamrul RUSSEL, P. Ravi SELVAGANAPATHY, Chan Y. CHING *

* Corresponding author: Tel.: +1 905 525 9140; Fax: +1 905 572 7944; Email: chingcy@mcmaster.ca (Chan Y. CHING)
Department of Mechanical Engineering, McMaster University, Canada

Keywords: Micropump, SWCNT, Pressure Head

Microelectronics thermal management in many applications requires novel active cooling methods with higher cooling capacity as typical passive techniques, such as the use of heat pipes, carbon foams or commonly used active techniques, such as forced convective cooling can be inadequate due to the increasing trend towards higher circuit packaging density. High performance chips are projected to dissipate over 360W by 2018 while still operating below their typical safe design temperature of 100 °C [1]. Among various active cooling techniques, microchannel liquid cooling is promising and has been shown to achieve a cooling capacity as high as 1 kWcm-2 [2]. A novel cooling approach for electronic devices would be to integrate a micropump with the microchannel heat sink within the processor chip. This would require adequate pumping of the cooling fluid to achieve the required flow rates. Among various available micropumps, the ion drag electrohydrodynamic (EHD) micropump is particularly promising due to its small form factor, low power consumption, ability to work with dielectric heat transfer fluids, good controllability and absence of any moving parts.

Ion drag EHD micro-pumps have been studied under different operating conditions and the pressure generated is reported to have a quadratic dependence on the applied electric field [3-5]. The electric field in a device with given electrode material, configuration and geometry depends further on the applied potential and electrode surface topology. Asymmetry between the emitter and collector electrodes in a micropump has shown to enhance the charge injection within the dielectric liquid [6, 7] which allows the pump to operate at a much lower applied potential with better pressure head. The asymmetry and pump performance can be further enhanced by incorporating micro/nano features with sharp asperities on the electrodes as it reduces the work function of the electrode [8] and thus reduces the energy barrier between the working fluid and the electrode material. The objective of this work is to investigate the charge injection and pressure characteristics in HFE 7100 of micropumps with different electrode surface topology.

The micropumps had 100 pairs of planer electrodes with the emitter electrodes having half the width of the collector electrodes (40 µm). The microchannel height was 100 µm. Details of the fabrication process can be found in [7], which produced electrodes with atomically smooth surfaces. SWCNT was electrophoretically deposited onto the emitter electrodes following the technique of Gao et al. [9]. Experiments were performed with both smooth and SWCNT deposited on patterned gold electrodes. The charge injection and pressure head was significantly higher for the pumps with SWCNT deposited electrode when compared to the no deposition case, which are shown in Fig. 1 and 2. The threshold voltage required for the onset of charge injection is less for the pumps with SWCNT electrode than for the smooth electrode pumps (Fig. 1). The slope is steeper, which indicates a higher charge injection for the pumps with SWCNT electrodes. This resulted in a significantly higher pressure (Fig. 2) when compared to the pump with no deposition.

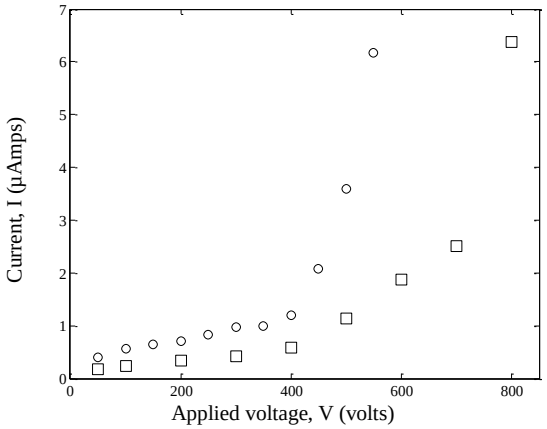

Fig. 1: I-V characteristics of planer µ-pump (○ without deposition, □ SWCNT deposited on emitter electrodes)

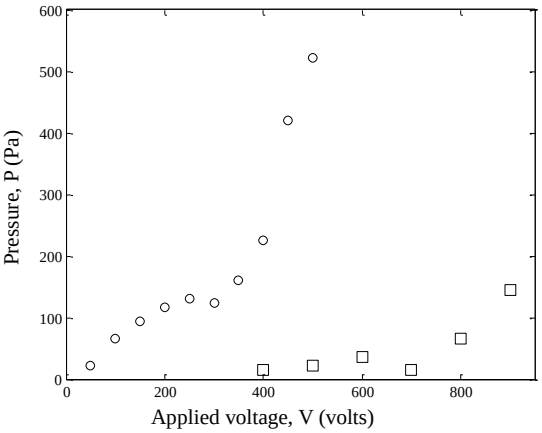

Fig. 2: Static pressure at different applied voltage of planer µ-pump (○ without deposition, □ SWCNT deposited on emitter electrodes)

1. DTI, *Developments and trends in thermal management technologies-a mission to USA.* report of a DTI global watch mission, 2006.
2. Jiang, L., M. Wong, and Y. Zohar, *Forced convection boiling in a microchannel heat sink.* Microelectromechanical Systems, Journal of, 2001. **10**(1): p. 80-87.
3. Pickard, W.F., *Ion drag pumping. II. Experiment.* Journal of Applied Physics, 1963. **34**(2): p. 251-258.
4. Coletti, G. and R. Bozzo. *A contribution to the evaluation of electrohydrodynamic pumps for insulating oils.* in *Electrical Insulation and Dielectric Phenomena, 1996. IEEE 1996 Annual Report of the Conference on*. 1996: IEEE.
5. Ahn, S.-H. and Y.-K. Kim, *Fabrication and experiment of a planar micro ion drag pump.* Sensors and Actuators A: Physical, 1998. **70**(1): p. 1-5.
6. Darabi, J., et al., *Design, fabrication, and testing of an electrohydrodynamic ion-drag micropump.* Microelectromechanical Systems, Journal of, 2002. **11**(6): p. 684-690.
7. Kazemi, P.Z., P.R. Selvaganapathy, and C.Y. Ching, *Electrohydrodynamic micropumps with asymmetric electrode geometries for microscale electronics cooling.* Dielectrics and Electrical Insulation, IEEE Transactions on, 2009. **16**(2): p. 483-488.
8. Xue, M., et al., *Understanding of the correlation between work function and surface morphology of metals and alloys.* Journal of Alloys and Compounds, 2013.
9. Gao, B., et al., *Fabrication and electron field emission properties of carbon nanotube films by electrophoretic deposition.* Advanced materials, 2001. **13**(23): p. 1770-1773.

4th Micro and Nano Flows Conference
UCL, London, UK, 7-10 September 2014

Optimal microscale water cooled heat sinks for targeted alleviation of hotspot in microprocessors

Chander Shekhar SHARMA [1], Manish K. TIWARI [2], Dimos POULIKAKOS [1,*]

* Corresponding author: Tel.: +41 44 632 27 38; Fax: +41 44 632 11 76; Email: dpoulikakos@ethz.ch
1: Department of Mechanical and Process Engineering, ETH Zurich, 8092 Zurich, Switzerland
2: Department of Mechanical Engineering, University College London (UCL), Torrington Place, London WC1E 7JE, UK

Keywords: Microchannels, Hotspot-targeted cooling, Electronics cooling, Hotspots

Hotspots in microprocessors arise due to non-uniform utilization of the underlying integrated circuits during chip operation. Conventional liquid cooling using microchannels leads to undercooling of the hotspot areas and overcooling of the background area of the chip resulting in excessive temperature gradients across the chip. These in turn adversely affect the chip reliability, cause mechanical stresses at the chip–substrate and chip–heat sink interfaces and result in circuit imbalances. This problem becomes even more acute in multi-core processors where most of the processing power is concentrated in specific regions of the chip called as cores. We present an analytical method for quick design and optimization of a microchannel heat sink for targeted cooling of hotspots in water cooled microprocessors. The method utilizes simplifying assumptions and analytical equations to arrive at the first estimate of a microchannel heat sink design that distributes the cooling capacity of the heat sink by adapting the coolant flow and microchannel size distributions to the microprocessor power map. This distributed cooling in turn minimizes the chip temperature gradient. The method is formulated to generate a heat sink design for an arbitrary chip power map and hence can be readily utilized for different chip architectures. It involves optimization of microchannel widths for various zones of the chip power map under the operational constraints of maximum pressure drop and pumping power limit for the heat sink. Additionally, it ensures that the coolant flows uninterrupted through its entire travel length consisting of microchannels of varying widths. The resulting first design estimate significantly reduces the computational effort involved in any subsequent CFD analysis required to fine tune the design for more complex flow situations arising, for example, in manifold microchannel heat sinks.

4th Micro and Nano Flows Conference
UCL, London, UK, 7-10 September 2014

Constant depth microfluidic networks based on a generalised Murray's law for Newtonian and power-law fluids

Konstantinos ZOGRAFOS [1,*], Robert W. BARBER [2], David R. EMERSON [2], Mónica S. N. OLIVEIRA [1]

* Corresponding author: Tel.: +44 (0) 1415745051; Email: konstantinos.zografos@strath.ac.uk
1 James Weir Fluids Laboratory, Department of Mechanical and Aerospace Engineering, University of Strathclyde, G1 1XQ, Glasgow, UK
2 Centre for Microfluidics and Microsystems Modelling, STFC Daresbury Laboratory, Daresbury, Warrington, UK

Keywords: Microfluidics, Non-Newtonian fluids, Murray's law, Biomimetics, Bifurcating networks

In this work, we study numerically the flow of Newtonian and power-law fluids through microfluidic bifurcating networks of rectangular cross-section and constant depth inspired by the biomimetic principle of Murray's law.[1] The original relationship governing the optimum ratio between the diameters of the parent and daughter vessels established by Murray is valid for networks with circular cross-section and has recently been extended[2] to consider other arbitrary cross-sections that are typical of lab-on-a-chip applications. We use an in-house code to perform computational fluid dynamics calculations to assess the extent of the validity of the proposed design for Newtonian, shear-thinning and shear-thickening fluids under different flow conditions.

1 Background

The ideal relationship for the ratio between the diameters of the parent and daughter branches throughout the arterial system was first discussed by Murray, based on the principle of minimum work.[1] Murray's law was originally derived for channels of circular cross section and states that the cube of the diameter of the parent vessel, equals the sum of the cubes of the diameters of the daughter vessels. Barber and Emerson[2] adapted the underlying biomimetic principle to extend this relationship to rectangular and trapezoidal shaped symmetric bifurcations of constant depth as illustrated in Figure 1. The suggested design methodology can be used to create micro-channels using typical fabrication processes, such as photo- and soft-lithography and etching, based on the hydraulic diameter D_h and the Poiseuille number, *Po*, of the desired channel.[2]

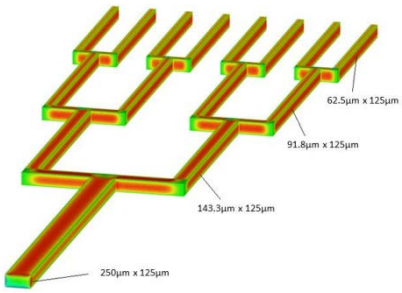

Figure 1: Wall shear stress distribution along the microfluidic network ($\alpha_0 = 0.5$; $X = 1$). Red corresponds to the maximum wall shear stress and green to zero.

Considering a symmetric system, the volumetric flow rate halves at each bifurcation and it can be shown that when $\alpha_i(1+\alpha_i)Po(\alpha_i^*) = (2X)^i \alpha_0(1+\alpha_0)Po(\alpha_0^*)$,[2] the shear stresses obey the following relationship $\bar{\tau}_i = \bar{\tau}_0 X^i$, where $\bar{\tau}_0$ and $\bar{\tau}_i$ are the mean shear stresses acting on the wetted perimeter of the parent and daughter channels (with the subscript i representing the i^{th} generation), respectively; $\alpha_i = d/w_i$ is the ratio of depth to the width for each channel generation; and X is the so called branching parameter. When $X = 1$, Murray's law is obeyed and the average wall shear stresses are homogeneous along the bifurcating network. By changing the branching parameter, this methodology offers a control function that can be used to design microfluidic distribution systems.

2 Numerical Techniques

We consider incompressible and isothermal, non–Newtonian fluid flow and solve the continuity and the momentum equations together with a constitutive equation for the stress-strain relationship. In our work, we use the power-law model, which describes the viscosity as a function of the shear rate such that $\eta(\dot{\gamma}) = K\dot{\gamma}^{n-1}$. Depending on the values of the power-law index n, the fluid is considered to be shear thickening ($n > 1$), shear thinning ($n < 1$), or Newtonian ($n = 1$).
The set of equations describing the flow are solved with an in-house numerical code based on a fully implicit finite volume method using collocated meshes.[3] The convective terms are discretised using high resolution interpolating schemes while for the diffusive terms a first order Euler implicit scheme is employed to discretise the time-dependent terms.

3 Overview of the Results

The examination of the biomimetic principle of Murray's law is achieved using a series of computational fluid dynamics simulations, considering non-Newtonian fluid flow inside rectangular shaped ducts of constant depth (d = 125 μm) and a parent channel width of 250 μm (Figure 1), for different branching parameters X. We consider a power-law fluid with density ρ = 1000 kg m^{-3}and consistency index $k = 10^{-3}$ N s^{n}m^{-2}. Initially, creeping flow conditions (Reynolds number, $Re \rightarrow 0$) are examined for different power-law indices within the range $0.2 \leq n \leq 3$. Tangential shear stress distributions and flow resistance along the microfluidic system are analysed for all cases and it was found that the biomimetic principle works well for Newtonian and power-law fluids when $\alpha_0 = 0.5$ and $X = 1$. A number of simulations using different *Re* were also performed to assess the flow characteristics and examine the limits of the validity of the biomimetic rule for power-law fluids under different flow conditions.

References

1. C.D. Murray, Proc Natl Acad Sci USA **12** (1926) 207-214
2. R. W. Barber, D. R. Emerson, Microfluid Nanofluid **4** (2008) 179-191.
3. P.J. Oliveira, F.T. Pinho, G.A. Pinto, J Non-Newtonian Fluid Mech **79** (1998) 1-43.

Acknowledgements

The numerical code used in this work was developed within CEFT and the authors are thankful for the development provided by Afonso, Alves, Pinho and Oliveira.

An experimental study of dynamic flow of nanofluid with different concentrations

Jiaju Hong[1], Paul Glover[2], Yuying Yan*
1 HVACR & Heat Transfer Research Group, Faculty of Engineering, University of Nottingham, UK
2 Sir Peter Mansfield Magnetic Resonance Centre, Physics and Astronomy, University of Nottingham, UK
*Corresponding to yuying.yan@nottingham.ac.uk, Tel: +44(0)1159513168

Abstract:

Current reported data of nanofluid concentration is almost all based on TEM observation, which is in a static situation. No data of dynamic concentration during flow is reported. In the present study, an experimental measurement based on nuclear magnetic resonance (NMR) of monitoring the dynamic concentrations of nanofluid flow is carried out. It is demonstrated that the ferrofluid with Fe_3O_4 as its nanoparticles coated with surfactant as a special type of nanofluid can be used as T2 contrast agent in NMR scanning as well as a magnetic and thermal sensitive nanoparticle solution that would enhance heat transfer.

Key words: nanofluid, dynamic concentration, NMR

The study of the influence of morphology anisotropy of clusters of superparamagnetic nanoparticle on magnetic hysteresis by Monte Carlo simulations

Rong Fu[1], Clive Roberts[2], Yuying YAN[1]*

*Corresponding author: Tel.: +44 (0) 115 951 3168; Fax: +44 (0) 115 95 13159;
Email: yuying.yan@nottingham.ac.uk
[1]Energy & Sustainability Research Division, Faculty of Engineering, University of Nottingham, University Park, Nottingham NG7 2RD, UK
[2]School of Pharmacy, University of Nottingham, University Park, Nottingham NG7 2RD, UK

ABSTRACT

Nowadays, extensive attentions have been focussed on the study of induction heating implanted magnetic nanoparticle under AC magnetic field for cancer hyperthermia treatment. Colloidal cluster composed of superparamagnetic nanoparticle has shown great potential for efficient hyperthermia heating. However, the relationship between cluster properties and heating efficiency is not clear. In this work, we investigate the influence of morphology anisotropy of cluster of superparamagnetic nanoparticle on magnetic hysteresis by Monte Carlo simulation. Five kinds of clusters with different shapes and structure are studied. We find that the morphology anisotropy of cluster changes the magnetic loss by affecting the tendency of cluster to remain magnetically aligned with the field orientation. A large aspect ratio of the length of cluster along the field orientation to the width perpendicular to the orientation can increase the amount of energy converted per cycle significantly. Lacking morphology anisotropy will make the magnetic hysteresis of cluster numb to the manipulation of cluster properties.

Keywords: hyperthermia; Superparamagnetic; dipole interaction; Monte Carlo; Cluster.

4th Micro and Nano Flows Conference
UCL, London, UK, 7-10 September 2014

Laminar Fluid Flow in Microchannels with Complex Shape

Maria B. ATMANSKIKH, Pavel T. ZUBKOV *, Olga V. RUSAKOVA

* Corresponding author: Tel.: +79123950810; Email: pzubkov@utmn.ru
Institute of Mathematics and Computer Sciences, Tyumen State University, Russia

Keywords: Laminar Flow, Microchannels, Viscosity, Numerical Simulation

Laminar flow of newton incompressible fluid with constant viscosity in system of channels (Fig.1) is considered. It's demonstrated that there are infinitely many stationary solutions with equal boundary conditions. Possible flow fields and ways of practical realization are studied. Solutions are investigated numerically, scheme of calculation is described partially in [1].

[1] Patankar S.V., *Numerical Heat Transfer and Fluid Flow. New York: Hemisphere*, **1980**, 200 p.

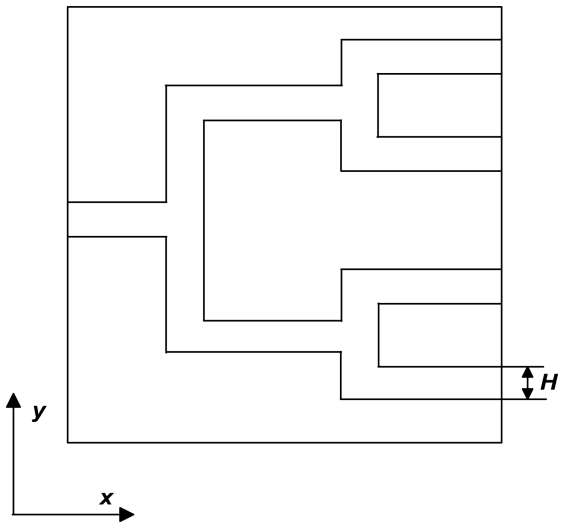

Fig. 1. Geometry of the channel

4th Micro and Nano Flows Conference
UCL, London, UK, 7-10 September 2014

Numerical study for magnetic fluid by lattice Boltzmann method

Wenning ZHOU, Yuying YAN*

* Corresponding author: Tel.: +44 (0)115 9513168; Email: yuying.yan@niottingham.ac.uk
HVACR & Heat Transfer Research Group, Faculty of Engineering, University of Nottingham, UK

Keywords: ferro-fluids, LBM

Magnetic fluids, also known as ferrofuids, are a particular class of colloidal suspensions of nanoscale ferromagnetic particles in a liquid carrier, which respond to the presence of an external magnetic field. These functional fluids show complex behaviour under the influence of an applied magnetic field. It has been a subject of intense research due to its overwhelming importance in wide range field. Over the last decade, lattice Boltzmann method (LBM), a meso-scope method based on discrete kinetic theory, has emerged as a powerful tool for the numerical investigation of a broad class of complex flows, including multiphase flows and multi-component flows. The LBM model has been recently extended to magnetic fluid. In this paper, we report two LBM models for magnetic fluid based on the scale investigated. In the first model, the effect of the external magnetic field on the flows will be investigated by employing a vector-valued particle distribution function into the LBM model. The evolution of the magnetic field can be then properly formulated in terms of a kinetic BGK like equation similar to Boltzmann's equation. The corresponding Lorentz force will be also incorporated into the LBM model. In order to investigate the particle-particle and particle-fluid interactions, a two-phase LBM model is presented. In this model, magnetic fluid is treated as a magnetic particle suspension. On the scale of interest to colloidal suspensions, Brownian motion, which is driven by fluctuations in the fluid stress tensor, becomes non-ignorable. The particle Brownian motion effect is included into this model based on fluctuation dynamics. At last, several simulation cases are conducted based on these two models. The results show that the lattice Boltzmann method could be a capable method for the simulation of complex magnetic fluid hydrodynamics.

4th Micro and Nano Flows Conference
UCL, London, UK, 7-10 September 2014

Gas recognition based on physiochemical parameters determined by monitoring diffusion rates in microfluidic channels

Ali Hooshyar Zare[1], Sobhan Erfantalab[1], Vahid Ghafarinia[2], Faramarz Hossein-Babaei[1*]

* Corresponding author: Tel.: ++98 (0) 21 88734172; Fax: +98 (0) 21 88768289; Email: fhbabaei@yahoo.com, fhbabaei@kntu.ac.ir
[1]Electronic Materials Laboratory, Electrical Engineering Department, K. N. Toosi University of Technology, Tehran 1635-1355, Iran
[2]Department of Electrical and Computer Engineering, Isfahan University of Technology, Isfahan, 84156-83111, Iran

Keywords: Microfluidics, Gas flow, Gas analysis, Langmuir parameter, Diffusivity

Abstract:
Monitoring the diffusion progress rates of different gases in a microfluidic channel affords their discrimination by the comparison of their temporal profiles in a high-dimensional feature space [1, 2]. Here, we demonstrate gas recognition by determination of their three important physiochemical parameters via a model-based examination of the experimentally determined diffusion rates in two different cross-section channels. The system utilized, schematically presented in Fig.1, comprises two channels with respective cross-sectional diameters of 1 mm and 50 µm. The open end of both channels are simultaneously exposed to the analyte, and the temporal profiles of the diffusion rates are recorded by continuous resistance measurements on the chemoresistive sensors spliced to the channels at the other end. Fitting the solutions of the diffusion equation to the experimental profiles obtained from the large cross-section channel results in the diffusivity of the analyte (D). The results of small cross-section channel, however, fit the solutions of a modified diffusion equation which accounts for the adsorption of the analyte molecules to the channel walls, as well. The latter fitting process results in the Langmuir parameter (b) for the analyte-channel wall interactions and the population of the effective adsorption sites on the unit area of the walls. The allocation of these three meaningful parameters to an unknown gas affords its recognition or discrimination from the other gases examined.

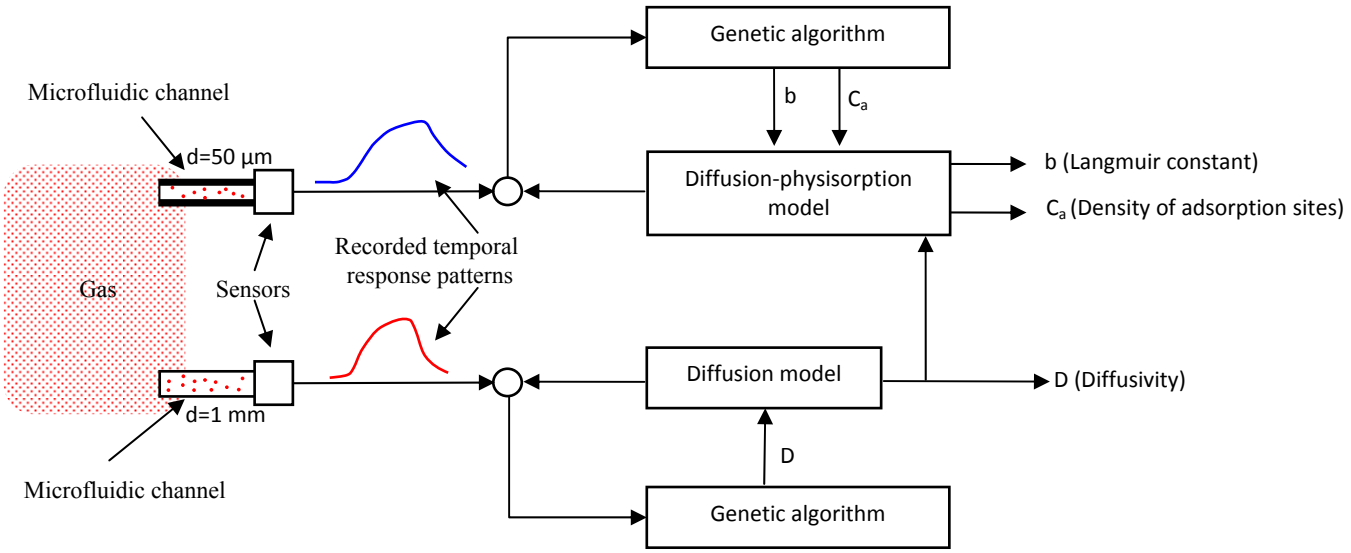

Fig.1. The schematics of the experimental system utilized.

References:

1. F. Hossein-Babaei and V. Ghafarinia, Gas analysis by monitoring molecular diffusion in a microfluidic channel, Analytical Chemistry, 82 (2010) 8349-8355.
2. F. Hossein-Babaei, M. Paknahad and V. Ghafarinia, A miniature gas analyzer made by integrating a chemoresistor with michrochannel, Lab on a Chip, 12 (2012) 1874-1880.

4th Micro and Nano Flows Conference
UCL, London, UK, 7-10 September 2014

Numerical study of the transition of convective boiling in micro channels

Qingming Liu*, Björn Plam

* Corresponding author: Tel.: ++46 (8)7907454; Email: qingming@kth.se
Department of Energy technology, Royal institute of Technology, Sweden

Keywords: Micro Flow, Numerical, Boiling, micro-channels, coupled level set and vof

A three dimensional numerical study on the transition of convective boiling from nucleate boiling to bubbly flow in a micro-channel with diameter of 0.64 mm was conducted. R134a was used as working fluid and aluminum as micro-channels material. A constant velocity inlet boundary with mass flux 60 kg/m^2 s and 120kg/m^2 s and a heated boundary wall with constant heat flux (5kW/m^2) are applied. Coupled level set and volume of fluid (CLSVOF) method was chosen to capture the two phase interface while the geo-construction method was used to re-construct the two-phase interface. The growth of bubbles and the transition of flow regime was well-predicted by the simulation. Local heat transfer is significantly enhanced by evaporation occurring vicinity of the wall. However, total heat transfer was enhanced at a much lower degree due to the small contact area. The effects of inlet Reynolds number and heat flux are also studied.

4th Micro and Nano Flows Conference
UCL, London, UK, 7-10 September 2014

Microconfined flow behavior of red blood cell by image analysis techniques

Giovanna TOMAIUOLO[1,2*], Luca LANOTTE[3], Antonio CASSINESE[4], Stefano GUIDO[1,2]

* Corresponding author: Tel.: ++39 081 7682261; Fax: ++39 081 2391800; Email: g.tomaiuolo@unina.it
1 Dipartimento di Ingegneria Chimica, dei Materiali e della Produzione Industriale, Università di Napoli Federico II, Italy
2 CEINGE Biotecnologie avanzate, Napoli, Italy
3 Laboratoire Charles Coulomb, Université UM2 de Montpellier, France
4 CNR-SPIN and Dipartimento di Scienza Fisiche, Università di Napoli Federico II, Italy

Keywords: Red blood cells, Deformability, Clustering, Microcirculation

Introduction

In microcirculation *in vivo*, red blood cells (RBCs) travel through microvessels with diameter smaller than cell size in order to allow optimal gas transfer between blood and tissues. In such microconfined conditions RBC shape departs from the classical biconcave geometry at rest by taking deformed configurations, resembling a bullet or a parachute, depending on flow rate and microvessel diameter [1]. The high RBC deformability is mainly due to the viscoelastic properties of the cell membrane, especially shear modulus and surface viscosity. Pathological alterations of RBC deformability are known to be implicated in several diseases, including diabetes, thalassemia, and sickle cell disease [2]. In light of such pathophysiological relevance, the measurement of RBC deformability has been the subject of a number of studies from single cell analysis (micropipette aspiration and optical tweezers) to flow techniques (ektacytometry and rheoscopy). Recently, microfluidic techniques, that are suitable to testing a large number of cells in a physiologically relevant flow field, have been applied to design flow geometries resembling the microvascular network [3, 4]. In this work, we report on an imaging-based *in vitro* systematic fluid dynamic investigation of RBC suspensions flowing either in microcapillaries or in a microcirculation-mimicking device containing a network of microchannels of diameter comparable to cell size. RBC membrane rheological behavior is investigated by analyzing the transient behavior of RBC shape in confined flow and by measuring the membrane viscoelastic properties in converging/diverging microchannels. The comprehension of the single cell behavior led to the analysis of the RBC flow-induced clustering.

Methods

Fresh venous blood samples, drawn from healthy consenting donors and used within 4 h from collection, are diluted with ACD anticoagulant and human albumin to a concentration of 1% for single cell experiments, or 10% by volume for clustering. Images of the flowing RBCs are acquired by a high speed video camera (operated up to 1000 frames/s) and by using a high magnification oil immersion objective (100x). The experiments are carried out either in 4.7, 6.6 or 10 μm diameter silica microcapillaries [5-7] and in a microfluidic device [8]. The latter is made of PDMS and is fabricated by using soft-lithography techniques with SU-8 as photoresist. The network pattern consists of a network of bifurcating channels of decreasing width (down to 10 μm), including converging–diverging flow sections, to mimic human microcirculation network.

Results

In steady state experiments, the classical parachute-like shape observed *in vivo* is found *in vitro*, and is dependent on the imposed pressure drop [5]. An increasing trend is observed, with a leveling-off of cell length with increasing RBC velocity. The cell shape evolution as a function of time, from the biconcave disk shape at rest to the deformed one during flow, is studied by start-up experiments, where the RBC time constant is also measured [6]. The time scale of the transient process is independent on the applied pressure drop and the measured value for healthy cells (0.1 s) is in agreement with previous micropipette data [9]. In order to study the effect of reduced deformability of the RBC membrane, the flow behavior of glutaraldehyde (GA)-hardened RBCs has been also analyzed. Hardened RBCs exhibit a faster shape evolution at higher GA concentration, thus showing that the corresponding time scale becomes shorter at increasing cytoskeleton elasticity [6]. RBC membrane viscoelastic properties, such as viscosity and elasticity, which are the main factors affecting cell deformability, has been measured by using a converging-diverging PDMS microchannels [8]. The shape change of the RBCs flowing in the divergent channel is elicited by the fluid dynamics of the flow field and can be described by using the Kelvin–Voigt model [10], which is based on the parallel combination of a spring and a dashpot, the two elements being associated with the elastic and viscous response of the cell membrane, respectively. Moreover, single RBC surface area is measured, providing an useful parameter that lacks in routine clinical tests [7]. The comprehension of the single cell behavior leaded to the analysis of the RBC flow-induced clustering. Cluster size and velocity is investigated as a function of the applied pressure drop and of the microcapillary residence time, including the effect of polydispersity [11].

Conclusions

This work concerns a systematic investigation of RBC deformation and clustering in artificial microcapillaries with diameter comparable to cell size and in PDMS-based microfluidic devices. We provide for the first time a through quantitative comparison with theoretical predictions from the literature, and find a good agreement with no adjustable parameters. The system presented in this work could be also used to evaluate the effects of drugs on cell deformability in microcirculation.

References

[1] S. Guido, and G. Tomaiuolo, C. R. Physique **10** (2009).
[2] S. Shattil *et al.*, *Hematology: Basic Principles and Practice* (Churchill Livingstone, Philadelphia, 2000).
[3] S. Shevkoplyas *et al.*, Microvasc Res **65** (2003).
[4] M. Abkarian *et al.*, Biomed Mater **3** (2008).
[5] G. Tomaiuolo *et al.*, Soft Matter **5** (2009).
[6] G. Tomaiuolo, and S. Guido, Microvasc Res **82** (2011).
[7] G. Tomaiuolo *et al.*, Cytom Part A **81** (2012).
[8] G. Tomaiuolo *et al.*, Lab Chip **11** (2011).
[9] E. Evans, and P. La Celle, Blood **45** (1975).
[10] R. Hochmuth, P. Worthy, and E. Evans, Biophys J **26** (1979).
[11] G. Tomaiuolo *et al.*, Phys Fluids **24** (2012).

4th Micro and Nano Flows Conference
UCL, London, UK, 7-10 September 2014

Deformability-based red blood cell separation in deterministic lateral displacement devices

Timm KRUEGER [1,2,*], Peter V. COVENEY [2]

* Corresponding author: Tel.: +44 (0)131 650 5679; Fax: +44 (0)131 650 6554; Email: timm.krueger@ed.ac.uk
1: School of Engineering, The University of Edinburgh, Scotland, UK
2: Centre for Computational Science, University College London, UK

Keywords: Cell Separation, Micro Flow, Deterministic Lateral Displacement, Deformability, Simulation

Deterministic lateral displacement (DLD) devices are commonly used to separate cells and particles by taking advantage of their intrinsic properties (*e.g.* size). The underlying principle is that finite particle sizes lead to volume-exclusion effects during flow through micro-structured geometries. Different particles therefore see different streamlines, which in turn can lead to particle separation. Advantages of DLD devices compared to alternative separation techniques are label-free and continuous operation modes and relatively easy integration into existing lab-on-chip devices.

DLD has previously been employed to separate blood components by their size [1], to enrich leukocytes [2] or to detect parasites in blood [3]. Deformability effects of red blood cells (RBCs) are usually either neglected or declared to be detrimental. Only recently, it has been shown experimentally that one can obtain a so-called deformable particles *fingerprint* by measuring their apparent diameter in DLD devices as a function of applied pressure gradient and therefore shear stress [4].

In order to investigate the behaviour of deformable RBCs in DLD devices, we have performed high resolution computational fluid dynamics simulations based on a combination of the lattice-Boltzmann and finite-element methods. We find that DLD devices can be employed to separate RBCs by deformability, which is, for example, relevant for the detection of malaria-infected cells. We further provide a detailed examination of RBC deformation during their passage through the DLD device as a function of capillary number (an indicator of cell deformability). In particular, we link the deformation characteristics of the RBCs to their apparent size.

References

[1] J.A. Davis, D.W. Inglis, K.J. Morton, D.A. Lawrence, L.R. Huang, S.Y. Chou, J.C. Sturm, R.H. Austin. *P. Natl. Acad. Sci.* **40** (2006), 14779—14784

[2] D.W. Inglis, M. Lord, R.E. Nordon. *J. Micromech. Microeng.* **21** (2011), 054024

[3] S.H. Holm, J.P. Beech, M.P. Barrett, J.O. Tegenfeldt. *Lab Chip* **11** (2011), 1326—1332

[4] J.P. Beech, S.H. Holm, K. Adolfsson, J.O. Tegenfeldt. *Lab Chip* **12** (2012), 1048—1051

4th Micro and Nano Flows Conference
UCL, London, UK, 7-10 September 2014

Non-classical Thermal Physics in Force-driven Micro-channel Gas Flows

Rho Shin MYONG [1,*]

* Corresponding author: Tel.: +82-55-772-1645; Fax: +82-55-772-1580; Email: myong@gnu.ac.kr
1 Department of Aerospace and System Engineering and Research Center for Aircraft Parts Technology, Gyeongsang National University, South Korea

Keywords: Micro Gas Flow, Non-classical Thermal Physics

The study of flow and thermal characteristics in gases associated with micro- and nano-devices remains as an important scientific topic. Previous studies [1-3] had revealed that the fundamental physics in micro- and nano-scale realm is significantly different from the physics found in conventional macro-scale problem. For instance, it was shown by various studies that the classical Navier-Fourier theory cannot predict the correct flow physics of the force-driven Poiseuille gas flow. In particular, the classical theory was not able to describe the non-monotonic temperature distribution across a micro-channel [1, 3].

The one-dimensional force-driven (or acceleration-driven) Poiseuille flow is defined as a stationary flow in an infinitely long channel under the action of a constant external force parallel to the walls. In a previous study based on a nonlinear couple constitutive relation (NCCR) derived from the Boltzmann equation via the moment method [3], it was shown that the term of coupling of force and viscous shear stress appearing in the constitutive equation of heat flux is responsible for the unusual feature of the central temperature minimum, which is in stark contrast with conventional monotonic quartic profile. However, there exist some unresolved issues such as how the coupling of force and shear stress can affect the flow and thermal characteristics when it is combined with the Navier law.

In the present study, the fundamental physics, in particular, non-classical thermal characteristics in micro-channel gas flows is investigated on the basis of non-Fourier law embedded in NCCR. First, the effects of the force-stress coupling term on thermal behavior are examined in detail in both classical and non-classical framework. It is shown that the ultimate source behind the non-monotonic temperature distribution is the coupling term in the constitutive equation of heat flux, irrespective of the nature of the constitutive equation of viscous stress, classical or non-classical. Second, the thermal characteristics such as the temperature and heat flux distributions for various Knudsen numbers are investigated in order to understand the complex interaction between the force and the rarefaction (or the size of the channel). It is shown that the central temperature reaches minimum value in whole flow field after a critical Knudsen number. Lastly, it is demonstrated that the so-called Knudsen minimum in mass flow rate is directly related to the non-classical thermal behavior due to the force-stress coupling term. In other words, the increase of average temperature within the channel after a threshold Knudsen number in transitional regime is responsible for the minimum, indicating a dominant role of thermal aspects on general flow physics in non-classical gas flow regimes.

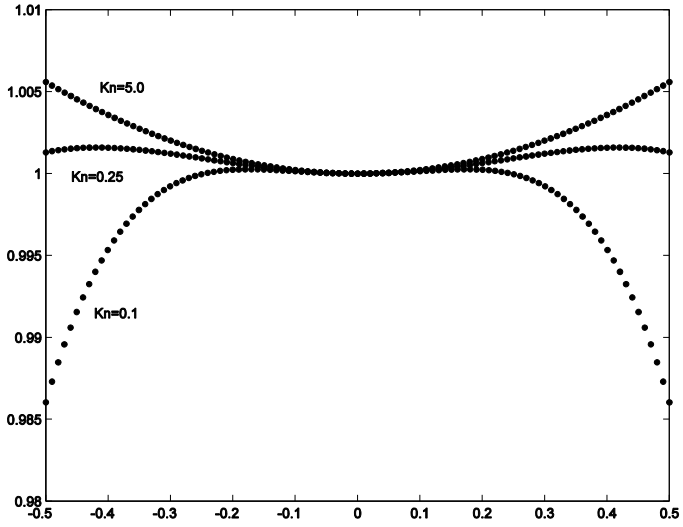

Figure 1 Temperature distribution in the force-driven compressible Poiseuille gas flow for various Knudsen numbers calculated by a nonlinear couple constitutive model.

References

[1] Tij, R., Santos, A., "Perturbation analysis of a stationary nonequilibrium flow generated by an external force," J. Stat. Phys. **76**, 1399 (1994)

[2] Chen, S., Tian, Z., "Simulation of thermal micro-flow using lattice Boltzmann method with Langmuir slip model," Int. J. Heat Fluid Flow **31**, 227 (2007)

[3] Myong, R.S., "A full analytical solution for the force-driven compressible Poiseuille gas flow based on a nonlinear coupled constitutive relation," Phys. Fluids **23**, 012002 (2011)

4th Micro and Nano Flows Conference
UCL, London, UK, 7-10 September 2014

Heat Flux Distribution in the Force-driven Poiseuille Flow by Molecular Dynamics

Ravichandran RANJITH [1], Jae Hyun PARK [1], Rho Shin MYONG [1,2,*]

* Corresponding author: Tel.: +82-55-772-1645; Fax: +82-55-772-1580; Email: myong@gnu.ac.kr
1 Department of Aerospace and System Engineering, Gyeongsang National University, South Korea
2 Research Center for Aircraft Parts Technology, Gyeongsang National University, South Korea

Keywords: Heat flux, Force-driven Poiseuille flow, LAMMPS

The Poiseuille flow is a flow type where the fluid is constrained between two infinitely long plates and forced to move parallel to the direction of plates by applying a constant force or pressure gradient. In this work, the force-driven Poiseuille flow is modeled by molecular dynamics simulation and the temperature and heat flux distributions are studied. The simulation is aimed to study the behavior of heat flux distribution, both normal and non-negligible tangential heat flux, for different values of applied force (driving force) and different Knudsen numbers. Previously, the non-negligible tangential heat flux distribution has been described by a continuum theory based on nonlinear coupled constitutive relations [1] and compared with DSMC results. This work is an attempt to study the same phenomenon using molecular dynamics simulations [2].

The simulation domain consists of both fluid and wall atoms and it is periodic in all the three dimensions. The fluid atoms are constrained only in the y-direction by solid walls that are modeled by layers of wall atoms and maintained at constant temperature. The flow is driven by applying a driving force in the x-direction on all the fluid atoms in the simulation. The software used for simulation is LAMMPS (Large-scale Atomic/Molecular Massively Parallel Simulator), distributed by Sandia National Laboratories. LAMMPS is a classical molecular dynamics code which can be used to model atoms as a parallel particle simulator at the atomic, meso, or continuum scale.

The normal heat flux as well as the non-negligible tangential heat flux is studied for different values of applied force and Knudsen number. When the driving force is increased from weak flow limit to higher value, the evolution of heat flux and its dependence on Knudsen number are observed. As preliminary results, the peculiar velocity and temperature profiles are shown in Figs. 1 and 2, respectively.

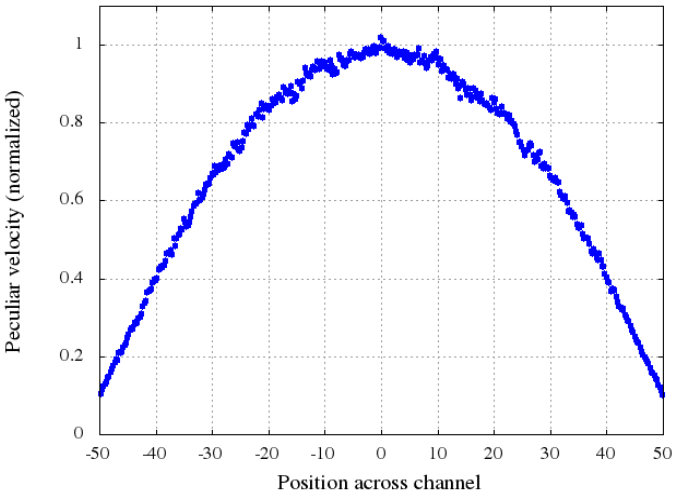

Figure 1 Peculiar velocity across the channel.

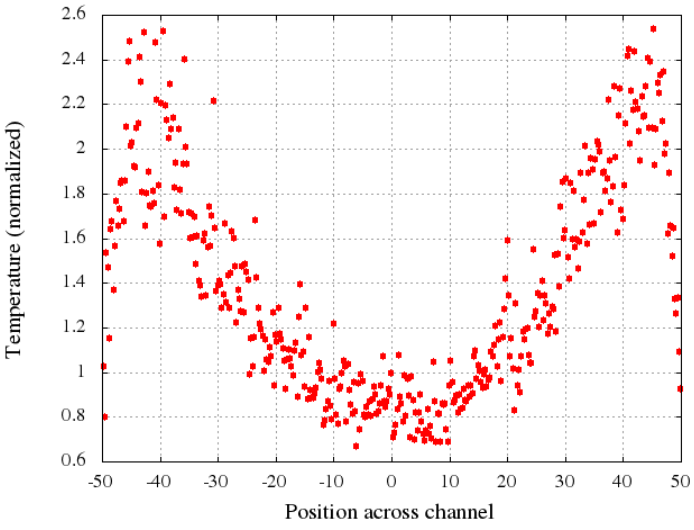

Figure 2 Temperature across the channel.

References

[1] Myong, R.S., "A full analytical solution for the force-driven compressible Poiseuille gas flow based on a nonlinear coupled constitutive relation," Phys. Fluids **23**, 012002 (2011)
[2] Todd, B.D., Evans, D.J., "Temperature profile for Poiseuille flow," Phys. Rev. E **55-3**, 2800 (1997)

4th Micro and Nano Flows Conference
UCL, London, UK, 7-10 September 2014

Fluid drag-reducing effect and mechanism of superhydrophobic surface with micro-nano textures

Jingxian ZHANG [1], Zhaohui YAO [1,*], Pengfei HAO [1], Haiping TIAN [2], Nan JIANG [2]

* Corresponding author: Tel.: ++86 10 6277 2558; Email: yaozh@tsinghua.edu.cn
1 Department of Engineering Mechanics, Tsinghua University, P.R. China
2 School of Mechanical Engineering, Tianjin University, P.R. China

Keywords: Superhydrophobic surface, Micro-nano textures, Drag reduction, PIV

Superhydrophobic surfaces have excellent self-cleaning, low skin friction and antifouling properties, which bring wide range of potential applications in industrial, medical and marine fields.

In this paper, drag-reducing property and mechanism of superhydrophobic surface are investigated. Superhydrophobic surfaces are fabricated using the spray coating method (Aljallis et al., 2010). The coating is composed of hydrophobic nanoparticles and formed dispersed micro clusters which are similar to the micro papillae of a lotus leaf. The morphology of the surface with the superhydrophobic coating is examined using scanning electron microscope (SEM), shown in Fig.1.

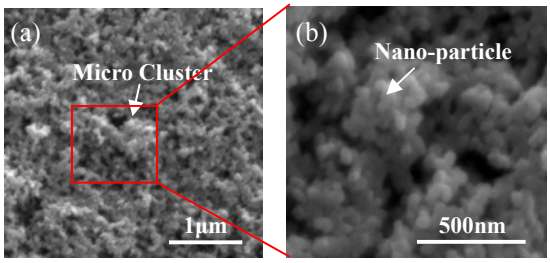

Fig. 1. Scanning electron microscope (SEM) images of the superhydrophobic coating. The arrow in (a) indicates a micro cluster, whose details are shown in (b).

The contact angle and rolling angle are measured as the wetting properties of the superhydrophobic coating. The contact angle is measured to be 161° and the rolling angle is measured to be lower than 1° of a 10μL water droplet.

In the following experiment, a channel and a flat plate in macroscopic scale are prepared, with the superhydrophobic coating sprayed on the measured surface (marked with red in Fig.2). According to the schematic illustrate in Fig. 2, two experimental apparatus are fabricated. Fluid drag and flow velocity field over the superhydrophobic surface are measured at different Reynolds numbers, controlled by an adjustable micro-pump. Superhydrophobic surfaces are settled where the flow is presumed to be fully developed in a time-averaged sense. As shown in Fig. 2, the Pressure drop and velocity field of the flow over the superhydrophobic surface are measured using the Particle image velocimetry (PIV) technology and micro pressure sensor (Lu et al., 2010), marked by a red dotted line box.

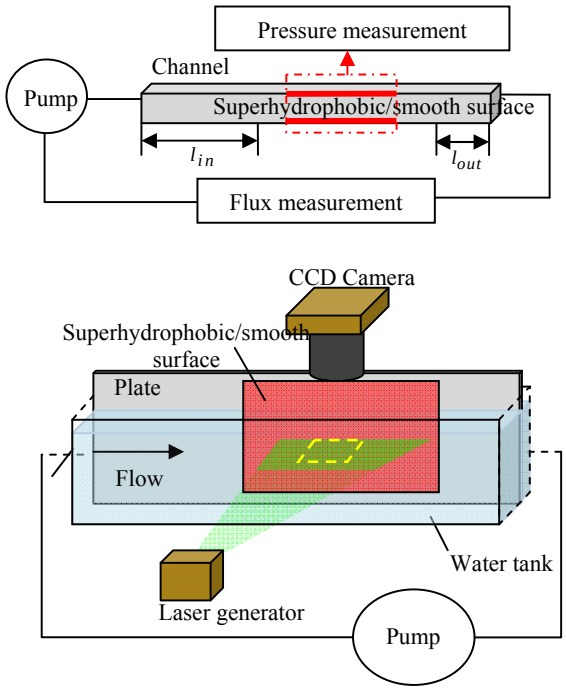

Fig. 2. Schematic of the experiment for flow in the channel (top panel) and flow over the flat plate (bottom panel).

Significant drag reduction is observed both in the channel and plate case with the superhydrophobic surface. For the channel flow, A 54% drag reduction is observed both in laminar and turbulent flow over Re range from 500 to 5000. For flow over a plate, there is a 19% reduction on the total stress in the whole boundary layer at Re_δ =12000. Suppressions of the turbulence intensities and the Reynolds shear stress are found, which may cause the drag reduction.

Foundation: National Natural Science Foundation of China (No. 11272176)

References

Aljallis, E., Sarshar, M. A., Datla, R., Sikka, V., Jones, A., & Choi, C. H., 2013. Experimental study of skin friction drag reduction on superhydrophobic flat plates in high Reynolds number boundary layer flow. Physics of Fluids (1994-present), 25(2), 025103.

Lu, S., Yao, Z.H., Hao, P.F., Fu, C.S., 2010. Drag reduction in ultrahydrophobic channels with micro-nano structured surfaces. Science China, Physics, Mechanics & Astronomy, 2010.7.

4th Micro and Nano Flows Conference
UCL, London, UK, 7-10 September 2014

Study on Thermal Conductivity of Gas and Solid in Nano-porous Aerogel

Gui Hua TANG *, Cheng BI, Bo FU

* Corresponding author: Tel.: +86-29-82665319; Fax: +86-29-82665445; Email: ghtang@mail.xjtu.edu.cn
MOE Key Lab of Thermo-Fluid Science and Engineering, School of Energy and Power Engineering,
Xi'an Jiaotong University, Xi'an 710049, China

Keywords: thermal conductivity, nanoporous-aerogel, gas phase, solid phase

Nano-porous aerogel has an ultra low thermal conductivity and is usually used as the super insulator. Aerogel has a complex structure with a three-dimensional network skeleton consisting of interconnected spherical nano-particles, and the heat transfer in aerogel can be attributed to three modes of heat conduction in solid backbone, thermal radiation, and heat transfer among gas molecules. To evaluate the insulation performance of the aerogel, we focus on studying the thermal conductivity of gas phase and solid phase in the aerogel.

Since the pore-size distribution has significant effect on the gaseous thermal conductivity, we present a modified model based on the previous theoretical models to take into account the random and non-uniform pore-size distribution, and the predicted results from the present model are in more agreement with available data than those of the existing models.

The heat transfer via the solid phase of the aerogel depends on the lattice vibration/localized atomic vibrations (phonons/atoms) and is limited by the scattering of the phonons/atoms at a distance of the mean free path/inter-atomic spacing. Based on the superlattice nanowire model, we propose a modified model to predict the effective thermal conductivity of aerogel solid backbone. We study both the size effect and interfacial resistance effect on the thermal conductivity of the aerogel backbone. The solid thermal conductivity of the aerogel calculated by the present model is in good agreement with that by the minimum thermal conductivity model, and also agrees well with available experimental data.

To investigate the coupled heat transfer between the solid and gas phases of the aerogel, we develop a three-dimensional numerical model to simulate the heat conduction in the aerogel. The effects of aerogel particle size and pore size are introduced into the numerical model to improve the prediction accuracy. The numerical model is validated by available experimental data and theoretical couple model, and it is proved that the present model have a higher performance to predict the thermal conductivity of the aerogel.

The modified gaseous thermal conductivity model:

$$\lambda_g = \sum_{i=1}^{n} \Phi_i K(D_i)$$

$$\Phi_i = \begin{cases} 0 & D_i \in [D-3\sigma, D-\sigma) \quad D_i - 3\sigma > 0 \\ \dfrac{\Delta D}{\sqrt{2\pi}\sigma} e^{\frac{(D_i-D)^2}{2\sigma^2}} & D_i \in [D-\sigma, D+\sigma] \\ \dfrac{2\Delta D}{\sqrt{2\pi}\sigma} e^{\frac{(D_i-D)^2}{2\sigma^2}} & D_i \in (D+\sigma, D+3\sigma] \end{cases}$$

where, n is the number of the pores, i is the pore index, Φ_i is the contribution to the total porosity, $K(D_i)=\lambda_0/(1+2\beta Kn)$ is the gaseous thermal conductivity with respect to the pore-size D_i, λ_0 is the thermal conductivity of the gas in free space, β is a coefficient depending on the accommodation coefficient and the adiabatic coefficient of the gas, and Kn is the Knudsen number, D is the mean pore diameter, and σ is the standard deviation in the Gauss distribution function.

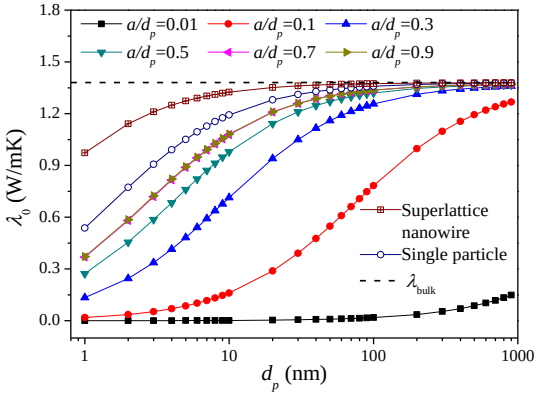

Fig. 1 Effective thermal conductivity of silica aerogel backbone

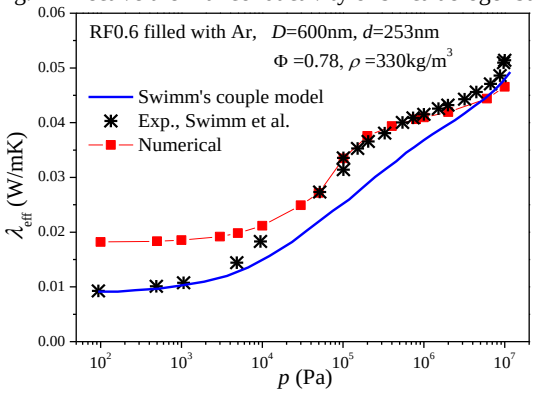

Fig. 2 Comparison between the present numerical model and theoretical couple model

Reference

[1] C. Bi, G. H. Tang, W. Q. Tao, J Non-Cryst Solids, 358 (2012) 3124-3128.
[2] M. G. Kaganer, Thermal Insulation in Cryogenic Engineering, Israel Program for Scientific Translations, Jerusalem, 1969.
[3] C. Bi, G. H. Tang, Int. J. Heat Mass Transfer, 64 (2013) 452-456.
[4] K. Swimm, G. Reichenauer, S. Vidi, H. P. Ebert, Int. J. Thermophys. 30 (2009) 1329-1342.

4th Micro and Nano Flows Conference
UCL, London, UK, 7-10 September 2014

Modeling of on-chip (bio)particle separation and counting using 3D electrode structures

Barbaros Çetin*, Soheila Zeinali

Corresponding author: Tel.: +90 (312) 290-2108; Fax: +90 (312) 266-4126
Email: barbaros.cetin@bilkent.edu.tr, barbaroscetin@gmail.com
Microfluidics & Lab-on-a-chip Research Group, Mechanical Engineering Department
İhsan Doğramacı Bilkent University 06800 Ankara Turkey

Keywords: Microfluidics, lab-on-a-chip, dielectrophoresis, particle separation, particle counting

In many devices using lab-on-a-chip technology, the manipulation and quantification of (bio)particles is required in a variety of biomedical applications such as drug screening, disease detection and treatment For manipulation of particles at such small scales, electrical techniques such as electrophoresis and dielectrophoresis (DEP) are very suitable [1]. DEP is the movement of particles in a non-linear electrical field due to the interaction of the particle's dipole and spatial gradient of the electrical field. DEP can induce both negative and positive forces on the particles depending on the dielectrical properties of the particles and the suspending medium. For an AC field, DEP force is also function of the frequency of the field which makes DEP force tunable for a given particle. Each (bio)particle has a distinct morphology; hence, a distinct *dielectric signature* which is the function of its type, its interior structure, and its state. This unique dielectric signature makes DEP a *label-free and sensitive selection tool*. Using this dielectric signature, DEP can be utilized to discriminate and identify (bio)particles from other particles or to detect and isolate diseased or damaged (bio)particles without any need for labeling the (bio)particles [1].

For the quantification or counting of the bioparticles, flow cytometer, fluoresence-activated cell sorting (FACS) and magnetic-activated cell sorting (MACS) are common techniques used in conventional laboratory environment. Although these techniques are robust, they require complex and expensive instruments, trained personnel and use of bulky and expensive external hardware and high end microscope set-ups [2]. Moreover, these instruments have a very limited level of portability and integrability with other analysis tools [3]. One alternative to these techniques is the electrical sensing. Common practice for the electrical sensing based particle counting is to flow a particle in a channel whose size is comparable with the particle size and to monitor the impedance of the channel. Since the electrical properties of the (bio)particles are different than that of the buffer solution, a peak can be detected as the (bio)particles are moving across a sensing section.

One major issue about the DEP-based microfluidic devices is the throughput. Their throughput is low compared to other conventional manipulation techniques [1]. One way to increase the throughput is to increase the channel dimensions. For the devices with planar and embedded electrodes, the electric field has fringe-like nature (see Figure 1). Therefore, the height of the device cannot be increased. The strong electric field and DEP force exists in a confined region over the electrodes (DEP force decreases drastically in height direction). The particles need to flow in the vicinity of this confined region. For trapping devices, the width of the channel can be increased to increase the throughput; however, this is not a solution for continuous flow devices. The same issue also exists for on-chip counting devices based on impedance measurements. One way to increase the performance of the DEP-based separation and the impedance-based counting is to use 3D electrodes at the sidewalls. Which eliminates the fringe-like structure of the electric field lines.

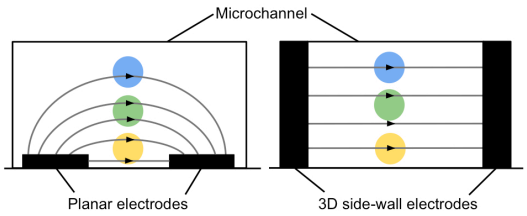

Figure 1: Electric field within a microchannel with planar and 3D side-wall electrodes

In this study, a numerical modeling using COMSOL Multiphysics for the separation and counting of (bio)particles is developed and the performance of the planar and 3D electrode structures are compared. Microfluidic devices with an asymmetric pair (for separation) and a symmetric pair (for counting) of electrodes are considered. The effect of the geometrical parameters, material properties, flow rates, particle size and applied voltage on the device performance is discussed. The fabrication procedure of 3D electrode structures is also addressed.

References

1. B. Cetin, D. Li, Electrophoresis, 32, 2011, 2410–2427
2. E.P. Dupont, E. Labonne, Y. Maruyama, C. Vandevyver, U. Lehmann, M.A.M. Gijs, E. Charbon, *Senors and Actuators B: Chemical*, 2012, 174, 609-614.
3. Y.-H. Lin, G.-B. Lee, *Biosensors ans Bioelectronics,* 24, 2008, 572-578.

4th Micro and Nano Flows Conference
UCL, London, UK, 7-10 September 2014

The Leidenfrost Phenomenon on Surfaces with Hydrophobicity Transitions

Gail R. DUURSMA [1,*], Ross KENNEDY [1], Khellil SEFIANE [1]

1: School of Engineering, The University of Edinburgh, King's Buildings, Mayfield Road, Edinburgh EH9 3EX, UK
* Corresponding author: Tel.: ++44 (0)131 6504868; Fax: ++44 (0)131 6506551; Email: Gail.Duursma@ed.ac.uk

Keywords: Leidenfrost, Boiling, Microstructure, Hydrophobicity

The lifetime of a droplet released on a hot plate decreases when the temperature of the plate increases. But above some critical value of the temperature, the lifetime suddenly increases. This is due to the formation of a thin layer of vapour between the droplet and the substrate. This layer plays a double role: first it thermally isolates the droplet from the plate and second it allows the droplet to "levitate." This effect was discovered by Leidenfrost in 1756, but remains an active field of research nowadays, motivated by a wide range of applications. The Leidenfrost point is a function of microstructure of the surface. For example, Kwon *et al*. (2013) showed that on a structured surface composed of a grid of 10 micron cylinders, the Leidenfrost temperature varies by up to 50 K for pillar spacing varying from 50 microns to 80 microns, see Figure 1 (a). In this work, surfaces with different microstructures were prepared such that there is a sharp transition (boundary) between a region of moderate hydrophobicity and a region of strong hydrophobicity. Samples of the microstructure are shown in Figures 1 (b-d) below. The Leidenfrost point was identified in experiments using water drops of average size 0.007 ml and the behaviour of the drop was recorded using a high-speed digital camera. If the drop is placed on the boundary between structured sections, the drop becomes asymmetric. Drop motion may also be observed and some occurrences of drop spinning have been seen. In this paper we present experimental data on Leidenfrost behaviour of drops placed on the boundary between surfaces with different micro-structures.

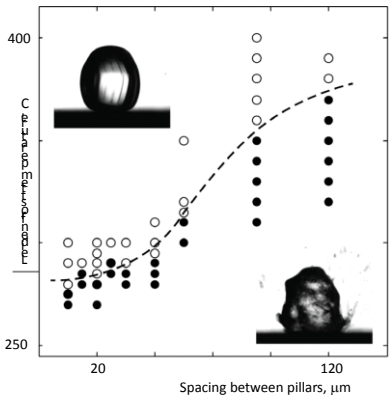

(a)

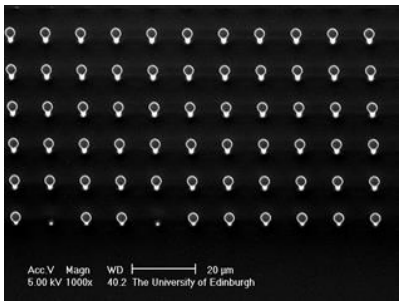

(b)

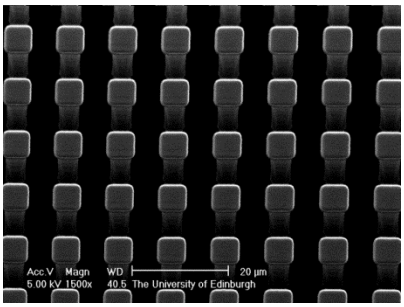

(c)

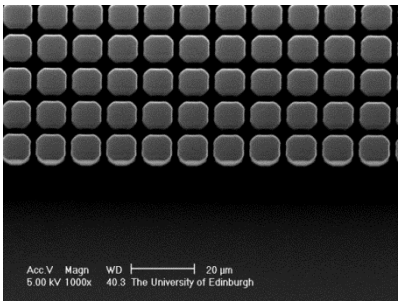

(d)

Figure 1: (a) Dependence of Leidenfrost temperature on structures, Micro-structured (b-d) surfaces use for Leidenfrost experiments

References

Hyuk-min Kwon, James C. Bird, and Kripa K. Varanasi, *Increasing Leidenfrost point using micro-nano hierarchical surface structures* Applied Physics Letters **103**, 201601 (2013); doi: 10.1063/1.4828673

4th Micro and Nano Flows Conference
UCL, London, UK, 7-10 September 2014

Reactive oxygen species by water containing nanobubbles and its role in the improvement of barley seed germination

Shu LIU[1], Seiichi OSHITA[1,*], Yoshio MAKINO[1]

* Corresponding author: Tel.: ++81 03 58415362; Fax: ++81 (0)1895 256392; Email: aoshita@mail.ecc.u-tokyo.ac.jp
1Graduate School of Agricultural & Life Sciences, The University of Tokyo, Japan

Keywords: Nanobubble, Reactive oxygen species, Barley seed, Germination, Fluorescent detection, Microscope spectrophotometer

1 Introduction

In recent years, water containing nanobubbles (NBs) has attracted peoples' great concern in the biological field. NBs' promotion effect on the physiological activity of living organisms has been verified in many areas, such as hydroponic cultivation (Liu et al. 2013), fermentation (Kurata et al. 2008), fishery (Ebina et al. 2013) etc. However, the mechanism of the biological impact at this stage is not clear.

Reactive oxygen species (ROS) can act as secondary messengers in signal transduction pathways that control processes as diverse as plant growth and development, stress response and programmed cell death. Passardi et al. (2006) found that the ROS played a vital role in growth by facilitating the required cell wall loosening for cell elongation. Meanwhile, it has been reported that the reactive oxygen species such as hydrogen peroxide enhanced germination and released residual dormancy of barley seeds (Ishibashi et al. 2010). The generation of ROS caused by NBs can be a reasonable explanation for the NBs' enhancement of physiological activity of living organisms.

2 Materials and methods

In this paper, Aminophenyl Fluorescein (APF) was used as a fluorescent reagent for the detection of ROS generation by NBs. APF itself has almost non-florescent intensity. After APF reacts with ROS, a substance with strong fluorescent intensity will be generated. The fluorescence intensities were measured at excitation wavelength of 490nm and fluorescence emission wavelength of 515nm with a fluorescence spectrophotometer (F-7000, Hitachi High-Tech Co. Ltd., Japan). As for the control water, 5 m mol/L APF reagent (Sekisui Medical Co., Ltd.) was diluted 5000 times with phosphate buffer (0.1mol/L, pH 7.4). Then the oxygen NBs was introduced into the control water through a micro-bubble generator (OM4-GP-040, Aura Tec Co. Ltd., Japan) at a constant temperature of 20 ℃. After 10 minutes, 30 minutes and 60 minutes generation time, the samples were used for the fluorescent intensity measurement.

Besides, the generated ROS in the barley seed cells were also measured in the geminated seeds in the water containing NBs and in distilled water respectively. The dissolved oxygen (DO) concentrations of the water containing NBs was adjusted to be the same as those of the distilled water through a mixed-gas flow regulator (Log MIX-D100A-0050/0052, FRONTO Co. Ltd., Japan). After 22 hours dipping, the geminated seeds in each group were incubated in 2mM nitroblue tetrazolium (NBT) in 10mM Tris-HCl buffer (pH 7.34) at room temperature for 30 minutes. Then the seeds were cut longitudinally into 100μm slices with a cutting machine (Leica CM1950, Leica Biosystems Co. Ltd., Japan). ROS was visualized as deposits of dark-blue insoluble formazan compound using microscope spectrophotometer (MSV-5000, JASCO Co. Ltd., Japan).

3 Results

Two repetitive experiments showed that the fluorescent intensity in the APF solution increased gradually with NBs generation time. When water contains a large amount of NBs, a scattered beam can be observed due to Tyndall effect caused by NBs (Najafi et al. 2007). Besides, NBs are inherently hydrophobic, which will drive them to adhere to the glass wall causing cuvette surface scattering. The scattering of NBs causes the decrease of fluorescence intensity. At the same time the DO concentration of NBs water was above 40mg/L after 60 minutes oxygen NBs generation. The quenching effect of oxygen may also cause the decrease of fluorescence intensity. Although the two factors above can mask the fluorescence intensity generated by ROS, the fluorescence intensity of the water containing NBs still increased with bubble generation time, which proved that oxygen NBs can generate ROS.

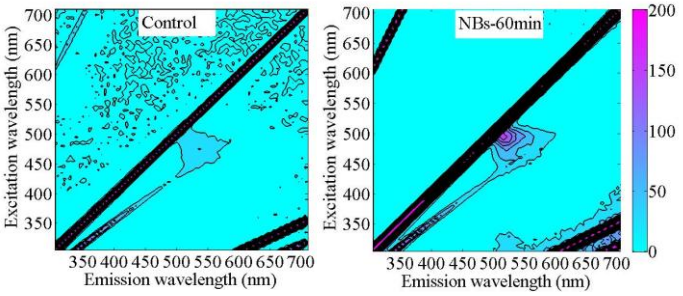

Figure 1 The fluorescence intensity of APF solution before and after oxygen NBs generation (NBs were generated in 60 minutes)

According to the results from seed staining experiment, both the images from the microscope and the results from the absorbance measurement approved that the seeds dipped in the water containing NBs can generate more ROS comparing to those in the distilled water.

4 Conclusions

In summary, NBs not only can generate ROS in the water but also can stimulate the barley seed to generate the ROS inside the seed. Once fully understanding NBs' promotion of living organism growth is achieved, the manipulation of NBs will develop a new technology in agricultural applications.

4th Micro and Nano Flows Conference
UCL, London, UK, 7-10 September 2014

Heat transfer characteristics of hybrid microjet – microchannel cooling module

Tomasz Muszynski[1], Rafal Andrzejczyki[1]
1: Gdansk University of Technology, Faculty of Mechanical Engineering, Department of Energy and Industrial Apparatus
Narutowicza 11/12, 80-233 Gdansk, Poland
E-mail: Tomasz.Muszynski@pg.gda.pl, Rafal.Andrzejczyk@pg.gda.pl

Keywords: microjets, heat transfer intensification, microchannels

ABSTRACT

The paper presents the experimental investigation of heat transfer intensification in a microjet-microchannel cooling module. Applied technology takes benefits from two very attractive heat removal techniques. When jets are impinging on the surface, they have a very high kinetic energy at the stagnation point, also in microchannels boundary layer is very thin allowing to obtain very high heat fluxes.

Micro-channel heat sinks for chip cooling applications have been studied extensively. Main benefit from using micro-channel heat sinks is their ability to achieve high heat transfer coefficients using coolant flow rates that are very low. Smaller than those required with standard sized channels. In experimental studies microchannels achieve heat removal rates up to 790 W/cm2 using water as working fluid, Tuckerman and Pease (1981). However, this advantage is realized with a very large temperature rise along the direction of fluid flow as well as large pressure drop, both of which are very undesirable in result in high pumping power and non uniform heat flux.

Jet impingement experimental studies demonstrated the effectiveness of jet impingement at maintaining very low thermal resistances, especially in the jet's stagnation zone, Garimella and Rice (1995). Main drawback of using a single jet to cool the surface is large variation of surface temperature caused by a diminishing heat transfer coefficient away from the stagnation point. Multiple jets are often used to reduce those variations. Problems arise due to flow blockage between closely spaced jets especially for jets that are situated towards the center of the cooled surface.

Main objective of this paper was to experimentally investigate the performance of a microjet-microchannel cooling module. Intense heat transfer in the test section has been examined and described with precise measurements of thermal and flow conditions. Reported tests were conducted under steady state conditions for single phase liquid cooling.

Obtained database of experimental data were compared to standard cooling techniques, and compared with superposed semi-empirical models for minichannels and microjet cooling, Mikielewicz and Muszynski (2009). Gathered data with analytical solutions and numerical computer simulation allows the rational design and calculation of hybrid modules and optimum performance of these modules for various industrial applications .

References

Tuckerman D.B., Pease R.F.W., "High-performance heat sinking for VLSI", IEEE Electron. Dev. Lett., EDL-2 (1981), pp. 126–129

Garimella, S.V., and R.A. Rice. "Confined and submerged liquid jet impingement heat-transfer." Journal of Heat Transfer, 1995: 871-877.

Mikielewicz, D, and T Muszyński. "Experimental study of heat transfer intensification using microjets." Int. Symp. on Convective Heat and Mass Transfer in Sustainable Energy. 2009.

4th Micro and Nano Flows Conference
UCL, London, UK, 7-10 September 2014

Microchannel Fluid Flow and Heat Transfer by Lattice Boltzmann Method

Rahouadja ZARITA [1*], Madjid HACHEMI [1]

* *Corresponding author:* ***Tel****.:+213 665187631;* ***FAX****:+21324817047;E-mail:*
rahouadja@yahoo.fr
1 *LEMI, University M'hamed Bougara of Boumerdes, Algeria*

Keywords: Lattice Boltzmann method, micro channel, MEMS, heat transfer

Micro flow has become a popular field of interest due to the advent of micro electromechanical systems (MEMS). In this work, the lattice Boltzmann method, a particle-based approach, is applied to simulate the two-dimensional micro channel fluid flow. We simulated fluid flow and heat transfer inside microchannel, the prototype application of this study is micro-heat exchangers. The main incentive to look at fluidic behaviour at micron scale is that micro devices tend to behave much differently from the objects we are used to handling in daily life. The choice of using LBM for micro flow simulation is a good one owing to the fact that it is based on the Boltzmann equation which is valid for the whole range of the Knudsen number. Slip velocity and temperature jump boundary conditions are used for the microchannel simulations with Knudsen number values covering the slip flow. The lattice Bhatnagar-Gross-Krook single relaxation time approximation was used. The results found are compared with the Navier-Stokes analytical and numerical results available in the literature and good matches are observed.

4th Micro and Nano Flows Conference
UCL, London, UK, 7-10 September 2014

Scalability of mass transfer in Taylor flow in capillaries

Valentina NAPPO, Simon KUHN *

* Corresponding author: Email: simon.kuhn@ucl.ac.uk
Department of Chemical Engineering, University College London, UK

Keywords: Taylor Flow, Mass transfer, Capillary, Two phase flow, Scale up

Chemical reactions between components present in gas and liquid phase represent an important class of reactions in chemical industry. The rate of such gas-liquid reactions is often limited by mass transfer, which depends on the hydrodynamics of the gas-liquid flow. In order to correctly predict the transport processes in these multiphase systems, a detailed knowledge of the transport mechanisms on different scales is needed.

In the past, batch systems were widely used for this kind of reactions, but the research efforts over the past decade produced microstructured devices for flow chemistry, which provide several advantages over these conventional reaction systems [1]. In micro-devices the small dimension of the channels results in a significant higher specific interfacial surface area between the gas bubbles and the liquid phase, which results in an increased mass transfer coefficient compared to conventional systems. However, micro-reactors are characterized by an inadequate throughput for industrial applications, for this reason scale-up of these systems is necessary. In this light, the ACS-GCI-Pharmaceutical Roundtable has specifically identified the demand for novel concepts for continuous reaction systems [2].

The most common two phase flow regime occurring in micro-structured and monolith reactors is Taylor flow, which consists of an alternating sequence of gas bubbles and liquid slugs. The length of the gas bubbles is larger than the channel diameter and a thin liquid film separates the gas bubbles from the channel walls.

In this work two-phase flow in circular capillaries with three different diameters (0.5 mm, 1.55 mm and 3.2 mm) is experimentally studied. Water is used as the liquid phase and air or CO_2 as the gas phase. Such a study of Taylor flow in single straight capillaries is particularly interesting because it allows to obtain accurate data that relate mass transfer coefficients to the fluid-dynamic conditions inside the channel.

The range of capillary diameters in this work is chosen in order to investigate system hydrodynamics and transport processes on both micro- and milli-scale. When the interfacial forces dominate over gravity then the channel can be classified as a micro-scale system, and one proposed criterion is based on the Laplace constant: if the diameter of the channel is smaller than the Laplace constant then the influence of the gravity on the system is negligible in comparison to that of the interfacial forces, and the channel can be considered a micro-channel. For the system air-water at ambient temperature and pressure the calculated Laplace constant is 2.7 mm so the 0.5 and 1.55 mm capillaries can be classified as micro-systems, while the 3.2 mm capillary is on the milli-scale.

A non-reactive system (air-water) is used to determine the influence of capillary diameter and superficial gas and liquid velocities on the flow regime, while a reactive system (CO_2-water) is used to investigate the mass transfer. The reactors used are transparent straight capillaries, which allow optical access in order to collect images by means of a high speed camera. The images collected from the camera provide information about the bubble generation frequency, bubble size distributions, and reaction conversion. The absorption of CO_2 in an alkaline solution is particularly suitable as a model reaction as it occurs in the absence of a catalyst, and the conversion of the reactants can be monitored through the value of pH. These measurements allow a quantification of the mass transfer coefficient k_La.

The experimental results are compared with literature, and in addition we will develop correlations to predict the values of k_La for both the milli and the micro systems for a range of Capillary number between 10^{-2} and 10^{-4} and for $Re < 10^3$.

The obtained results will contribute to quantifying the effect of two-phase flow hydrodynamics at each scale on the mass transfer coefficients and their scalability across several orders of length scale.

References

[1] Ehrfeld, Hessel, & Loewe, Microreactors: New Technology for Modern Chemistry. Wiley-VCH, Weinheim, Germany, 2000.
[2] Jiménez-González et al. (2011) OPRD, 15, 900-911.

4th Micro and Nano Flows Conference
UCL, London, UK, 7-10 September 2014

Microfluidic interactions between red blood cells and drug carriers by image analysis techniques

Rosa D'APOLITO[1], Francesca TARABALLI[2], Silvia MINARDI[3], Xuewu LIU[2], Sergio CASERTA[1], Armando CEVENINI[4], Ennio TASCIOTTI[2], Giovanna TOMAIUOLO[1,5*], Stefano GUIDO[1,5]

* Corresponding author: Tel.: ++39 081 7682261; Fax: ++39 081 2391800; Email: g.tomaiuolo@unina.it
1 Dipartimento di Ingegneria Chimica, dei Materiali e della Produzione Industriale, Università di Napoli Federico II, Italy
2 Department of NanoMedicine, The Methodist Hospital Research Institute, Houston, TX, USA
3 National Research Council of Italy - Institute of Science and Techonology for Ceramics
4 Department of Molecular Medicine and Medical Biotechnology, Università di Napoli Federico II, Italy
5 CEINGE Biotecnologie avanzate, Napoli, Italy

Keywords: Red blood cells, Microparticles, Microcirculation, Drug delivery

Introduction

Human blood is a complex non-Newtonian biological fluid consisting in a suspension of cells in plasma, a protein-rich Newtonian fluid. The blood cells are mainly red blood cells (RBCs or erythrocytes) white blood cells and platelets. One of the most remarkable properties of RBCs is their high deformability, that allow the flow even through microcapillaries of diameter smaller than their size [1-5]. The peculiar properties of RBCs needs to be considered when designing a drug delivery strategy based on systemically administered carriers and the delivery efficiency has to be evaluated, by analyzing the distribution of micro-carriers within blood vessels radius [6]. Recently, computational modeling has been used to demonstrate that, while nano-particles (diameter about 100 nm) present an uniform radial distribution and limited near-wall accumulation when flowing with RBCs, micro-particles (diameter about 1 μm) tend to accumulate near the tube wall [7], due to the deformability properties of RBCs [7]. Although a number of numerical works on particles radial distribution in tube flow [6, 8, 9] is present in literature, to our knowledge experimental investigations on the influence of RBC flow on particle migration, and the importance of particle properties, are still lacking. Here, we report on an *in vitro* flow-based imaging method to investigate the fluid dynamic influence of RBCs on micron sized drug carriers.

Methods

Fresh venous blood samples were supplemented with ACD anticoagulant and human albumin to a final concentration of 10% by volume and used in a microfluidic system with controlled geometries. The experiments were carried out either in 50 or 100 μm diameter silica capillaries that mimicked the hydrodynamic conditions of human microcirculation, such as laminar flow and physiological pressure (10-35 mmHg). Since particles size and shape are believed to influence their distribution in circulation [10, 11], three types of micro-carriers (spherical, discoidal and oblate) [12-14], with sizes ranging between 3 and 5 microns, were tested in the study. Images of the flowing RBCs and micro-particles were acquired by a high speed video camera (up to 1000 frames/s) at high magnification (100x).

Results

The transport and distribution of micro-particles in a suspension of deformable RBC under shear flow is related to: i) the migration of RBC towards the vessel centerline due to their deformability, leaving a cell-free layer near the vessel wall; ii) the cross-flow migration of micro-particles towards the vessel wall due to their hydrodynamic interactions with RBCs; iii) the radial distribution of micro-particles in the presence of RBC; iv) the effect of the micro-particle's shape on its margination (i.e. the accumulation of particles near blood vessel walls) dynamics. In the absence of RBCs every type of particle showed an uniform radial distribution, moving with the same velocity of the fluid field. In presence of RBCs, instead, the particles located near or at the centerline drifted laterally, moving towards the wall and accumulated in the cell-free layer, in a shape dependent manner.

Conclusions

The aim of this work is to elucidate the mechanisms that regulates the transport of injectable carriers in microcirculation and to help the design of micro-particles with physical and chemical features optimized for vascular delivery. This study suggests that the therapeutic efficacy of micro-carriers could be ultimately affected by their interactions with circulating cells and by their behavior in the microvasculature.

References

[1] S. Guido, and G. Tomaiuolo, C. R. Physique **10** (2009).
[2] G. Tomaiuolo *et al.*, Soft Matter **5** (2009).
[3] G. Tomaiuolo, and S. Guido, Microvasc Res **82** (2011).
[4] G. Tomaiuolo *et al.*, Cytom Part A **81** (2012).
[5] G. Tomaiuolo *et al.*, Lab Chip **11** (2011).
[6] H. Zhao, E. S. G. Shaqfeh, and V. Narsimhan, Physics of Fluids **24** (2012).
[7] T.-R. Lee *et al.*, Scientific Reports **3**, 2079 (2013).
[8] H. Lan, and D. B. Khismatullin, International Journal of Multiphase Flow **47** (2012).
[9] S. Bhattacharya, D. K. Gurung, and S. Navardi, Physics of Fluids **25**, 033304 (2013).
[10] J. Tan *et al.*, Microfluidics and Nanofluidics **14** (2013).
[11] F. Gentile *et al.*, Journal of Biomechanics **41** (2008).
[12] D. Fine *et al.*, Advanced Healthcare Materials **2** (2013).
[13] J. O. Martinez *et al.*, Chinese Science Bulletin **57** (2012).
[14] J. O. Martinez *et al.*, Biomaterials **34** (2013).

4th Micro and Nano Flows Conference
UCL, London, UK, 7-10 September 2014

Local Regulation of Arterial Tone: an Insight into Wall Dynamics Using Mathematical Models

Etienne BOILEAU [1,*], Dimitris PARTHIMOS[2], Perumal NITHIARASU [1]

* Corresponding author: Tel.: +44 (0)1792 604176; Email: e.boileau@swansea.ac.uk
1 Swansea University, Computational Bioengineering and Rheology, Swansea SA2 8PP, UK
2 Cardiff University School of Medicine, Institute of Molecular and Experimental Medicine, Wales Heart Research Institute, cardiff CF14 4XN, UK

Keywords: Vasomotion, Smooth Muscle, Complex dynamical system, Mass Transport, Computational Model

Summary

We present herein a first attempt to integrate large and small scale phenomena within an image-based computational domain. The aim of the present study is to highlight some of the underlying mechanisms that govern cellular interaction in the vascular wall, using a nonlinear model of vasomotion. We show that macroscopic rhythmic activity and emergent phenomena can indeed reflect ion movements at the level of the individual cell.

Background

Healthy vessels are characterised by an ability to adapt to the conditions imposed by the local environment, and respond to changes in blood flow by dilating or contracting. The vascular smooth muscle is responsible for these spontaneous fluctuations in vessel diameter, that are not caused by changes in heart rate or blood pressure, and are referred to as ‘vasomotion’. Vasomotion is thought to contribute to the enhancement of lymphatic drainage and microcirculatory mass transport, thereby reflecting the critical role of resistance vessels in regulating interstitial tissue pressure and delivery of oxygen and nutrients.

At a smaller scale, arterial contractions are dependent on cellular ionic transport mechanisms. A number of mathematical models have been proposed to described smooth muscle dynamics, inter-cellular communication and ion wave propagation. In the present formulation, the excitation-contraction coupling, or electrochemical coupling, is primarily controlled by movements of the ion calcium Ca2+ into and out of the cytoplasm. The intracellular oscillator is identified by the cyclic Ca2+ -induced Ca2+ release from ryanodine-sensitive stores (RyR CICR) of the sarcoplasmic reticulum (SR).

Methods

The nonlinear system of ordinary differential equations contains three variables describing movements of Ca2+ in the cytosol, in the SR and variations in the membrane potential. Simulations are produced by numerical integration of this system with an adaptive Runge-Kutta-Merson algorithm. We use different spatial domains: a two-dimensional rectangular array of approximately 6000 cells, representing a single layer of smooth muscle cells, and image-based computational domains. Each cell is coupled to its nearest neighbours. The nature of coupling between adjacent cells remains difficult to ascertain. In the current formulation we explore the consequences of either Ca 2+ or electrical coupling, by assuming a simple gradient driven flux between neighbouring cells coupled via gap junctions.

Results

The smooth muscle layer contains cells that are quiescent, in an under- or over-stimulated state, in terms of Ca2+ availability, and cells that are oscillating spontaneously. Within this range, the oscillatory regime is maintained at a physiological level. By controlling a given number of parameters, we are then able to reproduce various pharmacological interventions.

We investigate the effect of coupling on synchronization and entrainment. Weakly coupled cells are dominated by local dynamics and chaotic patterns. For stronger Ca2+ coupling, discrete pacemaker nodes become prominent, and these are eventually dominated by one or two nodes, resulting in clear wave fronts, as illustrated in Fig. 1.

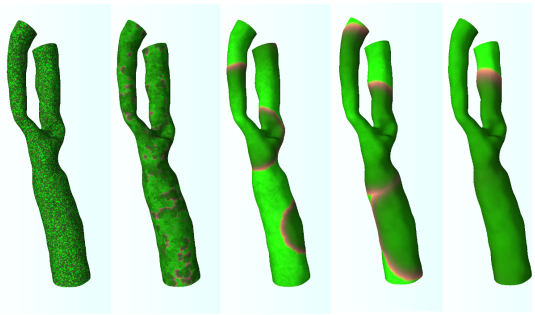

Figure 1: Computational modelling results illustrating the emergence of propagating wavefronts. A gradual transition of uncorrelated oscillatory activity into coherent patterns is observed under conditions of increased intercellular Ca2+ coupling from left to right.

4th Micro and Nano Flows Conference
UCL, London, UK, 7-10 September 2014

Optimization of Actuation Protocol to Enhance Mass Transfer Rate in a Laminar Flow

Erell BONNOT[1], Philip A. LISK [1], Md. Taifur RAHMAN[1], Robert POLLARD[2], Robert BOWMAN[2], Evgeny V. REBROV[1*]

[1] School of Chemistry and Chemical Engineering, Queen's University Belfast, BT9 5AG, Belfast, UK
[2] Centre for Nanostructured Media, School of Mathematics & Physics, Queen's University Belfast, BT7 1NN, Belfast, UK
* Corresponding author: Tel.: +44 (0)2890974627; Email: e.rebrov@qub.ac.uk

Keywords: Magnetic microparticles, optimization, magnetic actuation, quadrupole.

The use of micrometric magnetic particles (MMPs) in chemical synthesis offers the advantage of a large specific surface for chemical binding, in combination with a high mobility imposed by the long range magnetic forces acting on them. Functionalized magnetic microparticles can also act as a support for homogeneous and heterogeneous catalysts and their magnetic actuation enhances mass transfer in laminar flow. To achieve the maximum enhancement in mass transfer rate, one should increase their superficial velocity (Re number) and at the same time provide an external force on the boundary layer by acceleration/deceleration of the MMPs.

The experimental setup, designed for the actuation of magnetic microparticles consists of a quadrupolar set of iron bars with a cross section of 2.5 cm × 2.5 cm connected to four horizontal coils. The coils, connected to 2 separate DC power supplies (Kepco BOP 100-2ML) were coupled in two perpendicular pairs by two conductive iron bases. A time-varying magnetic field was generated in a PDMS circular cell with a diameter of 13 mm positioned in the centre of the set-up between the four iron bars. Experiments were performed with a single magnetic MMP and an array of 50-100 magnetic microparticles located in the cell filled with acetonitrile. The whole system was placed over the X-Y stage of an optical microscope to allow the observation of the particle motion in the fluid. The maximum magnetic field strength obtained (for a voltage of 100V applied to the coils) corresponds to 125 kA/m for set of coils 1 and 145 kA/m for set of coils 2.

Sinusoidal functions $V_1=V_{01}\cdot\sin(\omega t)$ and $V_2=V_{02}\cdot\sin(\omega t+\varphi)$ were applied to the two sets of coils to produce a rotating magnetic field, here: V_{01}, V_{02} are the maximum voltages, ω is the frequency and φ is the phase shift. The design parameters were changed as follows: ω between 0.10 and 0.70 Hz, V_{0i} between 25 and 100 V and φ between 60 and 130 degrees. For each set of parameters, the trajectory of the microparticle was monitored over several periods of rotation and the average angular velocity and average angular acceleration were calculated. Then, to optimize the actuation protocol, an objective function has been defined as $f=\tilde{\theta}+\tilde{\dot{\theta}}$, where $\tilde{\theta}$ is the dimensionless average angular velocity being the ratio of the average velocity over 50 s to the maximum velocity, $\tilde{\dot{\theta}}$ is the dimensionless angular acceleration being the ratio of the avegare acceleration over 50 s to the maximum acceleration:

$$\tilde{\theta}=\frac{\theta}{\theta_{\max}},\tilde{\dot{\theta}}=\frac{\dot{\theta}}{\dot{\theta}_{\max}}$$

The goal of this work was to find the maximum value of f as a function of design parameters ω, V and φ.

Under alternating magnetic field, the microparticle follows a circular trajectory with a radius close to that of the microfluidic cell. Figure 1 shows the effect of parameters ω and V on the objective function. The particle velocity increases with the frequency of magnetic field. However at frequencies above 65 mHz, the particle starts to oscillate near a single magnetic pole which results in a decrease of the average velocity. The maximum value of f of 1.10 is achieved at a frequency of 0.65 mHz for a voltage between 80 and 90 V corresponding to a velocity of 10 $mm.s^{-1}$ (Re=5.4) for a 250 µm particle. The acceleration changes in a more complex way.

In this study, the optimum set of parameters has been found corresponding to the maximum value of the objective function of 1.25.

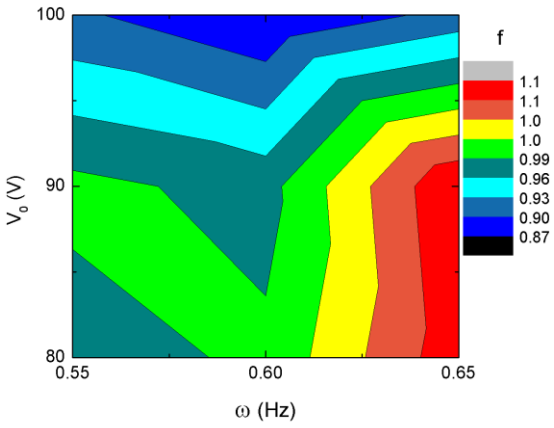

Figure1. Objective function f as a function of frequency (ω) and amplitude (V_0) of the sine function. Particle size: 250 µm, φ =90º.

Acknowledgement

The financial support provided by the European Research Council (ERC) project 279867, is gratefully acknowledged.

4th Micro and Nano Flows Conference
UCL, London, UK, 7-10 September 2014

Experimental Investigation on the Behavior of Artificial Magnetic Cilia

Andrea MARUCCI, Giovanni P. ROMANO*

* Corresponding author: Tel.: ++39 0644585913; Fax: ++39 0644585250; Email: giampaolo.romano@uniroma1.it
Dept. Mechanical & Aerospace Engineering. University of Roma "La Sapienza", Rome, ITALY

Keywords: Micro Flow, Magnetic Cilia, Micro-Mixer, Micro-Pumps

In the present work, the flow field induced by the movement of artificial cilia under the effect of a magnetic field is investigated. The aim of the work is to determine under which geometrical configuration of the cilia a net flow rate or net mixing are obtained. Therefore, the application of this device is derived as a micro-pump or micro-mixer respectively.

1 Theoretical background

The use of micro-devices is nowadays widely increasing due to applications in medical devices, Biomedicine, micro-sensors and control, micro-mixers and pumps (Laser & Santiago, 2004, Kallio 2010). Specifically, it is challenging to design systems at micro-scales which could ensure net flow rates or mixing without any direct contact with external parts to avoid contamination.
To this end, the use of magnetically actuated cilia received a large attention (Ramos 2007, Khaderi *et al.* 2011). Indeed, under the hypothesis of metachronal movement, ensemble of cilia ensures that a net flow rate is possible (Vogel 1996). Therefore, it is important to verify under which conditions such flow rate is possible and what is its effective amplitude. On the other hand, even if a net flow rate is not achieved, it is still possible that the movement of the cilia ensured an effective mixing of the flow with injected scalar solution.

2 Device specifications

A rotating disk with a magnetic element is placed under the plate containing the cilia which are themselves coated by a magnetic paint. Images of the whole rotating disk with the three cilia geometries are presented in Figure 1 with the measurement regions reported into red dotted boxes. The cilia are mounted radially and under the action of the rotating magnetic field (clockwise in Figure 1), they display an oscillating behavior, by moving in the direction of rotation and then turning back into the initial position. The attention is here focused onto the geometrical configuration of the cilia and specifically on the inclination angle in respect of the rotating magnetic field.

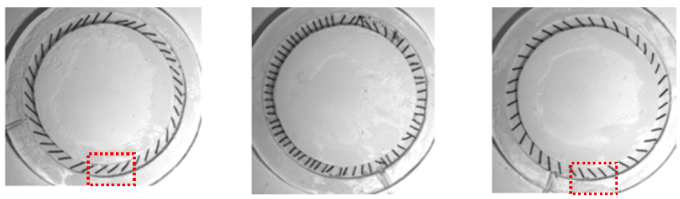

Figure 1. The three tested geometries for the artificial cilia.

Three values have been tested, *i.e.* 30° in the direction of rotation, 0° (radial position) and -30° in the direction opposite to the rotation.
The size of the imaged region is around 10 mm × 13 mm (corresponding to 3 to 4 cilia) and images are acquired through a high-speed camera with a spatial resolution of 1024 pixel × 768 pixel. Two consecutive frames are analyzed in order to determine the flow tracer displacements during the alternating motion of the cilia using the Particle Image Velocimetry (PIV) technique.

3 Main results

In the following plots (Figure 2), the average vector field is shown for the cilia inclined by 30° (on the left, as shown also in Figure 1) and by -30° (on the right as also in Figure 1). In the former case, there is a net volumetric flow rate towards the left part (just the direction of rotation) equal to about 60 mm^3/s. The region of the flow which contributes to such a movement is mostly derived from the constant motion concentrated at the cilia root. On the other hand, in the second case, two counter-rotating vortices are clearly noticed which give a null flow rate. In instantaneous plots, the oscillating behavior of the cilia is overlapped to this flow field, thus indicating a micro-pump type application for the cilia inclined by 30° and a micro-mixer one for those inclined with zero or a negative angle in respect to the direction of rotation of the magnetic field.

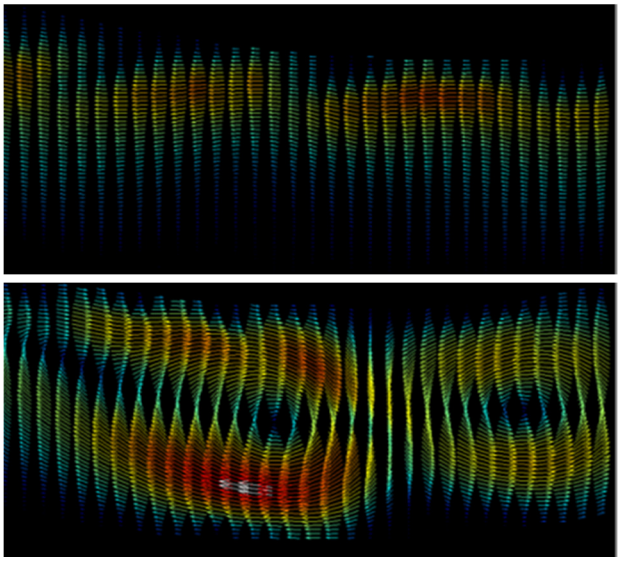

Figure 2. Examples of average vector fields.

4th Micro and Nano Flows Conference
UCL, London, UK, 7-10 September 2014

Variation of Important Non-Dimensional Numbers During Bubble Growth at Nucleation Site in Microchannels

Sambhaji T. KADAM[1], Ritunesh KUMAR[1,*]

* Corresponding author: Tel.: (+91) 4240734; Fax: (+91) 7324 240761; Email: ritunesh@iiti.ac.in
1 Mechanical Engineering Department, Indian Institute of Technology Indore, MP, India
Keywords: Microchannel Bubble growth, Nucleation site, Non-dimensional numbers

Abstract

Two phase flow in heat sink initiates at Onset of Nucleate Boiling, where the first bubble emerges in the downstream flow direction. Bubble nucleation and growth in microchannel heat sinks is very conspicuous phase as the growing bubble can completely block the flow cross-section area at high heat flux. Hence, microchannels are more susceptible to flow boiling instability. In this paper effort has been put to study the bubble dynamics during bubble growth at nucleation site for microchannel in terms of non-dimensional energy ratio numbers and their variation from bubble inception until departure. New non dimensional energy ratio is also proposed, which can be useful to differentiate inertia control and thermal diffusion control region during bubble growth at nucleation site.

4th Micro and Nano Flows Conference
UCL, London, UK, 7-10 September 2014

Comparative study of heat transfer and pressure drop during flow boiling and flow condensation in minichannels

Dariusz Mikielewicz[1], Rafał Andrzejczyk[1], Blanka Jakubowska[1], Jarosław Mikielewicz[2]
1: Gdansk University of Technology, Faculty of Mechanical Engineering, Department of Energy and Industrial Apparatus
Narutowicza 11/12, 80-233 Gdansk, Poland
2: The Szewalski Institute of Fluid-Flow Machinery PAS, ul. Fiszera 14, 80-231 Gdansk, Poland
E-mail: Dariusz.Mikielewicz@pg.gda.pl, rafal_andrzejczyk@wp.pl, jakubowska.blanka@gmail.com, jarekm@imp.gda.pl

Keywords: microjets, heat transfer intensification, boiling,

Flow boiling and flow condensation are often regarded as two opposite but symmetrical phenomena. Their description, however, with a single correlation has yet to be suggested. In the case of flow boiling in minichannels there is mostly encountered the annular flow structure, where the bubble generation is not present. Similar picture holds for the case of inside tube condensation, where annular flow structure predominates. In such case the heat transfer coefficient is primarily dependent on the convective mechanism.

In case of flow boiling/flow condensation in minichannels there is mostly encountered the annular flow structure [2], where the bubble generation/collapse is not present. In such case the heat transfer coefficient is primarily dependent on the convective mechanism, modeled in the majority of approaches from literature in terms of the Martinelli parameter. The difficulty in devising a general method for pressure drop and heat transfer calculations, applicable to both flow condensation and flow boiling, lies in the fact that the non-adiabatic effects are not included into the present in literature models. Non-adiabatic effects alter the shear stress in flow boiling as well as in flow condensation and, in authors opinion, are the main explanation why up to date approaches to common modeling of flow boiling and flow condensation fail to devise a single robust model for that purpose. Correct modelling of that heat flux enables to predict a thinner liquid film thickness in boiling and thicker in condensations at otherwise exactly the same flow conditions.

In the paper a method developed earlier by authors [3,1] is applied to calculations of pressure drop and heat transfer coefficient for flow boiling and also flow condensation for some recent data collected from literature for such fluids as R245fa, R600a, R134a, R1234yf and other. In case of modelling the annular flow the modification of interface shear stresses between flow boiling and flow condensation are considered through incorporation of the so called blowing parameter, which differentiates between these two cases of phase change. The shear stress between vapour phase and liquid phase is generally a function of non-isothermal effects. That is a major reason why that up to date approaches, considering the issue of flow boiling and flow condensation as symmetric, are failing in that respect. The way forward is to incorporate a mechanism into the convective boiling term responsible for modification of shear stresses at the vapour-liquid interface. Such mechanism has been presented earlier by the authors in [3]. In case of annular flow it contributes to thickening and thinning of the liquid film, which corresponds to condensation and boiling respectively. There is however a different influence of heat flux on the modification of shear stress in the bubbly flow structure, where it affects bubble nucleation. In case of bubbly flow structure the effect of applied heat flux is considered. As a result a modified form of the two-phase flow multiplier is obtained, in which the non-adiabatic effect is clearly pronounced.

In the paper presented will be comparisons with well established correlations for calculations of pressure drop and heat transfer coefficient. These results will be compares also with the predictions obtained by authors own model for pressure drop calculations as well as heat transfer coefficient. Satisfactory consistency of the latter model with experimental data for both flow boiling and flow condensation has been found.

References

1. Mikielewicz D., Mikielewicz J., A common method for calculation of flow boiling and flow condensation heat transfer coeffi-cients in minichannels with account of nonadiabatic effects, Heat Transfer Engineering, Volume 32, (13-14), 1173-1181, 2011.
2. Revellin R., Thome J.R., Experimental investigation of R134a and R245fa two-phase flow in microchannels for different flow conditions, Int. J. of Heat and Fluid Flow, 28, 63-71, 2007.
3. Mikielewicz D., Andrzejczyk R., Wajs J., Mikielewicz J., A general method for calculation of two-phase flow pressure drop in flow boiling and flow condensation, ECI 8th International Conference on Boiling and Condensation Heat Transfer, Lausanne, Switzerland, 3-7 June, 2012.

4th Micro and Nano Flows Conference
UCL, London, UK, 7-10 September 2014

Comparison of heat transfer characteristics in surface cooling with boiling microjets of water, ethanol and HFE7100

Dariusz Mikielewicz[1], Tomasz Muszynski[1]
1: Gdansk University of Technology, Faculty of Mechanical Engineering, Department of Energy and Industrial Apparatus
Narutowicza 11/12, 80-233 Gdansk, Poland
E-mail: Dariusz.Mikielewicz@pg.gda.pl, Tomasz.Muszynski@pg.gda.pl

Keywords: microjets, heat transfer intensification, boiling,

Accurate control of cooling parameters is required in ever wider range of technical applications. It is known that reducing the dimensions of the size of nozzle leads to an increase in the economy of cooling and improves its quality. Present study describes research related to the design and construction of the nozzles and microjet study, which may be applied in many technical applications such as in metallurgy, electronics, etc.

Using liquids such as water, boiling is likely to occur when the surface temperature exceeds the coolant saturation temperature. Boiling is associated with large rates of heat transfer because of the latent heat of evaporation and because of the enhancement of the level of turbulence between the liquid and the solid surface, Garimella and Rice (1995). This enhancement is due to the mixing action associated with the cyclic nucleation, growth, and departure or collapse of vapour bubbles on the surface. In the case of flow boiling, such as boiling under impinging jets, the interaction between the bubble dynamics and the jet hydrodynamics has significant effect on the rate of heat transfer. The common approach used to determine the rate of boiling heat transfer is by using a set of empirical equations that correlate the value of the surface heat flux or the heat transfer coefficient with the fluid properties, surface conditions, and flow conditions

These correlations do not provide much insight into the underlying physical mechanisms involved in the boiling heat transfer problem, Liu and Zhu (2002). The alternative approach is to use mechanistic models. There have been a number of mechanistic models developed for the case of pool boiling and for the case of parallel flow boiling. In the latter case, the boiling heat transfer phenomenon is more complicated due to the strong coupling between the flow, the thermal field, and bubble dynamics.

The basis of microjet technology is to produce laminar jets which when impinging the surface have a very high kinetic energy at the stagnation point, Mikielewicz and Muszynski (2009), Mikielewicz et al (2013). Boundary layer is not formed in those conditions, while the area of film cooling has a very high turbulence resulting from a very high heat transfer coefficient. Applied technology of jet production can result with the size of jets ranging from 20 to 500μm in breadth and 20 to 100μm in width. Presented data are used in order to validate semi-empirical theoretical model of surface cooling by evaporating microjet impingement in the stagnation point.

Main objective of this paper was to investigate the physical phenomena occurring on solid surfaces upon impingement of the single microjet in case of three fluids. Intense heat transfer in the impact zone of microjet has been examined and described with precise measurements of thermal and flow conditions of microjets. Reported tests were conducted under steady state conditions for surface cooling by single microjet producing an evaporating film.

Obtained database of experimental data with analytical solutions and numerical computer simulation allows the rational design and calculation of microjet modules and optimum performance of these modules for various industrial applications .

References

Garimella S.V., Rice R.A. (1995). Confined and submerged liquid jet impingement heat-transfer, Journal of Heat Transfer, vol.117, pp. 871–877.

Liu Z-H, Zhu Q-Z, (2002). Prediction of critical heat flux for convective boiling of saturated water jet impinging on the stagnation zone, Journal of Heat Transfer, vol. 124, pp. 1125-1130.

Mikielewicz D., Muszynski T. (2009). Experimental study of heat transfer intensification using microjets, Int. Symp. on Convective Heat and Mass Transfer in Sustainable Energy, Hammamet, Tunisia.

Mikielewicz D., Muszyński T., Mikielewicz J. (2013). Model of heat transfer in the stagnation point of rapidly evaporating microjet// Archives of Thermodynamics. Vol. 33, No. 1, pp.139-152.

4th Micro and Nano Flows Conference
UCL, London, UK, 7-10 September 2014

Influence of metallic porous microlayer on pressure drop and heat transfer of stainless steel plate heat exchanger

Jan Wajs[1], Dariusz Mikielewicz[1]
1: Gdansk University of Technology, Faculty of Mechanical Engineering, Department of Energy and Industrial Apparatus
Narutowicza 11/12, 80-233 Gdansk, Poland
E-mail: Dariusz.Mikielewicz@pg.gda.pl, janwajs@pg.gda.pl

Keywords: porous microlayer, heat transfer intensification, plate heat exchanger

Efficient heat production and distribution is very important from the economical and natural resources depletion points of view. Therefore an extensive research and development efforts have been undertaken in the area of heat transfer intensification over the past couple of decades. They refer to the one-phase convection and also to the boiling/condensation conditions. Nowadays we can observe a tendency to miniaturization in any field of life, but especially in the technical applications. At the same time, in the area of energy technology very important are the problems of high fluxes heat transfer. This is the reason why this new challenges require high efficiency of system components, especially high efficient and small capacity heat exchangers. It is known that in the recuperators the heat transfer coefficients on both sides of partition are the most significant and they determined their capacity. Because the overall heat transfer coefficient depends on the lowest value between the heat transfer coefficients, a special care should be given to the heat transfer conditions on the weaker side in the heat exchanger.

Plate heat exchangers have been widely used in power engineering, chemical processes and many other industrial applications due to their good effectiveness and compactness. Nevertheless there are still investigations going toward the more efficient and smaller size plate heat exchangers trough heat transfer intensification, because this kind of heat exchangers could be also prospectively applied in the heat recovery systems.

Recently a number of investigations on plate heat exchangers were reported in professional literature. Unfortunately, rather limited data for units with high performance microsizes, enhancement structures are available. Among them could be found works by Matsushima and Uchida (2002) who tested a brazed plate heat exchanger with a novel pyramid-like structure with R22 as working fluid. The structural features were 1.5 mm in height, hence, not in the microsized region, and the evaporation heat transfer coefficients were estimated to be 1.5–2 times higher than those of regular herringbone-type plates. A novel nano- and microporous structures were shown by Furberg et al. (2009). Their aim was to enhance pool boiling heat transfer caused by R134a with over one order of magnitude higher values in comparison with a plain machined copper surface. They presented an experimental study of the plate heat exchanger evaporator performance with and without this novel enhancement structure applied to the refrigerant channel. The knowledge and experiences connected with the passive heat transfer enhancement in the plate heat exchangers were also presented by Wajs and Mikielewicz (2013).

In the of paper the experimental analysis of passive heat transfer intensification in the case of plate heat exchanger has been conducted. The passive intensification was obtained by a modification of heat transfer surface, which was covered by a metallic porous microlayer.

The experiment was accomplished in two stages. In the first stage the commercial stainless steel gasketed plate heat exchanger was investigated, while in the second one – the identical heat exchanger but with the modified heat transfer surface. The direct comparison of thermal and flow characteristics between both devices was possible due to the assurance of equivalent conditions during the experiment. Equivalent conditions mean the same volumetric flow rates and the same media temperatures at the inlet of heat exchangers in the corresponding measurements' series. Experimental data were collected for the one-phase convective heat transfer and for boiling conditions in the water-ethanol system. The heat transfer coefficients were calculated using the Wilson method.

References

Matsushima H., Uchida M. (2002). Evaporation performance of a plate heat exchanger embossed with pyramid-like structures, J. Enhanced Heat Transfer, vol.9, pp. 171–179,

Furberg R., Palm B., Li S., Toprak M., Muhammed M. (2009). The use of a nano- and microporous surface layer to enhance boiling in a plate heat exchanger, Journal of Heat Transfer, vol. 131, doi: 10.1115/1.3180702,

Wajs J., Mikielewicz D. (2013). Effect of surface roughness on thermal-hydraulic characteristics of plate heat exchanger, Key Engineering Materials (in print),

Wajs J., Mikielewicz D. (2013). Heat transfer intensification by enlarged surface roughness in the plate heat exchanger. 8th International Conference on Multiphase Flow, Jeju, Korea.

4th Micro and Nano Flows Conference
UCL, London, UK, 7-10 September 2014

Pool Boiling Enhanced by Electric Field Distribution in Micro Sized Space

Ichiro Kano [1,*]

* Corresponding author: Tel.: ++81 (238)22 6257; Fax: ++81 (238)22 6257; Email: kano@yz.yamagata-u.ac.jp
1 Department of Mechanical engineering, Yamagata University, JPN

Keywords: Dielectric devices, Dielectric liquid, Electrohydrodynamics, Cooling, Thermal management

This paper describes results from an experimental and theoretical study of the effect of Electrohydrodynamic (EHD) force on the boiling curve of pool boiling. A dielectric liquid, which is fluorinated liquid, was selected as a working fluid. A boiling surface was electrically grounded, and an electrode was placed above the boiling surface at various heights of 200-400 μm. The slits were made in the electrode, whose width was several hundred micro meters, so as to remove vapor bubbles from the boiling surface by electrostatic force. From theoretical equation, critical heat flux (CHF) is depending on the electric field strength, the electrode height, and the total length of the slits. In this study, the effect of these parameters on the maximum heat flux was investigated experimentally and theoretically. As a result, the theoretical equation predicted the experimental results well. The maximum CHF showed 76 W/cm^2 at the electric field of -5 kV/mm, the electrode height of 400 μm, and the total slits length of 114mm, which was about four times over pool boiling.

1 Experimental facility

In order to create the high electric field and produce EHD convection over the boiling surface, a micro-sized electrode shown on Fig. 1 was used. The width of the slits, *Ws*, was changed from 400 to 500 μm that was designed to be larger than the bubble size at departure of 168 μm. The widths of the electrodes, *We*, was changed from 1000 to 1500 μm and the total length of the slits, *Ls*, was changed from 87 to 128 mm. The boiling process took place on the 15 mm diameter top surface of an oxygen-free copper block.

2 Experimental results

Figure 2 shows the heat flux as a function of wall super heat. The electrode was placed above the boiling surface at height of 400 μm. In this figure, the heat flux for the pool boiling is showed to compare with that with the application of electric field. The boiling process was changed in four regions (A-B, B-C, C-D, and D-CHF). The maximum heat flux shows 65 W/cm^2 while the maximum heat flux for pool boiling shows 22 W/cm^2.

The ratio of the critical heat flux, $q_{EHD\ max}$, with the application of electric field to that for pool boiling, q_{max}, was compared with the theoretical results as shown in Fig 3. The EHD enhancement was sufficiently detected by the theoretical results.

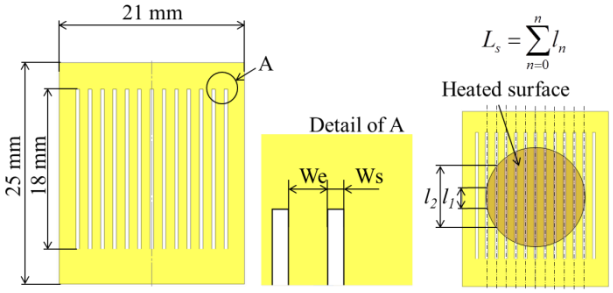

Fig. 1 Electrode geometry

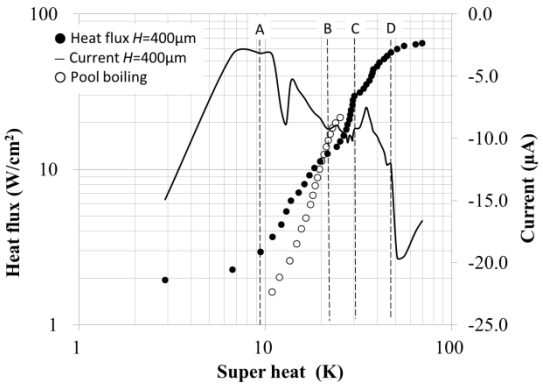

Fig. 2 Relationship between heat flux and current as a function of wall superheat at *E*= -5 kV/mm
(*Ws* = 400 μm, *We* = 1000 μm, *Ls* = 128 mm)

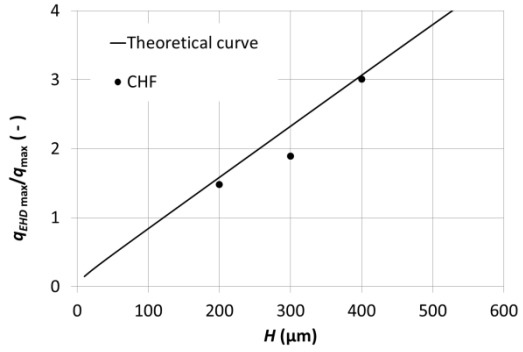

Fig. 3 Enhancement for CHF by electric field at *E* = -5 kV/mm

4th Micro and Nano Flows Conference
UCL, London, UK, 7-10 September 2014

Similarities in Dielectrophoretic and Electrophoretic Traps

Nichith CHANDRASEKARAN [1], Ramki MURUGESAN [1], Jae Hyun PARK [2,3,*]

* Corresponding author: Tel.: +82 (0)55 772-1585; Fax: +82 (0)55 772-1580; Email: parkj@gnu.ac.kr
1 School of Mechanical and Aerospace Engineering, Gyeongsang National University, South Korea
2 Department of Aerospace and System Engineering, Gyeongsang National University, South Korea
3 Research Center for Aircraft Parts Technology, Gyeongsang National University, South Korea

Keywords: dielectrophoretic trap, Paul trap, random motion, universality

Dielectrophoresis (DEP) is the motion of suspended particles in solvent resulting from polarization forces induced by an inhomogeneous electric field. DEP has been utilized for various biological applications such as trapping, sorting, separation of cells, viruses, nanoparticles, etc. Also, the analysis of DEP trap has been so far focused on the static features by employing the time-averaged ponderomotive force components while the dynamic features of DEP trapping (e.g. random motion) have not been attracted. However, the recent study about aqueous electrophoretic Paul trap showed a close relation between particle properties and the random motions, which cannot be understood via the ponderomotive effects. The random motion would be critical when the particle size shrinks to nanoscale, in which the random motion become comparable to the particle size.

In the present study, we consider the planar quadrupole dielectrophoretic trap (planar QDT, see Figure 1), in which four electrodes are aligned mutually perpendicular and pointing towards the trap center. The oscillating (AC) electric fields are applied to the electrodes such that the phase angle of the field between adjacent electrodes is 180˚. Such geometrical configuration is exactly same as that of planar Paul trap (planar PT) which is typically used to trap the charged atom and ions in low pressure environment [2].

Although both planar QDT and PT employ the quadrupole electrodes with AC field, their analyses are quite different: For DEP traps, people have mostly been interested in the static characteristics, which is governed by the ponderomotive components. However, for PT the rigorous understanding of dynamic features (e.g. stability) including static ones has been established with the aid of Mathieu function theory. It enables an accurate estimation of particle random motion at longtime limit.

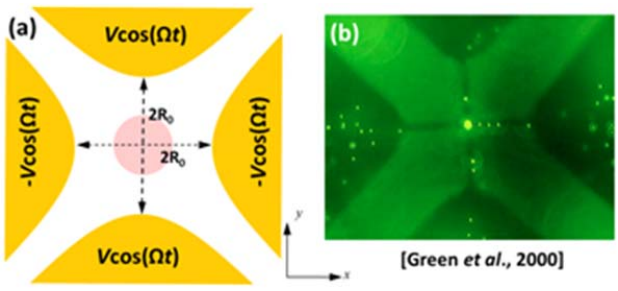

Figure 1 (a) Schematic of quadrupole Paul/dielectrophoretic traps; (b) Trapping of sub-micro particles with quadrupole dielectrophoretic trap (experiment) [1]

Considering all the above, in the present study we are pursuing two issues: (1) Establishment of a universal theoretical protocol applicable to both planar QDT and PT; (2) Accurate estimation of random fluctuation in QDT. In order to do that, we consider the instantaneous formulation of DEP force and the random noise modeled by Wien process. Then, the equation of motion of planar QDT has become quite similar with that of planar PT:

$$\frac{d^2x}{d\tau^2} + b_{DEP}\frac{dx}{d\tau} + [a_{DEP} - 2q_{DEP}\cos(2\tau - \phi)]\,x = W_{DEP}(\tau) \qquad \text{for QDP}$$

$$\frac{d^2x}{d\tau^2} + b_{PT}\frac{dx}{d\tau} + [a_{PT} - 2q_{PT}\cos(2\tau)]\,x = W_{PT}(\tau) \qquad \text{for PT}$$

where b_{PT}, a_{PT}, q_{PT}, b_{DEP}, a_{DEP}, and q_{DEP} are the system parameters, and the dynamic features of trap are determined by them.

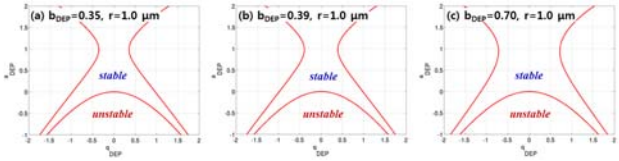

Figure 2 Stability plot for μ-trap with various b_{DEP}-values: (a) b_{DEP} = 0.35; (b) b_{DEP} = 0.39; (c) b_{DEP}= 0.70.

The random motions are estimated by the direct computation of the equation of motion averaged over the sufficient repetitions. Also, we develop the pseudo-potential expression of the fluctuation and it can be validated through comparison with the direct computation.

The present study will enable to identify the comprehensive dynamics of planar QDT including random fluctuation. It will be a milestone in designing the nanoscale QDTs.

References:

[1] N G Green, A. Ramos, and H. Morgan, J. Phys. D: Appl. Phys. **3**, 632 (2000).
[2] W. Paul, Rev. Mod. Phys. **62**, 531 (1990).

4th Micro and Nano Flows Conference
UCL, London, UK, 7-10 September 2014

A novel micro-separator using the capillary separation effect with locally populated micro-pin-fin structure

Bin An[1], Jinliang Xu [1,2,*], Dongliang Sun [2,*]

* Corresponding authors: Jinliang Xu, Tel.: ++86 (10)61772058; Email: xjl@ncepu.edu.cn
Dongliang Sun, Tel.: ++86 (10)61772079; Email: dlsun@ncepu.edu.cn
1 State Key Laboratory of Alternate Electrical Power System with Renewable Energy Sources, North China Electric Power University, Beijing, 102206, China
2 Beijing Key Laboratory of Multiphase Flow and Heat Transfer, North China Electric Power University, Beijing, 102206, China

Keywords: Micro-separator, Micro-pin-fin, Capillary effect, Optimal design.

Phase separation is an important process in many chemical engineering applications, such as reactive processes and thermal separation processes of components. Given that microstructure engineering is becoming more important in fields of chemical engineering, such as distillation and absorption, the phase separation in mini or micro assemblies should be dealt with. Generally, the gas/vapor–liquid phase separation can be achieved through mechanisms such as gravity, centrifugal forces, impingement and surface tension forces.

In this paper a novel micro-separator was proposed using the capillary separation effect. The micro-pin-fins are locally populated in a rectangular microchannel, forming an enclosed region with micro pores as the boundaries. Thus, the microchannel cross section is divided into two symmetrical side regions close to the microchannel side wall and a center enclosed region. When a two-phase stream interacts with the enclosed region boundary with micro-pores, the gas phase is prevented from entering the center enclosed region to enforce the gas phase flowing in the two side regions. Meanwhile, the liquid phase is flowing towards the center enclosed region. Thus, the two-phases are separated. Many parameters are involved in the capillary separation process.

A mathematical model was proposed. The Volume of Fluid (VOF) method deals with the two-phase interface tracking. A non-uniform grid system was used to compute the near pore area and the two-phase interface. The separation efficiency and the pumping power were selected as the optimal parameters. A set of cases were computed. The effect of various operating parameters such as the two-phase flow rates as well as the separator configuration parameters such as pin-fin size and distribution are analyzed based on the computation results. It is found that the proposed micro-separator is wonderful to have high separation efficiency with small pumping powers. In addition to these, the phase separation concept is extended to develop a perfect micro-condenser. This is due to the ultra-thin liquid film generated by the separated flow paths of the two-phases. Condensation heat transfer and its mechanism were investigated.

4th Micro and Nano Flows Conference
UCL, London, UK, 7-10 September 2014

Design of an air-flow microchamber for microparticles detection

Elena BIANCHI [1] & Francesca NASON [1], Marco CARMINATI [2], Lorenzo PEDALÀ [2], Luca CORTELEZZI [1,3], Giorgio FERRARI [2], Marco SAMPIETRO [2], Gabriele DUBINI [1,*]

* Corresponding author: Tel.: ++39 02 2399 4254; Fax: ++39 02 2399 4286; Email: gabriele.dubini@polimi.it
1 Politecnico di Milano, Dept. of Chemistry, Materials and Chemical Engineering, Lab. of Biological Structure Mechanics, Milan, Italy
2 Politecnico di Milano, Dept. of Electronics, Information Science and Bioengineering, Milan, Italy
3 McGill University, Dept. of Mechanical Engineering, Montreal, QC H3A 2K6, Canada

Keywords: air pollution, atmospheric dust, PM10, microparticles detection

1. Introduction

The effect of pollution on air quality is nowadays a major concern, especially in metropolitan and industrialized areas. Several studies [1] demonstrated that airborne particulate matter (PM) can be harmful to human health. According to the size, PM can penetrate further into the respiratory system [2]: particles smaller than 2.5 µm (PM2.5) can reach the bronchioles, while the 2.5-10 µm particles (PM10) are trapped by the cilia from the nose to the bronchi. A few instruments, mainly based on optical detection, are available on the market for the monitoring of air in urban areas and critical workplaces [3]. Emerging microelectronic and MEMS technologies could be successfully adopted for the miniaturization of the devices, aiming at developing less expensive and bulky systems, dedicated to personal and pervasive monitoring, while preserving single-particle screening and sizing capability. In this context we designed a microfluidic device in order to capture and deposit PM10 and PM2.5 on top of microelectrodes for detection and characterization (granulometry) by means of high-sensitivity (aF range) microcapacitance measurements.

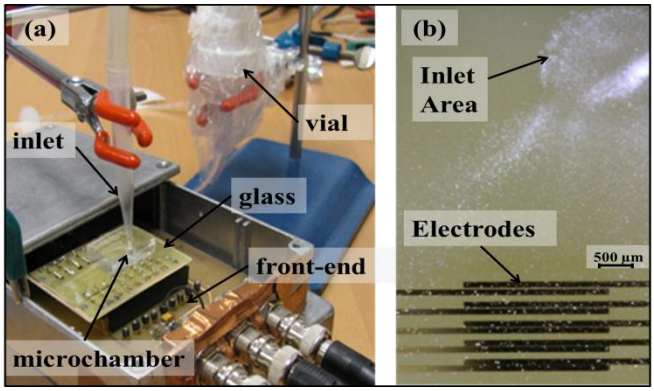

Fig. 1 (a) Set up: vial, nozzle-shaped inlet, PDMS chamber, glass substrate with the electrodes plugged in the low-noise analog front-end. (b) Monolayer of particles on the glass substrate altering the interelectrodes capacitance.

2. Materials and Methods

Planar gold electrodes were microfabricated on a glass substrate for the detection of particles by electrical impedance measurements. The design of the microfluidics consists in a 10 mm wide, 200 µm high and 15 mm long micro-chamber fabricated by soft lithography, to be positioned on the glass surface, in correspondence of the electrodes. An air flow seeded with micrometric particles is injected into the chamber through a nozzle-shaped inlet tubing properly oriented (Fig. 1a). The outlet has the same aspect ratio as the chamber, 10 mm × 200 µm. The loading process relies on the extraction of a small fraction from a suspension created by forcing pure air flow (HEPA filter 0.2 µm) in a vial containing a selected powder sample as a substitute for airborne PM10, (microtalc powder, Mondo Minerals BV, Amsterdam, 8 µm average diameter and ε_r ~2.4). The small fraction is then injected into the microchamber where the fluid dynamic field induces the dispersion of particles into a low density monolayer on the glass surface. Since the sensitive region is significantly smaller than the glass surface, the presence of single particles laying on this area can be detected.

3. Results and discussion

The configuration of the vial and the tubing connecting the vial to the chamber results in a successful extraction of a particle fraction, suitable for obtaining a well dispersed monolayer of particles on the glass surface. The monolayer is not homogeneously distributed along the bottom of the chamber: higher surface density can be found in the proximity of the inlet (Fig. 1b), gradually decreasing towards the outlet. Tuning the location of the electrodes with respect to the inlet is critical for depositing on the sensitive region (4 µm gap) the desired dust surface density and to perform single particle detection (Fig. 2).

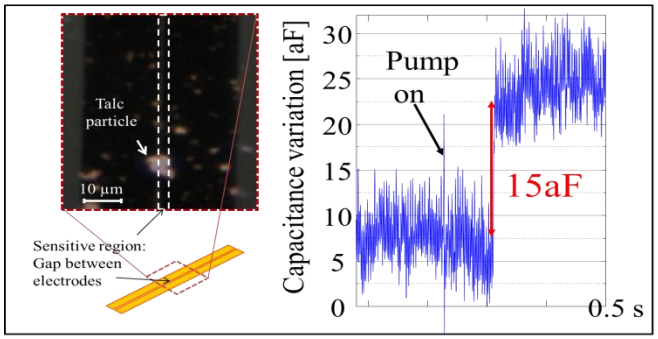

Fig.2 (a) Particles deposited in the sensitive region between the electrodes and (b) the corresponding real-time capacitance measurement showing a single detection event of 15 aF increase, consistent with a ~8 µm talc microparticle.

4. References

[1] Gilles J.A. et al. *Environ. Sci. Technol. 35(6): 1054 -1063* (2001)
[2] Matè et al. *Sci. Total Environ.* 408(23): 5750-5757 (2010)
[3] Carminati M. et al. *Proc. IEEE EESMS*: 1-6 (2011)

4th Micro and Nano Flows Conference
UCL, London, UK, 7-10 September 2014

Microfluidic Platform for Adherent Single Cell High-Throughput Screening

Paola OCCHETTA[1], Chiara MALLOGGI[2], Andrea GAZANEO[1], Mara LICINI[1], Alberto REDAELLI[1], Gabriele CANDIANI[2], Marco RASPONI[1*]

* Corresponding author: Tel.: +39 (02) 2399 3377; Email: marco.rasponi@polimi.it
1 Department of Electronics, Information and Bioengineering, Politecnico di Milano, Milano, Italy
2 Department of Chemistry, Materials and Chemical Engineering "Giulio Natta", Politecnico di Milano, Milano, Italy

Keywords: Microfluidics, Single Cell, High-Throughput Screening, Chaotic Mixing, Gene Delivery

Introduction

Traditionally, *in vitro* investigations on biology and physiology of cells rely on averaging the responses eliciting from heterogeneous cell populations. These tests are unsuitable for assessing the individual cell behavior and evolution upon external stimulation. Single cell assays represent a promising tool aiming at pursuing the direct and deterministic control over these cause-effect relationships guiding cell behavior [1]. Herein, a single-cell level microfluidic platform is presented for isolation and culture of a large number of individual adherent cells into defined spatial configurations, exploiting a dynamic variation of fluidic resistance. The platform represents a powerful and versatile tool for high-throughput screenings on single cells, integrating gradient generator which allows for delivering both soluble factors and non-diffusive molecules under spatio-temporally controlled chemical patterns.

Materials and Methods

The presented single cell microfluidic platform consists of two functional elements: a gradient generator and a cell culture region. Two input ports deliver through the gradient generator six linear dilutions to as many downstream culture units. Each unit is independently addressable and includes 48 culture chambers.
The cell trapping mechanism, optimized by means of Computational Fluid Dynamic models (CFD, Comsol Multiphysics), exploits an automatic variation of hydraulic resistance within the culture chamber. It presents (i) an upper, large opening which allows the entrance of both cells and diffusive media/conditioning factors, and (ii) a smaller bottom trapping junction controlling the variable fluidic resistance before and after cell trapping (Fig 1).

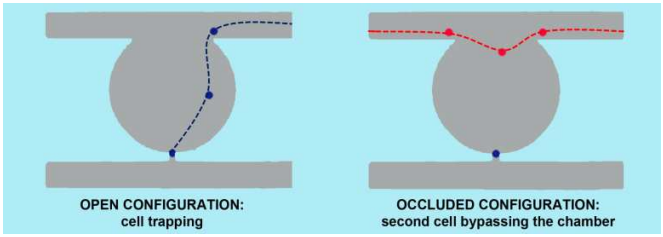

Fig 1. *Single cell trapping mechanism within a culture chamber (top view)*

The gradient generator has been designed by means of computational analyses for mixing both soluble factors and non-diffusive molecules, aiming at creating linear concentration patterns. For this purpose, herringbone (HB) structures were added on top of the channels constituting the gradient layout, aiming at triggering chaotic secondary flows thus decreasing the diffusion length and, eventually, increasing the mixing efficiency (Fig 2) [2].
Preliminary biological experiments were conducted with U87-MG glioblastoma cell line to evaluate both trapping efficiency and device compatibility for adherent single cell cultures.

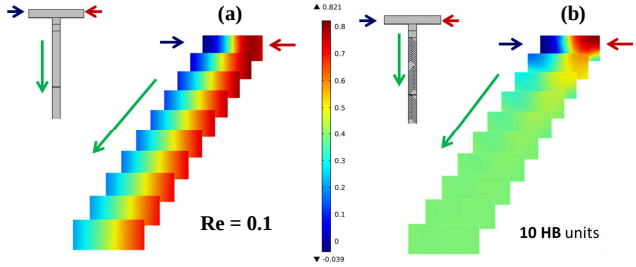

Fig 2 *CFD simulation results (Re=0.1) showing the flow mixing along a channel geometry (a) without and (b) with HB.*

Results and discussion

The functionality of the two functional units was assessed in terms of (i) cell trapping efficiency and (ii) soluble and non-diffusive molecules mixing efficiency. The proposed trapping mechanism allows to efficiently fill the six culture units with individual cells (cell ø 16 µm) within few minutes, exploiting a pressure driven control.

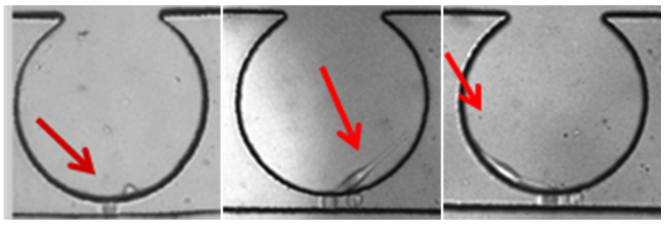

Fig 3. *Single cell culturing within a culture chamber*

The generation of specific concentration patterns was then demonstrated. In particular a linear concentration gradient of cells was obtained by perfusing chondrocytes (ø 10 µm) through the HB chaotic gradient generator, extending the potentiality of the device for high-throughput screening over a wide range of molecules and particles. Finally, single cells seeded within the device were cultured for 7 days, showing the platform is a versatile and biocompatible tool for monitoring individual cell behavior over time (Fig 3).

Conclusion

The presented microfluidic platform represents a powerful tool for high-throughput screenings at a single-cell level. Combining a high trapping efficiency with the ability to generate concentration patterns over a wide range of factors, the device will be useful for optimizing gene delivery and cell transfection protocols.

References

[1] Hong, S., Q. Pan, and L.P. Lee, *Single-cell level co-culture platform for intercellular communication.* Integr Biol, 2012. **4**(4): p. 374-80.
[2] Kee, S.P. and A. Gavriilidis, *Design and characterisation of the staggered herringbone mixer.* Chem Eng J, 2008. **142**(1): p. 109-121.

4th Micro and Nano Flows Conference
UCL, London, UK, 7-10 September 2014

Microdevices for Continuous Sized Based Sorting by AC Dielectrophoresis

Emre ALTINAGAC [1,*], Yavuz GENC [1], Huseyin KIZIL [2], Levent TRABZON [3], Ali BESKOK [4]

* Corresponding author: Tel.: +9 (0)5462591989; Email: altinagac@itu.edu.tr
1 Department of Nanoscience & Nanoengineering, Istanbul Technical University, Turkey
2 Faculty of Chemical and Metallurgical Engineering, Istanbul Technical University, Turkey
3 Department of Mechanical Engineering, Istanbul Technical University, Turkey
4 Department of Mechanical Engineering, SMU Lyle School of Engineering, USA

Keywords: AC Dielectrophoresis, Field-Flow-Fractionation, Microfluidics, Lab-on-a-Chip

Lab-on-a-Chip devices (LOCs) provide inexpensive and efficient solutions for integrating several laboratory functions on a single chip of only a few centimeters in size. LOCs are used for biomedical and environmental applications, such as, fluid transport, drug delivery, diagnosis of viruses and bacterias and manipulation of particles for focusing and separation applications. The particle movements can be observed without labeling the particles which put this technique forward for biological cell and submicron scale particle separations.

Dielectrophoresis (DEP) is a force acting on a dielectric particle when it is subjected to a non-uniform electric field which can be a DC or an AC field. Contrary to electrophoresis (EP), suspended particles do not need to have a surface charge, DEP only occurs when there are induced charges in non-uniform field. A dielectric particle polarizes under a non-uniform electric field and there is a net dipole moment acting on it. [1,2]

The time averaged dielectrophoretic force on the particle is given by [3]:

$$F_{DEP} = 2\pi\varepsilon_0\varepsilon_m a^3 Re(f_{cm})\nabla E^2$$

Where ∇E^2 is the gradient of the root mean square of the electric field, f_{cm} is the Clausius-Mossotti (CM) factor which is a function of particle and fluid properties, determines the direction of the dielectrophoretic force and Re(…) indicates the real part of CM factor, a is the diameter of the particle [3].

Particles interact with non-uniform electric fields in two ways: particles are either trapped in regions where the local electric field lines are intense which is called positive dielectrophoresis (pDEP), or pushed from this regions which is called negative dielectrophoresis (nDEP). The electrical properties of the particles and the frequency of the applied electric field determine the behavior of DEP.

In this project, various microfluidic devices are designed for separating microparticles and cells. The flow behaviors of particles for each design are modeled and simulated using COMSOL Multiphysics 4.3a software. Polystyrene particles in different diameters (3.2 μm and 9.8 μm) are used in our experiments and we plan to do the experiments with circulating tumor cells (CTCs).

Array of interdigitated electrodes are used to create electric field gradients along the microchannel and placed at 45° angle to repel the particles from the electrodes. Total force caused by the both hydrodynamic drag force and nDEP on particles causes them to deflect along the electrode geometry. Over the length of the device, larger particles deflect more than the smaller particles according to formula of F_{DEP} and that makes the separation of particles in different sizes is possible.

LOCs which have a Ti interdigitated electrode layer on a glass substrate and a PDMS microchannel is fabricated to investigate the most effective design for separating particles based on their sizes. The standard photolithography techniques and lift off processes are used in order to obtain the LOC devices.

Interdigitated electrodes are placed either only on the bottom glass substrate or both of the bottom and top glass substrate to increase the efficiency of the separation. Stronger electric field gradients are generated by devices which have an electrode layer on both of the bottom and top substrate on the contrary the fabrication steps are complex compared with the one-sided electrode based devices. We also added a focusing region before the particles reach to electrodes which prevents the randomly distribution of the particles across the channel and makes the separation more efficient.

Dielectrophoresis is an effective method to separate particles in different sizes and even living cells without any damage which put this technique forward for further investigations and analysises on collected/trapped cells. We investigate the different parameters and present the most effective method for separation of particles in different sizes by AC Dielectrophoresis.

---

[1] Castellanos, A., Ramos, A., Gonzales A., Green, N.G., and Morgan, H. (2003). Electrodynamics and Dielectrophoresis in Microsystems: Scaling Laws, in *Journal of Physics D: Applied Physics*, 36, p. 2584-2597.

[2] Morgan, H., and Green, N.G.O (2003). *AC Electrokinetics: Colloids and Nanoparticles,* (Research Studies Press, United Kingdom).

[3] N.G. Green, A. Ramos, & H. Morgan. *Journal of Electrostatics, 56*, 235-254. (2002).

4th Micro and Nano Flows Conference
UCL, London, UK, 7-10 September 2014

Three-dimensional multi-level heat transfer model of silica aerogels

He LIU, Zeng Y. LI*, Xin P. ZHAO and Wen Q. TAO
*corresponding author: Tex: + 86 29 82665446; Fax: + 86 29 82665445; Email: lizengy@mail.xjtu.edu.cn
Key Laboratory of Thermo-Fluid and Science and Engineering, Ministry of Education
School of Energy and Power Engineering, Xi'an Jiaotong University, Xi'an 710049, P.R. China

Key words: silica aerogels, DLCA，Monte Carlo，effective thermal conductivity

Silica aerogels have extraordinary properties resulting from their highly porous nanostructures of nanoparticle aggregation as shown in Fig 1(a) made by sol-gel process and supercritical drying. Because of the nano-sized pores and interconnected long particle chains, silica aerogels have been used as super insulating material. Description of heat transfer model of silica aerogels has interested many scientists since 30 years. One kind of thermal conductivity model is based on a cubic array of unit cell structure of spherical full density nanoparticles or rods[1,2]. The other is a numerical model using fractal structure[3]. However, these models neglect the influence of random nature of the real structure and the helium pycnometry experiment shows that the measured skeletal density of silica aerogels is smaller than the amorphous silica density[4].Therefore, a porous secondary nanoparticle aggregate structure is more feasible in which the secondary nanoparticle is accumulated by primary particles.

This paper focuses on the heat conduction of silica aerogels based on a 3-D heat transfer model generated by Diffusion-limited cluster aggregation(DLCA) while the secondary particles are developed by the Monte Carlo method which allowing the packing with arbitrary size distribution of spheres[5]. We further develop a fractal thermal conductivity model which related to the tortuosity, fractal dimension, porosity, size distribution of micro pores and the ratio of λ_s/λ_g[6]. Finally the effective thermal conductivity of the Multi-level model will be analyzed and the relation between the structure parameters and the effective thermal conductivity will be obtained.

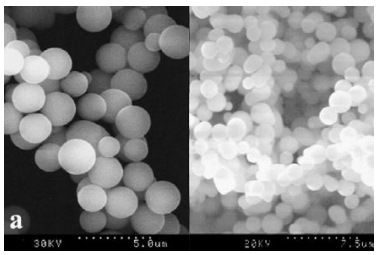

(a) SEM and TEM pictures of silica aerogels (Moner-Girona et al., 2003)

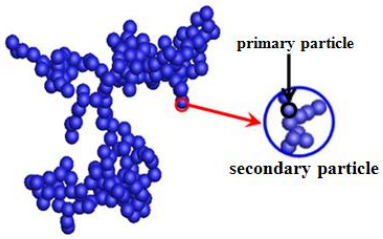

(b) 3-D heat transfer model(developed by DLCA)

Fig.1 The microstructure and heat transfer model of silica aerogels

Reference:

[1] Zeng, S.Q., Hunt, A., Grief, R., 1995. Geometric structure and thermal conductivity of porous medium silica aerogel. J. Heat Transfer 117(4), 1055–1058.

[2] Wei, G.S., Liu, Y.S., Zhang, X.X., et al., 2011. Thermal conductivities study on silica aerogel and its composite insulation materials. Int. J. Heat Mass Transfer 54 (11–12), 2355–2366.

[3] Spagnol, S., Lartigue, B., Trombe, A., et al., 2008. Modeling of thermal conduction in granular silica aerogels. J.Sol-Gel Sci. Technol 48(1–2), 40–46.

[4] Fricke, J., Tillotson, T., 1997. Aerogels: production, characterization, and applications, Thin solid films 297(1–2), 212–223.

[5] Reyes, S.C., lglesia, E., 1991. Monte Carlo simulations of structural properties of packed beds. Chem. Eng. Sci. 46(4), 1089–1099.

[6] Yu, B.M., Chen, P., 2002. Fractal models for the effective thermal conductivity of bidispersed porous media Monte Carlo simulations of structural properties of packed beds. J. Thermophys Heat Transfer 16(1), 22–29.

4th Micro and Nano Flows Conference
UCL, London, UK, 7-10 September 2014

The gas leakage dynamic flow in nanoporous silica aerogel under different pressure difference

Xin P. ZHAO, Zeng Y. LI*, He LIU and Wen Q. TAO

*corresponding author: Tex: +86 29 82665446; Fax: +86 29 82665445; Email: lizengy@mail.xjtu.edu.cn
Key Laboratory of Thermo-Fluid and Science and Engineering, Ministry of Education
School of Energy and Power Engineering, Xi'an Jiaotong University, Xi'an 710049, P.R. China

Keywords: DSMC, Gas Leakage, Silica Aerogel

Silica aerogel is a kind of nonporous material which has properties such as high porosity (80%-99.8%), low density (0.003-0.500 g/cm^3), high specific surface area (500-1200 m^2/g) and low thermal conductivity (0.017- 0.021Wm^{-1}K^{-1}, in air, 300K)[1,2]. It has excellent properties on thermal insulation, filter, chemo catalysis and other aspects[2]. The nano structure of silica aerogel is similar as pearl-necklace network formed by sol-gel process. The heat transfer in silica aerogel includes the heat conduction through solid skeleton and gas phase, and thermal radiation. In most cases, the heat transfer through gas plays a dominant role[2].

Generally, the gaseous thermal conductivity in silica aerogel is much lower than that in free space because the gas molecules are constrained by the complex structure of solid framework. However, the gas leakage dynamic flow may weaken the thermal insulating performance of silica aerogel if there exists a pressure difference from the aerogel materials to the working environment.

In the present study, three-dimensional (3D) diffusion-limited cluster-cluster aggregation (DLCA) method is adopted to generate the complex inner structure of silica aerogel (Figure 1)[4]. The gas flow and mass transfer in silica aerogel under different pressure difference between internal silica aerogel and atmosphere is predicted by using 3D direct simulation Monte Carlo (DSMC) method[5]. The permeability will be obtained and compared with the related experimental results[6]. Finally, the effect of the gas leakage dynamic flow on the thermal insulating performance of silica aerogel will be discussed.

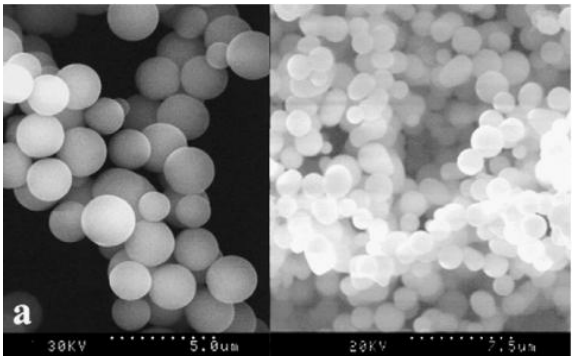

(a)The TEM picture of silica aerogel

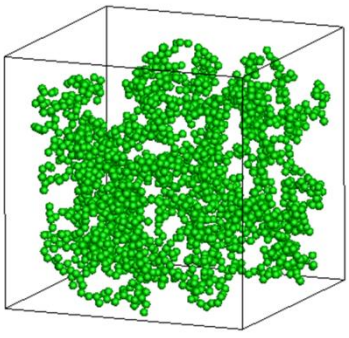

(b) Structure of silica aerogel generated by DLCA

Fig.1. The structure of silica aerogel

References:

[1] Dorcheh S, A., and Abbasi M. H.. Silica aerogel; synthesis, properties and characterization. Journal of materials processing technology 199.1 (2008): 10-26.

[2] Hüsing, Nicola, and Ulrich S. Aerogels—airy materials: chemistry, structure, and properties. *Angewandte Chemie International Edition* 37.1‐2 (1998): 22-45.

[3] Stumpf C, Von Gässler K, Reichenauer G, et al. Dynamic gas flow measurements on aerogels [J]. Journal of non-crystalline solids, 1992, 145: 180-184.

[4] Meakin, Paul, and Remi J. The effects of restructuring on the geometry of clusters formed by diffusion‐limited, ballistic, and reaction‐limited cluster–cluster aggregation. The Journal of

chemical physics 89 (1988): 246.

[5] Bird G.A, *Molecular Gas Dynamics and the Direct Simulation of Gas Flows (Clarendon, Oxford, 1994).*

[6] Hosticka B., et al. Gas flow through aerogels. Journal of non-crystalline solids 225 (1998): 293-297.

4th Micro and Nano Flows Conference
UCL, London, UK, 7-10 September 2014

Flow Boiling Heat Transfer of Refrigerant R-134a in Copper Microchannel Heat Sink

Vladimir V. Kuznetsov*, Alisher S. Shamirzaev

* Corresponding author: Tel.: +7 (383)3307121; Fax: +7 (383)3308480; Email: vladkuz@itp.nsc.ru
Kutateladze Institute of Thermophysics SB RAS, Russian Federation

Keywords: Flow Boiling, Microchannel Heat Sink, Refrigerant, Heat Transfer, Pressure Losses

In recent years, flow boiling in microchannels has received considerable attention due to its capability for thermal management of microelectronics and development of the microevaporators for a wide range of applications. Despite the fact, that this problem was addressed in many studies, flow boiling heat transfer in microchannel heat sink is still not fully understood. When one reduces the channel size, a wide variety of phenomena, which are not typical for conventional tubes, become apparent. The degree of their manifestation depends not only on the geometric scale, but also on the shape of channels, heat fluxes, pressure, etc. In this paper we study heat transfer at flow boiling of refrigerant R-134a in horizontal microchannel heat sink made from copper. The primary objective of this study is to establish experimentally how the heat transfer coefficient and pressure drop correlate with heat flux, mass flux and vapor quality.

The microchannel plate was made using a jeweler's saw. It contained 21 microchannels with 335x930 μm cross-section and fin thickness of 650 μm at total plate thickness of 2.5 mm. The top of microchannel plate was covered by 0.5-mm copper plate. The microchannel plate and heating block were soldered into the stainless steel framework which had two sections divided by the partition sheet for the local heat flux measurements. The test section was thermally insulated and heat losses were determined for different heat sink temperatures. The refrigerant R-134a was fed from the condenser through the filter and flow controller to the pre-evaporator via the pump. Then it went through the pre-evaporator to achieve the flow with desired vapor quality, passed to the microchannel heat sink and came to the condenser. The liquid flow rate was measured by the flow controller with an accuracy of 0.022 g/sec. Wall temperatures were measured by insulated thermocouples with 0.5 mm diameter along two lines at the distances of 5 mm, 15 mm, 25 mm, and 35 mm from the micro-channels inlet. The pressures and temperatures in the inlet and outlet chambers of test section were measured using the static and differential pressure probes and insulated thermocouples.

The local heat transfer coefficients were determined using the measurements of heat sink wall temperatures. Corresponding saturation temperatures in the microchannels were determined using linear approximation of pressure drop in the microchannels. The heat transfer coefficient was determined using the model of fin efficiency and for most experiments the fin efficiency exceeded 0.98. The vapor quality at the heat sink inlet was determined through the heat generated in the steam generator and the liquid temperature at the steam generator inlet. We verified the measurement procedure via the tests on measuring the distribution of heat transfer coefficient along the length of heat sink during the subcooled flow of refrigerant. The measured heat transfer coefficients agreed well with the prediction for laminar thermally developing flow.

Distribution of local heat transfer coefficients along the length and the width of the microchannel plate were measured in the range of external heat fluxes from 50 to 500 kW/m^2; the mass flux was varied within 150-600 kg/m^2 s, and the static pressure was varied within 6-10 bar. The variation of the inlet vapor quality for fixed heat flux shows that local heat transfer coefficients are weakly sensitive to the vapor quality and not sensitive to the flow rate. For refrigerant R-134a flow boiling in the microchannel heat sink, the obvious impact of the heat flux on magnitude of heat transfer coefficient was observed. It shows that the nucleation boiling is the dominant mechanism of heat transfer at R134a flow boiling, but the entrance effects have a strong influence on the value of inlet heat transfer coefficients. Another important mechanism of flow boiling heat transfer in microchannel heat sink at heat fluxes higher 30 kW/m^2 is a slight suppression of nucleate boiling at vapor quality growth. At heat flux less than 30 kW/m^2 evaporation of liquid film can be the dominant mechanism of heat transfer at high vapor quality. A new model of flow boiling heat transfer was proposed and verified experimentally in this paper; this model accounts the nucleate boiling suppression and liquid film evaporation heat transfer. This model predicts the reduction of heat transfer coefficients at high vapor quality if the nucleate boiling suppression is dominant. If the interface shear stress at high mass flux is sufficiently high to produce an extremely thin liquid film, the model predicts the enhancement of heat transfer at high quality for flow boiling in microchannel heat think with refrigerant R-134a as the working fluid.

The determination of friction pressure losses at adiabatic two-phase flow using wall thermocouple measurements shows that the Lockhart-Martinelli correlation with the value of the constant C recommended by Chisholm is in good agreement with experimental data. Also the inlet and outlet pressure drops in the chambers of heat sink were determined from total pressure drop measurements. They are in agreement with the calculation using the separated flow model. It allows one to determine the friction pressure drop for flow boiling in microchannel heat sink using the separated flow model calculation and measured total pressure drop. Comparison of the data on friction pressure losses during flow boiling with calculations according to the Lockhart-Martinelli correlation shows the additional pressure losses due to phase change in the microchannels.

This work was partially supported by the RFBR, grant 11-08-01140-a and Department EMEMP RAS, project No. 4.3.

4th Micro and Nano Flows Conference
UCL, London, UK, 7-10 September 2014

Lab-on-Chip for testing Myelotoxic effect of drugs and chemicals

Marco RASPONI[1], Andrea GAZANEO[1], Arianna BONOMI[2], Paola OCCHETTA[1], Loredana CAVICCHINI[2], Valentina COCCE[2], Gianfranco B. FIORE[1], Augusto PESSINA[2], Alberto REDAELLI[1,*]

* Corresponding author: Tel.: +39 02 2399 3375; Fax: +39 02 2399 3360; Email: alberto.redaelli@polimi.it
1 Department of Electronics, Information and Bioengineering, Politecnico di Milano, IT
2 Department of Biomedical, Surgical and Dental Sciences, Università degli Studi di Milano, IT

Keywords: Microfluidics, Microfluidic device, Clonogenic test, CFU-GM, CB MNC, Cell culture

Introduction

In 2006 the European Centre for the Validation of Alternative Methods (EVCAM) has approved the Colony Forming Unit-Granulocytes-Macrophages (CFU-GM) test, which is the first and currently unique test applied to evaluate the myelotoxicity of xenobiotics *in vitro*.
The current test [1] is a clonogenic assay based on the study *in vitro* of the acute effect of toxicants on bone marrow progenitors under maximally stimulatory cytokine concentrations [2]. It consists in seeding bone marrow progenitors in a methylcellulose semi-solid medium (to avoid cell spreading) and counting the colonies of cells formed by the surviving progenitors which are still able to demonstrate clonogenic activity after toxicant exposure.
In this context, our objective was to miniaturize and optimize the current state-of-art *in vitro* myelotoxicity test by developing a Lab-on-Chip (LoC) platform [3] consisting of a high number of bioreactor chambers with screening capabilities in a high-throughput regime.

Materials and Methods

The LoC architecture consists of two functional elements: a culture region and a gradient generator. The culture region is organized in six units, each composed by three lines of 10 culture chambers. The gradient generator delivers six linear dilutions of xenobiotic agents (concentrations ranging from 1 to 0, step 0.2) from two input ports to the culture units.

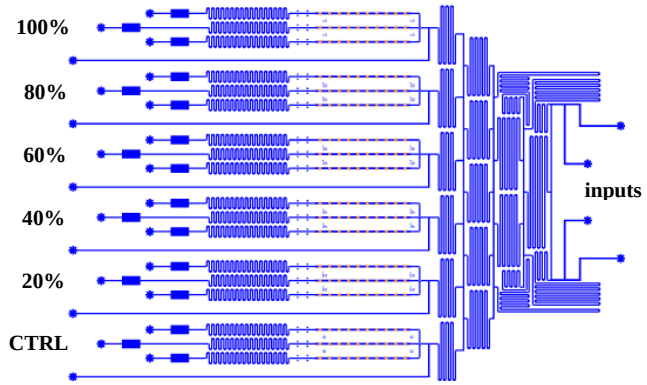

Fig. 1 *Lab on Chip device layout. Two input ports (together with two service ports) are represented on the right.*

The fluidic channels are 35µm high and 100µm wide whereas the culture chamber is cubic (side 150µm). Chamber dimensions and number have been chosen to host at least three progenitor cells in each culture unit, being i) 10 the target number of cells seeded in each chamber, and ii) 1% the population clonogenicity factor.
To assess the optimal perfusion rate for uniform cell seeding and subsequent culturing, preliminary cellular tests have been conducted using cord blood mononuclear cells (CB MNCs). Briefly, an amount of 30µl of cell suspension (concentration of 500,000 cells/ml) was simultaneously injected into each input port through a syringe pump. For this purpose, two flow rates were investigated, 0.1 and 0.2 µl/min, and the number of cells in each chamber was quantified after 12 hours through direct observation.

Results and discussions

The LoC platform was validated both in terms of cell seeding uniformity and biocompatibility during a 4 day culture. The optimal seeding flow rate was assessed for obtaining a homogenous distribution of cells among the chambers. The seeding conditions tested, 0.1 and 0.2 µl/min, provided distributions of cells in each chamber equal to 9.36 ± 6.90 and 11.84 ± 9.51, respectively.
Furthermore, the cytocompatibility of the LoC was evaluated by culturing CB MNCs (Stem Cell Technologies) in Iscove's modified Dulbecco's medium (IMDM, EuroClone) containing 30% (v/v) fetal bovine serum (FBS, GE Healthcare) and 10 ng/ml recombinant human granulocyte/ macrophage colony-stimulating factor (RELIATech). Upon 4 days of culture, an increase in the number of cells was recorder, with a final number of cells/chamber equal to 21.22 ± 13.32, thus suggesting early colonies formation.

Fig. 2 *Example of microscopy image of two subsequent chambers filled with CB MNCs. Cells were seeded at a flow rate of 0.2µl/min.*

Conclusions

In this study, a LoC device integrating high-throughput screening capabilities was presented. The proposed platform could represent a powerful tool in the hematotoxicity test field, offering high reproducibility and experimental costs, related to amount of drugs required and quantification of colony forming unit cells.

References

[1] Pessina A, Albella B, Bayo M, Bueren J, Brantom P, Casati S, et al. *Application of the CFU-GM assay to predict acute drug-induced neutropenia: an international blind trial to validate a prediction model for the Maximum Tolerated Dose (MTD) of myelosuppressive xenobiotics.* Toxicol Sci 2003:75: 355-367.
[2] Lewis ID, Rawling T, Dyson PG, Haylock DN, Juttner DN, To LB. *Standardization of the CFU-GM assay using hematopoietic growth factors.* J Hematother 1996; 5: 625-630.
[3] McDonald, J.C. et al. *Fabrication of microfluidic systems in poly(dimethylsiloxane).* Electrophoresis. 2000; 21:27-40.

4th Micro and Nano Flows Conference
UCL, London, UK, 7-10 September 2014

Investigation of laser induced phosphorescence and fluorescence of acetone at low pressure for molecular tagging velocimetry in gas microflows

Hacene SI HADJ MOHAND*, Feriel SAMOUDA, Christine BARROT, Stéphane COLIN

Université de Toulouse; INSA, UPS, Mines Albi, ISAE, ICA, France
* Corresponding author: Tel.: ++33 (0)5615 59894; Fax: ++33 (0)5615 59950; Email: sihadjmo@insa-toulouse.fr

Keywords: gas microflow, rarefied gas, molecular tagging, fluorescence, phosphorescence, acetone

A number of microfluidic applications involve gas microflows in the slip flow regime, characterized by a velocity slip and a temperature jump at the wall. Various models are proposed in the literature but experimental data mainly concern flowrate measurements. Local information on velocity fields is nevertheless necessary to improve the discussion on theoretical models for slip boundary conditions. The molecular tagging velocimetry (MTV) could be a well-suited technique, as it avoids using particles subjected to Brownian motion. MTV uses seeding molecules, such as acetone, which can be turned on tracer once excited with a UV laser. The tagged region is registered at two successive times -the first time can correspond to fluorescence signal and the second one to phosphorescence signal- and the velocity field can be deduced from the displacement of the tagged region. The resolution, however, is constrained by the laser beam diameter, with a typical minimum value of the order of 30 µm, which requires operating in channels with a hydraulic diameter around 1 mm. For this reason, microflows in the slip flow regime should be analyzed with Knudsen similitude, reducing the pressure in order to reach Knudsen numbers in the range [10^{-3}-10^{-1}]. Preliminary velocity profiles have been obtained at atmospheric pressure, i.e. in the continuum flow regime (Samouda et al., 2013). Applying the technique to rarefied gas flow requires a precise knowledge of acetone luminescence properties at low pressure, which is not documented in the literature.

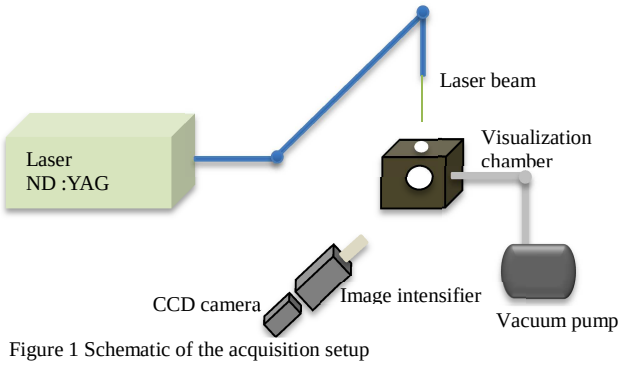

Figure 1 Schematic of the acquisition setup

The fluorescence and phosphorescence properties of liquid acetone under 266nm wavelength excitation have been studied by (Tran et al., 2006), who demonstrated that the fluorescence intensity of liquid acetone was not pressure dependent in the range of [1-15 bars], and observed a phosphorescence lifetime around 1 µs, much smaller than in the vapor phase (200µs) and also insensible to the pressure. Phosphorescence properties of liquid and vapor acetone excited at 308 nm were studied at atmospheric pressure by (Charogiannis & Beyrau, 2013). The phosphorescence signal of vapor acetone in nitrogen gas was found to be slightly decreasing with time and exhibited a much lower intensity signal than the fluorescence one.

In the present paper the pressure dependence of acetone vapor luminescence in argon gas is investigated in a pressure range from 5×10^{2} to 10^{5} Pa. A 266 nm wavelength Nd: YAG laser was used to excite acetone molecules, which reemission signal was collected with a CCD camera coupled to an image intensifier (Fig. 1). At atmospheric pressure, the early phosphorescence signal at t = 0.1 µs after tagging is 500 times lower than the fluorescence signal observed up to a t = 5 ns. From t = 0.1µs to 100µs the phosphorescence is regularly decreasing with time. For pressures between 10^{4} and 10^{5} Pa, the fluorescence intensity is not dependent on the pressure but below 10^{4} Pa the fluorescence intensity is strongly decreasing with pressure. The same behavior is observed with the phosphorescence signal but its intensity starts decreasing sooner, at 4×10^{4} Pa (Fig. 2). The systematic analysis of fluorescence and phosphorescence of acetone molecules shows that although the signal is dramatically reduced at 10^{3} Pa, the use on the on-chip integration technique permits to extract an exploitable signal at t = 50 µs, which allows analyzing argon flows

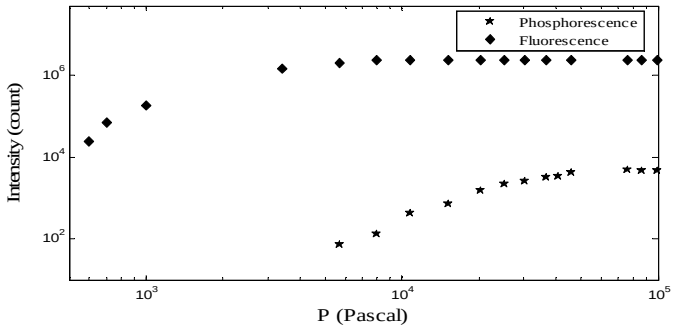

Figure 2 Vapor acetone in argon fluorescence intensity (◊), and phosphorescence intensity (*) at 0.1µs delay vs pressure

at Kn =5.5×10^{-3} or helium flows at Kn =1.7×10^{-2}, which correspond to the required range for velocity measurements in the slip flow regime. The possibilities and limitations of MTV for experimental analysis of rarefied microflows are then discussed.

References:

Charogiannis, A., & Beyrau, F. (2013). Laser induced phosphorescence imaging for the investigation of evaporating liquid flows. *Exp Fluids, 54*(5), 1-15.

Samouda, F., Colin, S., Barrot, C., Baldas, L., & Brandner, J. J. (2013). Micro molecular tagging velocimetry for analysis of gas flows in mini and micro systems. *Microsyst Technol*. DOI 10.1007/s00542-013-1971-0.

Tran, T., Kochar, Y., & Seitzman, J. (2006). Measurements of acetone fluorescence and phosphorescence at high pressures and temperatures. *44th aerospace sciences meeting and exhibit*. Nevada.

4th Micro and Nano Flows Conference
UCL, London, UK, 7-10 September 2014

A model of oxygen dynamics in the cerebral microvasculature

Chang Sub PARK [1,*], Stephen J. PAYNE [1]

* Corresponding author: Tel.: ++44 (0)1865 617696; Fax: ++44 (0)1865 617703; Email: chang.park@eng.ox.ac.uk
1: Institute of Biomedical Engineering, Department of Engineering Science, University of Oxford, UK

Keywords: Microcirculation, Oxygen dynamics, Oxygen extraction fraction

Introduction

The brain requires constant supply of blood and oxygen. In the microvasculature, this is achieved by complex interconnectedness between capillary vessels. Understanding oxygen dynamics to changes in cerebral microvasculature properties will provide valuable information of the effects of oxygen supply to different pathological conditions, such as ischaemic stroke. For example, an increase in cerebral metabolic rate of oxygen ($CMRO_2$) has been observed in hypoperfused brain tissue during ischaemia, but the causes are unclear. A solution for the oxygen extraction fraction (OEF), and hence $CMRO_2$, for a capillary network is provided here as a first step to understanding these complex dynamics.

Methods

General capillary networks are generated to solve for the oxygen transport. A specific algorithm is used to generate physiologically accurate capillary networks [1] based on histological data from experiments [2]. In order to obtain the OEF, the fraction of oxygen removed by the brain from the blood, and hence the $CMRO_2$, it is necessary to solve for the concentration within the capillary networks. This is achieved by solving the convection driven one-dimensional mass transport equation with the following assumptions:

1. Poiseuille flow with individual vessel viscosity.
2. Oxygen diffuses through the vessel walls at a linearly proportional rate.
3. Oxygen in the tissue is consumed immediately such that the concentration can be considered to be effectively zero.

The unsteady 1-D mass transport equation can then be expressed as:

$$\frac{\partial C(x,t)}{\partial t} + U\frac{\partial C(x,t)}{\partial x} = -\lambda C(x,t)$$

where C(x,t) is the oxygen concentration, U is the velocity and λ is the product of the surface permeability and the fraction of oxygen concentration in the plasma. An analytical solution of the concentration for a single vessel is obtained using the Laplace Transform. This is then applied to solve for the concentration in the whole capillary network. This approach is an extension of that proposed by Park and Payne for the capillary residue function [3]. Given a constant inlet concentration, the outlet concentration can be solved by calculating the flows, transit times and values of λ in each of the vessels, and knowledge of all pathways from the inlet to the outlet. The OEF can then be expressed as:

$$OEF = 1 - \frac{1}{Q_{net}}\sum_{i,j}^{out} Q_{ij}\prod_{k,l}^{i}\frac{Q_{kl}e^{-\lambda_{kl}T_{kl}}}{\sum_m Q_{ml}}e^{-\lambda_{ij}T_{ij}}u\left(t-\sum_{k,l}^{i}T_{kl}-T_{ij}\right)$$

where Q is the flow, T is the transit time and u(t) is a step function. The subscripts represent the different nodes in the capillary network.

Results and discussion

A step function was considered for the capillary inlet concentration. The magnitude was decreased to 75% at t=25s. λ was considered to be constant here as an initial approach. Figure 1 shows the variation of the overall network OEF, and the mean, 25th and 75th percentile OEF (<OEF>, OEF_{25} and OEF_{75} respectively) of the individual vessels with time. The sudden drop in inlet concentration causes a sharp decrease in OEF followed by a gradual recovery back to the steady state solution. The gradual recovery of OEF, which is due to a constant proportion of oxygen diffusing into the tissues irrespective of the vessel inlet concentration, determines the time taken for the oxygen to reach the outlet after the change in inlet concentration. The OEF changes observed in the individual vessels are more gradual since the change in the individual vessel inlet concentration occurs at different times. OEF_{25} and OEF_{75} show a significant degree of heterogeneity in OEF between the different vessels, which is due to the heterogeneity of the transit times through the vessels as well as the interconnectedness leading to multiple pathways available. Note that the network OEF is greater than <OEF>. The complex interconnectedness in the capillary network, which leads to multiple pathways, allows for a more efficient oxygen extraction.

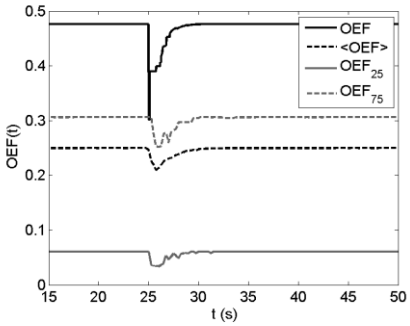

Figure 1: Dynamic OEF.

Conclusion

A sudden change in inlet concentration leads to a sharp change in OEF followed by a gradual recovery. The time to achieve steady state solution determines the time taken for the oxygen to reach the outlet. There is a degree of variability in the individual vessel OEF due to the heterogeneity of the transit times. We next plan to quantify the effects of morphological properties on OEF and to explore how dynamic OEF varies under a range of different conditions.

Acknowledgements

This work was supported by the Centre of Excellence for Personalized Healthcare funded by the Wellcome Trust and EPSRC under grant no. WT 088877/Z/09/Z.

References

[1] Su et al. *Microcirculation*, 19: 175–187, 2012.
[2] Cassot et al. *Microcirculation*, 13:1-18, 2006.
[3] Park and Payne. *Interface Focus*, 3:20120078, 2013.

4th Micro and Nano Flows Conference
UCL, London, UK, 7-10 September 2014

Electrophoretic manipulation of multiple-emulsion droplets

Andreas M. SCHOELER [1,*], Dimitris N. JOSEPHIDES [1], Ankur S. CHAURASIA [1], Shahriar SAJJADI [1], Patrick MESQUIDA[1]

* Corresponding author: Tel.: ++44 (0)207 848 2902; Email: andreas.schoeler@kcl.ac.uk
1: Department of Physics, Kings College London, UK

Keywords: Electrophoresis, Micro Flow, Emulsion, Carrier Mobility

1 Introduction

Double emulsions (W/O/W and O/W/O) are an attractive tool in biomedical engineering as they offer liposomes delivery vehicles [1], microcapsules [2], controlled content release [3] or living cells encapsulation [4], although it is not always easy to achieve efficient microscopic droplet manipulation. While electrophoretic manipulation of simple drops has been reported in the literature [5], complex or structured drops, such as drop-in-drop or drop-in-drop-in-drop, have not received any attention yet.

2 Experimental Method

a) b)

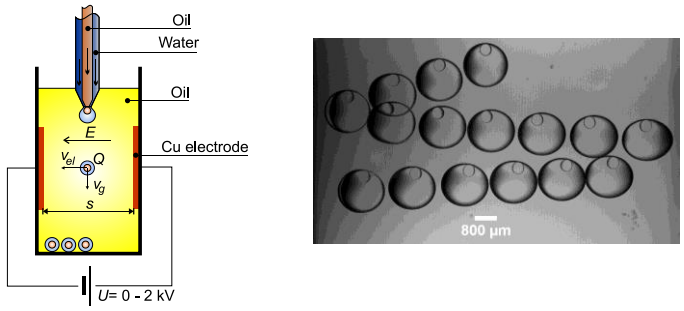

Figure 1 a) Vertical set-up for electrophoretic measurements. b) Back-and-forth motion of the O/W/O droplet between the two electrodes while continuing to slowly fall due to gravity. Both oil phases are silicone oil.

Individual oil in water droplets are injected into the oil and sink to the bottom of the cuvette with a gravitational terminal velocity, v_g. Once the droplet reaches the middle between the Cu electrodes separated by a distance, s, the voltage, U, is applied, creating a homogenous electric field, E, that causes the droplet carrying a net charge, Q, to be displaced with a horizontal velocity component, v_{el}, due to Coulomb force.

3 Results

This is a first report on electrophoretic manipulation of structured drops, both (O/W)/O and (W/O/W)O droplets. Water shells have been created that allow the electrophoretic manipulation of oil droplets in an oil environment. It was found that the inner droplet regardless of size and composition does not affect the electrophoretic motion caused by the application of an electric field neither before nor after the outer water shell has made contact with an electrode. Furthermore it has been observed that the surface charge of the shell can be altered through contact with a biased electrode and remains constant regardless of the inner droplet size. The method presented could be used for the manipulation of oil droplets in a continuous oil phase or for the transportation of microbial cells, e.g. enzymes, that would otherwise be killed, even at low electric field strengths.

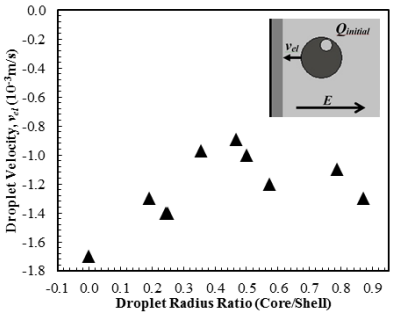

Figure 2 Electrophoretic droplet velocity, v_{el}, of an (o/W)/O droplet (in the presence of 2.30g/l SDS) with varying oil core size before contact with an electrode (inset).

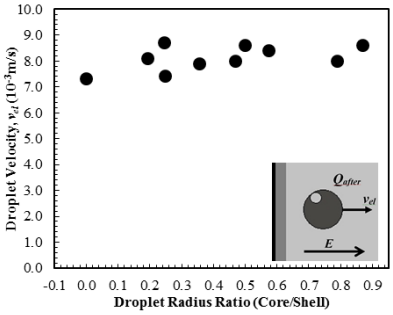

Figure 3 Electrophoretic droplet velocity, v_{el}, of an (o/W)/O droplet (in the presence of 2.30g/l SDS) with varying oil core size after contact with an electrode (inset).

4 References

[1] H.C. Shum, D. Lee, I. Yoon, T. Kodger, D.A. Weitz, Langmuir 24 (2008) 7651.

[2] P.W. Chen, R.M. Erb, A.R. Studart, Langmuir 28 (2012) 144.

[3] A. Abbaspourrad, N.J. Carroll, S.H. Kim, D.A. Weitz, J Am Chem Soc 135 (2013) 7744.

[4] C.J. Martinez, J.W. Kim, C.W. Ye, I. Ortiz, A.C. Rowat, M. Marquez, D. Weitz, Macromol Biosci 12 (2012) 946.

[5] A.M. Schoeler, D.N. Josephides, S. Sajjadi, C.D. Lorenz, P. Mesquida, J Appl Phys 114 (2013) 144903

4th Micro and Nano Flows Conference
UCL, London, UK, 7-10 September 2014

Explosive Vaporization of Water and Isopropyl Alcohol on a Flat Microheater

Vladimir V. Kuznetsov*, Igor A. Kozulin

* Corresponding author: Tel.: +7 (383)3307121; Fax: +7 (383)3308480; Email: vladkuz@itp.nsc.ru
Kutateladze Institute of Thermophysics SB RAS, Russian Federation

Keywords: Explosive Vaporization, Microheater, Pulse heating, MEMS

MEMS control systems, such as ink jet printers, optical switches and valves, use the explosive vaporization of metastable liquid for the rapid phase change. In recent years, experimental studies on explosive vaporization under pulsed heating on thin wires and rectangular microheaters were performed. Although these studies were focused on different aspects of the explosive vaporization, the patterns of rapid liquid–vapor phase transition and the characteristics of nucleation in liquid at high heat flux remain insufficiently understood. In this work, we experimentally studied the initial stage of explosive vaporization of a water and isopropyl alcohol on the surface of a flat microheater coated with a submicron silicon-carbide layer. Applying the optical method, we investigated the patterns of the liquid–vapor phase transition under pulse heating and obtained the characteristics of the nucleation in liquid at rate of temperature grows up to 800 MK/s.

The microheater is a multilayer thin-film resistor of the ThinkJet printhead. The resistor of 100 × 110 μm is a four-layer film was deposited layer-by-layer by the PECVD on a glass substrate. The first layer is a silica 1.1 μm layer, then follow a heat-emitting TaAl layer whose conduction is weakly dependent on the temperature, a 0.5 μmN_2O_4 layer, and a 0.25 μm SiC layer. This sandwich-like structure of the heater ensures high growth rates of the surface temperature under pulse heating. The microchip with the heater was immersed into working liquid. Single squared current pulses were applied to the microheater for heating up. The density of the heat flux into the liquid was about 400 MW/m^2, which yields less than 1.4 μs time of heating to the temperature of nucleation in water. The experiments were carried out at the atmospheric pressure. The initial liquid temperature was 20°C.

For studying explosive vaporization, an optical method for recoding the nucleation, vaporization, and dynamics of the vapor cavity was developed. It is based on measuring the intensity of He–Ne laser beam reflected regularly from the heater surface. As soon as microbubbles arise, the integral coefficient of regular reflectance begins to decrease and the inverted signal from the photodetector yields the dynamics of filling the heater surface with the microbubbles. Rectangular aperture in the image plane cuts out the necessary area of image of the resistor, which is then projected onto photodetector and processed by a fast ADC. A solid-state laser with pulse duration of about 20 ns and a videocamera were used to photograph different stages of the explosive vaporization.

Explosive vaporization of a liquid is characterized by the time of nucleation, the lifetime of the main bubble obtained during microbubbles coalescence, and the lifetime of the satellite bubble formed after collapse of the main bubble. Experimental data show that the time of the liquid heating for a nucleation start varied for water from 1.4 to 10 μs and for isopropyl alcohol from 0.9 to 5 μs. The nucleation in superheat liquid is explosive and lasts less than 350 ns. At the initial stage of nucleation, the bubbles are nonuniformly distributed over the heater surface, they are few in number, and at the instant of bubble emergence we observe emitting of diverging pressure waves. The number of bubbles at nucleation in isopropyl alcohol is more than in order exceeds the number of bubbles at nucleation in water.

Since in the described experiments the aperture cut off the beam may exceed the heater surface, the different stages of the bubble growth and collapse outside the heater were observed. At relative time τ_r less than 0.926, the vaporization is characterized by a good repeatability both in the nucleation time and in the lifetime of the main bubble. The relative vaporization time τ_r is equal to the ratio of time of the beginning nucleation to time of thermal power switch off. At $\tau_r \geq 1$, not only the lifetime of the bubble decreases, but also the nucleation time because its final stage takes place under switched off heat power. This yields the threshold relative vaporization time above which we do not observe the developed nucleation under pulse heating.

It was obtained that at growth rates of the surface temperature less 200 MK/s, the nucleation temperature in water on the silicon carbide surface is lower than the temperatures of kinetic and thermodynamic spinodals. It allows determine the decreasing of nucleation work due to the poorly wetting of silicon carbide surface. The heat flux into the liquid, surface temperature and surface temperature growth were determined for measured time of nucleation by numerical solving the one-dimensional heat conduction equation for a multilayer heater with regard to the heat production in the TaAl layer. When the rate of temperature growth exceeds 400 MK/s a nucleation occurs at the temperature closed to thermodynamic spinodal temperature.

The presented data show that the optic method ensures a high accuracy of measuring the characteristics of explosive evaporation under pulse heating. Using this method it was obtained that the temperature of nucleation on the silicon carbide surface achieves the temperature of thermodynamic spinodal if the rate of temperature growth exceed 400 Mk/s.

This work was supported, in part, by the Siberian Branch of the Russian Academy of Sciences under Integration project No. 74.

4th Micro and Nano Flows Conference
UCL, London, UK, 7-10 September 2014

Experimental µPIV and Numerical Analysis of a Fluid Flowing into a T-microjunction

Giacomo PUCCETTI [1,*], Beatrice PULVIRENTI [1], Gian Luca MORINI [1]

* Corresponding author: Tel.: +39 0512090540; Email: giacomo.puccetti2@unibo.it
1 DIN – Alma Mater Studiorum Università di Bologna,
Laboratorio di Microfluidica, Via del Lazzaretto 15, Bologna 40131, I

Keywords: Micro Flow, T micro-junction, microPIV, Microchannel

In this work an experimental campaign by means of the use of the micro PIV technique for the analysis of the mixing of the water into a T-microjunction is described.
The T-microjunction is made as intersection of two glass microchannels with a squared cross-section with a side of 300 µm. The mixing of the flows is obtained by means of an injection of a secondary water flow in perpendicular direction with respect to the main straight stream of water. The µPIV apparatus used in this work, is composed by a pulsed Nd:YAG (λ = 532 nm) monochromatic laser (*NanoPIV, Litron Lasers*), an inverse microscope (*Eclipse T2000, Nikon*) and a sensitive large-format interline-transfer CCD camera (*Sensicam, PCO*). The illumination light is delivered to the inverse microscope through beam-forming optics, which consists of a variety of optical elements that sufficiently modify the light so that it fill the back of the objective lens, and thereby broadly illuminate the microfluidic device. The illumination light is reflected upward towards the objective lens by an antireflective coated mirror designed to reflect wavelength 532 nm and transmit 560 nm. An air immersion lens with a numerical aperture NA = 0.25 and magnification M = 10 is used. The sensitive large-format interline-transfer CCD camera is used to record the particle image fields. Fluorescent seeding (*Invitrogen, FluoSphere*) is dispersed in both the fluids. The particle tracer presents a diameter of 1.0 µm, a density of ρ = 1.05 g/cm^3, orange coloration, a carboxylate coating and emitting a radiation wavelength of 560 nm when it is illuminated with a green light (λ = 532 nm).
The T junction has been modeled numerically by using OpenFOAM v.2.2.2. The flow solver is a finite-volume scheme, with an implicit second order scheme to solve momentum. The continuity equation is converted into a pressure-correction equation. A PISO algorithm solves iteratively the coupled pressure and momentum equations to obtain a converged pressure field and divergence-free velocity field. The capability of the software to simulate the flow of a fluid within a T junction in the macro-scale is assessed through several benchmarks and comparison with the literature. In the micro-scale, the hydrodynamics of water within the T junction is considered. The validation of the numerical results is carried out by comparing the water velocity profiles obtained experimentally.
The local flow velocity and the pressure distribution within the microchannel are calculated numerically for a different ratio between the velocity of the secondary flow and the one of the main stream. By these results the instantaneous and average pressure drop along the channel and within the T junction are obtained.

4th Micro and Nano Flows Conference
UCL, London, UK, 7-10 September 2014

Pore-scale Study on Two-phase Flow in Porous Media

Zhenyu Liu*, Huiying Wu

* Corresponding author: Tel.: ++86 (021) 34205299; Fax: ++86 (021) 34205299; Email: zhenyu.liu@sjtu.edu.cn
School of Mechanical Engineering, Shanghai Jiao Tong University, China

Keywords: Pore Scale, Two Phase Flow, VOF Method, Microfluid Flow

Macroscopic approaches are commonly adopted to describe the transport phenomena in porous media, which are based on averaging pore-scale processes over the representative elementary volume. The understanding of two-phase flow at the pore scale is of great importance because the pore-scale characteristics of flow and heat transfer has a major influence in the porous media. The pore-scale study provides a bridge between the pore scale and macro scale representation, and it has attracted more and more attention in recent years. This paper reviews currently available pore-scale experimental and predictive techniques for two-phase flow in porous media. The different analytical and numerical models for two phase flow in the small complex structures are summarized. The pore-scale models based on a realistic description of the pore space can be used to predict two-phase flow and heat transfer. The pore-scale modeling can be used to investigate the averaging effects and describe the detailed phenomena in porous media. The available experimental methods are presented, which include the pore-scale experiment on samples of porous media, the reconstruction of porous media using images obtained from X-ray microtomography or CT, etc. The pore scale model established in this work is available to simulate two-phase flow and heat transfer of pore fluids under the order of micrometer with VOF method, which can predict microfluid flow in complex geometry.

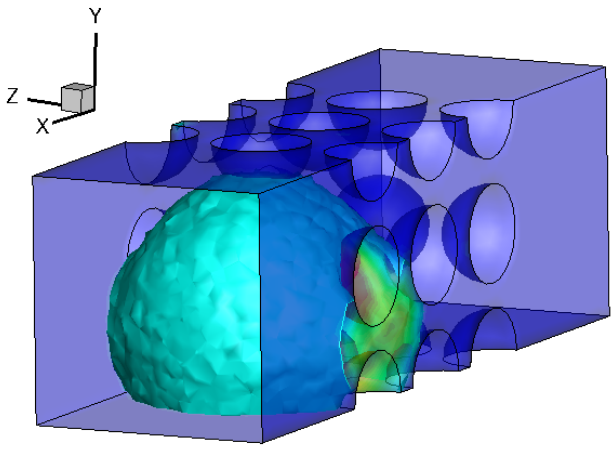

Figure 1. Hydrophobic wall leads to a fast removal of water (Contact angle 135^{o})

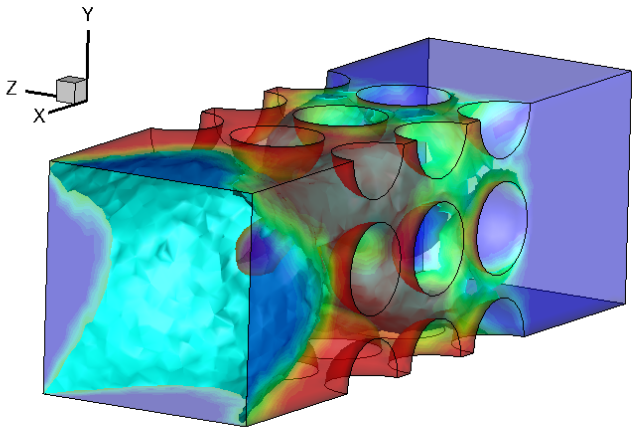

Figure 2. Hydrophilic wall leads to a fast removal of water (Contact angle 45^{o})

Acknowledgements
This paper is supported by the National Natural Science Foundation of China through grant no. 51306119, the National Basic Research Program of China (973 Program) through grant no. 2012CB720404.

4th Micro and Nano Flows Conference
UCL, London, UK, 7-10 September 2014

Analysis of the flow and mass transfer around non confined bubbles in a microchannel

David MIKAELIAN [1,*], Nathalie TARCHICHI [1], Benoit SCHEID [1], Benoît HAUT [1]

* Corresponding author: Tel.: +3226502917; Fax: +3226502910; Email: dmikaeli@ulb.ac.be
1 Laboratory of Transfers, Interfaces and Processes (TIPs), Université Libre de Bruxelles, Belgium

Keywords: Microfluidics, Microchannel, Bubbly flow, Liquid-gas absorption, CFD

Microfluidic devices are more and more used because they allow using les reactants, controlling more rigorously the involved processes and lowering the risk due to the use of high quantity of hazardous materials.

In this work, the flow and the mass transfer around bubbles in a microchannel are analyzed experimentally and numerically in the bubbly flow regime.

In the experimental part, the absorption of CO_2 in methanol is studied using a T-junction configuration (the width of the gas and the liquid microchannels are respectively w_d=30 µm and w_c=200 µm) and long serpentine microchannels (see Fig. 1).

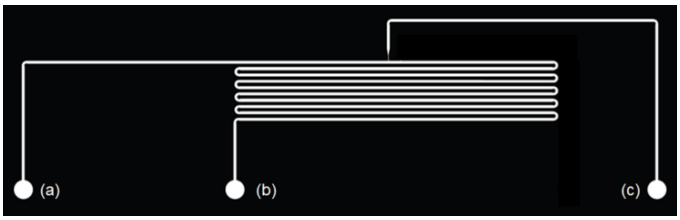

Figure 1: Micro-absorber device with: (a) the methanol inlet, (b) the outlet and (c) the CO_2 inlet.

The microchannels are made in PDMS by soft lithography and sealed with a glass plate. CO_2 is used as the dispersed phase and methanol as the continuous phase. The methanol is colored with a common food dye to achieve a better visualization contrast. The gas is injected at a constant pressure using a FLUIGENT device, while the methanol is injected at a constant flow rate using a syringe pump. The generated bubbles are recorded with a high speed camera. It allows observing the absorption phenomenon by monitoring the bubbles along the microchannel.

In the numerical part, simulations of the flow and the mass transfer are realized around a spherical bubble of diameter d in a microchannel of length L and with a square cross-section of width w, in a reference frame attached to the bubble. Therefore, one quarter of the microchannel with a bubble at its center is drawn (see Fig. 2) and meshed with the software Gambit 2.4. The grid independency is checked and the equations of continuity, Navier-Stokes and mass transfer are solved for the meshed volume using the software Ansys Fluent 14.5. Periodic boundary conditions are used to mimic the presence of a chain of bubbles and to analyze the influence of each bubble on the other ones.

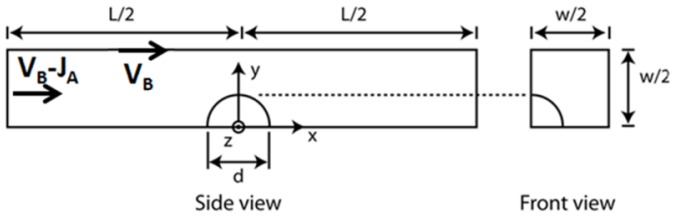

Figure 2: Model microchannel in the reference frame attached to the bubble (with V_B the velocity of the bubble and J_a the total inlet velocity)

Numerical simulations of the flow and the mass transfer are realized for different bubble diameters and different total inlet velocities. The flow and mass transfer fields are analyzed around the bubbles in the microchannel in order to better understand the phenomena that are present or dominant. An example of the concentration profile around a bubble with a diameter of 150 µm in a square microchannel with a width of 200 µm and a length of 5000 µm is provided in Fig. 3.

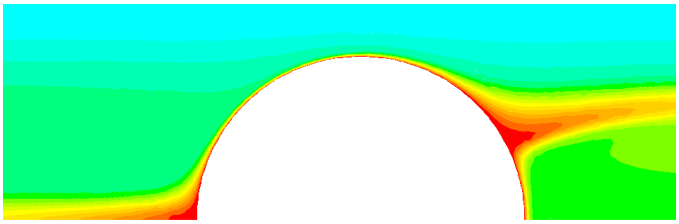

Figure 3: Concentration profile around a bubble diameter of 150 µm in a square microchannel with a width of 200 µm and a length of 5000 µm

For each numerical simulation of a given bubble diameter and a given total inlet velocity, the velocity of the bubble is determined such as the force on the bubble along the flow direction vanishes. Correlations are then established for V_B/J_a and also for Sherwood number as a function of the ratio d/w, Re and Sc. From these correlations, it is possible to establish a set of equations whose resolution will lead to the evolution of the diameter of the bubble along the microchannel. This calculated profile can then be compared to the results of the experimental part.

4th Micro and Nano Flows Conference
UCL, London, UK, 7-10 September 2014

Synthesis of Silver Nanoparticles using Non-Fouling Microfluidic Devices with Fast Mixing

Razwan BABER [1], Luca MAZZEI [1], Nguyen TK THANH [2,3], Asterios GAVRIILIDIS [1,*]

* Corresponding author:Tel.: +44 (0) 20 7679 3811; Fax: +44 (0) 20 7383 2348; Email: a.gavriilidis@ucl.ac.uk
[1]Department of Chemical Engineering, University College London, UK
[2]UCL Healthcare Biomagnetic and Nanomaterials Laboratories
[3]Department of Physics, University College London, UK

Keywords: Mixing time, Impinging jet, Nanomaterials, Nanocrystallisation

Silver nanoparticles (NPs) are used in a wide variety of applications such as biomedicine, optics, electronics, sensors and catalysis. The application of silver NPs is affected by the properties they display which are mainly determined by their size. It is well known that concentrations of reagents in the reaction affect size, shape and polydispersity of the synthesized NPs.

The use of traditional micromixers presents challenges for the synthesis of nanoparticles mainly arising from fouling of the reactor due to accumulation of nanomaterial on the walls of the reactor. This results in poor repeatability of nanoparticle synthesis leading to unreliable experimental results. To counter this effect, the use of techniques such as droplet based flow are used to keep the nanoparticles away from the wall [1].

This study addresses the synthesis of silver NPs using a non-fouling microfluidic device (impinging jet reactor (IJR) [2]). Our experiments with batch reactors, split and recombine mixer or a simple T-mixer have produced non-repeatable results for silver NP synthesis, thus an IJR is employed to address the issues associated with fouling of channel walls. Initial experiments indicate that the synthesis of silver nanoparticles is highly repeatable (UV-Vis spectra peak absorbance of several repeated experiments varied by 0.3% using the IJR compared to 13% variance using a T-mixer). Following the establishment of a non-fouling system, it is expected that the mixing efficiency plays a significant role in the morphological parameters of the resultant NPs.

During batch experiments involving the addition of a small volume of concentrated reagent to a larger volume of dilute reagent, it was observed that by keeping the absolute concentration of reagents constant but changing the mixing order of precursor and reducing agent resulted in different NP shapes. This consisted of small spherical particles or formation of a significant amount of nanoplates and nanorods (1), confirming the importance of mixing.

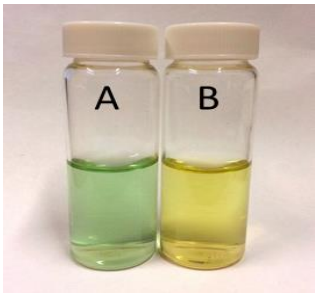

Figure 1: *Silver NPs synthesized in a batch reactor A) forming nanoplates and nanorods and B) forming nanospheres*

Using the IJR, small changes to the NPs occur with incremental changes in flow rates (and hence mixing efficiency). Based on these findings, mixing has been characterized using the 'Villermaux Dushmann' reactions [3]. Using the Interaction by Exchange with the Mean (IEM) model [4], the mixing time is inferred from experimental results. Experiments show that there are changes in NP morphology (size and polydispersity) with incremental changes in flowrate (Figure 2). Using the IJR, at lower flowrates the appearance of nanoplates seems to more prevalent whereas at higher flowrates the nanoplates seem to be less prevalent (or not present). Mixing time is in the order of 100 ms.

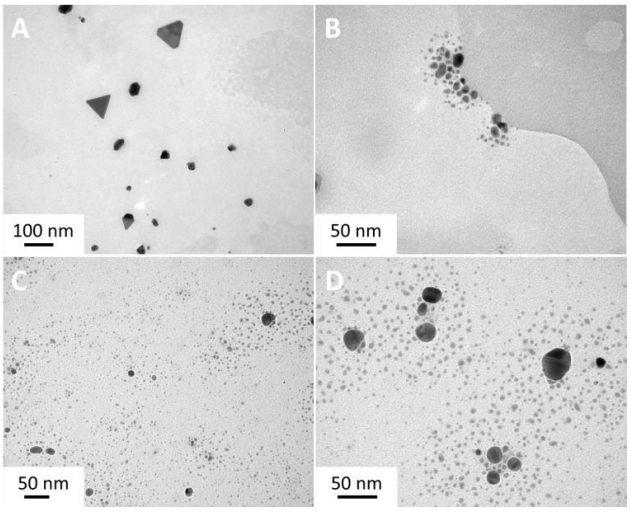

Figure 2: *TEM Images of silver NPs synthesized using impinging jet reactor at a total flow rates of (A), (B) 10 ml/min and (C), (D) 20 ml/min*

References:

1. Zhao, C.-X., et al., *Nanoparticle synthesis in microreactors.* Chemical Engineering Science, 2011. **66**(7): p. 1463-1479.
2. Hessel, V., H. Löwe, and F. Schönfeld, *Micromixers—a review on passive and active mixing principles.* Chemical Engineering Science, 2005. **60**(8–9): p. 2479-2501.
3. Commenge, J.-M. and L. Falk, *Villermaux–Dushman protocol for experimental characterization of micromixers.* Chemical Engineering and Processing: Process Intensification, 2011. **50**(10): p. 979-990.
4. Baldyga, J. and J.R. Bourne, *Comparison of the engulfment and the interaction-by-exchange-with-the-mean micromixing models.* The Chemical Engineering Journal, 1990. **45**(1): p. 25-31.

4th Micro and Nano Flows Conference
UCL, London, UK, 7-10 September 2014

ELECTROMAGNETIC ACTUATED STIRRING IN MICROBIOREACTORS ENABLING EASIER MULTIPLEXING & FLEXIBLE DEVICE DESIGN

Matthew J. DAVIES [1], Ian MUNRO [2], Christabel K.L. TAN[2], Mark C. TRACEY[2], Nicolas SZITA[1,*]

* Corresponding author: Tel.: ++44 (0)20 76794418; Fax: ++44 (0)20 72090703; Email: n.szita@ucl.ac.uk
1: Department of Biochemical Engineering, University College London, UK
2: School of Engineering and Technology, University of Hertfordshire, UK

Keywords: MicroBioReactor, Stirring, Electromagnet, Duplex

Development of a **novel electromagnetically (EM) actuated stirring** method, for use in microbioreactors, is reported. The design flexibility afforded by this new method is demonstrated by fermentation of the **gram-positive bacteria *S. carnosus*** in a **diamond-shaped reactor** and a **duplex microbioreactor system**.

Introduction

Microbioreactors, initially developed to aid in bioprocess development [1], have also found application in strain optimisation for synthetic biology [2]. The ability to *in situ* monitor fermentation variables and multiplex reactor chambers, relevant to both applications, is a direct result of the microscale dimensions of microbioreactors. Many different passive and active [3] mixing methods have been developed for a wide variety of microfluidic devices. Despite these developments mixing in microbioreactors still provides some challenges as a result of the specific conditions required for microorganism growth, operational monitoring, and ease of multiplexing. Additionally, rotating permanent magnets to drive stirrer bars, as previously implemented [1, 4], require a circular reactor chamber to prevent stagnant zones, which makes reactor priming challenging. Here, we present for the first time an EM actuated stirring method, which is not hard-linked with a particular reactor shape, facilely enables optical access for condition monitoring between the EMs, and has the potential for easy multiplexing.

Experimental

The microbioreactor is designed in a cassette format comprised of 4 separate layers (Fig 1a). Three of the four layers are micromilled in polycarbonate with the fourth, cast in PDMS. Manually fabricated EMs are mounted axially underneath each corner of the reactor chamber (Fig 1b), and direct the movement of a magnetic bead within the reactor chamber. EM activation is controlled using an Arduino Mega2560. Mixing results from the motion of a 1 mm magnetic bead moving to each activated EM in turn. Stirring was visualised using colored dyes and a USB microscope. Video was analyzed by eye to determine mixing time. The fermentation was performed using *S. carnosus* TM300 grown in a defined medium. Optical density was monitored as an indirect measure of bacterial growth. The duplex reactor was formed by placing two fluidically independently addressed reactor chambers, sharing the central EM on a single reactor body, with the Arduino code duplicating electromagnet timing for both microbioreactors.

Results

Bubble-free priming of the diamond-shaped reactor device was achieved without any user interaction. Different mixing patterns were tested. A mixing time of 3.4 seconds resulted from actuating the solenoids in two loops (60 ms actuation time) followed by a figure of 8 (100 ms actuation time). Mixing in both chambers of the duplex microbioreactor was demonstrated to be almost identical (Fig 2). Finally, growth of the *S. carnosus* in a fermentation demonstrated the ability of the EM stirring to sustain bacterial growth (Fig 3).

Conclusion

The stirring method presented here facilitates **flexible implementation** of microfluidic chamber designs, **rapid mixing**, and **straightforward multiplexing** of microbioreactors, while still enabling the microbioreactor to **sustain, and monitor, bacterial growth**. Future work will include CFD modelling of the bead and fluid motion, to enable directed mixing optimisation, and further integration of growth condition monitoring and multiplexing.

References

1. "Development of a multiplexed microbioreactor system for high-throughput bioprocessing", N. Szita et al., Lab on a Chip, **5**, 819 (2005)
2. "Microfluidic approaches for systems and synthetic biology", N. Szita et al., Current Opinion in Biotechnology, **21**, 517 (2010)
3. "Microfluidic mixing: a review", C. Y. Lee et al., International Journal of Molecular Sciences, **12**, 3263 (2011)
4. "Development of a single-use microbioreactor for cultivation of microorganisms", D. Schäpper et al., Chemical Engineering Journal, **160**, 891 (2010)

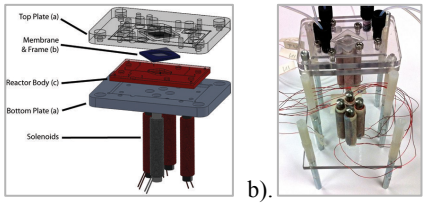

a). b).

Figure 1a). Microbioreactor cassette and b). Duplex EM arrangement.

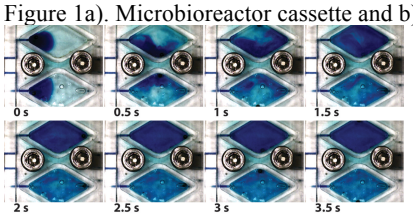

Figure 2. Still sequence showing close agreement in mixing behaviour between the two chambers of the duplex microbioreactor.

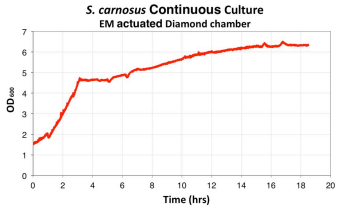

Figure 3. Plot of OD against time for a continuous culture fermentation of *S. carnosus*.

4th Micro and Nano Flows Conference
UCL, London, UK, 7-10 September 2014

Effective Transport Template for Particle Separation in Microfluidic Bumper Arrays

Stefano CERBELLI [1,*], Massimiliano GIONA [1], Fabio GAROFALO [2]

* Corresponding author: Email: stefano.cerbelli@uniroma1.it
1 Dept. of Chemical Engineering, Sapienza Università di Roma, IT
2 Dept. of Mechanical Engineering, Technical University of Eindhoven, UK

Keywords: Particle Sorting, Deterministic Lateral Displacement, Diffusion

As micro-fabrication techniques make it possible to produce micrometer-sized geometries with unprecedented resolution, an increasing number of prototypes are being continuously proposed, which realize classical engineering operations based on altogether new design principles. The separation method referred to as *Deterministic Lateral Displacement* (Huang et al., *Science* (2004) **304**, 987-990) constitutes one such example, where an elegant use of simple fluid dynamic ideas allows to perform in an efficient way the size-based separation of a multi-disperse population of micrometer-sized objects suspended in a carrier fluid, be them solid particles, bacteria, blood components or even drops of an immiscible phase.

A typical realization of a device exploiting this principle is constituted by a shallow rectangular channel filled with a periodically ordered array of identical obstacles arranged along a Cartesian lattice. The lattice is given an angle, say Θ_l, with respect to the lateral walls of the channel. A pressure-driven flow, entraining the multi-disperse suspension crosses the array of impermeable obstacles. The geometry is designed so that the typical size of the objects in the mixture is comparable to the gap between adjacent obstacles. Figure 1 provides a schematic representation of the separation mechanism for the case where the lattice angle is given by $\Theta_l = 1/3$. The red thick lines represent critical streamlines of the Stokes flow through the periodic array of obstacles. These critical streamlines define flux tubes that extend throughout the domain. The separation mechanism can be explained by assuming that a generic finite-sized particle is constrained to follow the streamline through its center until it comes into contact with an obstacle. At the collision, the particle starts to glide around the obstacle and eventually detaches from it by following a different streamline. According to this simplified model, one observes two qualitatively different behavior of particle dynamics: small particles tend to remain constrained within a single flux tube (zig-zag mode), whereas larger particles change flux tube at each collision with an obstacle (displacement mode). The critical particle size separating the two separation modes is given by the condition that the particle radius be equal the the minimal width of the flux tube immediately adjacent to any given obstacle. A number of experiments involving solid-particle or even cell suspensions, provided a qualitative validation of this simple interpretation scheme for the separation mechanism, even though it has been recognized that the impact of thermal fluctuations on separation efficiency should not be neglected if an accurate design of the separation device is sought. In more recent studies (Cerbelli et al, (2013), *Microfluidics & Nanofluidics* **15**, 431-449**)** it has been showed how the superposition of thermal fluctuations to the simple kinematic scheme described above can have a significant influence not only on the average direction attained by particles of a given size, but also on the dispersion of individual particles about the average particle current.

It has been found that enhanced dispersion regimes, hindering separation efficiency far beyond what could be predicted from the value of bare particle diffusivity, can arise as a consequence of the interaction between thermal fluctuations and flow structure. The scope of this work is to analyze the practical consequences of these dispersion regimes in device geometries and operating conditions that are typically used in practical implementations of this separation technique. Specifically, we show the occurrence of effective transport regimes which are characterized by an average particle velocity and a typically anisotropic large-scale dispersivity. Also, we provide numerical evidence that the dispersivity enhancement may depend sensitively on particle size, especially for particles dimensions that are close to the critical size. We expect the conclusions of this analysis to be especially relevant for possible further scale-down of this process to the separation of mesoscopic objects in the range of hundreds of nanometers.

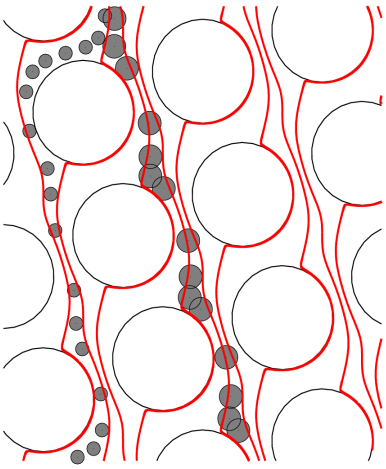

Figure 1: Critical streamlines of the single phase Stokes flow through a tilted periodic array of cylindrical obstacles (thick red lines). The gray circles display the paths of finite-sized particles dragged by the surrounding fluid through the obstacle lattice

4th Micro and Nano Flows Conference
UCL, London, UK, 7-10 September 2014

Experimental Study of Slug Flow for Condensation in a Square Cross-Section Micro-Channel at Low Mass Velocities

Georges EL ACHKAR [1,*], Marc MISCEVIC [2], Pascal LAVIEILLE [2]

* Corresponding author: Tel.: +33 (0)491106890; Fax: +33 (0)491106969; Email: georges.elachkar@laplace.univ-tlse.fr
[1] Institut Universitaire des Systèmes Thermiques Industriels (IUSTI), Aix-Marseille Université, France
[2] LAboratoire PLAsma et Conversion d'Energie (LAPLACE), Université de Toulouse III - Paul Sabatier, France

Keywords: Condensation, Micro-channel, Square Cross-Section, N-Pentane, Flow Patterns, Elongated Bubbles, Heat Transfer

The increase integration of the electronic systems in the satellites results obviously in an increase of the dissipated heat fluxes. The area of the satellites radiative panels becomes thus insufficient, leading to thermal control problem of the electronic systems. One solution to solve this problem is to increase the radiation temperature of the satellites panels using heat pumps. In the off nominal operation of these heat pumps, very low mass velocities of the working fluid may be encountered. However, most of the studies on condensation flows available in the literature were carried out at high mass velocities of several hundreds of $kg.m^{-2}.s^{-1}$, and concerned particularly the flow regimes and the heat transfer. Studies on the condensation flows at much lower mass velocities are thus required [1,2]. Besides, the gravitational field influences significantly the distribution of the vapour and liquid phases in the condensers. In a space application context, it is important to operate in condition of low impact of gravity. A possible solution in terrestrial environment is to reduce the size of the channels [3].

In this study, condensation flows in a cross-flow air-cooled micro-condenser were investigated for mass velocities lower than 12 $kg.m^{-2}.s^{-1}$, with n-pentane used as the working fluid. This micro-condenser consisted of a transparent single square cross-section micro-channel placed horizontally, having inner and outer edges of 553 and 675 mm, respectively, and a real length exposed to the coolant of 196 mm. One of the specificities of the experimental bench was the choice of the air as a coolant so that the external heat transfer is limiting. In order to determine accurately the value of the external heat transfer coefficient, a special technique developed in a previous study and based on Laser Induced Fluorescence was used again [4].

Three main flow zones were identified, similarly to those observed in a circular cross-section micro-channel of nearly equal hydraulic diameter [1,4]: annular zone, intermittent (or elongated bubbles) zone and spherical bubbles zone. The intermittent zone was investigated from a thermo-hydraulic point of view by a simple visualization of the vapour and liquid phases distribution using a high-speed camera. The condensation of the elongated bubbles was studied by following these bubbles from the moment of their detachment till they become spherical. The evolutions of their mean displacement and condensation velocities were determined as a function of their mean length and the mass velocity of the fluid. The resulted curves showed a linear relationship between the mean condensation velocity and the mean length of the elongated bubbles. Hence, the evolution of the mean latent heat flux density released by phase change (elongated bubbles collapse) was determined as a function of the mean elongated bubbles surface (Fig. 1), showing an almost constant curve except for the transition zone between the intermittent and spherical bubbles zones.

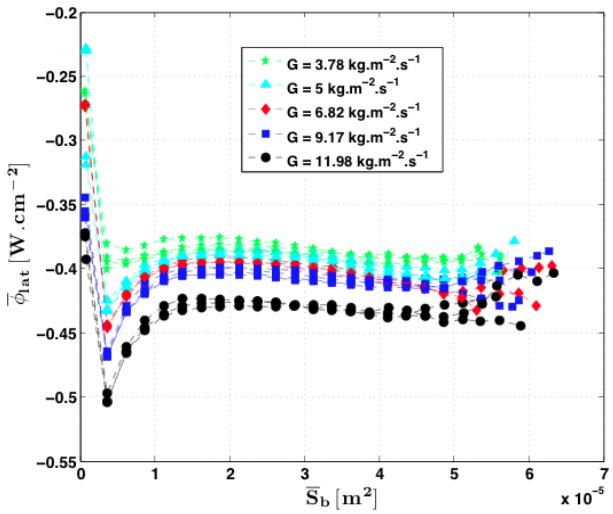

Figure 1: Evolution of the mean latent heat flux density released by the elongated bubbles collapse as a function of the mean bubbles surface during condensation flows of n-pentane inside a square cross-section micro channel for different mass velocities.

References

[1] B. Médéric, P. Lavieille, M. Miscevic, Heat transfer analysis according to condensation flow structures in a minichannel, Exp. Therm. Fluid Sci. 30 (2005) 785-793.
[2] G. El Achkar, M. Miscevic, P. Lavieille, J. Lluc, J. Hugon, Flow patterns and heat transfer in a square cross-section micro condenser working at low mass flux 59 (2013) 704-716.
[3] B. Médéric, M. Miscevic, V. Platel, P. Lavieille, J-L. Joly, Experimental study of flow characteristics during condensation in narrow channels: the influence of the diameter channel on structure patterns, Superlattices and Microstructures 35 (2004) 573-586.
[4] G. El Achkar, P. Lavieille, J. Lluc, M. Miscevic, Heat transfer and flow distribution in a multichannel microcondenser working at low mass fluxes, Int. J. Heat Mass Transfer 54 (2011) 2319-2325.

4th Micro and Nano Flows Conference
UCL, London, UK, 7-10 September 2014

A CFD and FEM Approach to a Multicompartmental Poroelastic Model for CSF Production and Circulation with Applications in Hydrocephalus Treatment and Cerebral Oedema

John C. VARDAKIS[1*], Dean CHOU[1], Brett J. TULLY[2] & Yiannis VENTIKOS[3]

* Corresponding author: Email: john.vardakis@eng.ox.ac.uk
1 Institute of Biomedical Engineering and Department of Engineering Science, University of Oxford, Oxford, UK, dean.chou@eng.ox.ac.uk
2 Oxyntix Ltd., Department of Engineering Science, University of Oxford, Oxford, UK, brett.tully@oxyntix.com
3 Department of Mechanical Engineering, University College London, Torrington Place, London, UK, y.ventikos@ucl.ac.uk

Keywords: Cerebrospinal Fluid (CSF), Aquaporins, Multiple-Network Poroelastic Theory (MPET), Hydrocephalus, Cerebral Oedema

Brain diseases affect over one quarter of the European population, at an estimated cost of over €450 billion [1]. Age-related variations are imposing huge challenges to the global healthcare system. Diseases of old-age, such as Dementia are exerting substantial pressures on society through growing numbers and costs. At the same time, medical experts and policy makers are increasingly aware that the efficacy and economy of therapy is strongly connected with the personalization of treatment.

Hydrocephalus (HCP) is a neurological disorder characterized by an active distension of the cerebral ventricles. It has no known cure and current treatment methods display unacceptably high failure rates. The two prominent treatment methods - shunt implants and endoscopic third ventriculostomy – are both surgical interventions that are statistically indistinguishable in terms of available clinical survival data and efficacy of short or long term success [2, 3].

This study proposes the implementation of a Multiple-Network Poroelastic Theory (MPET) model (Figure 1a) coupled with a finite element method and finite-volume computational fluid dynamics (CFD) for the purpose of studying, in detail, the transport of water within a patient-specific cerebral environment reconstructed from T2 weighted MRI data [4]. The advantage of using the MPET representation is that it allows the investigation of fluid transport between CSF, brain parenchyma and cerebral blood.

A key novelty in the CFD model (Figure 1b) is the amalgamation of anatomically accurate choroid plexuses with their feeding arteries and a simple relationship relaxing the constraint of a unique permeability for the CSF compartment. This was done in order to account for the Aquaporin-4-mediated swelling characteristics. This model is used to demonstrate the impact of aqueductal stenosis and fourth ventricle outlet obstruction (FVOO). The implications of treating such a clinical condition with the aid of endoscopic third (ETV) and endoscopic fourth (EFV) ventriculostomy were considered. The greatest reversal of the effects of atresia come by opting for ETV rather than the more complicated procedure of EFV [5].

Finally, we also present a coupled multidimensional (1D, 2D and 3D) MPET-FEM framework (Figure 1c) with application to HCP and Cerebral Oedema.

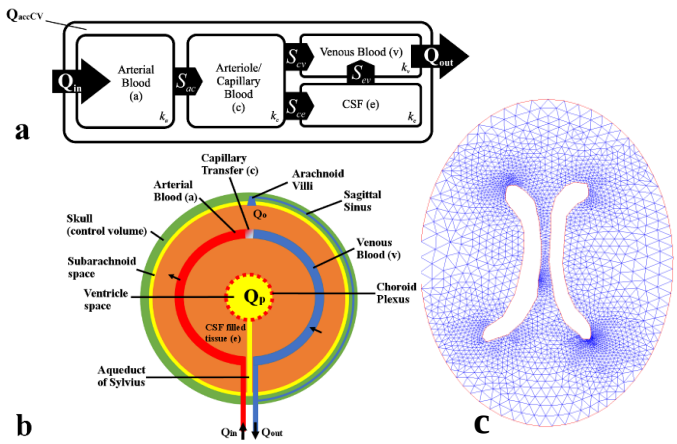

Figure 1: *(a) The schematic represents the transfer restrictions placed on the MPET model. For example, it can be seen that flow is prohibited between the CSF and arterial network. (b) In our MPET model, the ventricles are connected to the subarachnoid space via an anatomically accurate representation of the ventricular system. The two arrows in the figure denote directional transfer between arterial blood and CSF filled tissue and finally CSF filled tissue and venous blood. (c) An example of a coarse triangular mesh of an adult skull, parenchyma and extracted ventricles used for the 2D FEM-MPET model.*

References

1. A. Gustavsson, "Cost of disorders of the brain in Europe 2010", *European Neuropsychopharmacology,* vol. 21, pp. 718-779, 2011.
2. J. Drake, V. Kulkarni and J. Kestle, "Endoscopic third ventriculostomy versus ventriculoperitonial shunt in pediatric patients: a decision analysis", *Childrens Nervous System,* pp. 467-472, 2009.
3. A. V. Kulkarni, J. M. Drake, J. R. Kestle, C. L. Mallucci, S. Sgouros and S. Constantini, "Endoscopic Third Ventriculostomy Vs Cerebrospinal Fluid Shunt in the Treatment of Hydrocephalus in Children: A Propensity Score - Adjusted Analysis", *Neurosurgery,* vol. 67, pp. 588-593, 2010.
4. B. Tully and Y. Ventikos, "Cerebral water transport using multiple-network poroelastic theory: application to normal pressure hydrocephalus", *Journal of Fluid Mechanics,* vol. 667, pp. 188-215, 2011.
5. J. C. Vardakis, B. J. Tully and Y. Ventikos, "Exploring the Efficacy of Endoscopic Ventriculostomy for Hydrocephalus Treatment via a Multicompartmental Poroelastic Model of CSF Transport: A Computational Perspective", *PLOS ONE,* in press.

4th Micro and Nano Flows Conference
UCL, London, UK, 7-10 September 2014

Nanoscale Prediction of Graphite Surface Erosion by Highly Energetic Gas – Molecular Dynamics Simulation –

Ramki MURUGESAN [1], Nichith CHANDRASEKARAN [1], Jae Hyun PARK [2,3,*]

* Corresponding author: Tel.: +82 (0)55 772-1585; Fax: +82 (0)1895 256392; Email: parkj@gnu.ac.kr
1 School of Mechanical and Aerospace Engineering, Gyeongsang National University, South Korea
2 Department of Aerospace and System Engineering, Gyeongsang National University, South Korea
3 Research Center for Aircraft Parts Technology, Gyeongsang National University, South Korea

Keywords: Surface Erosion, Rocket Nozzle, Highly Energetic Gas, Molecular Dynamic Simulation

Graphite is widely used as materials for rocket-nozzle inserts due to its excellent thermophysical properties as well as low density. However, during the operation of rockets, the surface of the graphite nozzle is subjected to very high heat fluxes and the undesirable erosion of the surface occurs (see Figures 1(a) and 1(b)). This phenomenon is most considerable at the throat, in which the heat-transfer rate reaches maximum. Any throat erosion can cause severe reduction of rocket performance. For most solid-rocket applications, an increase in the throat-area of more than 5% is usually not tolerated [1].

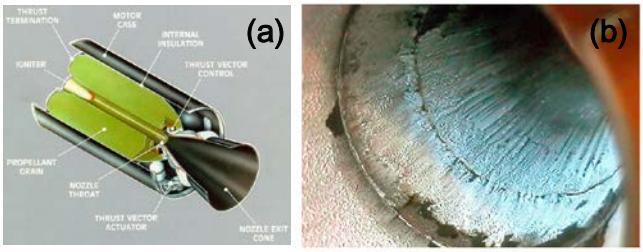

Figure 1 (a) Typical solid-rocket motor; (b) Rocket nozzle after experiencing erosion.

A popular expression for surface erosion was developed by Boyarintsev and Zvyanginby using the theoretical formula for chemical kinetics and heat/mass transfer in boundary layer [2]. The key parameter for this expression is the heat transfer coefficient and it is estimated by the simple Bartz relation [3]. Although it requires a number of empirical parameters varying with the surface types, it has been used for the last several decades. Recently, the strong demand for faster and more reliable design for rocket nozzle drives us to the development of more fundamental relations for surface erosion. In the current study, we pursue this by using extensive molecular dynamics (MD) simulations. As shown in Figure 2, a number of combustion gas molecules (e.g. CO_2 and H_2O) are bombarded to the graphite surface. Their injection velocities are assigned by the sum of thermal velocities from Maxwellian distribution and flow velocity. Flow velocity and temperature are obtained from continuum analysis of the combustion chamber. Since the temperature of gas-surface interface is about several thousand Kelvin, the carbon atoms in the graphite might be easily dislocated by the impact of gas molecules. To our knowledge, it is the first time to observe the erosion behavior at such high temperature in molecular level (e.g. nanoscale).

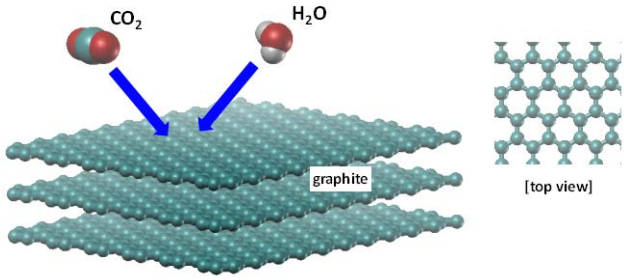

Figure 2 Bombardment of carbon dioxide and water molecules onto graphite surface.

The MD simulations are performed by LAMMPS with NVE ensemble and AIREBO or REBO potential for graphite. Since the surface is not metallic, the charge transfer effects during impingement are neglected. Through these simulations, in this study we obtain the erosion rate and heat flux profiles with diverse flow velocity and temperature conditions, then to build a molecule-level model for graphite surface erosion due to highly energetic gas. This new model is expected to be a milestone in efficient design of rocket nozzle.

References:

[1] G. P. Sutton and O. Biblarz, Rocket Propulsion Elements, 6th ed. (John Wiley & Sons, Inc., New York, 2001).
[2] V. I. Boyarintsev and Yu. V. Zvyagin, *Proc. 5th Int. Heat Transfer Conf.*, pp.264-268.
[3] D. R. Bartz, *J. Jet Propul.*, 27, 49 (1957).
[4] S. J. Plimpton, J. Comput. Phys. 117, 19 (1995).

4th Micro and Nano Flows Conference
UCL, London, UK, 7-10 September 2014

A Model For Uphill Droplet Motion

Felipe M. MANCIO REIS [1,2], Pascal LAVIEILLE [1,2], Marc MISCEVIC [1,2,*]

* Corresponding author: Tel.: +33 (0)5 61 55 83 07 ; Fax: +33 (0)5 61 55 60 12 ; Email: marc.miscevic@laplace.univ-tlse.fr
[1]Université de Toulouse, UPS, INPT, LAPLACE (Laboratoire Plasma et Conversion d'Energie), 118 route de Narbonne, F-31062 Toulouse
[2]CNRS, LAPLACE, F-31062 Toulouse, France

Keywords: dynamic contact angle, contact angle hysteresis, wettability gradient, droplet hydrodynamic model

It is considered that two-phase systems are among the most efficient systems to exchange large heat fluxes. These systems are based on the latent heat associated to a change of state of matter, i.e. a phase transition such as the boiling of a liquid, the evaporation of a droplet, or the condensation of a vapour. Even if two-phase systems are effective, their control under microgravity conditions is not yet completed, as the gravity forces do not allow the evacuation of the dispersed phase anymore. The present work deals with the use of surface tension forces induced by heterogeneous wettability to solve this problem. It is considered that a heterogeneous wettability property of a solid surface enables the mechanical non-equilibrium of the embryos forming on the wall. Dynamic contact angle of a droplet on a tilted surface (with an angle α compared to the horizontal) with a wettability gradient have been widely studied in the literature from both experimental and theoretical point of views [1-3]. The most common approach is based on hydrodynamic theory consisting in the balance between the driving force (F_d) and the viscous force (F_v). The driving force is directly related to the wettability gradient and gravity in the case of (α<0), and the viscous force corresponds to the integral of the viscous stress over the base of the droplet. Due to the singularity of viscous dissipation near the contact line, there are several studies regarding this viscous force, Subramanian et al. [2] proposed the viscous force model chosen in this study.

The Young equation corresponds to an equilibrated force balance on a static wedge of an interface. If an external action modifies the geometry of the problem, a new contact angle appears, i.e. the dynamic contact angle. The sum of the vectors will be perturbed and, consequently unbalanced. A new force exerts by the interface to compensate this situation, thus the droplet shrinks or spreads. If we assume that the forces are always unbalanced, a wetting force arises on the triple line causing the continuous motion of the liquid. Nevertheless, the contact angle hysteresis that is related to the roughness and the chemical heterogeneities on the surface, prevent the motion. The contact line pinning, i.e. contact angle hysteresis, has prove to be a major experimental problem, that's why a hydrodynamic model has been realised in order to describe the motion of a droplet on a heterogeneous surface. The aim of the model presented in this paper is to establish the velocity (U) of the centre of mass of the droplet taking into account the contact angle hysteresis. It is also possible to determine the spreading velocity and the shape of the droplet during the movement. The model allows us to know the setting in motion conditions. The results obtained have been first compared to experimental data from Moumen et al. [3]. To our knowledge, this model taking into account contact angle hysteresis is the first one that shows a so good agreement with the experimental data (Figure 1). This agreement suggests that the hypothesis that the contact angle hysteresis reduces the driving force is consistent in order to explain the behaviour of the drops on the gradient surface. The model can then be used to analyse the mainly governing parameters of the motion. A study of the effect of the fluid physic properties, surface characteristics, gradient and contact angle hysteresis will be presented. A particular attention will be paid considering water as the working fluid.

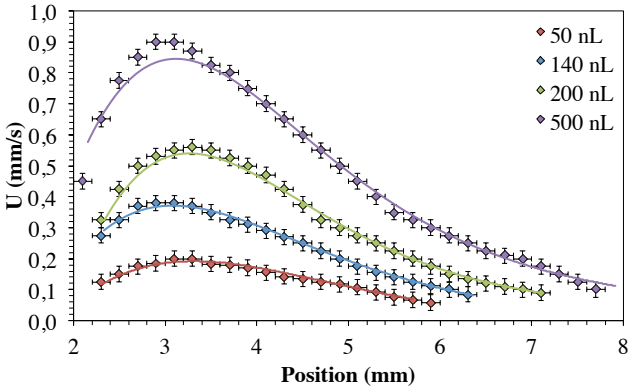

Figure 1 Comparison between the measured [3] and predicted velocities for a drop which volume is 500 nL.

Acknowledgement: this work is funded by the European Space Agency Microgravity Application Program "MANBO" (Multiscale ANalyses BOiling).

References:

1. Manoj K. Chaudhury, George M. Whitesides, "How to make water run uphill", Science 1992, Vol. 256
2. R. S. Subramanian, N. Moumen, and J. B. McLaughlin, "Motion of a droplet on a solid surface due to a wettability gradient", Langmuir 2005, Vol. 21, No. 25, 11844-11849
3. M. Moumen, R. S. Subramanian, and J. B. McLaughlin, "Experiments on the motion of drops on a horizontal solid surface with wettability gradient", Langmuir 2006, Vol. 22, No. 6, 2682-2690

4th Micro and Nano Flows Conference
UCL, London, UK, 7-10 September 2014

Novel Microgels Fabricated On Microfluidic Devices

Bingyuan LU, Theoni GEORGIOU, Nicole PAMME

* Corresponding author: Tel.: +44 (0)1482 465476; Email: B.Lu@2012.hull.ac.uk
Department of Chemistry, University of Hull, UK

Keywords: Microgels, Microfluidics, Polymerisation, Droplets, T-junction, Flow Focusing

We present the use of microfluidic devices for the fabrication of novel functional microgels towards their use as drug delivery vehicles, achieved by the on-chip generation of droplets and their subsequent polymerisation either on- or off-chip.

Microgels are gel particles formed of polymer networks that show potential for the delivery of both hydrophilic and hydrophobic drugs[1]. However, the preparation of monodisperse microgel particles from droplets containing monomers, crosslinkers and initiators can be challenging when using conventional emulsion or precipitation polymerisation techniques. Microfluidic devices provide an excellent format for the generation of monodispersed droplets due to the precise manipulation of fluids and flow rates within the microchannels. Immediate polymerisation of each droplet can then be realised to prevent monomers or crosslinkers from dissolving into the surrounding immiscible phase, ensuring the reproducible synthesis of high quality microgels.

The two main strategies for generating droplets in microfluidic devices are the use of T-junction and flow focusing geometries, both introduce droplets of a "dispersed phase" (DP) into a "continuous phase" (CP)[2]. Both designs were utilised here to generate oil-in-water droplets. The influence of the flow rates of each phase on the size of the produced droplets was investigated. It was found that when the flow rate of the CP was held constant and the DP flow rate was increased, the droplets became larger. On the other hand, when the flow rate of the DP was held constant, the droplets became smaller as the flow rate of the CP was increased (Fig.1).

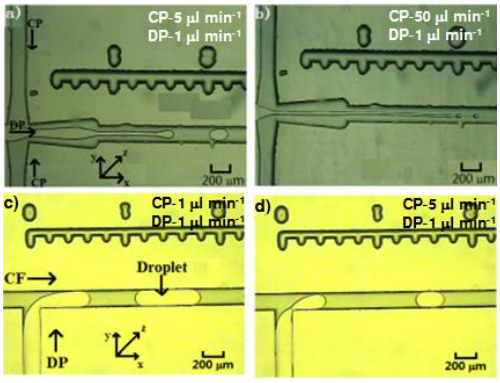

Fig. 1 Photographs of the change in size of droplets when the flow rate of dispersed phase (DP) was maintained at 1 µl min^{-1} while the continuous phase (CP) flow rate was varied. (a) Droplets formed by the flow focusing design with a CP flow rate of 5 µl min^{-1} and (b) 50 µl min^{-1}. (c) Droplets generated via a T-junction design at CP flow rates of 1 µl min^{-1} and (d) 5 µl min^{-1}.

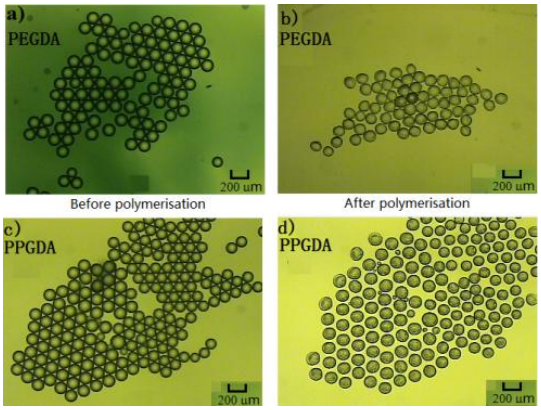

Fig. 2 Photos of the change in (a-b) PEGDA and (c-d) PPGDA microgels before and after polymerisation.

By varying the relative flow rates appropriately, droplets smaller than 200 µm could be generated (CV 2-4 %) in both chip geometries, while droplets of less than 50 µm diameter (CV 8-14 %) could be produced in the flow focusing design when very high flow rates of CP were used relative to the DP flow rates.

In order to fabricate microgels, various combinations of monomers, crosslinkers and initiators were added to the DP (chloroform). Once the droplets had been generated, thermo/photo polymerisation was achieved by UV irradiation (365 nm) to form the microgel. Three types of microgels were formed using this setup: poly(ethylene glycol) diacrylate (PEGDA), poly(propylene glycol) diacrylate (PPGDA), and tetrahydropyran acrylate (THPA). Fig.2 demonstrates how hydrophilic PEGDA microgels became transparent as they absorbed water from the CP, while PPGDA microgels remained cloudy due to their hydrophobicity. THPA/PEGDA amphiphilic microgels demonstrated a responsiveness to pH due to a build up of electrostatic force in high pH.

In conclusion, we have demonstrated the fabrication of hydrophilic, hydrophobic and amphiphilic microgels via the generation of droplets in microfluidic devices and their subsequent polymerisation either on- or off-chip. The microgels showed high monodispersity, while on-chip polymerisation reduces the loss of reagents from the dispersed phase into the continuous phase.

References

[1] Dadsetan et al., *Acta Bio.*, **2013**, 9(3): p. 5438-5446.
[2] Zhao et al., *Chem. Eng. Sci.*, **2011**, 66(7): p. 1394-1411.

4th Micro and Nano Flows Conference
UCL, London, UK, 7-10 September 2014

Electrodiffusion Method of Near-Wall Flow Diagnostics in Microfluidic Systems

Jaroslav TIHON*, Vera PENKAVOVA, Petr STANOVSKY, Jiri VEJRAZKA

* Corresponding author: Tel.: ++420 220390250; Email: tihon@icpf.cas.cz
Institute of Chemical Process Fundamentals, Academy of Sciences of the Czech Republic, CZ

Keywords: Electrodiffusion Method, Wall Shear Stress, Microchannel Flow, Backward-Facing Step

Introduction

The electrodiffusion technique [1], which has been until now used only for the near-wall flow diagnostics on larger scales, can be promising for both, scientific experiments and microdevice diagnostics. The electrodiffusion sensors prepared by the photolithography have been already applied to investigate the structure of near-wall turbulence in channel flows and their applications in microfluidic systems have been just considered. New microfabrication techniques enable us to produce microfluidic devices with precisely shaped microelectrodes. It offers a possibility to use such electrodiffusion sensors for near-wall flow investigations in various microfluidic systems (e.g. in complex channel geometries often used as micromixers, or possibly in multiphase microfluidic systems dealing with bubbles and drops.)

Electrodiffusion method

The electrodiffusion sensor works as a small electrode, on which a fast electrochemical reaction takes place, when a small polarization voltage is applied to it. The electric current passing through the electrode is the measured quantity. The current signal I provided by a simple strip probe is controlled by convective diffusion and depending on the wall shear rate γ according to the well-known Léveque formula

$$I = 0.807\, n F\, c_0\, w l^{2/3} D^{2/3} \gamma^{1/3}, \qquad (1)$$

where n is the number of electrons involved in the electrochemical reaction, F is the Faraday constant, l is the length of the strip sensor in the mean flow direction, w is its width, c_0 is the bulk concentration of the active ions, and D is their diffusivity in the solution. The main advantage of this technique is that the wall probes provide information about the flow in the near wall region without any disturbances imposed on the studied velocity field.

Classical versatile sensors are fabricated from platinum foils or wires, which are glued into a stainless steel tube acting as an auxiliary electrode. A novel technique for fabrication of plastic microfluidic systems with integrated metal microelectrodes (called technique of sacrificed substrate) has been developed at ICT Prague [2]. Several micrometer thick gold sensors built-in into a plastic substrate exhibit good mechanical resistance and smoothness.

Microchannel flow experiments

A test chip designed to test electrodiffusion sensors fabricated by the method of a sacrificed substrate consists of an array of gold strips embedded into a Plexiglas plate. Twenty working cathodes (160 μm strips) separated by 40 μm insulating gaps are located between two large anodes (10 mm strips). The plate with microelectrodes serves as a top cover (roof wall) of a flat calibration microchannel. It has a rectangular cross-section (with 800 μm height and 10 mm width) and a length of 80 mm. The active surface of sensors is delimited by a sealing placed between the microchannel and test plate so that it forms side walls of the microchannel. The design of the test plate enables us to use gold strips as individual or double (two-strip) sensors, thus to investigate also the microchannel flows with possible separations and reattachments. Water with a small addition equimolar potassium ferro/ferricyanide is used as a suitable electrochemical system.

The electrodiffusion sensors have been first tested by the measurement of polarization curves (see Figure 1). The currents measured from individual sensors differentiated less than 0.5%. The results of sensor calibrations carried out under steady laminar flow conditions then follow very well a cubic root dependence on the wall shear rate prescribed by Eq.1.

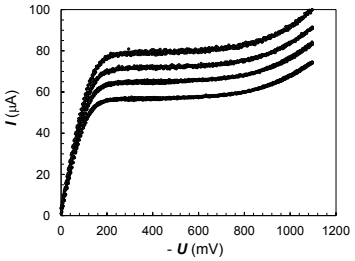

Figure 1. Limiting diffusion currents measured at different flow rates (for γ=3120, 4690, 6250, and 7810 s^{-1}).

Also the measured transient current response to the polarization set-up is found to be in good agreement with the Cottrell asymptote describing the initial period of unsteady diffusion:

$$I = zFc_0 wl\sqrt{D/(t\pi)}. \qquad (2)$$

The practically same values of diffusion coefficient are obtained from the results of steady and unsteady calibrations (D = 6.9 10^{-10} m^2/s), thus verifying the proper functioning of sensors.

After calibration measurements, the chip with microsensors has been mounted into a microchannel provided by a step change in its height from 400 μm (inlet section) to 800 μm (outlet section). The axial profiles of wall shear stresses have been measured for different Re values. The different flow-recirculation zones have been identified downstream the step and high magnitudes of near-wall flow fluctuations observed at reattachment regions. The characteristic frequencies of these pulsations have been provided.

Conclusions

The chip with sensors fabricated by the method of a sacrificed substrate proved to be a reliable platform for electrodiffusion measurements carried out in microfluidics. Our first results obtained for separating/reattaching flow behind a backward-facing step placed in the microchannel demonstrate its applicability for the detection of near-wall flow reversal and the delimitation of flow-recirculation zones. However, other applications of these sensors in microfluidics (as investigation of near-wall turbulence, detection of moving bubbles or drops, or characterization of capillary waves on liquid films) are easily envisaged.

Acknowledgement
The support by Czech Science Foundation GACR through the contract P101/12/0585 is gratefully acknowledged.

References

1. T.J. Hanratty, J.A. Campbell, Fluid mechanics measurements (Washington, Hemisphere, 1983)
2. W. Schrott, M. Svoboda, Z. Slouka, D. Snita, Microelectron Eng, 86, 1340 (2009)

4th Micro and Nano Flows Conference
UCL, London, UK, 7-10 September 2014

Aerodynamic behavior of the bridge of a capacitive RF MEMS switch

Dragos ISVORANU [1,*], Stefan SOROHAN [2], Gabriela CIUPRINA [3]

* Corresponding author: Tel.: ++40 (0)213250704; Fax: ++40 (0) 213181007; Email: ddisvoranu@gmail.com
1 "Elie Carafoli" Department of Aerospace Sciences, University Politehnica of Bucharest (UPB), Romania (RO)
2 Department of Strength of Materials, Faculty of Engineering and Management of Technological Systems, UPB, RO
3 Department of Electrotechnics, Electrical Engineering Faculty, UPB, RO

Keywords: Capacitive switch, Coupled modelling, Vortex flows, Viscous damping

The present paper proposes a coupled 3D multiphysics model and presents the results of its transient simulation, for a RF MEMS capacitive switch of bridge-type.

Capacitive switches, with their large contact area, can handle more RF power than metal-to-metal contact switches and are therefore the preferred switches for applications requiring 100–500 mW of RF power. Their switching time is in the range of 1-200 μs. Their relatively small contact forces (50-1000 μN) ensure high reliability and a large number of operating cycles (~ 2-10 Billions). Capacitive switches can operate in the range 6 – 120 GHz and above due to their relatively small down-state capacitance (2–5 pF). Among all these parameters, the switching time is an important one, especially in applications in which the devices are required to change their states as fast as possible. Therefore, modelling strategies able to accurately predict the switching time of RF MEMS switches are needed.

There is an enormous literature on the modelling steps in the case of static regimes, useful to derive quantities such as the pull-in or pull-out voltages, based on the coupling between the mechanical and the electrostatic field formulations. However, in the dynamic case, neglecting or poor models of the aerodynamical behaviour may lead to unsatisfactory results [1].Most papers dealing with aerodynamic behaviour use mostly the squeeze film analysis mainly related to viscous damping characteristics [2]. Complex 3D geometries of the bridge were rarely taken into account in viscous damping assessment much less in the simulation of the full flow around the bridge of the switch. That is why, the present paper includes, beside the common assessment of the pull-in and pull-out voltages, bridge deflection, capacitance and mechanical behaviour. 3D fluid-structure analysis in order to catch the complex vortical unsteady fluid structures that have been identified in our preliminary finite element analysis tests for a simple geometric capacitive swich (Figs. 1 and 2).
The fluid structure interaction (FSI) simulation sustains time-varying viscous damping and modified time response of the bridge deflection compared to the actuation modulation especially when the amplitude of the forcing function is above pull-in voltage.
The simulations performed for the considered structures have been compared with results from the literature and with measurements.

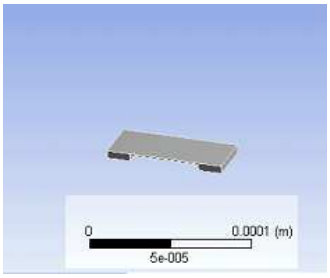

Fig.1 Geometry of the bridge

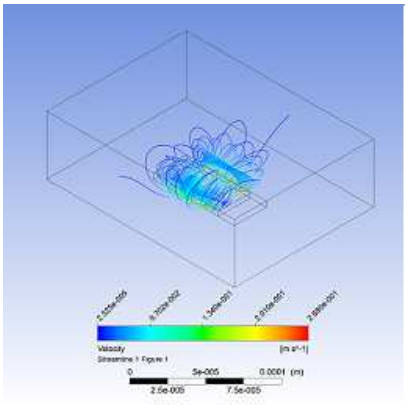

Fig.2 Vortical structures of the flow

References

[1] A Eriksson, (2005). Mechanical Model of Electrostatically Actuated Shunt Switch, Excerpt from the Proceedings of the COMSOL Multiphysics User's Conference 2005 Stockholm.
[2] P G Steeneken, Th G S M Rijks, J T M van Beek, M J E Ulenaers, J De Coster and R Puers, (2005). Dynamics and squeeze film gas damping of a capacitive RF MEMS switch, *J. Micromech. Microeng.* **15** 176.

Acknowledgment

This work has been funded by the Joint Research Project PN-II-PT-PCCA-2011-3, with the support of ANCS, CNDI – UEFISCDI, project no. 5/2012.

4th Micro and Nano Flows Conference
UCL, London, UK, 7-10 September 2014

A Hydrodynamic Study of Gas-Liquid Flow in a Micro-Packed Bed Reactor

Noor AL-RIFAI, Enhong CAO, Asterios GAVRIILIDIS*

* Corresponding author: Tel: +44 (0) 20 7679 3811; Fax: +44 (0) 20 7383 2348; Email: a.gavriildis@ucl.ac.uk
Department of Chemical Engineering, University College London, UK

Keywords: Micro-Fixed Bed, Flow Mapping, Multiphase Reaction

The high surface area-to-volume ratios associated with microreactors promote fast heat and mass transfer, making them particularly suited to highly exothermic and mass transfer limited reactions. Despite the cited advantages and the rather wide application of micro-packed beds in multiphase kinetic and mass transfer studies, their hydrodynamic characteristics are still poorly addressed in the literature. Deviations exist from what is commonly observed in the macroscale in terms of hydrodynamics and flow regime mapping due to a strong increase in the effect of capillary forces when scaling down reactor and particle size [1].

In this study, we examine the influence of gas and liquid flow rates on the flow regimes observed in a microstructured packed bed reactor. The focus of the work is flow regime mapping; onset of flow regime transition, and the contributory roles of particle size, morphology, bed length, fluid properties, and inlet flow conditions. The used silicon-glass microstructured reactor consists of serpentine channels (***Figure 1***) of rectangular cross-section (300µm D x 600µm W). The range of superficial liquid velocities studied are 0.001 to 0.2 cm/s while the superficial gas velocities range from 5 to 100 cm/s, utilising both aqueous and organic liquid feeds, and under both cold flow and typical oxidation reaction temperatures (120°C). To avoid flow maldistribution in macroscale reactors, typically a particle to tube diameter ratio less than 1/10 is recommended [2]; here we assess the applicability of this criterion to microreactors by studying a range of particles differing in size (10-90 µm) and morphology (glass beads and porous catalyst). The flow observation is carried out via microscopic visualisation of the contacting patterns between the phases.

The results show a strong dependency of the hydrodynamics on the gas and liquid flow rates. Increasing the gas to liquid velocity ratio results in a transition from "slug flow" where segregated regions of both gas and liquid slugs exist (***Figure 2A***), to a "gas-continuous trickle flow" where the bed is occupied by a continuous gas phase and the liquid is sheared to a more uniformly distributed thin film (***Figure 2F***). This effect is more pronounced at lower liquid flow rates where a lower gas flow rate is required to achieve the same flow pattern. The flow regime in the empty channel preceding the bed has a large influence on the hydrodynamics observed; slug flow at the packed bed inlet causes periodic wetting and drying of the particles and results in segregated regions of gas and liquid, whilst annular flow at the packed bed inlet results in a more stable liquid film.

Figure 1. *Micro-packed bed reactor*

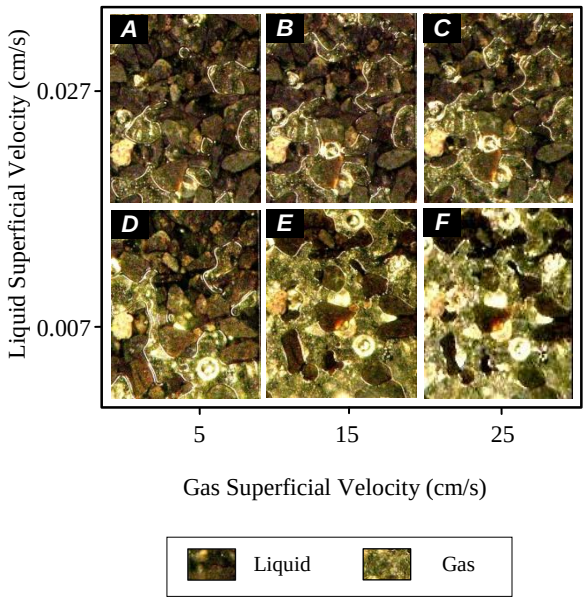

Figure 2. *Microscope images of the micro-packed bed at the different hydrodynamic conditions. Particles shown are Au-Pd/TiO_2 with an average particle size of 65µm.*

The classification of flow regimes will help to determine operating ranges for kinetic and mass transfer studies, and for process conditions optimisation. In kinetic studies, a steady flow regime (gas-continuous trickle) is more desirable to allow reproducibility and easy interpretation of kinetic data. This flow regime is also anticipated to have high mass transfer rates due to better spreading of the liquid film over the external packing area.

References

1. A. Faridkhou, M. Hamidipour, F. Larachi. Hydrodynamics of gas-liquid micro-fixed beds - Measurement approaches and technical challenges. *Chemical Engineering Journal*, **2013**, 223, 425-435.
2. V. Hessel, A. Renken, J.C. Schouten, J. Yoshida. Heterogeneous multiphase reactions. *Micro Process Engineering: A Comprehensive Handbook*, Wiley-VCH Verlag GmbH, Weinheim, **2009**.

4th Micro and Nano Flows Conference
UCL, London, UK, 7-10 September 2014

Design of passive micromixer for the enzymatic digestion of DNA

Ioanna K. KEFALA, Vasileios E. PAPADOPOULOS, George KOKKORIS, Georgia KARPOU, Despoina, MOSCHOU, George PAPADAKIS, and Angeliki TSEREPI*

* Corresponding author: Tel.: ++30 2106503264; Fax: ++30 210 6511723; Email: atserepi@imel.demokritos.gr
Department of Microelectronics, Institute of Advanced Materials, Physicochemical Processes, Nanotechnology & Microsystems, NCSR "Demokritos", Greece

Keywords: passive micromixer, microflow, microfluidics, Lab on Chip, LoC, DNA digestion

The basic idea and the vision that leads to the rapid development of Lab-on-a-Chip (LoC) systems is the integration of several functions of a (bio)chemical analysis laboratory on a chip. Microfluidic devices appropriate for transport, mixing, separation, and/or reactions, are necessary for LoC systems. Additionally, their operation defines the total performance of LoC systems; thus, their design is of crucial importance. For example, a well designed micromixer can reduce the analysis time and the footprint of a LoC system.[1]

The application of interest in this work is the enzymatic digestion of DNA with restriction enzymes that recognize and cut DNA at specific positions. Restriction enzymes are commonly employed to identify a change (known as single nucleotide polymorphism, SNP) in the genetic sequence that occurs at a site where these enzymes would normally cut. Effective mixing of the enzyme with the DNA sample is required to have a fast digestion process.[2]

The aim of the present work is the design, fabrication, and evaluation of a passive micromixer for the enzymatic digestion of DNA. Passive micromixers do not require external energy (besides the energy required for the pumping of the fluid) as opposed to active which use the disturbance generated by an external field for the mixing process.

The design of an efficient passive micromixer is achieved by testing several configurations including multiple inlets, zig-zag geometries,[3] split-and-merge geometries, helical flow patterns and expansion units[4] in terms of mixing efficiency. The basic characteristics of mixing the enzyme with the DNA sample is the low Reynolds number (<0.5) in the channel of the micromixer and the low diffusion coefficient of the enzymes (10^{-9} – 10^{-11} m^2/s). The channel dimensions are from 100 to 500 μm.

The testing of the configurations is accomplished by mathematical modeling and simulation. The mathematical problem is simplified to a diffusion problem of a solute (enzyme) into water (solution of DNA). The model consists of the continuity and Navier-Stokes equations as well as the mass conservation equation of the enzyme. The equations are solved in 3 dimensions inside the channel of the micromixer with a commercial code.

The preferable micromixer designs are fabricated on thin polyimide (PI) substrates. The fabrication technology is based on a) photolithography for patterning polymeric substrates through the use of photosensitive PI layers and b) lamination with a PI tape for sealing the microchannels. The final part of the micromixer channel (after completion of mixing) is intended to function as the DNA digestion microreactor. For this reason, a thin film copper microheater is fabricated (on commercially available copper clad PI) beneath the microchannel,[5] able to maintain the DNA-enzyme mixture at a temperature necessary for digestion (37^0 C).

The mixing performance of the fabricated device is *evaluated* by visualizing with off-chip gel electrophoresis the outcome of a digestion of a polymerase chain reaction (PCR) product with a restriction endonuclease. A 273 bp DNA was produced from human genomic DNA template.[6] The sequence of the amplified DNA fragment is part of the BRCA1 gene and is associated with breast cancer cases when a single base insertion occurs at the position 5382. The 273 bp DNA can be digested with the restriction endonuclease DdeI (NEB, R0175S) into two fragments of 20 and 253 bp, in respect. In Fig. 1, the results for a passive micromixer with multiple inlet configuration and zig-zag geometry are shown. In Fig. 1a, the concentration along the flow direction coming from simulation is shown. Fig. 1b shows the design of the micromixer as well as images of parts of the fabricated micromixer. The results of gel electrophoresis are shown in Fig. 1c; the DNA was completely digested which indicates that efficient mixing taking place within the microchannel also leads to rapid DNA digestion. This result involves a 7.5μl sample; the digestion was completed in 2.5 min.

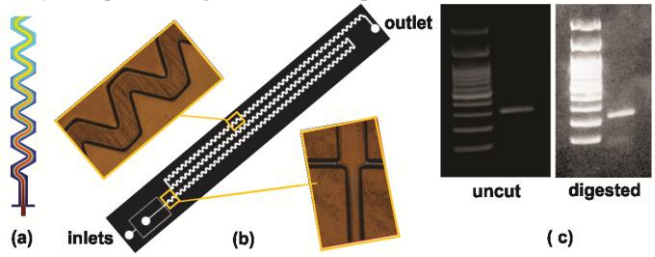

Figure 1. a) Concentration along the flow direction for the fabricated micromixer, b) The design of the fabricated micromixer and images showing magnified details (inlet junction, part of zig-zag channel). c) Gel images of uncut and digested 273 bp fragment.

[1]J. M. Ottino and S. Wiggins, Philos. T. R. Soc. A **362,** 923 (2004).
[2]L.-M. Fu and C.-H. Lin, Biomed Microdevices **9,** 277 (2007).
[3]W. Jeon and C. B. Shin, Chem. Eng. J. **152,** 575 (2009).
[4]A. P. Sudarsan and V. M. Ugaz, Lab on a Chip **6,** 74 (2006).
[5]E. Mavraki, D. Moschou, G. Kokkoris, N. Vourdas, S. Chatzandroulis, and A. Tserepi, Procedia Engineering **25,** 1245 (2011).
[6]G. Papadakis and E. Gizeli, Anal. Methods **10.1039/c3ay41143e** (2013).

4th Micro and Nano Flows Conference
UCL, London, UK, 7-10 September 2014

Continuous Flow vs. Stationary µPCR Devices on Ultra Thin Polymeric Substrates

Vasileios E. PAPADOPOULOS, Ioanna K. KEFALA, George KOKKORIS*, and Angeliki TSEREPI

* Corresponding author: Tel.: ++30 2106503238; Fax: ++30 210 6511723; Email: gkok@imel.demokritos.gr
Department of Microelectronics, Institute of Advanced Materials, Physicochemical Processes, Nanotechnology & Microsystems, NCSR "Demokritos", Greece

Keywords: microflow, heat transfer, PCR, microfluidics, DNA amplification, polyimide, µTAS, LoC, FCB technology

Polymerase chain reaction (PCR) can create copies of specific fragments of DNA by thermal cycling. A typical PCR includes denaturation of double-stranded DNA (at 95°C), annealing of primers (at 60 °C), and extension of the primer-bound sequences (at 72°C). Each thermal cycle can double the amount of DNA, and 20–35 cycles can produce millions of DNA copies.

µPCR devices can be categorized to stationary and continuous flow devices. The stationary devices resemble the conventional thermo-cyclers at their operation; the sample is static in a well and both the device and the sample undergo thermal cycling. One type of continuous flow devices comprises fixed loop devices where the sample moves through fixed temperature zones to achieve the required thermal cycling; the number of cycles is determined at the fabrication stage. A second type of continuous flow devices comprises closed loop devices where the sample circulates in the temperature zones. The number of thermal cycles can be adjusted at will during the operation.

Efficient and fast amplification as well as and low power consumption are of a great importance for a µPCR device. For efficient amplification, good temperature uniformity and precise temperature control in the three thermal zones are required.[1]

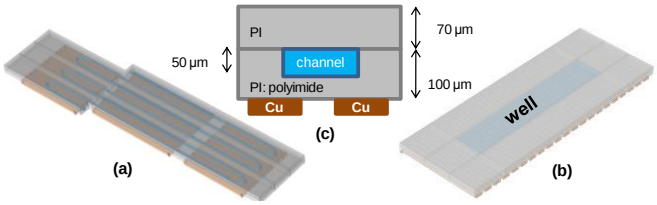

Figure 1. Schematic of a) 3 unit cells (3 thermal cycles) of a continuous flow fixed loop and b) a stationary µPCR device. c) Material stack of the devices integrated with thin metal heaters.

Since the early 1990s, several materials (Si, glass, and recently polymers), technologies, and designs have been utilized for fabrication of µPCR devices.[2] *In this work, continuous flow and stationary µPCR devices based on the same technology (material stack and fabrication process) are evaluated by simulation. In particular, a fixed loop µPCR device (Fig. 1a) is compared with a closed loop and a static (Fig. 1b) device in terms of temperature uniformity in the PCR zones, speed, and power consumption. All devices are based on flexible circuit board (FCB) technology*; the substrate is a biocompatible and thin (50 – 100 µm) polyimide (PI) layer coated with an even thinner metal layer on which resistive heaters are fabricated for sample thermal cycling. PI has been already used as a structural material for stationary µPCR devices.[3,4] Recently,[5] it has been used for fixed loop continuous flow devices but not for closed loop devices. *The aim of this work is the evaluation of FCBs as substrates for continuous flow and stationary µPCR devices.* The evaluation is performed by simulation of the µPCR performance with respect to temperature uniformity and power consumption. The mathematical model consists of the heat transfer equation which is coupled to momentum balance and continuity equations. The equations are numerically solved in 3d and at steady state by the finite element method implemented by a commercial code.

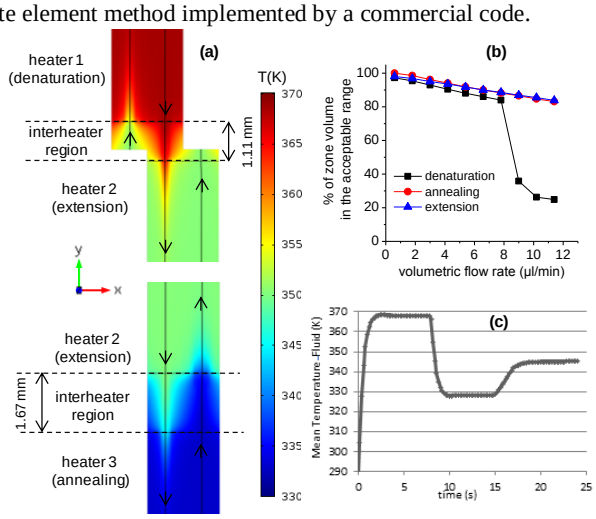

Figure 2. a) Temperature at a cross section (middle of the microfluidic channel height) of the unit cell of a fixed loop µPCR. The focus is on the interheaters region. Arrows show the direction of flow. b) The percentage of the volume of each zone in the acceptable temperature range (set point ±1.5 K) vs. flow rate. c) The mean temperature of fluid during one thermal cycle in a stationary µPCR.

In Fig. 2a the thermal "cross-talk" between different zones of a fixed loop µPCR is shown. The percentage of the volume of the zones in the acceptable temperature range (±1.5 K from the set point) is shown vs. the flow rate in Fig. 2b. The mean temperature of the fluid during one thermal cycle in the stationary µPCR is shown in Fig. 2c.

[1]Y. H. Zhang and P. Ozdemir, Anal Chim Acta **638,** 115 (2009).
[2]C. S. Zhang, J. L. Xu, W. L. Ma, and W. L. Zheng, Biotechnol. Adv. **24,** 243 (2006).
[3]B. Giordano, Analytical Biochemistry **291,** 124 (2001).
[4]K. Shen, X. Chen, M. Guo, and J. Cheng, Sensors and Actuators B: Chemical **105,** 251 (2005).
[5]D. Moschou, N. Vourdas, M. K. Filippidou, V. Tsouti, G. Kokkoris, G. Tsekenis, I. Zergioti, S. Chatzandroulis, and A. Tserepi, Proc. SPIE 8765, Bio-MEMS and Medical Microdevices **8765,** 87650L (2013).

4th Micro and Nano Flows Conference
UCL, London, UK, 7-10 September 2014

From Core-Shell Drops to Drops with Ultra-thin Shells via Non-confined Microfluidics

Ankur CHAURASIA *, Dimitris JOSEPHIDES, Shahriar SAJJADI

* Corresponding author: Tel.: ++44 (0)7795320616; Email: ankur.chaurasia@kcl.ac.uk
Department of Physics, King's College London, UK

Keywords: Microfluidics, non-confined, Core-shell, Ultra-thin shells

Introduction

For many biomedical, pharmaceutical and agricultural applications where encapsulation of payloads such as nutrients or living organisms (cells/tissues)[1] or a controlled release is needed, large core-shell drops (drop radius R~100µm-5mm) are required. Conventional confined microfluidic devices are limited to a rather small range of droplets because of difficulties associated with phase separation at low kinetic energies. A non-confined microfluidic device is introduced which can produce such large range of drop sizes with varying shell thickness under the maximum influence of buoyancy with inner and middle phase flows and quiescent outer phase. The device was made by introducing a circular glass capillary into a square capillary after both were cut to the desired sizes. The inner and outer surfaces of the capillaries were selectively treated to obtain desired affinities. The aligned channels were oriented vertically to maximize the buoyancy effect, schematic for which is shown in Figure 1a. Highly monodisperse drops (CoV< 3%) with ultra-thin shells were obtained by reducing the interfacial tension via a mixture of surfactants. Such drops are stable and excellent for controlled release[2] of the content.

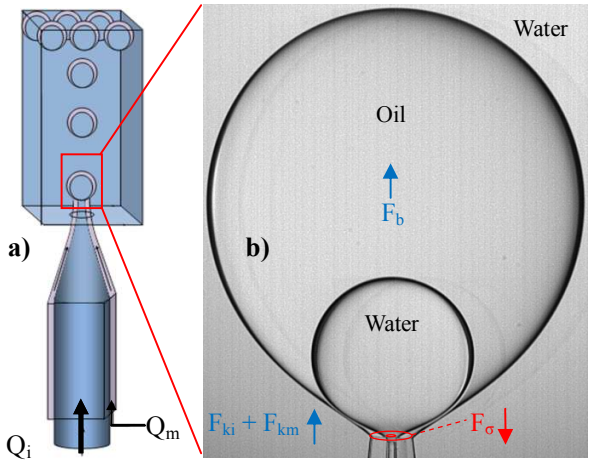

Figure 1 a) Microcapillary based device schematic where buoyancy effect is maximized for core-shell drop formation, b) shows different forces acting on the overall drop being formed at the tip.

A force balance model relating the buoyancy, kinetic and interfacial tension forces (Figure 1b) was applied to the overall drop that could predict the results rather well for a surfactant-free system where the dynamics of interfacial tensions were avoided, and satisfactorily when the surfactants were present. As a general statement, drops with wide range of shell thickness were produced. The shell thickness t was defined as, $t = R - r$. Using mass conservation, the relative thickness (t/R) was given by,

$$\frac{t}{R} = 1 - \sqrt[3]{\frac{Q_i}{Q_i+Q_m}} \quad (1)$$

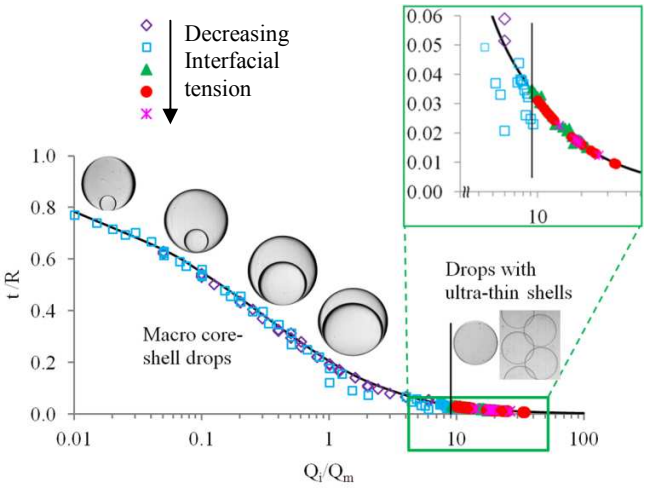

Figure 2 Relative shell thickness t/R versus Q_i/Q_m plot showing that drops with ultra-thin shells can be achieved by decreasing interfacial tension. Solid black line represents the mass balance (Equation 1).

Conclusion

Phase maps were generated to identify the process conditions (flow rates) and formulations (surfactants concentrations) with which core-shell drops could be produced. Drops with rather thick shells were formed at very low Q_i/Q_m and high interfacial tension (Figure 2) where the drop sizes ranged from 3-7mm with shell thickness t >100µm. Drops with ultra-thin shells, t ~1-5µm, were produced by decreasing the interfacial tensions, while the minimum relative shell thickness (t/R) obtained for ultra-thin shelled drops was ~ 0.01, which is similar to those formed using conventional microfluidic technique[3]. Such structures can be useful as delivery vehicles owing to high stability and low residual content left after the release.

References

[1] Manukian, ARS Inc. Gainsville FL, Hydrocapsules®: A New method for aqueous Drug Delivery, DDT Magazine Jan 2008.

[2] A Abbaspourrad, N. J. Carroll, S- H. Kim and D. A. Weitz, Polymer Microcapsules with Programmable Active Release, J. Am. Chem. Soc. 2013, 135, 7744-7750

[3] S- H. Kim, J. W. Kim, J- C Choc and D. A. Weitz, Double-emulsion drops with ultra-thin shells for capsule templates, Lab Chip, 2011, 11, 3162

4th Micro and Nano Flows Conference
UCL, London, UK, 7-10 September 2014

Margination of Micro- and Nano-Particles in Blood Flow and its Effect on the Efficiency of Drug Delivery

Kathrin MÜLLER[1], Dmitry A. FEDOSOV[1,*], Gerhard GOMPPER[1]

* Corresponding author: Tel.: +49 (0)2461 612972; Fax: +49 (0)2461 613180; Email: d.fedosov@fz-juelich.de
1 Theoretical Soft Matter and Biophysics, Institute of Complex Systems and
Institute for Advanced Simulation, Forschungszentrum Jülich, 52425 Jülich, Germany

Keywords: Red Blood Cell, Drug Carrier, Flow Migration, Margination Probability, Particle Distribution, Dissipative Particle Dynamics

Drug delivery by various micro- and nano-carriers offers the possibility of controlled transport of pharmaceuticals to targeted sites (e.g., cancerous tissue). Even though the fabrication of carriers of different sizes and shapes with a number of functionalities has made much progress in the last decade, their delivery including controlled particle distribution and adhesion within the body remains a great challenge. The adhesion of micro- and nano-carriers in blood flow is strongly affected by their distribution within the vessel cross-section. To investigate the adhesion potential of carriers of different shapes and sizes, we employ mesoscopic hydrodynamic simulations of blood flow in order to predict margination of carriers or their migration properties toward vessel walls. The margination of carriers is studied for a wide range of hematocrit values, vessel sizes, and flow rates, using a combination of two- and three-dimensional blood flow models. Two different particle shapes (spherical and ellipsoidal) and various sizes, ranging from about hundred nanometers to several micrometers, are considered. We find that the margination properties of particles worsen with decreasing carrier size. Spherical particles yield slightly better margination than ellipsoidal particles; however, adhesion of ellipsoidal carriers is expected to be superior due to a larger area for particle-wall interactions and a slower rotational dynamics of ellipsoids near a wall. As a conclusion, micron-size ellipsoidal particles seem to be favorable for drug delivery in comparison to sub-micron particles and spherically shaped carriers

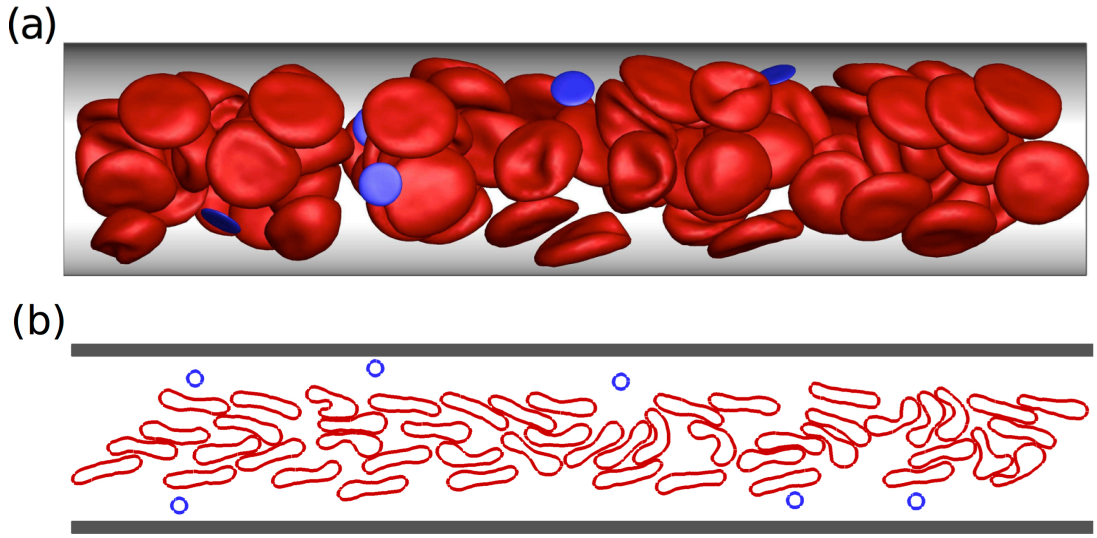

Figure 1. Snapshots of 3D and 2D simulations. RBCs are drawn in red. (a) A 3D simulation snapshot of blood flow for hematocrit of 30%. Suspended disc-like particles are colored in blue. (b) A 2D simulation snapshot of blood flow for hematocrit of 30%. The circle-shaped particles are drawn in blue.

4th Micro and Nano Flows Conference
UCL, London, UK, 7-10 September 2014

Experimental and numerical investigation on forced convection in circular tubes with nanofluids

Laura COLLA [1], Laurea FEDELE [1], Oronzio MANCA [2,*], Lorenzo MARINELLI [2], Sergio NARDINI [2,*]

* Corresponding author: Tel.: +39 081 5010217; Fax: +39 081 5010204; Email: oronzio.manca@unina2.it
1 Istituto per le Tecnologie della Costruzione, Consiglio Nazionale delle Ricerche, Corso Stati Uniti 4, 35127 Padova, Italy
2 Dipartimento di Ingegneria Industriale e dell'Informazione, Seconda Università degli Studi di Napoli, Via Roma 29, 81031 Aversa (CE), Italy

Keywords: Nanofluids, Forced convection, Tubes, Experimental measurements, Numerical simulations

In this paper an experimental and numerical investigation on forced convection flow of a water–Al_2O_3 nanofluid in a circular tube is presented. An assigned heat flux on the external surface of the tube is applied. Moreover, a numerical simulation of the experimental test section is accomplished in order to compare the numerical results with the experimental ones.

1 Experimental apparatus and numerical model

Heat transfer of fluids is very important to many industrial heating or cooling equipments. Convective heat transfer can be enhanced passively by changing flow geometry, boundary conditions or by enhancing the thermal conductivity of the working fluid. An innovative way of improving the thermal conductivity of base fluids is to introduce suspended small solid nanoparticles. Recently, several engineering applications of nanofluids have been accomplished. In fact, they have been studied to in such as many components and systems involved in applications such as automotive car radiators, refrigeration systems, electronic cooling, aerospace and energy thermal storage or solar energy. These applications are strongly related to convective heat transfer in ducts and tubes with different cross sections: triangular, circular, squared and so on.

The experimental apparatus is reported in Figure 1. It consists in: 5 circular tube in stainless steel, which represents the test section, 1 peristaltic pump, 9 two heat exchanges, 4 tank, 7 three ways valve, 10 discharge reservoir. Two manometers, 6, allow to evaluate the pressure value upstream and downstream the text section and an ultrasonic flow meter, 12, is employed to measure the mass flow rate. The heated part of the text section is 910 mm long with external and internal diameters equal to 12.66 mm and 21.55 mm. Ten thermocouples are allocated on the external surface to measure the wall temperature along the tube. One thermocouple is in the inlet section to measure the fluid entrance temperature. Six electrical resistances are placed on the external surface to obtain a maximum heat rate of 520 W. A thermally insulated material, with a thickness of 37 mm, is used to reduce the thermal losses toward the ambient.

The experimental runs were carried out for three heat rate equal to 200, 400 and 520 W with corresponding heat flux value of 2650, 5250 and 6850 W/m^2. The used volumetric flow rates were 200, 350 and 500 l/h. The corresponding Reynolds numbers varied between 5400 and 15000. The nanoparticles volumetric concentrations of Al_2O_3 were equal to 0%, 1% and 3%. The inlet temperature of the fluid in the test section is controlled by the chiller and set to the value of 20 °C.

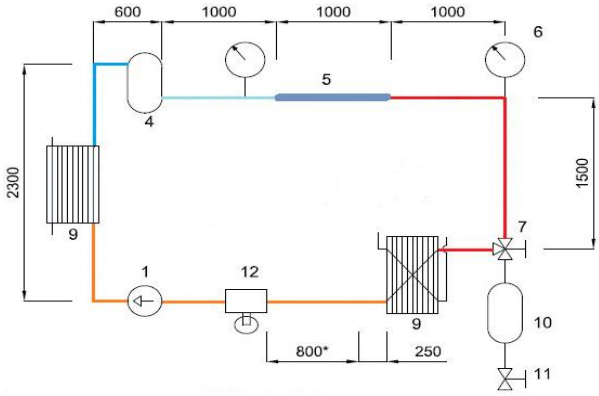

Figure 1. Sketch of experimental apparatus

The numerical simulations were accomplished on the experimental test section with the geometrical dimensions given in the previous paragraph. In the analysis, the fluid flow and the thermal field were assumed axial-symmetric and the cylindrical coordinates were considered. The fields were assumed two-dimensional and steady state. The single-phase model was employed in order to analyze the thermal and fluid dynamic behavior of the considered nanofluid. Moreover, the k-ε model was used to describe the turbulent fluid flow. At the channel exit section, the fully developed conditions were assumed, *i.e.* all axial derivatives were zero. On the external wall of the circular tube a uniform heat flux was assigned and the non-slip conditions were assumed on the internal wall.

Heat transfer coefficients were evaluated experimentally and numerically by means of temperature profiles and fixed wall heat fluxes. Comparisons in terms of wall temperatures and average Nusselt numbers were performed. Moreover, some performance evaluation criteria were estimated in order to compare the convective heat transfer enhancements with the pumping power increases.

4th Micro and Nano Flows Conference
UCL, London, UK, 7-10 September 2014

Droplet Initiated Rupture of High Viscosity Jets to Create Uniform Emulsions

Dimitris N. JOSEPHIDES *, Shahriar SAJJADI

* Corresponding author: Tel.: ++44 (0)207 848 2902; Email: dimitris.josephides@kcl.ac.uk
Department of Physics, Kings College London, UK

Keywords: Monodisperse, Viscous Droplets, Micro Flow, Emulsion, Core-shell, Droplet Templating

Monodisperse emulsions have found uses in many fields including agriculture, coatings and pharmaceuticals. Many methods exist to create monodisperse emulsions of various uniformities and these include micro engineered devices such as membranes and microchannel systems [1]. However one problem all these micro engineered devices suffer from is their inability to create highly uniform emulsions from very viscous or low interfacial tension materials. The reason for this is that most devices rely on a dripping flow regime of emulsion production to create high degrees of uniformity. When an emulsion's viscosity is increased, the feed rate at which a device can be used and remain in this dripping regime is significantly reduced. When devices are used at increased flow rates, jetting normally occurs increasing the polydispersity of the produced emulsion.

The potential to initiate drop formation of a middle phase around an internal drop has been briefly observed in other works involving the creation of core-shell emulsions through microfluidic means. This is where the rate at which internal droplets are formed dominate the total core-shell droplet creation rate [2,3]. However, this method has not been exploited in producing simple emulsions.

This work introduces a method to create a viscous single emulsion by using a core-shell template. Core-shell emulsion templates are created using a glass capillary based microfluidic device (figure 1) where the outer and middle phases are of high viscosity (≈100 cp).

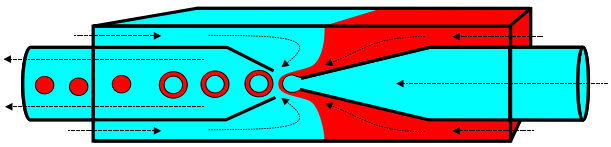

Figure 1: Schematic of the microfluidic device being used. The blue fluid represents the inner (i) and outer (o) phases, and the red fluid the middle (m) phase. Core shell drops are created which later destabilize downstream to create uniform single emulsions.

It is shown that if internal droplets are introduced into a viscous jet, at frequencies bellow a critical value, it will force the system from a jetting regime into a dripping mode creating monodisperse core-shell type droplets. These core-shell type droplets then rupture downstream creating a highly uniform single emulsion (figure 2). A comparison between a simple two-phase, and core-shell type three-phase method is conducted under similar conditions where highly monodisperse emulsions could not be created under simple conditions due to the viscosity of the chosen phases.

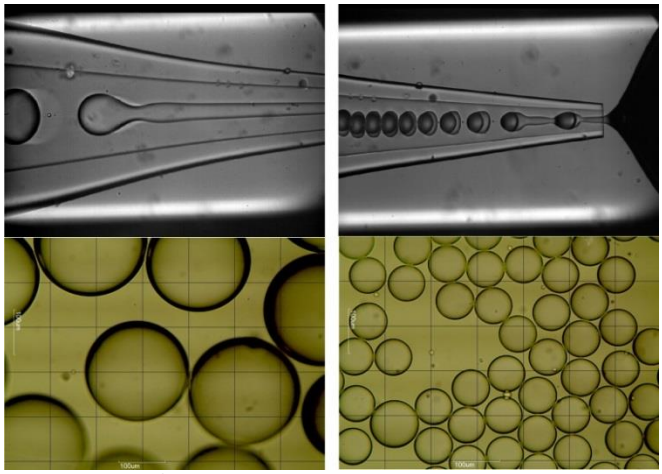

Figure 2: Left: Image shows jetting regime and resultant large polydisperse emulsion after collection. Due to the high viscosity nature of the fluids used the system is very prone to jetting (Q_o =1000 µl/hr Q_m=200 µl/hr Q_i=0 µl/hr). Right: Dripping core-shell regime achieved by incorporating an inner fluid of low viscosity and high interfacial tension into the jet. The resulting core shell droplets are highly unstable and separate to form a monodisperse single emulsion of high viscosity (Q_o =1000 µl/hr Q_m = 200 µl/hr Q_i = 200 µl/hr). Grid size is 100µm

The frequency (f_i) at which inner droplets must be generated in order to have sufficient distance (λ_i) between perturbations to induce jet rupture is found to be similar to that predicted by Rayleigh-Plateau instability theory (equation 1 and 2).

$$\lambda_i = \frac{v_m}{f_i} \quad (1) \qquad \lambda_{crit} = \pi D_{jet} \quad (2)$$

Higher frequencies were found not to result in core-shell production. The final simple droplet sizes after rupture can be further tuned by altering the size of the core and C_v < 2% in all cases studied.

References

[1] G. T. Vladisavljević, I. Kobayashi, and M. Nakajima, 'Production of uniform droplets using membrane, microchannel and microfluidic emulsification devices', Microfluidics and Nanofluidics, vol. 13, no. 1, pp. 151–178, Feb. 2012.

[2] R. Shah, H. Shum, A. Rowat, D. Lee, J. Agresti, A. Utada, L. Chu, J. Kim, A. Fernandeznieves, and C. Martinez, 'Designer emulsions using microfluidics', Materials Today, vol. 11, no. 4, pp. 18–27, Apr. 2008.

[3] H. C. Shum, A. Sauret, A. Fernandez-Nieves, H. A. Stone, and D. A. Weitz, 'Corrugated interfaces in multiphase core-annular flow', Physics of Fluids, vol. 22, no. 8, p. 082002, 2010

4th Micro and Nano Flows Conference
UCL, London, UK, 7-10 September 2014

Flow boiling heat transfer of a non-azeotropic mixture inside a single microchannel

Davide DEL COL *, Marco AZZOLIN, Stefano BORTOLIN

* Corresponding author: Tel.: ++39 049 8276891; Fax: ++39 049 8276896; Email: davide.delcol@unipd.it
Department of Industrial Engineering, University of Padova, IT

Keywords: Microchannels, Flow Boiling, Non-azeotropic mixture, Heat transfer

The worldwide alert about global warming has led to an increasing interest in new HVAC (heating, ventilation and air conditioning) technologies with low environmental impact. When considering this impact, both an indirect effect due to the energy consumption, and the consequent carbon dioxide emissions caused by the electricity production process, and a direct effect due to leakages of refrigerant must be taken into account. A way to achieve high heat transfer rates in compact heat exchangers is using microchannel technology. In addition to high heat flux applications, microchannels are viewed as appropriate options to reduce the charge of refrigerant, minimize the problems of release of potentially hazardous fluids in the atmosphere and allow to use natural fluids such as hydrocarbons and carbon dioxide. Proper understanding of microscale transport phenomena is fundamental for the design of microscale heat exchangers.

In the recent years much attention has been paid to the possible use of fluorinated propene isomers for the substitution of high-GWP (global warming potential) refrigerants. Even if they are widely commercialized, the HFOs (hydrofluoroolefins) cannot cover all the air-conditioner, heat pump, and refrigeration applications. In recent studies, it was found that the coefficient of performance (COP) and the capacity of heat pump cycles using HFO-1234ze(E) are significantly lower than those of the most widely used refrigerant, R410A (Koyama et al., 2010). The main causes are the small latent heat and vapor density of R1234ze(E). To improve the COP and capacity, in the latest literature it was attempted to blend R1234ze(E) into another refrigerant, R32 Although R32 is one of the HFCs, it has relatively low GWP and excellent thermodynamic characteristics. Therefore, a zeotropic mixture of R1234ze(E) and R32 can be effectively used in the field of air-conditioning due to their mild impact on environment. As the result of their drop-in test with R32/R1234ze(E) 0.5/0.5 by mass, Koyama et al. (2010) concluded that the tested binary mixture achieved a superior COP at some operating conditions, and this binary mixture is the most promising candidate to replace R410A.

It is worth mentioning that very limited data of mixture R32/R1234ze flow boiling are available in the literature and, to the best of authors' knowledge, no data have been taken inside microchannels. Hossain et al. (2013) measured the evaporation heat transfer coefficient of the mixture R1234ze(E)/R32 (55/45 mass%) inside a 6 mm tube. The effect of vapor quality, mass flux and saturation temperature on heat transfer coefficients have been analyzed. Kondou et al. (2013) performed flow boiling tests of the potential refrigerant R32/R1234ze(E) in a horizontal microfin tube of 5.21 mm inner diameter. The heat transfer coefficient and pressure drop are measured at a saturation temperature of 10°C, heat fluxes of 10 and 15 kW m^{-2}, and mass velocities from 150 to 400 kg m^{-2} s^{-1}.

In this paper, a mixture of R1234ze(E) and R32 (0.5/0.5 by mass) is under study. In particular the local heat transfer coefficient during flow boiling of this mixture in a single minichannel with 0.96 mm diameter is measured at 30°C saturation temperature. Tests are carried out with the experimental apparatus available at the Two Phase Heat Transfer Lab of the University of Padova. As a peculiar characteristic of the present technique, the heat transfer coefficient is not measured by imposing the heat flux; instead, the boiling process is governed by controlling the inlet temperature of the heating secondary fluid. On this regard the present data is new and original since the large majority of data in the literature is taken by means of Joule effect heating. For the determination of the local heat transfer coefficient, three parameters are measured: the local heat flux, the saturation temperature and the wall temperature. The heat flux is determined from the temperature profile of the secondary fluid in the measuring sector. The wall temperature is directly measured along the test section and the saturation temperature is obtained from the pressure measurements at the inlet and outlet of the test tube.

The flow boiling data taken in the present test section are discussed, with particular regard to the effect of heat flux, mass velocity, vapor quality and fluid properties. The heat transfer coefficients are compared against some predicting models available in the literature. The new experimental data are compared to flow boiling data of pure R1234ze(E) and R32. This allows to analyze the heat transfer penalization due to the mass transfer resistance of this zeotropic mixture and to assess available predicting models for evaporation of zeotropic mixtures.

References

Hossain, Md. A., Onaka, Y., Afroz, H.M.M., Miyara, A., 2013. Heat transfer during evaporation of R1234ze(E), R32, R410A and a mixture of R1234ze(E) and R32 inside a horizontal smooth tube. International Journal of Refrigeration 36, 465-477.

Kondou, C., BaBa, D., Mishima, F., Koyama, S., 2013. Flow boiling of non-azeotropic mixture R32/R1234ze(E) in horizontal microfin tubes. International Journal of Refrigeration http://dx.doi.org/10.1016/j.ijrefrig.2013.07.009

Koyama, S., Takata, N., Fukuda, S., 2010. Drop-in experiments on heat pump cycle using HFO-1234ze(E) and its mixtures with HFC-32. In: Proc. Int. Refrigeration and Air Conditioning Conf. at Purdue, West Lafayette, IN, No. 2514, pp. 1-8.

Photothermal Conversion Characteristics of Silver Nanoparticle Dispersions

Dongsheng WEN [1*], Hui ZHANG [2], Hui-Jiuan CHEN[1], Guiping LIN [3]

* Corresponding author: Tel.: ++44 (0)113 3431299; Fax: ++44 (0)113 3431009;
Email: d.wen@leeds.ac.uk

[1] School of Chemical and Process Engineering, University of Leeds, UK
[2] School of School of Energy and Power, North China Electric Power University, China
[3] School of Aeronautical Engineering, Beijing University of Aeronautics and Astronautics, China

Abstract: Nanoparticle-based direct absorption system is a recent development, which employs nanoparticles to absorb and convert solar energy directly into thermal energy within the fluid volume. This work reports for the first time the use of plasomic nanoparticles (PNPs) to improve the direct photo-thermal conversion efficiency. Rod-shaped silver nanoparticles are synthesized and used as an example to illustrate the photo-thermal conversion characteristics of PNPs and the effect of particle shape. The result reveals a significant role of particle morphology on the photo-thermal conversion efficiency (PTE). For spherical silver particles, constant specific absorption rate (SAR), ~0.14 kW/g, is observed and the PTE increases nearly linearly with the particle concentration. For rod-shaped silver nanoparticles, much higher SARs (2~5 kW/g) are obtained, and the PTE increases from 43% (pure DI water) to 61% at a low concentration of 0.0028%. It is suggested that the increased specific surface area and the absorption spectrum variation are the two main reasons for the strong heating effect of rod-shaped silver nanoparticles.

Keywords: Plasmonic nanoparticle, silver, nanofluids, nanowire, photo-thermal conversion, solar collector

4th Micro and Nano Flows Conference
UCL, London, UK, 7-10 September 2014

Analysis and design optimization of an integrated micropump-micromixer operated for bio-MEMS applications

Cesar A. CORTES-QUIROZ [1,*], Alireza AZARBADEGAN [2], Ian D. JOHNSTON [1], Mark C. TRACEY [1]

* Corresponding author: Tel.: ++44 (0)1707 284147; Fax: ++44 (0)1707 284147; Email: c.cortes-quiroz@herts.ac.uk
1 School of Engineering and Technology, University of Hertfordshire, UK
2 Department of Mechanical Engineering, University College London, UK

Keywords: Micropump-micromixer, Valveless Micropump, Pulsating Flow, Multi-objective Optimization

Microfluidic systems for biological and chemical applications necessitate mixing of reagents as a routine protocol. Many biosensors require two fluids to be mixed prior to their introduction to specific sensors. As an integrated device, consisting of pumps, mixer and sensor, the ability of the sensor to detect biomarkers depends on the mixing efficiency obtained in the whole integrated system. However, mixing in the micrometer scale is marred by the low Reynolds number and thus by the laminar flow that only facilitates mixing based on molecular diffusion. Various strategies towards achieving efficient mixing in microfluidic devices have been reviewed earlier [1].

In this study, we examine a generic device composed by two single chamber valveless micropumps connected to a simple T-type channel intersection, where efficient mixing is produced due to the pulsating flow generated by the micropumps. The characteristics of a feasible valveless micropump given by [2] have been used. A schematic view of the pumps and channels arrangement is shown in figure 1. Previous studies have demonstrated numerically and experimentally the advantages of using time pulsing inlet flows for enhancing mixing in channels [3, 4]. These reported studies implemented pulsating flows merely on the basis of theoretical sinusoidal equations for the inlet velocities of fluids to be mixed and they do not refer to any characteristic of the pumps that are required to achieve the resulting periodic flows.

We present the analysis and optimization of a microfluidic system using a Computational Fluids Dynamics (CFD) based multi-objective optimization method that was presented in [5]. This method integrates CFD with a set of optimization techniques that reduces the computational cost of the optimization process. In this study, the frequency f and the phase difference ϕ of the periodic fluid velocities (operation parameters) and the angle θ formed by the inlet channels at the intersection (geometric parameter) are the design parameters, whereas mixing quality, pressure drop and maximum shear strain rate in the channel are the performance parameters. The optimization enables the minimization of pressure drop and maximum shear strain and the maximization of the mixing quality. The Pareto front of the trade-off of performance parameters is obtained.

For an optimum design, mass fraction contours at different times on a horizontal mid-height plane of the mixing channel are depicted in figure 2. A simple and realistic microfluidic system has been studied and optimized for achieving high mixing quality with all the desirable parameters that enable manipulation of biological fluids in microchannels.

References

1. Hessel V, Lowe H, Schonfeld F, Micromixers: a review on passive and active mixing principles, Chem. Eng. Sci. **60**, 2479-2501 (2005).
2. Azarbadegan A, Cortes-Quiroz C A, Eames I, Zangeneh M, Analysis of double-chamber parallel valveless micropumps, Microfluidics and Nanofluidics **9**, 171-180 (2010).
3. Glasgow I, Aubry N, Enhancement of microfluidic mixing using time pulsing, Lab on a Chip **3**, 114-120 (2003).
4. Chen C-K, Cho C-C, A combined active/passive scheme for enhancing the mixing efficiency of microfluidic devices, Chem. Eng. Sci. **63**, 3081-3087 (2008).
5. Cortes-Quiroz C A, Zangeneh M, Goto A, On multi-objective optimization of geometry of staggered herringbone micromixer, Microfluidics and Nanofluidics **7** (1), 29-43 (2009).

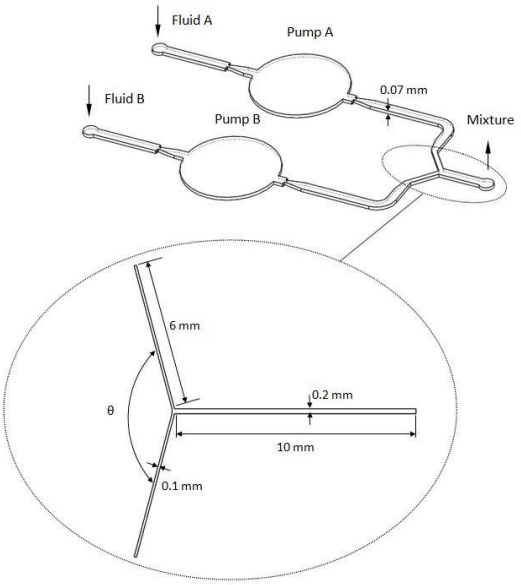

Figure 1. Schematic of the valveless pumps and mixing channel

.

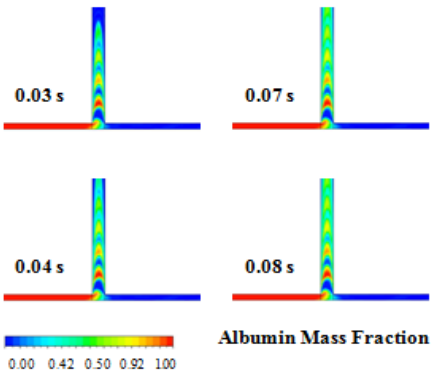

Figure 2. Mass fraction contours on a mid-height plane at different times (case: f = 100 Hz, $\phi = \pi$, $\theta = 180^{o}$).

4th Micro and Nano Flows Conference
UCL, London, UK, 7-10 September 2014

The Influence of Geometry on the Thermal Performance of Microchannels in Laminar Flow with Viscous Dissipation

Marcos LORENZINI [1,*], Nicola SUZZI [1]

* Corresponding author: Tel.: ++39 0543 374455; Fax: ++39 0543 374444 2; Email: marco.lorenzini@unibo.it
1 Department of Industrial Engineering – DIN Alma Mater Studiorum, Bologna, Forlì Campus, I

Keywords: Microchannel, Viscous Dissipation, Entropy generation

Microchannels are the building block of many micro flow devices (MFDs), among which micro heat exchangers (MFHXs)represent a significant group. The small dimensions allow very high heat transfer coefficients to be achieved even in laminar flow, and this, together with a high Area-to-Volume ratio make MFHXs attractive in many applications. The main drawback of these devices is the high frictional losses – especially for liquids – that affect the flow even under laminar conditions, which also make viscous dissipation no longer negligible. In order to enhance heat transfer, several strategies may be adopted at the macroscale, but for MFHXs actions are confined to the modification of the channel's morphological characteristics, such as the modification of the channels' cross-section. The extent to which a given change from the original conditions (which act as reference values) brings about an enhancement in the quantity which one aims at maximizing (objective function) is usually rated through performance evaluation criteria (PECs). These are based on an analysis in terms of the first law of thermodynamics, but in recent years also the second law is accounted for [1,2].

In the present work the fully developed steady laminar flow of a Newtonian liquid through a microchannel subject to H1 (uniform heat flux and uniform temperature along the heated perimeter of the cross-section) in the presence of viscous dissipation is investigated. Entropy generation numbers and PECs are employed to assess the influence of smoothing the corners of an initially rectangular cross-section, with an aspect ratio β ranging from 1 (square channel) to 0.03 (the case approaching two parallel plates) under four different types of geometrical constraints. The governing equations and the results are expressed in non-dimensional form to lend a general character to the treatment, with the strength of viscous dissipation is exemplified by the Brinkman number, which is demonstrated to increase its maximum significant value when corners of the cross-section are smoothen. The four geometrical constraints applied to the different PECs are: constant characteristic length of the cross section, hydraulic diameter, heated perimeter, cross-sectional area. The PECs considered are those normally employed [3] and belong to three families (VG, FG, FN), which corresponds to the quantity which is optimized under constraints (pumping power, conductance, heat transfer area), while the entropy number contains the contributions given by frictional losses and by heat transfer to entropy generation in the process.

The results are reported as a function of the non-dimensional radius of curvature and show the ratio of the value of each quantity at a given R_c to that for sharp corners (R_c=0) under the same geometrical constraints.

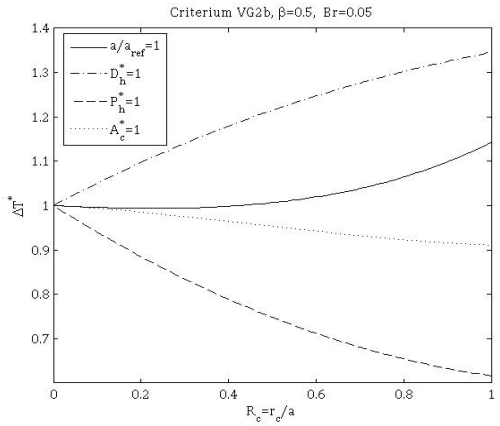

Also the entropy generation number is reported in the same way and give pieces of information on the extent to which smoother corners contribute to a fuller use of the available energy.

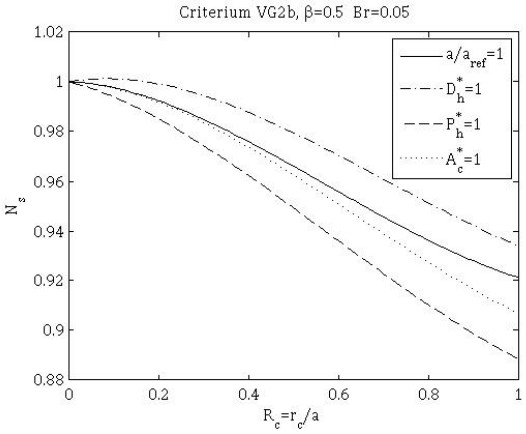

References

[1]. Chakraborty S. and Ray S. . Performance optimization of laminar fully developed flow through square ducts with rounded corners. *International Journal of Thermal Science*, vol.50, pp. 2522-2535, 2011.

[2]. Bejan A., Entropy Generation Through Heat And Fluid Flow. *Wiley-Interscience Publications.*

[3]. R. L. Webb. Principles of Enhanced Heat transfer. *Wiley-Interscience Publications*

4th Micro and Nano Flows Conference
UCL, London, UK, 7-10 September 2014

Development of interconnected silicon micro-evaporators for the on-detector electronics cooling of the future ITS silicon tracker in the ALICE experiment at LHC

Andrea FRANCESCON [1,2,3*], Giulia ROMAGNOLI [1], Alessandro MAPELLI [1], Paolo PETAGNA [1], Corrado GARGIULO [1], Luciano MUSA [1], John R. THOME [4], Davide DEL COL [2]

* Corresponding author: Tel.: ++41 (0) 22 76 70696; Email: andrea.francescon@cern.ch
1 CERN European Laboratory for Particle Physics, Physics Department, Geneva, Switzerland
2 DII Dipartimento di Ingegneria Industriale, University of Padova, Padova, Italy
3 INFN Istituto Nazionale di Fisica Nucleare, Sez. di Padova, Padova, Italy
4 EPFL École Polytechnique Fédérale de Lausanne, Lausanne, Switzerland

Keywords: Micro-channels, Micro-fabrication, Electronics cooling, Silicon particle detectors

ALICE (A Large Ion Collider Experiment) is the experiment at the CERN Large Hadron Collider (LHC) [1] designed to investigate the physics of nucleus-nucleus collisions. The ITS (Inner Tracking System) is the ALICE innermost detector dedicated to vertexing and particles tracking. In order to improve the ALICE physics performance, the actual ITS will be replaced with seven new layers equipped with Monolithic Active Pixel Sensors (MAPS). The three innermost layers, composing the ITS inner barrel, will be formed by 48 staves surrounding the beam pipe: each stave is composed by Pixel chips (15x30 mm^2) assembled in a row of 9 modules giving an active area of 15x270 mm^2 [2].

The MAPS electronics is expected to exhibits a power dissipation of 0.1-0.3 W/cm^2 over the chip surface, turning into a total power for the inner barrel ranging from 200 to 580 W. This power must be correctly removed in order to ensure proper working conditions for the chip: maximum temperature of 30°C, minimum temperature of 15°C (to avoid condensation on the electronics surface) and a maximum ΔT on the chip surface of 5°C. In order to meet these requirements, a dedicated on-detector cooling system based on flow boiling inside silicon micro-channels has been considered. The refrigerant to be used will be C_4F_{10} (perfluorobutane) for its dielectric characteristics and for radiation hardness. At room temperature (20°C) the saturation pressure for this fluid is p_{sat}=2.27 bar.

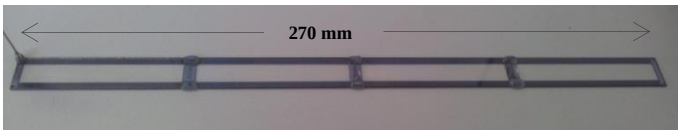

Figure 1 First prototype of interconnected silicon micro-evaporators for the ITS inner layers on-detector cooling.

When designing particle detectors for High Energy Physics (HEP) applications one of the key targets is the minimization of the material budget, a parameter accounting for the materials composing the detector and their interaction with particles. In order to minimize the material budget of the future ITS on-detector cooling system, a special frame design was developed and fabricated [3].

In the fabrication of silicon micro-evaporators, the maximum length of the device is limited by the diameter of the silicon wafers. This limitation, not significant for other applications (e.g. CPU cooling), is critical in this case where a long structure must be cooled. For cooling the ITS inner layers, a special prototype with interconnected silicon micro-channel frames was designed and fabricated using standard micro-fabrication techniques (Fig. 1). Since we are using 4" wafers at this stage of the development, four devices must be integrated in the final prototype in order to cover the length of the ITS inner layer stave. For the interconnection of the different devices, a dedicated micro-connector (Fig. 2) for bridging the flow between the frames was developed and successfully implemented into the prototype.

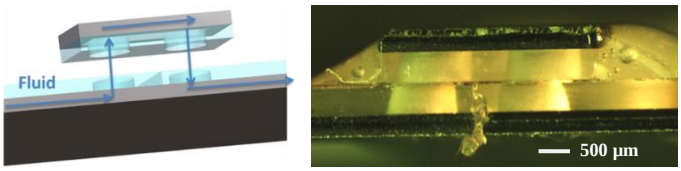

Figure 2 The micro-connector concept (left) and a section view of the connector installed at the interface between two frames

The prototype is designed with distribution lines, integrated into the silicon substrate, providing the fluid at the four evaporators in the liquid phase and recollecting the vapour from the outlet manifolds.

In the paper, the fluidic design of the system is discussed, the process flow for the micro-fabrication of the silicon micro-evaporators is reviewed and the assembly of the final prototype is shown. Then, thermal results of chip cooling with refrigerant flow boiling in micro-channels are presented and discussed.

References

[1] ALICE Collaboration, The ALICE experiment at the CERN LHC 2008 JINST 3 S08002

[2] ALICE Collaboration, Conceptual Design Report for the upgrade of the ALICE ITS, Tech. Rep. CERN-LHCC-2012-013. LHCC-P-005

[3] A. Francescon et al., Thermal management of the ALICE ITS detector at CERN with ultra-thin silicon micro-channel devices, in Proceedings from Ex-HFT8 World congress (2013).

4th Micro and Nano Flows Conference
UCL, London, UK, 7-10 September 2014

Mass Transfer Enhancement in a Microfluidic Cell with a Magnetic Microparticle by the Use of Alternating Magnetic Fields

Philip A. LISK[1], Farid AIOUACHE[2], Erell BONNOT[1], Robert POLLARD[3], Robert BOWMAN[3] and Evgeny V. REBROV[1*]

[*] Corresponding author: Tel.: ++44 (0)2890974627; Email: e.rebrov@qub.ac.uk
[1]School of Chemistry and Chemical Engineering, Queen's University Belfast, UK
[2]Department of Engineering, Lancaster University, Lancaster, UK
[3]Centre for Nanostructured Media, School of Mathematics & Physics, Queen's University Belfast, Belfast, UK

Keywords: Actuation, Laminar flow, Magnetic microparticles, Mass transfer

The impact of external alternating magnetic fields on a suspended magnetic microparticle (MMP) may lead to a fast particle movement. When the MMP possesses sorptive or catalytic properties, mass transfer on the liquid side is increased which leads to process intensification in many chemical and biomedical applications. Mass transfer of suspended particles in a microfluidic cell depends decisively on the mode of magnetic actuation. If a particle moves with a constant (angular) velocity, the thickness of the laminar liquid film that adheres to the particle remains constant. An increase in relative velocity leads to a reduction of the laminar boundary layer thickness around the particle, and thus, to an increase in the mass transfer coefficient. However if the particle experiences a force due to time dependent changes in the velocity, this leads to a thinning of the liquid boundary layer. Hence, liquid-side mass transfer could further be improved. To make use of this particle acceleration effect on mass transfer in laminar flow, a new reactor concept is required, which allows to influence local particle movement. This is possible when magnetic microparticles are used, as they react to external magnetic fields and, hence, their trajectories may be controlled. The particle trajectory and velocity depend on the absolute value and the gradient of magnetic field inside a quadruple magnetic actuator.

In this study, the effect of magnetic and hydrodynamic forces on MMP motion has been studied with Comsol Multiphysics. Using the AC/DC magnetic field module, a two-dimensional time dependent oscillating magnetic field has been simulated inside a circular cell with a diameter of 13 mm. The physical properties of acetonitrile were used for fluid properties inside the cell and a solid magnetic particle with a density of 1000kg/m^3 (size of 250, 500 or 750 μm) was introduced in the cell. The model consists of four equally sized and spaced iron electromagnets surrounding a circular interaction region. Magnets are separated into pairs producing sinusoidal magnetic fields at two different phases: $V_1=V_{01}\cdot\sin(\omega t)$ and $V_2=V_{02}\cdot\sin(\omega t+\varphi)$ (Figure 1), here: $V_{01,}$ V_{02}·are the maximum voltages at the coils, ω is the frequency and φ is the phase shift. The hydrodynamic resistance was simulated using the drag force. The design parameters were changed as follows: ω between 10 and 70 mHz, and φ between 60 and 130 degrees and the particle velocity and acceleration were calculated.

A fast reaction on the surface of the microparticle was chosen to obtain mass transfer rate. A reactant flow was fed to the cell with the magnetic microparticle via an inlet (constant velocity profile) and it was withdrawn via an outlet (constant pressure). Mass transfer was described by the Sherwood number which is a function of the Reynolds number and the Schmidt number. An additional term which accounts for acceleration of mass transfer due to acceleration/deceleration behavior of the microparticle was introduced.

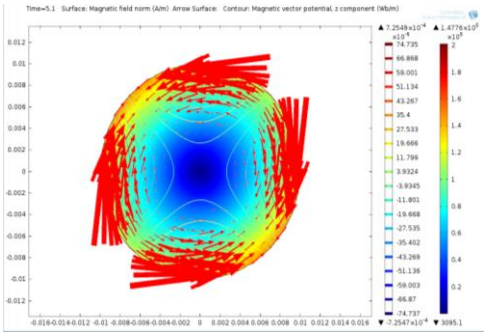

Figure 1 The intensity of the magnetic flux density including directional arrows of the magnetophoretic force represented by the magnetic field gradient squared (∇H^2).

For reference purposes, simulations were also made during conventional operation without magnetic actuation. Compared to this reactor without magnetic actuation, a magnetic actuation caused the mass transfer to be considerably enhanced.

Acknowledgement
The financial support provided by the European Research Council (ERC) project 279867, is gratefully acknowledged.

4th Micro and Nano Flows Conference
UCL, London, UK, 7-10 September 2014

Single and Two-phase Flow Pressure Drop and Heat Transfer in a Rectangular Metallic Microchannel

Mehmed R. OZDEMIR[1], Amirah M. SAHAR[1], Mohamed M. MAHMOUD[1*], Jan WISSINK[1], Tassos G. KARAYIANNIS[1]

* Corresponding author: Tel.: ++44 (0)1895 267132; Fax: ++44 (0)1895 256392; Email: tassos.karayiannis@brunel.ac.uk
1 School of Engineering and Design, Brunel University, UK

Keywords: Microchannel, Single phase flow, Flow Boiling

Abstract

This study presents experimental and numerical results for single phase heat transfer and pressure drop in a single rectangular microchannel using de-ionized water. Also, experimental flow boiling heat transfer results are included. The channel was made of oxygen free copper with 1 mm width and 0.39 mm height (D_h = 0.561 mm) and 62 mm length. Experimental conditions covered a Reynolds number range 200-3000 for single phase flow experiments and mass flux range 200 – 500 kg/m^2 for two phase flow boiling experiments. The heat flux range was 1695 – 3960 kw/m^2. The test section inlet pressure was 125 kpa. The numerical part was conducted for single phase flow only using the commercially available software ANSYS FLUENT at the same experimental conditions. Single phase experimental results will be compared with existing correlations as well as predictions from the CFD simulation. The experimental two phase flow boiling heat transfer results will be presented as flow patterns, local heat transfer coefficient versus local vapour quality and heat flux versus wall superheat (classical boiling curve).

4th Micro and Nano Flows Conference
UCL, London, UK, 7-10 September 2014

Challenges and Possibilities in Cooling Electronics Equipment

Mohamed M. MAHMOUD[1], Tassos G. KARAYIANNIS[1*]

* Corresponding author: Tel.: ++44 (0)1895 267132; Fax: ++44 (0)1895 256392; Email: tassos.karayiannis@brunel.ac.uk
1 School of Engineering and Design, Brunel University, UK

Keywords: Microchannel, Flow Boiling

Abstract

Thermal management of electronics systems has become a hot research topic in the last two decades. This was arising from the fact that continuous miniaturization of electronics systems with increasing processing speed will result in very high heat fluxes and local hot spots. In some applications, the conventional cooling techniques can not dissipate this high heat flux. As a result, the chip junction temperature may exceed its maximum allowable limit and consequently the performance and lifetime of system will decrease dramatically. Accordingly, in the last two decades, several experimental and numerical studies were directed towards this research area. These studies focused on: (i) understanding the physics of flow and heat transfer at micro scale level, (ii) testing prototypes for micro heat sinks, (iii) developing a miniature cooling system. The present paper reviews the different cooling schemes proposed by researchers for electronics cooling. The review discuses also the limitations, merits and demerits of each scheme. Due to the fact that the big challenge in this research area is to develop a reliable and efficient miniature cooling system, the review will shed the light on the attempts of researchers to develop a full miniature cooling system.

4th Micro and Nano Flows Conference
UCL, London, UK, 7-10 September 2014

Optimization of Drug-Eluting Stents

Franz Bozsak, Jean-Marc CHOMAZ, Abdul I. BARAKAT *

* Corresponding author: Tel.: ++33 (1) 6933 5268; Fax: ++33 (1) 6933 5292; Email: barakat@ladhyx.polytechnique.fr
Hydrodynamics Laboratory (LadHyX; CNRS UMR7646), Ecole Polytechnique, France

Keywords: Drug-Eluting Stent, Gradient-Free Optimization, Arterial Wall Transport, Drug Release, Strut Geometry

Drug-eluting stents (DES), which release anti-proliferative drugs into the arterial wall in a controlled manner, have drastically reduced the rate of in-stent restenosis relative to bare metal stents (BMS) and have therefore revolutionized the treatment of atherosclerosis. Several studies have suggested, however, that DES are associated with a higher risk of late stent thrombosis (LST) than BMS. Because drugs used in DES inhibit vascular endothelial cell proliferation, LST is thought to be due to delayed endothelial wound healing at the site of stent implantation. The goal of the present work is to devise optimal strategies for drug release from DES in order to minimize the likelihood of LST while simultaneously maintaining sufficiently high drug concentrations in the arterial wall to prevent restenosis.

1 Methodology

We have recently developed a two-dimensional axisymmetric computational model that describes the transport within the arterial wall of drugs released by DES [1]. In the model, the arterial wall is represented as a two-layer structure consisting of an intima and a media. Both layers are considered as porous structures with distinct transport characteristics. The model solves the Navier-Stokes equations to obtain the flow field in the arterial lumen and Darcy's law for the flow field in the porous arterial wall. To determine the concentration of the eluted drug, the advection-diffusion equation is solved both in the lumen and in the arterial wall with an additional reversible reaction term in the arterial wall to represent drug interactions with both endothelial cells and smooth muscle cells. Simulations are performed for the two most commonly used DES drugs, namely paclitaxel and sirolimus.

For the optimization, the objective is the delivery of efficacious but non-toxic drug concentrations to smooth muscle cells in order to prevent restenosis while ensuring minimal drug concentration at the endothelial cell surface to allow endothelial wound healing and hence limit thrombosis. To accomplish this objective, we formulate a cost function that is minimized using a gradient-free optimization algorithm based on the surrogate management framework [2]. In the current simulations, we wish to determine the optimal drug release strategy for both paclitaxel- and sirolimus-eluting stents. To this end, two variables are used in the optimization: the drug release rate from the stent and the initial drug concentration loaded onto the stent. Simulations of drug transport in the arterial wall are performed using the finite element commercial multi-physics code COMSOL (version 4.3), whereas the optimization routines are implemented in Matlab.

2 Results

The simulation results demonstrate that the optimal drug delivery strategies for paclitaxel-eluting stents and sirolimus-eluting stents are very different. For paclitaxel-eluting stents, we identified two distinct optima with widely different drug release times: a very fast (order of an hour) optimum and a slow (order of a year) optimum. Significantly, both of these optima require considerably lower initial drug concentrations than those used today (1-10 $\mu g/cm^2$ vs. the 50-100 $\mu g/cm^2$ in today's stents). In contrast, sirolimus-eluting stents have only a single viable optimum which lies in the slow release (order of a year) regime. The difference in the optimization results between the two drugs is attributable to differences in drug reaction dynamics. More specifically, while paclitaxel dissociation from cells following binding occurs over a time constant of ~200 hours, the unbinding time constant for sirolimus is only ~10 hours. Therefore, very fast drug delivery to the arterial wall, which is equivalent to rapidly flooding the wall with drug, is effective in the case of paclitaxel where the drug remains bound for an extended period of time but is ineffective in the case of sirolimus where rapid drug dissociation does not permit drug retention in the wall but leads instead to a situation where convection rapidly flushes out the drug from the arterial wall.

3 Conclusions

The present results offer possible explanations for recent trends in DES development, most notably drug-coated balloons that use paclitaxel as the drug of choice. Such a system operates in a manner that is largely similar to the fast-release paclitaxel optimum identified here. Our results also underscore the importance of detailed modeling of the arterial wall and the choice of eluted drug in any *in silico* DES design process. More broadly, the results demonstrate the potential for large improvements in DES design relative to today's designs and define guidelines for implementing these improvements, thus paving the way towards patient-specific DES design.

References:

1. Bozsak F, Chomaz JM, Barakat AI. Modeling the transport of drugs eluted from stents: physical phenomena driving drug distribution in the arterial wall. *Biomechanics and Modeling in Mechanobiology.* In Press.
2. Belitz P, Bewley T. New horizons in sphere-packing theory, part II: lattice-based derivative-free optimization via global surrogates. *Journal of Global Optimization* 56: 61-91, 2013.

4th Micro and Nano Flows Conference
UCL, London, UK, 7-10 September 2014

Two-phase aqueous-ionic liquid flows in small channels of different diameter

Dimitrios TSAOULIDIS [1], Qi LI [1], Maxime CHINAUD [1], Panagiota ANGELI [1,*]

* Corresponding author: Tel.: ++44 (0) 20 7679 3832; Fax: ++44 (0)20 7383 2348; Email: p.angeli@ucl.ac.uk
[1] Department of Chemical Engineering, University College London, Torrington Place, WC1E 7JE, London, UK

Keywords: Spent nuclear fuel reprocessing, Scale-up, Ionic Liquids, PIV

Driven by pressing demands for high-performance, safe, and sustainable flow processes, intensified small-scale systems find increasing applications in (bio)chemical analysis and synthesis, polymerization, fuel cells, micro-heat exchangers, and separation processes (solvent extraction). Many of these systems involve two phases, gas-liquid and liquid-liquid.

One of the main two phase processes is liquid-liquid extraction, which has been used widely in the nuclear energy cycle for the management of the radioactive waste from the nuclear reactor. Reprocessing can reduce the volume and toxicity of the nuclear waste for storage or disposal. However, in the extractions volatile organic solvents are used with high hazard ratings. Ionic liquids have become appealing alternatives to organic solvents because of their negligible volatility and flammability, high resistance to radiation, and good thermal stability at common industrial conditions, which reduce solvent loss and make them inherently safe and environmental friendly. Despite their benefits the industrial uptake of ionic liquids has been low mainly because of their high costs.

Operation in intensified, small-scale systems can reduce the solvent volume required, and make possible the implementation of expensive solvents such as ionic liquids. The reduction in volume is compensated by the high efficiencies achieved. Despite the absence of turbulence, mixing in small channels can be significantly enhanced as a result of short diffusion lengths, recirculation within phases, and convection induced by surface tension gradients. Moreover, the high surface to volume ratio increases the importance of interfacial phenomena and favours the formation of regular patterns with well characterized properties (such as segmented flow).

To increase throughput in small scale devices, scale out (instead of scale up) is used; this can however, require a prohibitively large number of small channels. An alternative approach would be to increase the channel sizes enough while still preserving the benefits of small scale operation, such as laminar flows and well defined, regular patterns. Scale out to desired throughputs would then involve a smaller number of channels.

In this work, the effects of channel size and flow rate on the hydrodynamic and mixing characteristics in ionic liquid/nitric acid two-phase flows were investigated by means of Particle Image Velocimetry (PIV). The measurements were carried out in a non-conventional way using continuous bright field illumination and high speed imaging. PIV provides multipoint information of the velocity inside one liquid with high accuracy and high spatial resolution in a non-intrusive way. Channels with sizes from 0.5 to 2 mm internal diameter and liquid flow rate ratios from 0.5 to 1 were used. Plug flow (segmented flow) was established for all the conditions tested. This study is complementary to an ongoing research on the use of ionic liquids for extraction applications in small devices relevant to spent nuclear fuel reprocessing.

4th Micro and Nano Flows Conference
UCL, London, UK, 7-10 September 2014

Heat transfer enhancement with gas-to-gas micro heat exchangers

Iris GERKEN [1,*], Juergen J. BRANDNER [1], Roland DITTMEYER [1]

* Corresponding author: Tel.: ++49 (0)721 60824094; Fax: ++49 (0)721 60823186; Email: iris.gerken@kit.edu
1 Institute of Micro Process Engineering (IMVT), Karlsruhe Institute of Technology (KIT), Germany

Keywords: Heat transfer enhancement, Heat exchanger, Energy efficiency, Gas heat transfer

Micro process engineering is named to provide several advantages in chemical and thermal process engineering due to micro structures with dimensions below millimeter scale. Micro heat exchangers have proved to exceed heat transfer performance in comparison to conventional sized heat exchangers due to an increased surface-to-volume ratio and small heat transfer distances. High heat transfer capabilities can be provided within compact micro heat exchangers.

As a disadvantage, the small dimensions of micro scale flow channels generate increased pressure losses compared to conventional devices for liquid and gas flows. Therefore, heat transfer enhancement in terms of modified geometries, e.g. pin fins, different channel flow path or channel cross sectional area, leads to additional pressure losses while enhanced heat transfer can be observed. Previous published literature demonstrates this contrarily behavior between improved heat transfer and increased pressure loss with various geometries of micro structures.

An overall assessment of heat exchangers with respect to both, heat transfer performance and fluid flow behavior, is still missing but needs to be considered. Previous studies present options for the overall assessment to compare augmented surfaces relative to smooth surfaces and in direct contrast to other augmented surfaces. In terms of micro structured heat exchangers a common comparison is between an augmented flow path with straight micro channels.

The second law of thermodynamics is an option for heat exchanger assessment and has been used by several authors for different approaches, namely due to entropy generation or exergy loss. During a process, heat and mass transfer result in an irreversibility, which is described by the second law of thermodynamics in terms of process entropy. Although entropy in a thermodynamic process can only be increased or decreased, published literature refers to the entropy changes as “entropy generation” or “entropy production”.

A consequence of entropy generation is the irreversibility resulting in exergy loss due to an increase of anergy, the content of energy which cannot be changed into work. Therefore, to compare and assess the performance of different heat exchangers the entropy generation or the exergy loss can be used.

Using liquids as heat transfer fluids, the behavior of micro heat exchangers is well described and understood. Little attention has been paid to heat transfer from gas to gas in micro channels. This can be attributed to some properties of gases, e.g. lower specific heat capacity compared to liquids and arising effects such as compressibility and rarefaction. Existing publications present an increased influence of longitudinal conduction in the separation wall between the two gas flows on gas-to-gas heat transfer processes.

The present study experimentally investigates the influence of different flow arrangements and different materials, i.e. their thermal conductivity, on heat transfer performance of an innovative gas-to-gas micro heat exchanger. Within the investigation co-current, counter current and cross flow arrangement have been evaluated. In addition, the wall separating the two gas flows has been exchanged to understand the influence of its thermal conductivity on heat transfer processes. The materials stainless steel, copper, aluminum and PEEK have been analyzed as materials separating the two gas flows with different partition foil thicknesses. The results present a strong dependence of wall thermal conductivity on heat transfer in micro scale.

Furthermore, a numerical comparison of two micro heat exchangers is introduced to examine an overall efficiency in terms of heat transfer augmentation and fluid flow behavior. In the present study, the exergy loss is used to assess the micro heat exchangers with an exergy loss in terms of fluid flow behavior and in terms of heat transfer behavior. The exergy loss reveals to depend only on input and output parameters, i.e. mass flow rates, specific heat capacities, gas constant, temperature (ambient, inlet, outlet), pressure (inlet, outlet) and thermal effectiveness (calculated with temperature at inlet and outlet of both fluids). An overall heat transfer performance has been calculated which sums up the exergy losses in terms of fluid flow behavior and heat transfer behavior. The overall assessment reveals the complexity of comparing fluid flow behavior and heat transfer performance which are not related to each other. In addition, using gas flows as working fluids, an increased impact of the exergy loss in terms of fluid flow behavior on the overall heat transfer performance has been determined.

Results of the experimental investigation of the gas-to-gas micro heat exchanger and the numerical comparison to detect an overall heat transfer efficiency will be presented in the conference contribution.

4th Micro and Nano Flows Conference
UCL, London, UK, 7-10 September 2014

The behaviour of von Willebrand factor in blood flow

Kathrin MÜLLER [1,*], Dmitry A. FEDOSOV [1], Gerhard GOMPPER [1]

* Corresponding author: Tel.: ++49 (0)2461 613913; Fax: ++49 (0)2461 613180; Email: k.mueller@fz-juelich.de
1 Theoretical Soft Matter and Biophysics, Institute of Complex Systems and Institute for Advanced Simulation, Forschungszentrum Jülich, 52425 Jülich, Germany

Keywords: Primary hemostasis, Polymer, Margination probability, Numerical modelling, Dissipative Particle Dynamics

The large multimeric protein von Willebrand factor (VWF) is essential in hemostasis. Under normal conditions, VWF is present in blood as a coiled passive polymer. However, in case of an injury, VWF is able to uncoil and bind to the vessel wall and flowing platelets. Thus, platelets are significantly slowed down and can adhere to the wall and close the lesion. Nevertheless, it is still not clear how the uncoiling of the VWF is triggered.
Numerical simulations help us better understand such complex processes. Using a particle-based hydrodynamic simulation method we study the behaviour of VWF in blood flow. The VWF is modelled as a chain of spheres (monomers) connected by springs. In addition, the monomers are subject to attractive interactions in order to represent realistically characteristic properties of the VWF observed in experiments. The behaviour of VWF is investigated under different conditions including a freely-suspended polymer in shear flow and a polymer attached to a wall. We also examine the migration of VWF to a wall (margination) depending on shear rate and volume fraction of red blood cells (RBCs). Furthermore, we monitor the stretching of the VWF in flow direction depending on its radial position in blood flow. Our results show that attractive interactions between monomer beads similar to those in VWF increase margination efficiency and significantly affect the extension of VWF at different radial positions in blood flow.

4th Micro and Nano Flows Conference
UCL, London, UK, 7-10 September 2014

Flow Boiling in Rectangular Microchannels: 1-D Modelling of the Influence of Inlet Resistance on Flow Reversal

Sateesh GEDUPUDI[1,*], David B.R. KENNING[2], Tassos G. KARAYIANNIS[2]

* Corresponding author: Tel.: ++91 (0)44 2257 4721; Email: sateeshg@iitm.ac.in
1: Department of Mechanical Engineering, Indian Institute of Technology Madras, Chennai, India
2: School of Engineering and Design, Brunel University, UK

Keywords: Confined Bubble, Flow Boiling, Micro-channel, Flow Instability

Parallel micro-channel heat sinks making use of flow boiling are a potential method of cooling devices that dissipate high heat fluxes, such as microprocessors. Inherent with the confined bubble growth in mini/micro-channels are the flow instabilities, which lead to uneven flow distribution between channels, temporary flow reversal and poor heat transfer due to intermittent dry-out. Empirical techniques employed as remedies include usage of flow resistance at the inlet to individual channels, Kandlikar et al (2006), and enhancement of bubble formation inside the channels, Agostini et al (2008).

Gedupudi et al. (2011) made an experimental observation of bubble growth in a single microchannel with and without inlet compressibility and presented a 1-D model to study the influence of inlet (upstream) compressibility conditions on local pressure fluctuations and flow reversal for various combinations of parameters, mostly without inlet resistance. The two upstream compressibility models considered were condensable vapour in a subcooled boiling region in an upstream preheater and non-condensable ideal gas subject to compression with polytropic exponent *n*. Compressibility due to subcooled boiling may occur in experimental rigs with electrical preheaters or in industrial applications in which heat can be supplied from a high temperature source through a heat exchanger. Compressibility due to accidental trapping of small volumes of non-condensable gas during filling or maintenance is highly likely in most applications.

The present work makes a detailed study of the effect of inlet resistance on maximum flow reversal distance, return time and local pressure fluctuation for different initial upstream compressible volumes, for water boiling at atmospheric pressure. The pressure drop through the inlet resistance is expressed as a multiple (F, a constant loss coefficient) of $\rho_l U_1^2/2$, where U_1 is the upstream liquid velocity. Figure 1 shows a typical effect of inlet restriction on flow reversal for water at 101 kPa in 0.3 x 1.5 x 40 mm channel, U_{1i}=0.4 m/s , q = 200 kW/m^2, L_A = 20 mm (midpoint of the channel) , G = 4 x10^{-5} m^3/Ns (constant). With the largest compressible volume and no inlet resistance, there is a strong flow reversal that nearly reaches the inlet plenum. This is much reduced by increasing *F*, with only small further improvement for *F* >20.

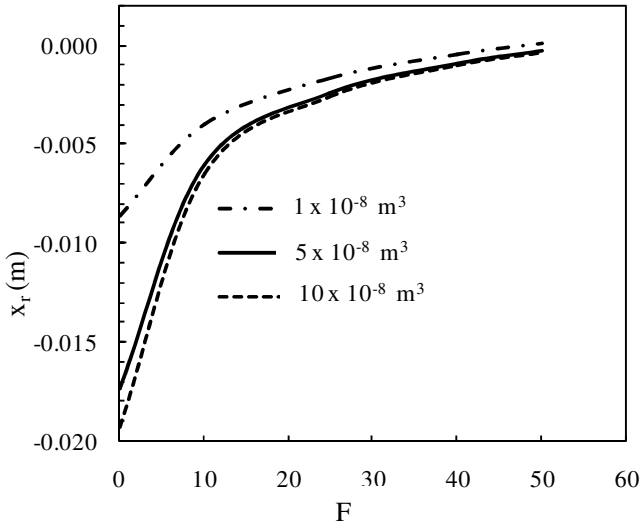

Fig. 1. Effect of inlet resistance on maximum flow reversal distance (negative) for three different inlet compressible volumes due to subcooled boiling.

This paper as a whole examines the size of inlet flow resistance required to control flow reversal driven by the confined growth of individual bubbles.

References

Kandlikar, S.G., Kuan, W.K., Willistein, D.A.,Borrelli, J., 2006. Stabilization of flow boiling in microchannelsusing pressure drop elements and fabricated nucleationsites, J. Heat Transfer 128, 389-396.

Agostini, B., Thome, J.R., Fabbri, M., Michel, B., Calmi, D., Kloter,U., 2008. High heat flux flow boiling in silicon multi-microchannels - Part I: Heat transfer characteristics of refrigerant R236fa, Int. J. Heat Mass Transfer 51 (2008) 5400-5414.

Gedupudi, S., Zu, Y.Q., Karayiannis, T.G., Kenning, D.B.R., Yan, Y.Y., 2011. Confined bubble growth during flow boiling in a mini/micro-channel of rectangular cross-section Part I: Experiments and 1-D modeling, Int. J. Thermal Sciences 50, 250-266.

4th Micro and Nano Flows Conference
UCL, London, UK, 7-10 September 2014

Numerical study and optimize the microchannel heat sink with pin-fin structure

Jin Zhao, Liang Gong*, Shanbo Huang

Department of Energy & Power EngineeringK, College of Pipeline & Civil Engineering, China University of Petroleum (East China), PRC

Keywords: Microchannel, Rectangular pin-fin heat sink, Optimization study, Numerical simulation

Abstract

The manifold microchannel (MMC) heat sinks have many advantages such as low thermal resistance, compact structure, little amount of coolant, low flow rate, uniform temperature distribution along the flow direction, etc. In this paper, numerical simulations are conducted to investigate flow and heat transfer characteristics of water through four kinds of optimized MMC structures. Simulation results indicate that rectangular pin-fin heat sink has a better heat exchange capacity than column pin-fin heat sink. Moreover, there exists an optimum manifold porosity in pin-fin microchannel heat sink based on the study of each model's cooling performance factor. Besides the influence of porosity on flow and heat transfer characteristics, there also exist a most appropriate rectangular pin fin located angle (around 30 degree) which could achieve the best heat transfer effect.

4th Micro and Nano Flows Conference
UCL, London, UK, 7-10 September 2014

Corner Accumulation Behavior of Spermatozoa in Microchannels

Reza NOSRATI [1], David SINTON [1,*]

* Corresponding author: Tel.: +1 (416) 978 1623; Fax: +1 (416) 978 7753; Email: sinton@mie.utoronto.ca
1 Department of Mechanical and Industrial Engineering, University of Toronto, 5 King's College Road, Toronto, Ontario, Canada

Keywords: Microfluidics, Microswimmer, Sperm Motility, Surface Accumulation

Understanding swimming behavior of spermatozoa in confined geometries, especially close to the boundaries, is of particular importance in reproduction, leading to new insights into both sperm selection techniques *in vitro* and sperm penetration mechanisms *in vivo*. Previous studies indicated that swimming microorganisms, including spermatozoa, accumulate near surfaces (Rothschild, 1963; Gaffney et al., 2011). Recently, Denissenko et al. (2012) indicated that migration ability of spermatozoa in a microchannel significantly depends on the channel geometry as human spermatozoa navigate along the channel corners. Here, we used microfluidic approaches to study corner accumulation behavior of bull spermatozoa in a microchannel. A rectangular microchannel is vertically aligned with a cylindrical observation chamber in the microfluidic device, as shown in Fig. 1. The distribution of migrating spermatozoa across the microchannels cross section is imaged at the time of exiting the channel using fluorescence microscopy, revealing a strong and non-random preference of spermatozoa to navigate against the channel corner. Results indicate that approximately 74% of spermatozoa accumulate close to the surfaces and only 26% of spermatozoa are bulk swimmers. Moreover, 49% of spermatozoa (i.e. 66% of wall swimmers) are corner swimmers (i.e. swimming close to the channel wall intersections) while 26% swim next to one wall. In conclusion, distribution of bull spermatozoa across a rectangular microchannel has been measured, showing much higher accumulation of spermatozoa near corners (intersection of the channel walls) than close to the free boundaries. In effect, about half of the microswimmers are concentrated geometrically, into only 4% of the cross-sectional area. This concentration effect significantly influences how these swimmers react to in-plane channel geometries both in artificial reproduction methods and *in vivo*. The distinction and quantification of wall vs. corner vs. bulk swimmers was enabled by the unique head-on microchannel imaging approach applied here.

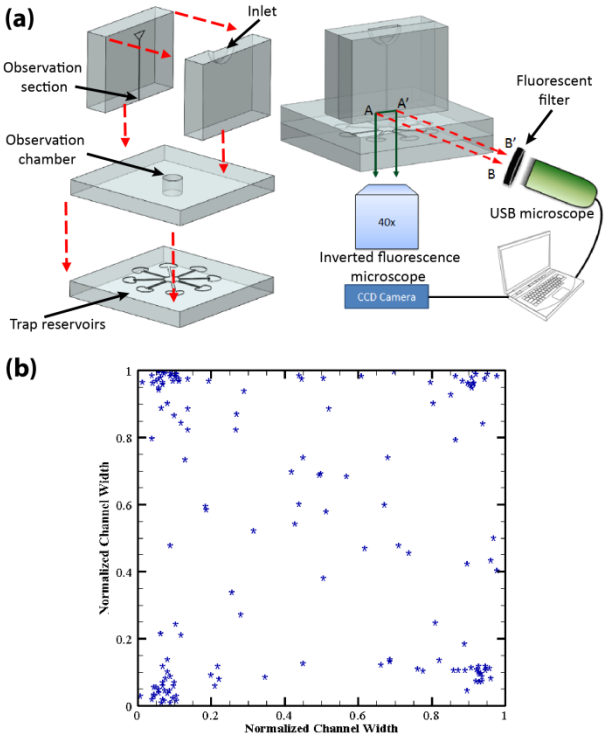

Fig. 1. Microfluidic device to study corner accumulation behavior of bull spermatozoa across a rectangular microchannel. *(a)* Schematic view of the device: a rectangular microchannel which is vertically aligned at the center of a cylindrical observation chamber. *(b)* Spatial distribution of 164 bull spermatozoa across the rectangular section of the microchannel at the exit of the channel, indicating strong corner accumulation behavior of migrating spermatozoa.

References

Denissenko, P., Kantsler, V., Smith, D. J., Kirkman-Brown, J., 2012. Human spermatozoa migration in microchannels reveals boundary-following navigation. Proc. Natl. Acad. Sci. U.S.A. 109(21), 8007–8010.

Gaffney, E.A., Gadêlha, H., Smith, D.J., Blake, J.R., Kirkman-Brown, J.C., 2011. Mammalian Sperm Motility: Observation and Theory. Annu. Rev. Fluid Mech. 43, 501–528.

Rothschild, L., 1963. Non-random Distribution of Bull Spermatozoa in a Drop of Sperm Suspension. Nature 198, 1221–1222.

4th Micro and Nano Flows Conference
UCL, London, UK, 7-10 September 2014

Effect of nanomaterial properties on thermal conductivity heat transfer fluids and nanomaterial suspension

Rohit S. KHEDKAR [1,*], Shriram S. SONAWANE [2], Kailas L. WASEWAR [2]

* Corresponding author: Tel.: +91 (0712)2779013; Email: rohit.chemin@gmail.com
1 Department of Chemical Engineering, Anuradha Engineering College (AEC), Chikhali, Maharashtra (India)
2 Department of Chemical Engineering, Visvesvaraya National Institute of Technology (VNIT), Nagpur, Maharashtra (India)

Keywords: Thermal conductivity, Enhancement, Nanofluids, Sonication, Maxwell and H – C model,

Energy has been rated as the single most important issue facing humanity in the current as well as next 50 years. Securing clean energy has become the top priority of most developed countries. Considering the rapid increase in energy demand worldwide, intensifying heat transfer process and reducing energy loss due to ineffective use have become an increasingly important task. Fundamentally, energy conversion and transportation occur at atomic or molecular levels, nanoscience and nanotechnology are expected to play a significant role in revitalizing the traditional energy industries and stimulating the emerging renewable energy industries.

Nanofluid is a modern engineering heat transfer fluid with superior potential for enhancing the heat transfer performance of conventional fluids such as water, ethylene glycol and oils. It is consisting of solid nanoparticles with sizes typically of 1–100 nm suspended in base fluids. Many attempts have been made to investigate its important thermal properties i.e. thermal conductivity; however no definitive agreements and idea have emerged about this property. This article reports the effect of different nanomaterial on thermal conductivity enhancement of nanofluids experimentally. TiO_2 Fe_3O_4 and Al_2O_3 nanoparticles dispersed in water and ethylene glycol with volume concentration of 0.5 – 4 vol. % are used in the present study. A transient hot-wire apparatus (KD2 pro) is used for measuring the thermal conductivity of nanofluids. The results show that all the heat transfer fluids show increase in thermal conductivity with addition of nanoparticles in it. The measured thermal conductivity of nanofluids increased as the particle concentrations increased and are higher than the values of the base liquids. This confirms the effect of volume concentration of nanoparticles on the thermal conductivity enhancement.

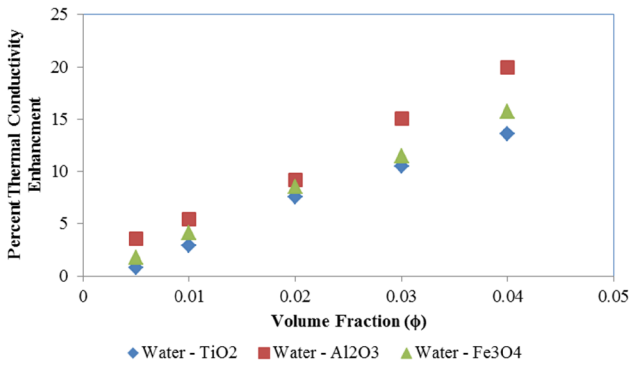

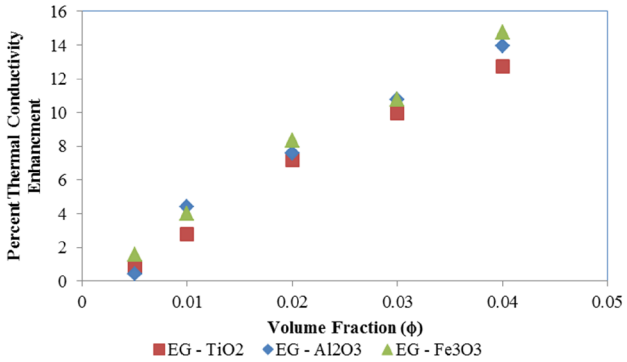

It is observed that Al_2O_3 nanoparticles based nanofluids shows higher enhancement in thermal conductivity as compared to TiO_2 and Fe_3O_4 nanoparticles based nanofluids for same volume concentration. This confirms the fact that thermal conductivity of nanofluids is also depends on nanoparticles material properties. We suggest that this phenomenon is because of actual thermal conductivity of nanomaterial. In universe alumina has highest thermal conductivity as compared to titania and ferrous oxide.

In further study, water and ethylene glycol were used as base fluids confirm the effect of heat transfer fluids properties on effective thermal conductivity. Results suggest that heat transfer fluids properties also important and viscosity of base fluids effect the effective thermal conductivity of nanofluids.

Experimental thermal conductivity results are compared with existing theoretical model of thermal conductivity. Comparative study shows that the measured thermal conductivity of nanofluids was quite different from the predicted values from the existing correlations for thermal conductivity.

References

R.P. Feynman, Plenty of Room at the Bottom, APS Annual Meeting, 1959.

Xuan, Y and Q. Li, Heat transfer enhancement of nanofluids. International Journal of Heat and Fluid Flow, 2000. 21(1): p. 58-64.

Maxwell, J.C., A Treatise on Electricity and Magnetism Clarendon Press, Oxford, UK, 1881. 1: p. 435.

Murshed, S.M.S., K.C. Leong, and C. Yang, Enhanced thermal conductivity of $Ti0_2$ - water based nanofluids. IJTS, 2005. 44(4): p. 367-373

4th Micro and Nano Flows Conference
UCL, London, UK, 7-10 September 2014

Grad's Moment Equations for Binary Gas-Mixture of Hard Spheres

Neeraj SARNA [1], Vinay Kumar GUPTA [1,*], Manuel TORRILHON [1]

* Corresponding author: Tel.: +49 (0)241 8098676; Fax: +49 (0)241 80 92600; Email: gupta@mathcces.rwth-aachen.de
1: Center for Computational Engineering Science,
Department of Mathematics,
RWTH Aachen University, Germany

Keywords: Moment Method, Binary Mixture, Kinetic Theory

The gas flow in micro-devices is an intriguing problem. Due to their small sizes, the mean-free-path of the gas molecules becomes comparable with the length scale of the problem. Thus, the Knudsen number (Kn)---which is defined as the ratio between mean-free-path and a length scale in the problem---for micro-devices is large ($Kn \geq 1$). Therefore, the Navier-Stokes-Fourier equations, which are suitable for the description of processes with $Kn \leq 0.1$, are no longer valid for flow description in micro-devices. So, one seeks for more elegant models for flow description in micro-devices and the models stem from kinetic theory.

The fundamental equation in kinetic theory is the Boltzmann equation, which is the evolution equation for the distribution function of the gas-particles and adequate for describing the flows for all Knudsen numbers. However, the direct solutions of the Boltzmann equation for micro-devices are very expensive. Nevertheless, the approximation methods in kinetic theory provide good remedy. In kinetic theory, the two most celebrated approximation methods, which provide approximate solution of the Boltzmann equation, are "Grad's method of moments" and "Chapman-Enskog expansion". The Grad's method of moment is based on approximating the distribution function with a series of orthogonal polynomials (usually Hermite polynomials) in velocity space and the unknown coefficients multiplied with the polynomials are evaluated in such a way that this approximated distribution function satisfies the definitions of moments considered. In the Chapman-Enskog expansion, the distribution function is expanded in terms of small parameter(s), which is Knudsen number usually, around an equilibrium distribution function. This expanded distribution function is substituted back in the Boltzmann equation and the coefficients of each power of small parameter from both sides are compared to obtain the constitutive relations. The coefficients corresponding to power zero of small parameter lead to Euler equations, that to power one, two and three lead to Navier-Stokes-Fourier equations, Burnett equations and super-Burnett equations, respectively. In principle, the process can be continued further, although it is almost impossible to obtain even super-Burnett equations with this method.

In addition to their complicated derivation procedure, the equations beyond Navier-Stokes-Fourier equations suffer from instability. The advantage of Grad's method of moment over the Chapman-Enskog expansion is that the moment equations obtained from former are always linearly stable, which has been shown in the literature for single gas. Nevertheless, the right-hand sides of the moment equations, referred to as *production terms*, are not easy to compute for different interaction potentials. In the past few years, we developed automated codes (in Mathematica), which can compute the production terms for different interaction potentials.

In this paper, we shall derive the Grad's moment equations for binary mixture of gases with hard sphere interaction potential and investigate the linear stability of the Grad's moment equations for binary mixture by discussing the damping coefficient and phase velocity. Furthermore, we shall study a diffusion problem in a one-dimensional channel to show the effects of some of the parameters, e.g., the mass ratio.

References:

1. Kremer, G. M. 2010, An Introduction to the Boltzmann Equation and Transport Processes in Gases. Berlin: Springer.
2. Struchtrup, H. 2005 Macroscopic Transport Equations for Rarefied Gas Flows. Berlin: Springer.
3. https://web.mathcces.rwth-aachen.de/CollisionIntegrals/

4th Micro and Nano Flows Conference
UCL, London, UK, 7-10 September 2014

Numerical Simulation of Microflows with Moment Method

Zhenning CAI [1,*]

* Corresponding author: Tel.: ++49 (0)1575 6378931; Email: caizn@pku.edu.cn
1 Center for Computational Engineering Science, RWTH Aachen University, Germany

Keywords: Micro Flow, Moment Equations, Boundary Condition, Finite Volume Method

A series of hyperbolic moment systems is derived for the Boltzmann equation with BGK-type collision term. These systems can be obtained through a slight modification in the deduction of Grad's moment equations, and such method is suitable for deriving systems with moments up to any order. The systems are equipped with proper wall boundary conditions so that the number of equations in the boundary conditions is consistent with the hyperbolic structure of the moment system. In our numerical scheme, a special mapping method is introduced so that the numerical efficiency is highly enhanced for systems with large number of moments. Our numerical results are validated by comparing with the DSMC results. Through the numerical solutions of systems with increasing number of moments, the convergence of the moment method can be clearly observed.

4th Micro and Nano Flows Conference
UCL, London, UK, 7-10 September 2014

Thermal conductivity of nanofluids in nanochannels

Michael FRANK [1,*], Nikolaos ASPROULIS [2], Dimitris DRIKAKIS [3]

* Corresponding author: Tel.: +44(0)1234755108; Email: m.frank@cranfield.ac.uk
1 Division of Engineering Sciences, Centre of Fluid Mechanics & Scientific Computing, Cranfield University, Cranfield, Bedfordshire, MK43 0AL, UK
2 Division of Engineering Sciences, Centre of Fluid Mechanics & Scientific Computing, Cranfield University, Cranfield, Bedfordshire, MK43 0AL, UK
3 Division of Engineering Sciences, Centre of Fluid Mechanics & Scientific Computing, Cranfield University, Cranfield, Bedfordshire, MK43 0AL, UK

Keywords: Nanofluid, Nano Flow, Micro Flow, Nanochannel, Argon, Copper

Suspensions of metallic particles in base fluid, called nanofluids, have been known to enhance the heat transfer capacity of the base fluid significantly, rendering them promising materials for thermal management applications. Experimental data available in the literature, present an increase of up to 150% in the thermal conductivity of the base liquid, when less than 1% w.t. of particles was added into the system (Choi, et al. 2001). However, the disagreement between results from different laboratories as well as the lack of an accurate theoretical framework governing the thermal behavior of nanofluids, hinders the development of the field and its commercial use (Keblinski, Eastman and Cahill 2005). Furthermore, even conventional fluids restricted in nanometer-sized structures such as nano-channels, exhibit behaviors radically different from their bulk equivalents (Sofos, Karakasidis and Liakopoulos 2009).

The present work studies the thermal properties of a nanofluid composed of copper particles suspended in liquid argon, enclosed within a channel of nano-meter sized diameters. The system is modeled using Equilibrium Molecular Dynamics (EMD), which has been extensively used for the calculation of transport properties of fluids in equilibrium, using the Green-Kubo relations (Sofos, Karakasidis and Liakopoulos 2009, Sarkar and Selvam 2007). Cases of different channel diameters were used to study the behavior of nanofluids within such nanofluidic scenarios.

The Green-Kubo relations were used to calculate the transport properties (thermal conductivity, viscosity and diffusion coefficient), of the system. In addition, density profiles close to the walls and the particle were calculated, in order to provide insight as to how the particle affects the structure of the liquid, and how that structure might be affecting its thermal properties. The angular momentum of the particle is also calculated in time, studying whether the rotational energy of the particle is correlated with the enhanced thermal properties. The position of the center of mass of the particle was also followed to understand the nature of its motion. Finally, the decay of the Heat Flux Autocorrelation Function (HFACF), used for the calculation of the thermal conductivity, is studied providing further insight in the heat transport mechanisms of nanofluids and the ballistic nature of phonons (Keblinski, et al. 2002).

Results show that with increasing channel width, resulting in decreasing volume fraction, the thermal conductivity deviates from the predictions of the effective medium theory based models. The thermal conductivity in the y-direction increases linearly with increasing wall distance. Although such conclusions were reached for pure liquids in channels, the authors have shown that the thermal conductivity converges to the bulk equivalent at 20σ whereas the current study shows that the effect of the wall distance is significant even at larger wall distances. This is attributed to the phonon scattering at the surface of the particle and the walls as indicated by the oscillating nature of the HFACF in the direction perpendicular to the wall.

In addition, the viscosity of the fluid drops linearly with increasing mass fraction of particles.

Bibliography

Choi, SUS, ZG Zhang, Wu Yu, FE Lockwood, and EA Grulke. "Anomalous thermal conductivity enhancement in nanotube suspensions." *Applied Physics Letters* 79, no. 14 (2001): 2252--2254.

Keblinski, P, SR Phillpot, SUS Choi, and JA Eastman. "Mechanisms of heat flow in suspensions of nano-sized particles (nanofluids)." *International journal of heat and mass transfer*, 2002: 855-863.

Keblinski, Pawel, Jeffrey A Eastman, and David G Cahill. "Nanofluids for thermal transport." *Materials Today* 8, no. 6 (2005): 36--44.

Sarkar, Suranjan, and R Panneer Selvam. "Molecular dynamics simulation of effective thermal conductivity and study of enhanced thermal transport mechanism in nanofluids." *Journal of applied physics*, 2007: 074302--074302.

Sofos, Filippos, Theodoros Karakasidis, and Antonios Liakopoulos. "Transport properties of liquid argon in krypton nanochannels: anisotropy and non-homogeneity introduced by the solid walls." *International Journal of Heat and Mass Transfer* 52, no. 3 (2009): 735--743.

4th Micro and Nano Flows Conference
UCL, London, UK, 7-10 September 2014

An investigation on the structural dynamics of human blood using high performance computations

Dong XU[1], Ante MUNJIZA[2], Eldad Avital[2], Chunning Ji[1], Efstathios KALIVIOTIS[3], John WILLIAMS[2]
* Corresponding author: Tel.: +++44 (0)20 7882 5306; Email: j.j.r.williams@qmul.ac.uk
1 State Key Laboratory of Hydraulic Engineering Simulation and Safety, Tianjin University, Weijin Road, Tianjin 300072, PR China
2 School of Engineering & Materials Science, Queen Mary, University of London, Mile End Road, London E1 4NS, UK
3 Department of Mechanical Engineering, University College London, Torrington Place, London, WC1E 7JE, UK

Keywords: red blood cells, aggregation, immersed boundary method, numerical simulation

Studies on the haemodynamics of human circulation are clinically and scientifically important. The flow of human blood is extremely complex due to the existence of the highly deformable red blood cells (RBCs), which are able to pass through capillaries smaller than their size. Under low shear forces the RBCs may clump together to form aggregations, which can significantly affect blood flow in the human circulatory system. To investigate the effect of deformation and aggregation in blood flow, a computational technique has been developed by coupling the interaction between the fluid and the deformable solids. This technique includes a three-dimensional finite volume method for the solution of the incompressible viscous (and turbulent if necessary) flows, the combined finite-discrete element method for computing the deformation of the RBCs, a Johnson, Kendall & Roberts model (JKR) (Johnson et al., 1971) to take account of the adhesion forces between the different RBCs and an iterative direct-forcing immersed boundary method to couple the fluid-solid interactions. The flow of 49,512 RBCs at 45% concentration and under the influence of aggregating forces was examined, improving the existing knowledge on simulating flow and structural dynamics of blood at a large scale: previous studies on the particular issue were restricted to simulating the flow of 13000 aggregative ellipsoidal particles at a 10% concentration. The simulation was carried out with full parallelization of the coupled fluid-solid code using spatial decomposition and high performance supercomputers. The large scale feature of the simulation has enabled a macroscale verification and investigation of the overall characteristics of RBC aggregations to be carried out. The results are in excellent agreement with experimental studies and, more specifically, both the experimental and the simulation results show uniform RBC distributions under high shear rates (60-100s^{-1}) whereas large aggregations were observed under a lower shear rate of 10s^{-1}. The statistical analysis of the simulation data also shows that the shear rate has significant influence on both the flow velocity profiles and the frequency distribution of the RBC orientation angles. The flow under the low shear rate also tended to have bi-phasic velocity profiles, which is mainly due to the formation of large scale aggregation clusters. The simulations also showed that there is an apparent cell-free-layer (CFL) under low shear rates (γ=10s^{-1}), which almost disappears as the shear rate increases.

4th Micro and Nano Flows Conference
UCL, London, UK, 7-10 September 2014

Multiphase measurement of blood flow in a microchannel

Joseph M. SHERWOOD [1, 3*], David HOLMES [2], Efstathios KALIVIOTIS [3], Stavroula BALABANI [3]

* Corresponding author: Tel.: ++44 (0)207 5491850; Email: joseph.sherwood@ic.ac.uk
1 Department of Bioengineering, Imperial College London, UK
2 Sphere Fluidics, Cambridge
3 Department of Mechanical Engineering, University College London, UK

Keywords: Blood flow, Microcirculation, Haematocrit, Multiphase

Detailed knowledge of how blood flows is of fundamental importance in understanding a wide range of physiological and pathological functions. The multiphase nature of blood, being composed of discrete cells suspended in a continuous medium, drastically alters its flow characteristics from those of a simple fluid such as water. However, these characteristics are often overlooked or considered unimportant in haemodynamic studies. When measured in rheometers, blood displays shear thinning properties; reported to be a result of red blood cell (RBC) aggregation at low shear rates and RBC deformation at high shear rates. Additionally, it has been observed that the viscosity of blood is highly dependent on the haematocrit (RBC concentration) and increases around 4 times as the haematocrit increases from 0 up to 0.45, the physiological haematocrit in the large arteries; in smaller vessels, the haematocrit is significantly decreased. It has been widely observed that RBCs migrate away from the wall, forming a region of low RBC concentration commonly termed a cell-free layer (CFL), in long straight vessel sections which is enhanced around bifurcations. It is often considered that the haematocrit is zero in the CFL and constant in the RBC core. However this is an oversimplification which has significant ramifications; local viscosity, and hence local velocity, are strongly affected by RBC concentration at a given location. Furthermore, the differences in velocities between the RBCs and the continuous fluid in which they are suspended (suspending medium, SM) are expected to be closely linked to the RBC concentration. We propose that to fully describe haemodynamics, both multiphase aspects of the fluid, namely the concentration and velocity of both phases, must be considered. In the present study, a system is developed which allows quasi-simultaneous multiphase measurements of human blood flowing through a sequentially bifurcating microchannel under a range of flow conditions.

Human blood was collected via venepuncture and mixed with 1.8 mg/ml EDTA to prevent coagulation. The samples were separated via centrifugation and the plasma and buffy coat removed. The RBCs were then washed twice in PBS and resuspended at the required haematocrit. Dextran 2000 at 5mg/ml was added to induce RBC aggregation and neutrally buoyant 1.1 µm fluorescent microparticles (Invitrogen) were added at a volume concentration of 0.1% to provide the velocity of the suspending medium. The experimental system comprised a polydimethylsiloxane (PDMS) microchannel bonded to a glass microscope slide with sequential 90° bifurcations and a 50x50µm cross section. The pressure in each branch of the channel was regulated using a Fluigent MFCS system. The microchannel was placed on an inverted microscope with a 10x air objective and illuminated alternately with laser and strobe illumination. Images were captured on a CCD camera and processed for time averaged velocity and haematocrit distributions, using a development of method described in a previous study (Sherwood et al. 2012).

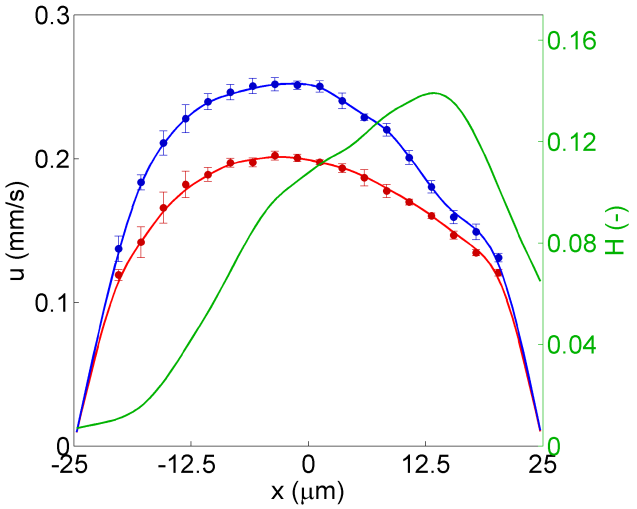

Figure 1: Sample velocity profiles for the RBCs (red) and suspending medium (blue) as well as the local haematocrit distribution (green) in the daughter branch of the 1st bifurcation.

As can be seen in Figure 1, the RBCs and SM show significantly different velocities: most notably, the RBC velocity is decreased relative to the SM (whereas they were similar in the parent branch). Additionally, both velocity profiles are skewed towards negative *x*, conversely to the haematocrit profile which is skewed towards positive *x*. This is evidence that the local distributions of haematocrit affect the velocity of both phases of the blood. A number of parameters, including flow rate, flow ratio, upstream conditions and the presence of absence of RBC aggregation, have a significant effect on the relationships between the velocity and concentration of both phases of the blood. Analysis of these parameters highlights the importance of considering the true multiphase nature of blood.

J.M. Sherwood, J Dusting, E. Kaliviotis, and S. Balabani, 'Hematocrit, Viscosity and Velocity Distributions of Aggregating and Non-Aggregating Blood in a Bifurcating Microchannel', *Biomechanics and Modeling in Mechanobiology*, (2012) Epub.

4th Micro and Nano Flows Conference
UCL, London, UK, 7-10 September 2014

Characterisation of the Mechanobiology of Stents *In-Vitro*

Luke BOLDOCK [1], Charlotte POITEVIN [1], Helen L CASBOLT [1], Sarah HSIAO [2], Paul C EVANS [2], Cecile M PERRAULT [1*]

* Corresponding author: Tel.: +44 (0)114 2220154; Email: c.perrault@sheffield.ac.uk
1: Department of Mechanical Engineering, University of Sheffield, UK
2: Department of Cardiovascular Science, University of Sheffield, UK

Keywords: flow mechanics, stent, shear stress, *in-vitro* assay, cardiovascular disease

1 Introduction

Coronary heart disease is the single biggest killer worldwide, accounting for 7 million deaths annually (Mackay and Mensah, 2004). The blockage of arteries due to plaque build-up (stenosis) associated with this disease currently has no cure, although treatments are available to alleviate symptoms. **M**inimally invasive treatment involving the insertion of a stent to widen the affected arteries is common. However, stent deployment has been associated with a 25% chance of restenosis and treatment of this complication carries a 30% chance of a major adverse cardiac event (Radke *et al*, 2003). Globally, 2 million people receive stents each year, with 80,000 in the UK alone (University College London, 2011). Optimising stented artery repair will reduce mortality and improve quality of life.

Current practice involves the use of drug-eluting and biodegradable stents (Bangalore *et al*, 2013), with the aim of inhibiting restenosis and promoting regrowth of vessel-lining endothelial cells. However, endothelial cells have now been shown to react to complex flow patterns and wall shear stress caused by the stent structure, disrupting repair (Van der Heiden *et al*, 2013). Furthermore, the distribution of chemicals (including the cells' own signaling mechanisms) is affected. To further explore this aspect of the stented artery, full characterisation of the system's fluid dynamics is necessary.

In-vitro study is required to obtain high-resolution, real-time flow patterns around intricate mesh stent structure. Previously, analogies of stent structure, e.g. ridged channels, have been used, which are inadequate for this aim. Therefore, we have developed a novel microfluidic system to accurately replicate *in-vivo* conditions.

2 *In-vitro* analysis of fluid dynamics

Straight sections of tubing were used to create a mould with which blocks of polydimethylsiloxane (PDMS), a silicone elastomer, could be created containing channels of circular cross-section. Balloon catheters were inserted into these channels to deploy pre-mounted, clinically used stents.
Stented channels can be readily connected to fluid reservoirs, with a peristaltic pump providing constant unidirectional flow. Flow rate, associated laminar shear stress and channel diameter can be adjusted to attain conditions comparable to those within the artery.

The high optical transparency of PDMS allowed FluoSpheres to be introduced to the fluid, and subsequently used to image flow using a fluorescent light microscope. Flow patterns were obtained at entry and exit of the stent, and around the complex structure of the mesh.
In parallel, the stented channel was studied *in-silico*, using a computational fluid dynamic model created by micro computed tomography of the PDMS block post-stent deployment.

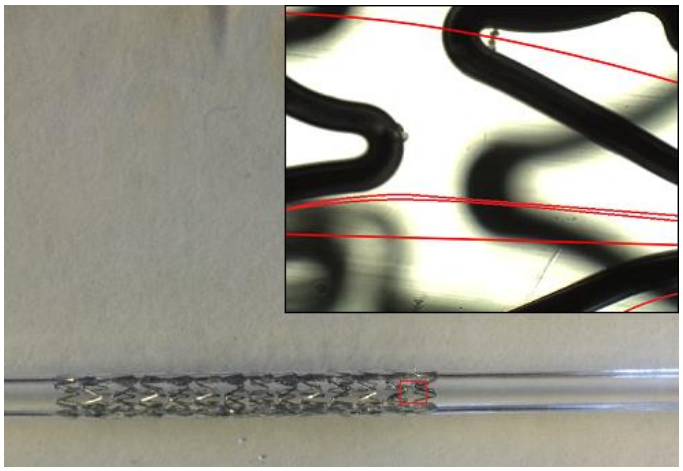

Figure 1: Deployed stent and tracked particle streamlines around struts (inset, 10x magnification). Flow is from right to left.

3 Conclusion

The use of a custom microfluidic system and PDMS rapid prototyping allowed for an *in-vitro* test which was simple, cost- and time-effective, yet an accurate model of the stented artery. *In-vitro* and *in-silico* analysis provided fluid dynamics data of far greater resolution than that possible by *in-vivo* study.

Furthermore, the biological compatibility of PDMS permits the introduction and direct analysis of endothelial cells within the system.

References

Bangalor, S. *et al*, 2013. Bare metal stents, durable polymer drug eluting stents, and biodegradable polymer drug eluting stents for coronary artery disease: mixed treatment comparison. Br. Med. J. 347, f6625.

Mackay, J. and Mensah, G., 2004. The Atlas of Heart Disease and Stroke. 48-49. World Health Organisation.

Radke, P., Kaiser, A., Frost, C. & Sigwart, U., 2003. Outcome after treatment of coronary in-stent restenosis. Eur. Heart J. 24, 266-273.

University College London, 2011. National Audit of Percutaneous Coronary Interventional Procedures. National Institute for Cardiovascular Outcomes Research.

Van der Heiden, K. *et al*, 2013. The effects of stenting on shear stress: relevance to endothelial injury and repair. Cardiovasc. Res. 99, 269-275.

4th Micro and Nano Flows Conference
UCL, London, UK, 7-10 September 2014

Simulation of Gas Micro Flows based on Finite Element and Finite Volume Method

Armin WESTERKAMP [1,*], Jonas BÜNGER [1], Manuel TORRILHON [1]

* Corresponding author: Tel.: ++49 (0)241 8098664; Email: westerkamp@mathcces.rwth-aachen.de
1 Center for Computational Engineering Science, RWTH Aachen University, Germany

Keywords: Kinetic Theory, Moment Methods, Rarefied Gas Flow, Micro Flow

The accurate prediction of rarefied gas flows via numerical simulation remains a challenging task nowadays. Although the branch of computational fluid dynamics (CFD) has undergone a remarkable development, rarefied gas flows have been excluded from this particular success story. While standard CFD relies on the applicability of the Navier-Stokes equations, choosing an appropriate equation set in the rarefied regime is by no means a straight forward task. In situations where the Knudsen number, which is defined as the mean free path divided by a macroscopic length scale, becomes large , the field of non-equilibrium thermodynamics comes into play. This in turn demands for a non-standard treatment.

It is widely accepted that kinetic theory in terms of the Boltzmann equation is able to meet those requirements. In comparison to the macroscopic point of view, that is dominant in standard fluid dynamics, kinetic theory comes along with a microscopic perspective on quantities like temperature and heat. This means in particular a shift from measurable quantities to a statistical description of molecules. But solving the Boltzmann equation numerically is almost forbiddingly expensive due to its high dimensionality. In addition to three spatial and one temporal dimension, also three dimensions in phase space are considered. The phase space thereby spans the space of all possible particle velocities.

The goal of this paper is to present an equation set for the macroscopic quantities, that goes beyond the Navier-Stokes-Fourier (NSF) system. The equations are obtained by considering moments of the probability density, which is the unknown in the Boltzmann equation. When deriving a moment system from the Boltzmann equation, there will always be more unknowns than equations. Therefore a closure has to be introduced which is the part where the modeling takes place. The Regularized 13 (R13) equation set is the result of such a moment closure procedure and states the main part of the paper. These equations have been introduced in [1] and are discussed in detail in the book [2]. They are believed to be accurate up to a Knudsen number of 0.5, while NSF already fails 0.01. In addition to the standard model, balance equations for the heat flux and stress tensor are added. These additional PDEs serve the purpose to resolve more of the non-equilibrium effects that happen on smaller scales. The closure which is used for R13 makes the equations overcome some of the drawbacks that are inherent to common moment systems.

When it comes to numerical simulation, the biggest competitor for moment equations is the Direct Simulation Monte Carlo (DSMC) method. This particle method is the quasi-standard for most rarefied regimes. But especially for slow flows DSMC becomes very noisy. The field of slow flows is intended to be one of the main application areas for R13. This is especially interesting when considering gas flows in micro systems. Since the macroscopic length scale becomes small, larger Knudsen numbers and therefore rarefaction effects may occur. In addition, those flows rarely come close to a Mach number of unity. In that sense the R13 equations can become a valuable contender, especially when considering engineering practice.

After introducing R13 and some of its properties, the numerical treatment states a major theme of the paper. Since we focus on slow flows, a linearized version of R13 is presented in detail. This set of equations is of elliptic nature, which in turn makes finite elements the method of choice. Special challenges that appear are e.g. Stokes-like saddle-point structures and complicated non-standard boundary conditions. But also the finite volume method has its advantages, in particular when it comes to time dependent problems. The strengths and weaknesses of both methods will be outlined. This is then followed by an outlook on future research topics related to R13.

References:

[1] H. STRUCHTRUP AND M. TORRILHON, *Regularization of Grad's 13 moment equations: Derivation and linear analysis*, Phys. Fluids, (2003).

[2] H. STRUCHTRUP, *Macroscopic Transport Equations for Rarefied Gas Flows*, Springer, 2005

4th Micro and Nano Flows Conference
UCL, London, UK, 7-10 September 2014

Experimental Apparatus for the Study of micro Heat Exchangers with Inlet Temperatures between -200 and 200 °C and Elevated Pressures

Anatoly Parahovnik [1,2], Nir Tzabar [2], Gilad Yossifon [1]

[1] *Faculty of Mechanical Engineering Technion-Israel Institute of Technology, Technion city 32000, Israel*
[2] *Rafael, Haifa, 3102102 Israel*

Keywords: Micro Channels, Recuperative Heat Exchanger, Gas Micro Flow, MEMS Fabricated

The current paper presents a test bench for micro-fabricated Recuperative Counter Flow Heat Exchanger (RCFHE), The investigated RCFHE is presented in Fig 1-3. The channels were formed using Deep Reactive Ion Etching (DRIE) on the middle layer and sealed with Pyrex glass covers on both sides by anodic bonding process

Schematic drawing of the test assembly can be seen in Fig 4.

Test bench is suitable for up to 200 K difference between inlets temperatures and operating pressures up to 32 MPa. The experimental setup allows controlling the physical state of the gas (i.e. temperature, pressure and flow rate) at the RCFHE inlets, point 1 and 3 and monitoring the gas state at the outlets, points 2 and 4. The bench has 5 controlled parameters and 5 more that are monitored and enables studying each of the hot and cold channels separately, as demonstrated experimentally.

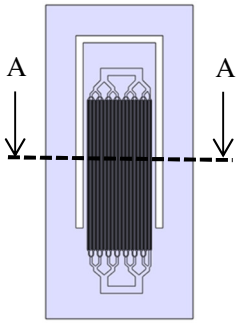

Figure 1 – silicon slide pattern

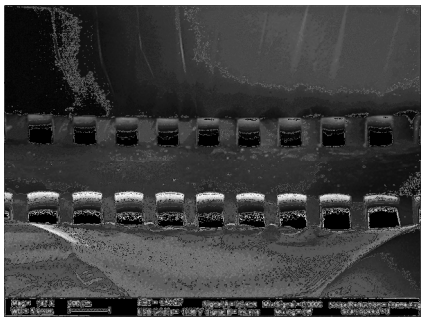

Figure 2 – SEM micrograph A-A cross section

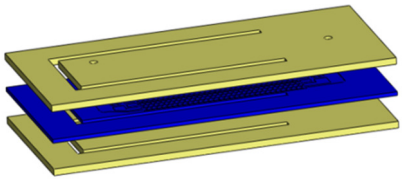

Figure 3 – Heat Exchanger Assembly

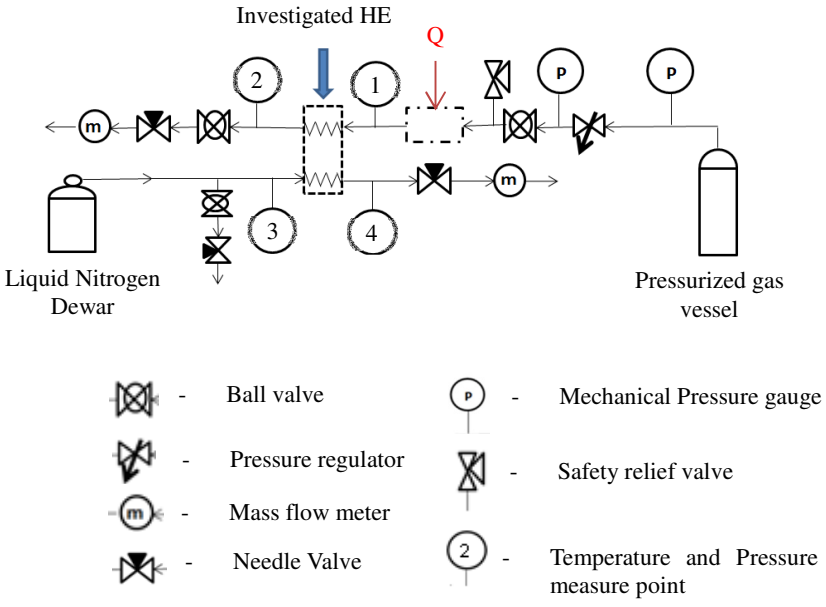

Figure 4 – Experimental test setup

4th Micro and Nano Flows Conference
UCL, London, UK, 7-10 September 2014

On the effect of the dynamic contact angle of a vapor embryo interface trapped in a nucleation site

Laetitia LÉAL [1], Marc MISCEVIC [2,*], Pascal LAVIEILLE [2], Frédéric TOPIN [3], Lounès TADRIST [3]

* Corresponding author: Tel.: ++44 (0)1895 267132; Fax: ++44 (0)1895 256392; Email: marc.miscevic@laplace.univ-tlse.fr
1 Department of Chemical Engineering, Ecole Polytechnique de Montreal, P.O. Box 6079, Stn. CV, Montreal, QC, Canada, H3C 3A7
2 Université de Toulouse ; UPS, INPT ; LAPLACE (Laboratoire Plasma et Conversion d'Energie) ; 118 route de Narbonne, F-31062 Toulouse cedex 9, France. CNRS ; LAPLACE ; F-31062 Toulouse, France
3 Aix-Marseille Université-CNRS Laboratoire IUSTI, UMR 7743, 5 Rue Enrico Fermi, Marseille 13453, France

Keywords: Nucleation, Cavitation, Boiling, Dynamic contact angle

Numerous heat transfer enhancement techniques have been developed to meet the growing needs in terms of heat transfer efficiency and of compactness. Those implementing the liquid-vapor phase-change are promising. However, one of the constraints of these techniques is the high temperature to be achieved for the onset of the boiling process. A technique for controlling the nucleation incipience temperature was proposed by Léal et al. [1, 2, 3]. It consists in simultaneously involving boiling and cavitation, using the dynamic deformation of a confinement wall. Indeed, nucleation can be obtained in two ways: by increasing the liquid temperature at constant pressure (boiling) or by decreasing the liquid pressure at constant temperature (cavitation). Thus, a decrease in pressure would then cause the decrease of the temperature necessary to the nucleation incipience. Furthermore, if the mechanisms governing nucleation were studied from the point of view of "boiling" and from the point of view of "cavitation", the simultaneous action of these two effects on the nucleation has not been analyzed yet.

An experimental device was designed to study the effect of the simultaneous boiling and cavitation on nucleation conditions. As previously mentioned, the control technique consists in imposing a dynamic deformation at a confinement wall that induces an oscillation of the liquid pressure over time to promote cavitation process. Furthermore, a heat flux is imposed to the system. Thus, boiling and cavitation processes are simultaneously involved.
The nucleation incipience superheats when the dynamic deformation is imposed to the confinement wall were measured experimentally. A strong decrease (up to 86%) in the superheat was obtained compared to the reference case (i.e without dynamic deformation). Experimental nucleation superheats were compared with those obtained by the "classical" theory of nucleation [4]. When the confinement wall is not deformed, the experimental nucleation incipience superheats are consistent with those theoretically obtained. By cons, when the dynamic deformation is imposed to the confinement wall, large discrepancies appear between the theoretical and experimental nucleation superheats. Thus, dynamics phenomena promoting nucleation appear to not been taken into account by the "classical" theory of nucleation.

New theoretical approaches taking into account some dynamic effects on nucleation are proposed in order to identify the main mechanisms involved in such a configuration.
For a highly wetting liquid (which is the case in the experimental configuration), the onset of nucleation takes place while the nucleus is trapped inside a cavity. The contact line is not attached to the geometrical singularity and can therefore move inside the cavity. The dynamic (including the hysteresis) of the contact angle can affect the conditions of nucleation. This study proposes a method to analyse the stability of the embryo and thus to predict the onset of nucleation. To describe the dynamic of the contact angle in a simplified manner, the study is limited to two configurations: 1) the contact line is fixed and the contact angle varies; 2) the contact line moves and the contact angle is a function of its velocity. This methodology does not replace the need for much detailed modeling phenomena that occur at these scales but simply provides an attractive alternative for capturing different phenomena and to guide future studies for understanding the experimental results.
This first conclusion of the model is that the decrease in the static liquid pressure has a weak effect on the superheat required to the onset of boiling (almost 2 K for a decrease in the liquid pressure of 0.1 bar). The boiling incipience appears to be more sensitive to the dynamic of the contact angle. A variation of this contact angle during an oscillation from 10 degrees to 90 degrees implies about 20K of reduction in the wall superheat at the onset of boiling. Thus, if dynamical effects lead to the change in the contact angle, it appears possible to obtain the onset of nucleation at very low superheat. As the liquid pressure is changed over time, the contact line moves with a certain velocity that changes the value of the contact angle. So, the effect of the dynamic (including hysteresis) of the contact angle appears as being the possible mechanism promoting nucleation in dynamic configuration.

The effect of boiling and cavitation phenomena on nucleation was first experimentally studied. Results highlight the fact that the "classical" theory of nucleation cannot describe such a configuration. New theoretical approaches were proposed in order to describe the dynamic effects which occur when the liquid pressure oscillates over time and when a heat flux imposed to the system. It then appears that the dynamic and the hysteresis of the contact angle may play a significant role in nucleation by simultaneous boiling and cavitation effects. Nevertheless, further theoretical and experimental studies are required on this subject in order to better understand their effects on nucleation.

Acknowledgements
Financial support from CNRS Energie CITAMPE PR09-3.1.3-2 and FNRAE SYRTIPE are gratefully acknowledged.

References
[1] Léal, L., Lavieille, P., Miscevic, M., Pigache, F., Tadrist, L., Control of pool boiling incipience in confined space: dynamic morphing of the wall effect. In International proceedings of the 3rd Micro and Nano Flows Conference, number 53, (2011)
[2] Léal, L., Lavieille, P., Miscevic, M., Pigache, F., Tadrist, L., Control of pool boiling incipience in confined space: dynamic morphing of the wall effect. Applied Thermal Engineering, 51(2):451–458, 2013.
[3] Léal, L., Étude des mécanismes de nucléation par action simultanée de l'ébullition et de la cavitation, PhD thesis, Université de Toulouse, École doctorale MEGeP, 2012.
[4] Carey, V. P., Liquid-vapor phase-change phenomena, Hemisphere Publishing Corporation, 1992.

4th Micro and Nano Flows Conference
UCL, London, UK, 7-10 September 2014

Flow pattern in inner cores of double emulsion droplets

Shaohua MA,[1,2] Joseph M. SHERWOOD,[3,4] Wilhelm T. S. HUCK[1,5,*] and Stavroula BALABANI[3,*]

* Corresponding author: w.huck@science.ru.nl; s.balabani@ucl.ac.uk
1. Department of Chemistry, University of Cambridge, Cambridge CB2 1EW, UK
2. Department of Chemistry, University of Oxford, Oxford OX1 3TA, UK
3. Department of Mechanical Engineering, University College London, London WC1E 7JE, UK
4. Department of Bioengineering, Imperial College London, London SW7 2AZ, UK.
5. Radboud University Nijmegen, Institute for Molecules and Materials, Heyendaalseweg 135, 6525 AJ Nijmegen, The Netherlands.

Keywords: Droplet, Microfluidics, Micro-particle Image Velocimetry, Flow Topology

Microfluidic droplets have been the subject of extensive research due to the wide ranging applications of this technology. Knowledge of the flow field inside the droplets is of paramount importance in order to tailor microdroplets to a specific application. For example, while intensive mixing is desirable for reaction/synthesis applications, a low shear environment might be preferred for cell encapsulation. Water-in-oil-in-water (w/o/w) double emulsions might be advantageous in cell encapsulation applications as the shear environment inside the droplets might protect shear sensitive cells. Furthermore, such systems are more compatible with commercial flow cytometry methods, such as fluorescence-activated cell sorting (FACS), owing to the fact that the carrier fluid in FACS is aqueous, whereas water-in-oil (w/o) droplets are carried by oil. The flow topology inside the inner cores of moving w/o/w double emulsions in microchannels determines the efficacy of their application and hence needs to be well understood.

In this study, micro-Particle Image Velocimetry (μPIV) was employed to characterize the flow field inside single w/o microdroplets as well as in the inner cores of w/o/w droplets of equal size moving in a rectangular microchannel. The multiphase flow system (water-in-HFE7500) employed in the study had a viscosity ratio, λ, between oil and aqueous phase of the order of unity (λ = 0.78) and both single and compound droplets filled the channels.

This viscosity contrast resulted in a weak recirculating flow pattern inside the w/o single droplet: the measured flow field exhibited a uniform low velocity flow field in the central region surrounded by small regions of reversed flow near the channel walls. This results in relatively low shear, which in practice could protect encapsulated samples like sperm cells in flow cytometry. Interestingly, this flow topology was maintained in the inner cores of w/o/w double emulsions for intermediate capillary numbers (*Ca*) ranging from 10^{-3} to 10^{-2}, and core morphologies varying from large plug to pancake cores. The core morphology affects the magnitude and distribution of the velocity in the droplets. The similarity in the flow pattern results from the fact that inner cores were located at the back of the outer droplet in such a way that inner and outer interfaces were in contact for half of the core surface area and separated by a thin lubricating film.

The inner cores of double droplets exhibit analogous flow topologies and velocity magnitudes with equally sized single droplets composed of the inner core and middle oil shell of double emulsions. Thus, double emulsions are suitable candidates to substitute single droplets in flow cytometry to protect screened cells and achieve higher cell viability recovery rate.

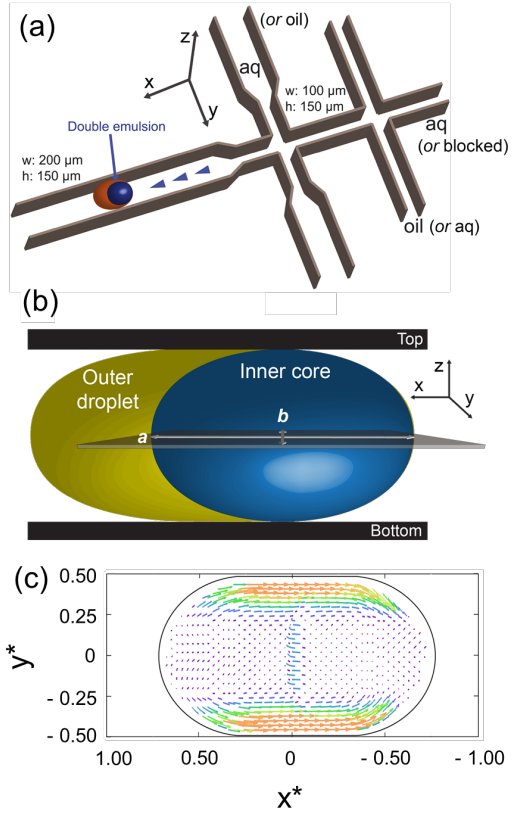

Figure 1. (a) 3D drawing of the microfluidic channel architecture. (b) Schematic of double emulsion system imaged showing focal plane, coordinate system and dimensions (c) Velocity vector field of the inner core of a w/o/w double emulsion.

4th Micro and Nano Flows Conference
UCL, London, UK, 7-10 September 2014

Measurement and Modeling of Void Fraction in High Pressure Condensing Flows through Microchannels

Brendon KEINATH [1], Srinivas GARIMELLA [2,*]

* Corresponding author: Tel.: +1 404-897-7479; Fax: +1 404-894-8496; Email: sgarimella@gatech.edu
1 Exxon Mobil, Houston, TX, USA
2 G.W. Woodruff School of Mechanical Engineering, Georgia Institute of Technology, Atlanta, GA, USA

Keywords: Microchannel, Condensation, Void Fraction, Visualization, Refrigerants

1 Abstract

Modeling the transport of heat and mass in condensing flows is of great importance for the design and improvement of condensation heat transfer equipment. Due to the inherent complexities of phase change in two-phase flow, nearly all available models contain varying degrees of empiricism. Many of these models rely on the prediction of the location of the vapor-liquid interface as a starting point for modeling heat, mass and momentum transfer. For in-tube condensation, the void fraction is used to infer the thickness of the liquid film and is a building block for pressure drop and heat transfer models. Thus, there is a need for accurate correlations for void fraction under varying flow conditions, particularly in mini- and microchannels.

The condensation of Refrigerant R-404A in tubes of diameter 0.508, 1.00, and 3.00 mm is investigated. Void fraction measurements are obtained using image analysis techniques on high speed video frames. Experiments were conducted on refrigerant R-404A throughout the entire condensation quality range ($0.05 < x < 0.95$) at varying mass fluxes ($200 \leq G \leq 800$ kg m^{-2} s^{-1}) and saturation temperatures from 30 to 60°C. At these saturation temperatures, condensation occurs over a wide range of mid to high reduced pressures ($0.38 \leq p_r \leq 0.77$). These high pressures are representative of actual operation of air-conditioning and refrigeration equipment, instead of extrapolating findings for adiabatic air-water mixtures at atmospheric pressure to high pressure refrigerant condensation. For all saturation temperatures, the void fraction approaches unity as the flow becomes completely vapor and approaches 0 as the flow becomes completely liquid. At both extremes, the measured results approach the homogeneous flow model. The influence of saturation temperature on void fraction is most pronounced in the quality range $0.25 < x < 0.75$. In addition, it was found that the influence of mass flux on void fraction was negligible for all saturation temperatures and tube diameters investigated.

The void fraction data obtained in this study were compared with several models from literature. The Baroczy [1] model predicts data the best but is physically inconsistent. As a result, a new drift flux void fraction model is developed to predict void fraction for condensing flows in microchannels. The model was developed for the R404A data and was compared with R-134a void fraction data from Winkler *et al*. [2]. Overall there is very good agreement and the model is able to predict 92.3% of the R-404A data and 81.6% of all refrigerant data within 25%. The resulting void fraction model can provide closure for pressure drop and heat transfer models.

2 References

1. Baroczy, C. J., 1965, "Correlation of Liquid Fraction in Two-Phase Flow with Applications to Liquid Metals," *Chemical Engineering Progress Symposium Series*. **61**(57): pp. 179-191.

2. Winkler, J., Killion, J., and Garimella, S., 2012, "Void Fractions for Condensing Refrigerant Flow in Small Channels. Part II: Void Fraction Measurement and Modeling," *International Journal of Refrigeration*. **35**(2): pp. 246-262.

4th Micro and Nano Flows Conference
UCL, London, UK, 7-10 September 2014

Microfluidic droplet control by photothermal interfacial flow

Muto MUTO [1,*], Masahiro MOTOSUKE [1,2]

* Corresponding author: Tel.: +81 (3)5876 717; Fax: +81 (3)5876 1326; Email: j4513652@ed.tus.ac.jp
1 Department of Mechanical Engineering, Tokyo University of Science, Japan
2 Research Institute for Science and Technology, Tokyo University of Science, Japan

Keywords: Microfluidics, Droplet, Photothermal Marangoni Effect, Laser-Induced Fluorescence

1 Purpose

Droplet-based microfluidics is the emerging field that can perform a variety of discrete operation, such as generation, manipulation, mixing, reaction or separation, of tiny amount of reagent or individual cell. Noncontact manipulation of droplets in a microfluidic platform can be achieved by using photothermal interfacial flow, namely the Marangoni convection due to a local temperature gradient given by an irradiation of heating light. This method provides noncontact, selective and flexible manipulation for droplets flowing in microchannel network. In this study, we investigated the quantitative determination of the driving force exerted on droplets generated by the photothermal Marangoni effect.

2 Methods

2.1 Generation of photothermal Marangoni flow

Temperature gradient around a droplet by the light irradiation generates spontaneous interfacial flow, *i.e.*, Marangoni effect, used for our method of droplet manipulation. When the heating light is irradiated into the liquid in the vicinity of a droplet, it generates the Marangoni convection and results in a pressure difference around the droplet. The driving force works on the droplet and moves it toward an area with lower pressure, that is, lower interfacial tension. The liquid-liquid interface in the present experiments has positive temperature dependence of the tension, and this means the droplet moves away from the heating light position.

2.2 Experimental system

In our study, oleic acid droplet was used as the dispersed phase. The continuous phase was buffer solution. In the continuous phase, a temperature-sensitive fluorescent dye (fluorescein) was added for laser-induced fluorescence to measure the temperature field. Also, an absorption dye was added into the buffer solution for enhancing the absorption of the heating light. A microfluidic device consisting of a PDMS (polydimethylsiloxane) channel and a glass substrate was used. The light from the red diode laser was irradiated into the microchannel. The droplet motion in the channel was obtained by a sCMOS camera connected to the microscope.

3 Results

3.1 Optically-manipulated pathway for microfluidic droplet

Under the laser heating, droplet in the channel flows avoiding the heated region due to the photothermal interfacial flow. Difference of trajectory pattern of droplets with different sizes the same laser irradiation is shown in Fig. 1. The result clearly shows that larger droplet has increased transportation distance from the heated area. Therefore, we thought the driving force of droplet depends on the droplet size and the temperature gradient.

3.2 Determination of driving force

Here, we evaluated the manipulation force for a droplet under photothermal surface activation under an assumption of a force balance between the photothermal Marangoni force and the drag force by the bulk channel flow as shown in Fig. 2. In order to determine the manipulation force F_M, the temperature difference at two edges of the droplet was measured by LIF. Based on Eq. (1), F_M can be related to ΔT and d.

$$F_M = AF_m = A\frac{\partial\sigma}{\partial T}\frac{\partial T}{\partial x}d^2 = A\frac{\partial\sigma}{\partial T}\Delta T d \qquad (1)$$

Fig. 3 depicts the calculation results. F_M linearly and quadratically increases as the increase of ΔT and d, respectively.

4 Conclusions

(1) Microfluidic droplet can be manipulated by heating based on photothermal Marangoni effect.
(2) Manipulation force by photothermal Marangoni effect was quantitatively evaluated with droplet diameter and temperature difference.

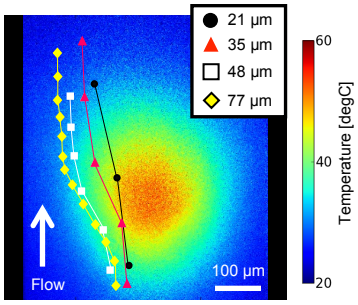

Figure 1: Trajectory of droplets

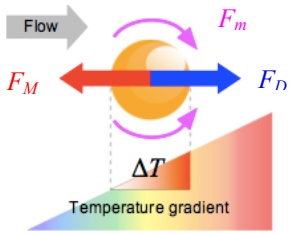

Figure 2: Force balance

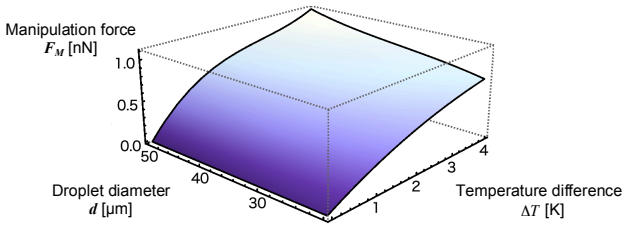

Figure 3: Manipulation force by photothermal Marangoni effect

4th Micro and Nano Flows Conference
UCL, London, UK, 7-10 September 2014

A particle flow specific boundary element formulation for microfluidic applications

Besim Baranoğlu, Barbaros Çetin*

Corresponding author: Tel.: +90 (312) 290-2108; Fax: +90 (312) 266-4126
Email: barbaros.cetin@bilkent.edu.tr, barbaroscetin@gmail.com
[1]Department of Manufacturing Engineering, Atılım University, Ankara 06836 Turkey
[2]Microfluidics & Lab-on-a-chip Research Group, Mechanical Engineering Department
İhsan Doğramacı Bilkent University 06800 Ankara Turkey

Keywords: Boundary element method, microfluidics, particle flow, Stoke's flow

Lab-on-a-chip (LOC) devices are the microfluidic platforms which can handle complex chemical and biological management and analysis for many practical applications. Manipulation of bioparticles within the microchannels is a key ingredient for many biomedical and chemical applications. Therefore, for an efficient design of microfluidic systems, the simulation of the motion of the bioparticle(s) with different shapes is crucial. In many applications of microfluidics, particles are under the action of electrical, magnetic and/or acoustic field together with the flow field. Particle trajectory is the result of the interaction of the particle with the fields that are present. One approach to model the particle trajectory within the microchannel is the stress tensor approach. In this approach, the field variables are solved with the presence of the finite-sized particle. The resultant force on the particle can be obtained by integrating the appropriate stress tensor on the particle surface. In each incremental movement of the particle, the field variables need to be resolved. In many studies, this approach has also been successfully implemented [1,2] to explore the nature of the bioparticle flow within a microchannel.

A rigorous simulation of the particle motion utilizing tensor approach requires massive remeshing. For methods involving domain discretization, such as finite element method (FEM) or finite volume method (FVM) not only the remeshing process is computationally expensive, but also at each remeshing step, some interpolating algorithms relating the field variables in the new mesh in terms of the variables of the old mesh are required which cause some loss in the accuracy. Moreover, the determination of the forces induced on the particles requires the calculation of gradient of the field variables. Therefore, for an accurate calculation of gradient of field variables, fine mesh is required on and within the close neighborhood of the particle surface. Due to the computationally expensive nature, only 2D models with relatively coarse mesh and the motion of single particle have been worked on using FEM. To overcome the remeshing problem for the simulation of particulate flow at macroscale, immersed boundary method [3] and fictitious domain method [4] have been proposed and implemented. Although these methods are computationally very efficient, to model the particle-particle interaction, some contact modeling is required which has a resolution that cannot be accepted for the simulation at microscale. Moreover, these methods are well established for flow simulations, but very rare studies exist for the coupling of flow with the electrical and/or magnetic fields.

Considering the microchannel networks within the LOC devices, typical flow speed is low (resulting in very low Reynolds number) and the inertia forces are negligible (in magnitude) when compared with the pressure or the viscous forces. The flow can be considered as the so-called creeping flow. The governing equations of the creeping flow are those of the Stoke's flow, which are linear partial differential equations suitable for solution with the Boundary Element Method. Since the BEM does not require meshing within the flow region and the exact calculation of the gradient of the field variables, and considering the linearity of the governing equations, it is a preferable tool for the simulation of the trajectory of bioparticles in a microchannel.

In this study, a formulation to track the motion of the particles within a microchannel flow is presented. The method involves the re-organization of the BE matrices that are evaluated for the flow problem, and through several manipulations, reducing the problem to a linear system of equations where the only unknowns are the motion parameters (eg., the translational and rotational velocities of the centers of gravity) of the particles. With such manipulation, the dimension of the linear system of equations to be solved is reduced drastically, resulting in a comparably fast solution. Since the presented manipulations are all matrix multiplications, the procedure can easily be parallelized. To assess the formulation presented, several benchmark studies from the literature are considered. Some results related with practical microfluidic applications are also presented. The present formulation offers an efficient numerical model to be used for the simulation of the particle trajectory for microfluidic applications and can easily be extended for 3D multiphysics simulations.

References

1. Y. Ai, S. W. Joo, Y. Jiang, X. Xuan, and S. Qian, Biomicrofluidics, 3 (022404), 2009, 1–14
2. Y. Ai, B. Mauroy, A. Sharma, and S. Qian, Electrophoresis, 32, 2011, 2282–2291
3. A. L. Fogelson, C. S. Peskin, J. Comp. Phys., 79, 1988, 50–69
4. R. Glowinski, T. W. Pan, T. I. Hesla, D. D. Joseph, and J. Periaux, J. Comput. Phys., 169, 2001, 363–426

4th Micro and Nano Flows Conference
UCL, London, UK, 7-10 September 2014

Measurement of Cavitation in a Sliding Bearing using Digital Holography

Jeremy M COUPLAND [1,*], Tian TANG [2], Laura AREVALO[3]

* Corresponding author: Tel.: +44 (0)1509 227506; Email: J.M.Coupland@lboro.ac.uk
1 Department of Mechanical and Manufacturing Engineering, Loughborough University, UK
2 Department of Mechanical and Manufacturing Engineering, Loughborough University, UK
3 Aragón Institute of Engineering Research, University of Zaragoza, Spain

Keywords: Digital holography, Cavitation, Sliding bearing, Piston ring

Cavitation bubbles are observed when the local pressure falls below the vapour pressure or saturation pressure of a liquid and are most frequently associated with the errosion of marine propellors and pump impellers. In 1886, however, Osborne Reynolds suggested that cavitation is also possible in the lubricant between bearing surfaces[1] and since then considerable effort has applied to the understanding and modelling of sliding or rolling contact bearings. In this case, assuming various boundary conditions, the Reynolds equation can be solved and this forms the basis of one-dimensional models such as the Swift[2]-Stieber[3] model, the JFO model[4] and Coyne and Elrod's model[5]. Although these models all provide reasonable estimates of engineering parameters such as load capacity and friction, they are based on substantially different assumptions and further work is required to understand the fundamental operation of bearings.

In this study digital holography was used to examine bubble formation within a glass sliding bearing. Digital holography collects the both the phase and amplitude of the transmitted wavefront and therefore contains quantitative information concerning the position and thickness of the cavitation bubbles.

Figure 1. shows the experimental configuration. In this case the sliding contact is between a cylindrical lens and a plane glass surface, lubricated with commercial engine oil (SAE 5W-30). The plane glass is driven by a motorized translation stage capable of bi-directional motion with controlled speed and acceleration. The digital holography system is shown in figure 2. The output of a Q-switched Nd:YLF laser illuminates the bearing and an image is formed on the CCD using a long working distance microscope objective. The image is mixed with a diverging reference wave from the same source such that a near image-plane hologam is recorded. After demodulation the holograms can be reconstructed to find the phase and amplituted of the wavefront in any focal plane and Figure 3.

This paper will discuss the demodulation process and how the information can be used to find parameters such as bubble position and shape.

Figure 1 Experimental configuration

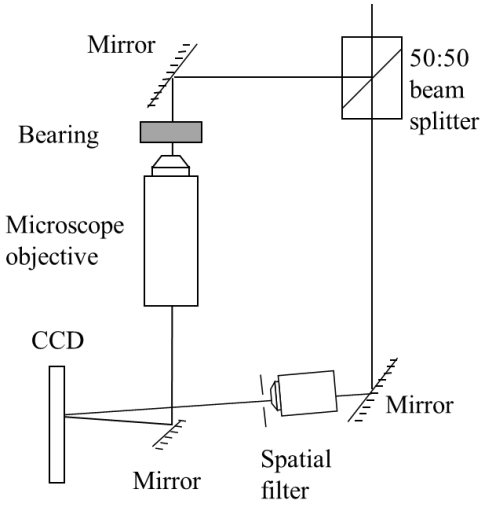

Figure 2 Digital holography system

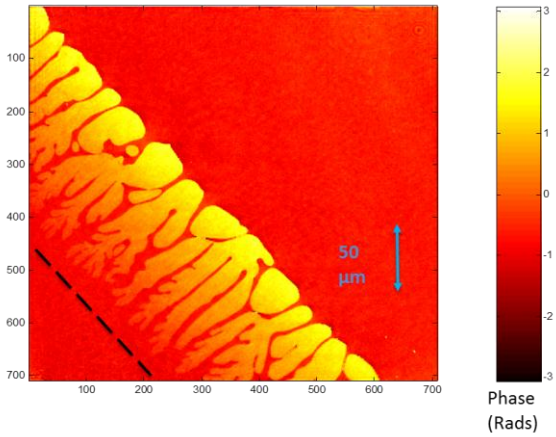

Figure 3 Phase change of a demodulated hologram

Reference

1. REYNOLDS, O. 1886. On the theory of lubrication and its application to Beauchamp Tower's experiments, Including an experimental determination of the viscosity of olive oil. *Philos. Trans. R. Soc. London Ser. A 177:157-233.*
2. SWIFT, W. 1933. The stability of lubricating film in journal bearing. *J. Inst. Civ. Eng. 233 (Pt. 1): 267-88.*
3. STIEBER, W. 1933. *Das Schwimmlager*. Berlin: Ver. Dtsch. Ing.
4. FLOBERG, L. 1974. Cavitation Boundary Condition with Regard to the Number of Streamers and Tensile Strength of the Liquid. *Cavitation and Related Phenomena in Lubrication, ImechE, England, pp. 31-36.*
5. COYNE, J. and ELROD JR, H. 1971. Condition for the Rupture of a Lubricating Film-Part II: New Boundary Condition for Reynolds Equation. *Journal of Lubrication Technology, vol. 93, pp. 156.*

4th Micro and Nano Flows Conference
UCL, London, UK, 7-10 September 2014

Experimental Investigation on Performance of silver Nanofliud in Absorber/Receiver of Parabolic trough collector

D. R Waghole [1,*], R .M. Warkhedkar [2], V.S.Kulkarni[3]

* Corresponding author: Tel.: ++91 (0)020 25431795; Fax: ++91 (0)020 25431795; Email: waghole@yahoo.com
1 Department of Mechanical Engineering, Government College of Engineering, A' bad, India
2 Departments of Mechanical Engineering, Government College of Engineering, Karad, India
3 Department of Math's, Mumbai University, Mumbai, India

Keywords: Nano Flow, nanocirculation, convection, Performance

This experimental investigation presents synthesis and characterizations of silver Nanoparticle. This study also deals with improvement in performance of absorber/Receiver using silver nanoparticle dispersed in DI water (De-Ionized water).The silver nanoparticle suspended in conventional fluid have superior heat transfer capabilities .The absorber of parabolic trough collector is tested for heat input ranging from 50 W/²-600 W/m² in four steps which is suitable for removing heat from solar system, process industries, power plants, automobile systems marine systems etc. The effect of various operational limits and test parameters such as heat input, volume fraction, fluid temperature, heat transfer coefficient are experimentally investigated. The silver nanoparticle is tested for volume concentration in the range of $0 \leq \Phi \leq 0.1$ %, $500 \leq Re \leq 6000$, *experimentally with average silver nanapartice diameter 10nm-400 nm. The Characterizations of silver nanoparticle is carried out using TEM, UV and SEM methodology for required sample of silver nanoparticle. The experimental results are evaluated in terms of performance matrices by direct measurements of fluid temperature and surface temperature in the absorber. A substantial reduction in thermal resistance of 23.152% observed for 0.00011% concentration of silver nanoparticle. The Nussult number for absorber of parabolic trough collector with silver nanofliud varied from 1.25 to 2.10 times in comparison that of water.*

4th Micro and Nano Flows Conference
UCL, London, UK, 7-10 September 2014

Droplet Microfluidics for High Throughput Biological Analysis

Helene ANDERSSON SVAHN [1,*]

* Corresponding author: Tel.: ++46 8 55 37 83 22; Email: helene.andersson.svahn@scilifelab.se
1 Div of Proteomics and Nanobiotechnology, Royal Institute of Technology, Science for Life Laboratory, Sweden

Keywords: Microfluidics, Point-of-care devices; Lab-on-a-chip technology, Droplet manipulation

The Nanobiotechnology group at the Royal Institute of Technology in Sweden is focusing on interdisciplinary research combining nanotechnology and microfluidics with various biotechnology and medical applications such as for example point of care tools and droplet microfluidics.

Droplet microfluidics is a technological platform that utilizes monodisperse aqueous droplets in a continuous biocompatible oil phase as controllable picoliter microreactors. The droplets are generated, manipulated and detected at rates of thousands of droplets per second in a microfluidic device. These characteristics and capabilities make droplet microfluidics uniquely suited for high throughput analysis of single cells, proteins and genetic material. Droplet manipulations include generation, fusion, splitting and sorting by fluorescence or droplet size. We have developed several droplet microfluidic assays such as homogeneous assays based on fluorescence polarization and a method for detection and analysis of cell surface biomarkers on individual human cells using enzymatic amplification in droplets. We also demonstrate high throughput sorting of droplets by size using deterministic lateral displacement, sorting droplets by cells content based on droplet shrinking. Another research focus is droplet-based assays for directed-evolution of industrially relevant enzymes.

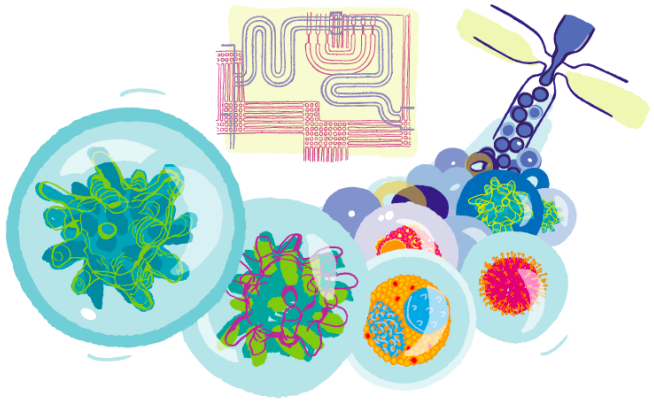

Figure 1. Artist's view of biological assays in droplet microfluidics

4th Micro and Nano Flows Conference
UCL, London, UK, 7-10 September 2014

Sample Preparation for Point of Care Molecular Diagnostics

Wamadeva BALACHANDRAN, RUTH McKAY, Pascal CROW, Branavan MANOHARANEHRU

* Corresponding author: Tel.: ++44 (0)1895 265774; Fax: ++44 (0)1895 256392; Email: emstwwb@brunel.ac.uk
Centre for Electronic Systems Research
School of Engineering and Design, Brunel University, UK

Keywords: Microfluidics, Microcengineering, Point-of-Care, Molecular Diagnostics

Nucleic acid amplification testing (NAAT) is becoming increasingly popular within point of care (POC) diagnostics due to the rapid, sensitive and specific results obtained. An integrated microengineered platform is under development for automated DNA extraction and isothermal amplification using micro volume samples. Challenges in sample preparation methods including nucleic acid extraction have inhibited the uptake of commercial POC devices. Nucleic acid extraction for POC devices is dominated by solid phase extraction with chaotropic salts on silica membrane columns and magnetic beads membranes. Solid phase extraction requires centrifugation whilst magnetic beads require an external magnet for separation. The other drawback to this method is the use of toxic guanidinium thiocyanate, which can inhibit downstream polymeraise chain reaction (PCR). This presentation reports a new method of DNA isolation using chitosan impregnated on an organic membrane embedded in a urine/swab sample collection device for diagnosis of sexually transmitted infections. Chitosan, a deacetylated form of chitin, has been shown to adsorb DNA in microfluidic devices by anion exchange. This method significantly reduces complexity associated with sample collection and nucleic acid extraction as DNA is bound to the membrane under acidic conditions and is eluted in alkaline conditions (Figure.1). The microfluidic device incorporates passive mixing of the lysis-binding buffers and sample.

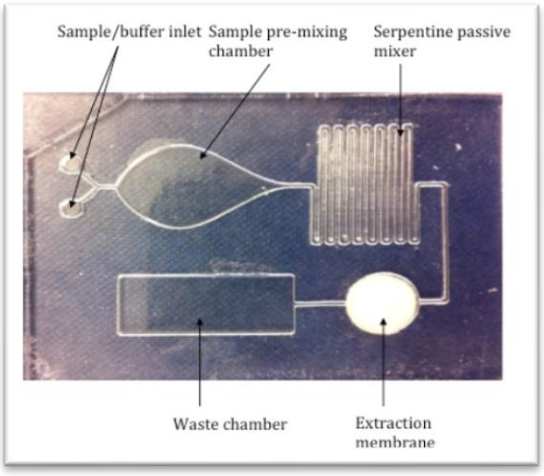

Figure 1: Microfluidic DNA extraction cartridge

Preliminary results have shown that the extraction efficiencies for this new membrane is comparable to the commercial Qiagen extraction method for 0.1ng/µL and 100ng/µL salmon sperm DNA spiked in phosphate buffered solution as well as *E.Coli* spiked in artificial urine solutions. The time for extraction is about one third that of Qiagen extraction method. Preliminary results obtained with DNA extraction using paper based microfluidic flow through devices will also be presented Ffigur 2 a &b).

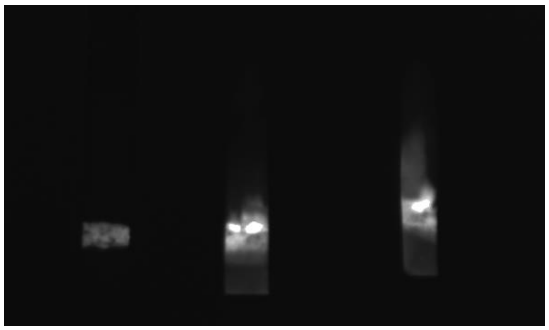

Figure 2.a: Chitosan modified test strips with 50mM DNA in pH 5.0 MES buffer bound to the test region

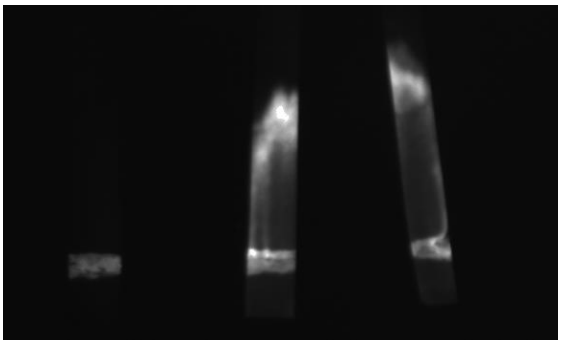

Figure 2.b: DNA being washed out of the test region with an elute buffer of pH of 9.0.

The results obtained using the BIO-RAD Gel DOC™ XR+ system and the associated image analysis software indicates that the sensitivity of detection of florescence labeled DNA is 1 pM.

4th Micro and Nano Flows Conference
UCL, London, UK, 7-10 September 2014

Co-current horizontal flow of a Newtonian and a non-Newtonian fluid in microchannels

Eyangelia-Panagiota ROUMPEA, Agathoklis D. PASSOS, Aikaterini A. MOUZA, Spiros V. PARAS*

* Corresponding author: Tel.: ++30 2310 996174; Email: paras@auth.gr
Chemical Engineering Department, Aristotle University of Thessaloniki, GR

Keywords: Two phase flow, Microchannels, Non-Newtonian fluid

Within the last decade, microchannel reactors have become a new and promising technology in chemical engineering aiming to more effectively use of both raw materials and energy. High heat transfer rates can be achieved because of the small diameter of the channels and the high specific surface area of microchannel reactors. Although many investigations deal with Newtonian liquid-liquid two-phase flow patterns in microchannels [1], to the authors' best knowledge studies on the flow behavior of non-Newtonian liquid–liquid flow in small dimension conduits were not found. In liquid–liquid systems various flow patterns can be observed, depending on the flow rate and the physical properties of both phases, the microchannel material and wettability and the geometry of the mixing zone [2].The effect of these parameters on both Newtonian and non-Newtonian fluid flow behavior must be carefully investigated, in order to fully understand the characteristics and patterns of two-phase flow in a microchannel. The slug flow regime that prevails in such microchannels is characterized by regular and periodic flow of a dispersed phase in a continuous liquid stream and provides enhanced heat and mass transfer rates when compared with its single phase counterpart [3]. For the optimal design of droplet-based microreactors the understanding of the hydrodynamics of the flow of long liquid droplets in continuous liquid phase is essential.

The present work aims to experimentally study the immiscible liquid-liquid two-phase flow patterns in a circular microchannel (*I.D.*= 580μm, 12cm long). Using two syringe pumps, the two fluids enter through two inlet arms that meet at a T-junction. Two aqueous glycerine solutions containing xanthan gum were used as non-Newtonian fluids (*shear thinning*) while kerosene was employed as the Newtonian fluid. Xanthan gum is a polysaccharide that acts as rheology modifier and renders the fluid non-Newtonian. Two Newtonian systems, namely water-kerosene and aqueous glycerin solution-kerosene, were used as reference. The physical properties of all fluids employed were carefully measured. The effect of the flow rate and the fluid properties of the two immiscible liquid phases on the flow pattern were thoroughly examined. The flow patterns were identified by recording the flow using a high sense *CCD* camera connected to a microscope and then examining the corresponding video images (***Fig. 1***). To eliminate image distortion caused by refraction due to the cylindrical wall, the microchannel was placed in a square cross-section Plexiglas box filled with the same fluid as the one in the corresponding experiment. During the experiments the flow rate of the continuous phase was kept constant to 50μL/min, while the flow rate of the dispersed phase varied between 50-200μL/min.

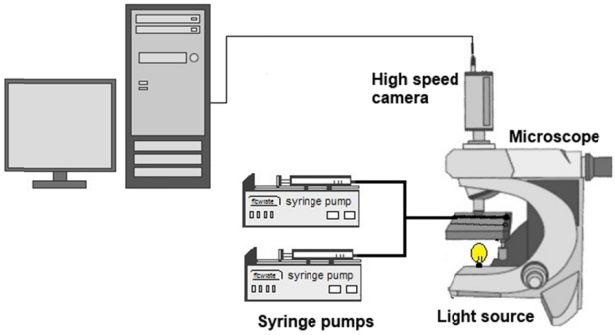

Fig. 1: *Experimental setup used in our study.*

Preliminary experiments in the micro-channel revealed that the flow patterns are the same, irrespective of the fluid that initially filled the tube. The main pattern observed in the tube is kerosene-slugs flowing in the non-Newtonian fluid (***Fig. 2***). The shape and the size of the slugs are highly affected by the flow rate of the two phases, the interfacial tension and the viscosity of both fluids. This study, currently in progress, is expected to provide interesting information on the transport phenomena occurring in this type of microreactors.

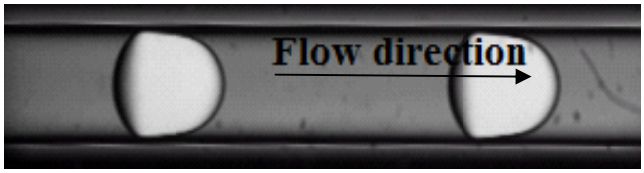

Fig. 2: *Typical flow pattern in the microchannel.*

References

1. Talimi, V., Muzychka, Y.S., Kocabiyik, S., 2012. A review on numerical studies of slug flow hydrodynamics and heat transfer in microtubes and microchannels. *Int J Multiphase Flow* **39**, 88–104.
2. Tsaoulidis, D., Dore, V., Angeli, P., Plechkova, N., Seddon, K., 2013. Flow patterns and pressure drop of ionic liquid – water two – phase flows in microchannels. *Int J Multiphase Flow* **54**, 1-10.
3. Gupta, R., Leun, S.S.Y., Manica, R., Fletcher, D.F., Haynes, B.S., 2013. Hydrodynamics of liquid–liquid Taylor flow in microchannels. *Chem Eng Sci* **92**, 180–189.

4th Micro and Nano Flows Conference
UCL, London, UK, 7-10 September 2014

Advances and Challenges in Computational Research of Micro and Nano Flows

Dimitris DRIKAKIS [1,*]

* Corresponding author: Tel.: ++44 (0)1895 267132; Fax: ++44 (0)1895 256392; Email: d.drikakis@cranfield.ac.uk
1 Department of Engineering Physics, Cranfield University, UK

Keywords: Micro Flow, Nano Flows, CFD, MD

The talk gives an overview of the current state of the art in computational research of micro and nano flows. It presents the development of multi-scale methods based on computational fluid dynamics and molecular dynamics and their application to a broad range of problems, including drag reduction, carbon capture nanotechnologies and biomedical engineering. It also uses specific examples to demonstrate how computational research can guide the development of novel technologies such as nanotechnology-based gas filters.

4th Micro and Nano Flows Conference
UCL, London, UK, 7-10 September 2014

Blood Flow *in silico*: From Single Cells to Blood Rheology

Gerhard GOMPPER [1,*]

* Corresponding author: Tel.: ++49 2461 61 4012; Fax: ++49 2461 61 3180; Email: g.gompper@fz-juelich.de
1 Theoretical Soft Matter and Biophysics, Institute of Complex Systems and Institute for Advanced Simulation, Forschungszentrum Jülich, D-52425 Jülich, Germany

Keywords: Microcirculation, Capillary Flow, Red Blood Cells

The flow behavior of vesicles and blood cells is important in many applications in biology and medicine. For example, the flow properties of blood in micro-vessels is determined by the rheological properties of red blood cells (RBCs). Blood flow is therefore strongly affected by diseases such as malaria or diabetes, where RBC deformability is strongly reduced. Furthermore, microfluidic devices have been developed recently, which allow the manipulation of small amounts of suspensions of particles or cells.

Of fundamental interest is here the relation between the flow behavior and the elasticity and deformability of the blood cells, their long-range hydrodynamic interactions in microchannels, and thermal membrane undulations [1]. We study these mechanisms by combination of particle-based mesoscale simulation techniques [2] for the fluid hydrodynamics with triangulated-surface models [3-5] for the membrane. The essential control parameters are the volume fraction of RBCs (tube hematocrit), the flow velocity, and the capillary radius.

In narrow channels, single red blood cells in capillary flow show a transition from the biconcave disk shape at low flow velocities to a parachute shape at high flow velocities [4,6]. For somewhat wider channels, other shapes such as slippers intervene between these states [6]. At higher volume fractions, hydrodynamic interactions are responsible for a strong deformation-mediated clustering tendency at low hematocrits, as well as several distinct flow phases at higher hematocrits, such as a zig-zag arrangement of slipper shapes [7]. For large vessels, blood behaves like a continuum fluid, which displays a strong shear-thinning behavior; our simulations show quantitatively how this behavior arises due to RBC deformability and cell-cell attraction [8]. Finally, the dynamics of RBCs is demonstrated to lead to a margination of white blood cells at intermediate hematocrits and not too large flow rates [9].

References

[1] D.A. Fedosov, H. Noguchi, and G. Gompper. *Multiscale Modeling of Blood Flow: From Single Cells to Blood Rheology.* Biomech. Model. Mechanobiol., advance online publication (2013). DOI: 10.1007/s10237-013-0497-9.

[2] G. Gompper, T. Ihle, D.M. Kroll, and R.G. Winkler. *Multi-Particle Collision Dynamics -- a Particle-Based Mesoscale Simulation Approach to the Hydrodynamics of Complex Fluids.* Adv. Polymer Sci. **221**,1 (2009).

[3] G. Gompper and D.M. Kroll. Triangulated-Surface *Models of Fluctuating Membranes.* In *Statistical Mechanics of Membranes and Surfaces*, 2nd edition, edited by D.R. Nelson and T. Piran and S. Weinberg (World Scientific, Singapore, 2004).

[4] H. Noguchi and G. Gompper. *Shape Transitions of Fluid Vesicles and Red Blood Cells in Capillary Flows.* Proc. Natl. Acad. Sci. USA **102**, 14159 (2005).

[5] D.A. Fedosov, B. Caswell, and G.E. Karniadakis. *A multiscale red blood cell model with accurate mechanics, rheology, and dynamics.* Biophys. J. **98**, 2215 (2010).

[6] D.A. Fedosov, M. Peltomäki, and G. Gompper. *Shapes and Deformation of Red Blood Cells in Microvessel Flows.* submitted (2013).

[7] J.L. McWhirter, H. Noguchi, and G. Gompper. *Flow-Induced Clustering and Alignment of Red Blood Cells in Microchannels.* Proc. Natl. Acad. Sci. USA **106**, 6039 (2009).

[8] D.A. Fedosov, W. Pan, B. Caswell, G. Gompper, and G.E. Karniadakis. *Predicting blood rheology in silico.* Proc. Natl. Acad. Sci. USA **108**, 11772 (2011).

[9] D.A. Fedosov, J. Fornleitner, and G. Gompper. *Margination of White Blood Cells in Microcapillary Flow.* Phys. Rev. Lett. **108**, 028104 (2012).

4th Micro and Nano Flows Conference
UCL, London, UK, 7-10 September 2014

Microfluidics for Energy Applications

David SINTON [1,*]

* Corresponding author: Tel.: ++1 416 978 1623; Fax: ++1 416 978 7753; Email: sinton@mie.utoronto.ca
1 Department of Mechanical and Industrial Engineering, University of Toronto, 5 King's College Rd, Toronto, Ontario M5S 3G8, Canada

Keywords: Microfluidics, optics, bioenergy, carbon management

Microfluidic methods developed primarily for medical applications have much to offer energy applications. This talk will describe my group's recent work in two such areas: (1) microfluidics and optics for bioenergy and (2) microfluidics for carbon management. Within the bioenergy theme, we are developing photobioreactor architectures that leverage micro-optics and microfluidics to cater both light and fluids to maximize productivity of microalgae. Within the carbon management theme we are developing a suite of methods to study pore-scale transport and reactivity in carbon sequestration and enhanced oil recovery. Results indicate potential for order of magnitude gains in photobioreactor technology and a 100-fold improvement over current subsurface fluid transport analysis methods.

4th Micro and Nano Flows Conference
UCL, London, UK, 7-10 September 2014

Unified Modeling Suite for two-phase flow, convective boiling and condensation in macro- and micro-channels

John R. THOME [1,*], A. CIONCOLINI [2]

* Corresponding author: Tel.: ++41 21 693 59 81/82; Fax: ++41 21 693 59 60; Email: john.thome@epfl.ch
1 Laboratory of Heat and Mass Transfer, École Polytechnique Fédérale de Lausanne, Switzerland
2 School of Mechanical, Aerospace and Civil Engineering, University of Manchester, UK

Keywords: Modeling, Two-phase flow, Boiling, Condensation

The present paper focuses on the unified modeling suite for annular flow that the authors have and continue to develop. First, the unified suite of methods is presented, illustrating in particular the most recent updates. Then, results for convective evaporation of refrigerants in non-circular multi-microchannel configurations for microelectronics cooling are presented and discussed. The annular flow suite includes models to predict the void fraction, the entrained liquid fraction, the wall shear stress and pressure gradient, and a turbulence model for momentum and heat transport inside the annular liquid film. The turbulence model, in particular, allows prediction of the local average liquid film thicknesses and the local heat transfer coefficients during convective evaporation and condensation. The benefit of a unified modeling suite is that all the included prediction methods are consistently formulated and are proven to work well together, and provide a platform for continued advancement based on the other models in the suite. Annular flow is of fundamental importance to the thermal design and simulation of micro-evaporators and micro-condensers for compact two-phase cooling systems of high heat flux components for the thermal management of computer chips, power electronics, laser diodes and high energy physics particle detectors. In micro-evaporators, annular flow is even more conspicuous than in macrochannels, since annular flow relegates bubbly and slug flows to only the first 3-10% of the vapor quality range. In convective condensation, annular flow is established almost immediately at the inlet of the channel and persists over most of the condensation process until the condensate floods the channel.

The purpose of the present paper is to present the unified modeling suite for annular flow that the authors have and continue to develop, focusing in particular on the prediction of the pressure drop and the heat transfer coefficient during convective evaporation in not only circular but most of all in non-circular multi-microchannels that are typical of microscale heat sinks. Presently, the unified annular flow modeling suite includes methods to predict the entrained liquid fraction, the void fraction, the walls shear stress, the frictional and total pressure gradients, and a turbulence model for momentum and heat transport inside the annular liquid film that allows *one method* for the prediction of the local average liquid film thickness and the local heat transfer coefficient during *both* convective evaporation and condensation ([1]-[8]). The practical advantage of a unified modeling suite is that all the included prediction methods are consistently formulated and are proven to work well together.

The heat transfer methods have been adapted to non-circular (rectangular and square) microchannels as well as the microchannels in a multi-port aluminum tube, without changing of the underlying equations but just stretching of the liquid film around the larger perimeter. Some examples of comparisons to the data are as follows:

Costa-Patry et al. ([9], [10]) for R245fa and R236fa flowing in 135 high aspect ratio silicon multi-microchannels is shown in Fig. 1. The channels were 85 μm-wide, 560 μm-high, aspect ratio of 6.56, hydraulic diameter of 136 μm, 12.7 mm-long, and separated by 47 μm-wide fins. Their heat transfer coefficients measured under non-uniform heat flux conditions are compared with the annular flow models predictions in Fig. 2, where both hot-spot and hot-row heat flux profiles have been tested.

Szczukiewicz et al. ([11],[12]) investigated two-phase flow evaporation of refrigerants R245fa, R236fa and R1234ze(E) flowing in 67 square cross section, silicon multi-microchannels, as shown in Fig. 3. The channels were 100x100 μm size, aspect ratio of 1.0, hydraulic diameter of 100 μm, 10.0 mm-long, and separated by 48 μm-wide fins. The agreement between measured data and predictions is quite satisfactory for R236fa and R245fa, while the R1234ze(E) data are somewhat underpredicted.

References

[1] Cioncolini, A., Thome, J.R., Lombardi, C., (2009a). Algebraic turbulence modeling in adiabatic gas-liquid annular two-phase flow. *Int. J. Multiphase Flow*, Vol. 35, pp. 580-596.

[2] Cioncolini, A., Thome, J.R., Lombardi, C., (2009b). Unified macro-to-microscale method to predict two-phase frictional pressure drops of annular flows. *Int. J. Multiphase Flow*, Vol. 35, pp. 1138-1148.

[3] Cioncolini, A., Thome, J.R., (2010). Prediction of the entrained liquid fraction in vertical annular gas-liquid two-phase flow. *Int. J. Multiphase Flow*, Vol. 36, pp. 293-302

[4] Cioncolini, A., Thome, J.R., (2011). Algebraic turbulence modeling in adiabatic and evaporating annular two-phase flow. *Int. J. Heat Fluid Flow*, Vol. 32, pp. 805-817.

[5] Cioncolini, A., Thome, J.R., (2012a). Entrained liquid fraction prediction in adiabatic and evaporating annular two-phase flow. *Nucl. Eng. Des.*, Vol. 243, pp. 200-213.

[6] Cioncolini, A., Thome, J.R., (2012b). Void fraction prediction in annular two-phase flow, *Int. J. Multiphase Flow*, 43, pp.72-84.

[7] Cioncolini, A., Thome, J.R., (2012c). Algebraic turbulence modeling in condensing annular two-phase flow: preliminary results, *ECI 8th International Conference on Boiling and Condensation Heat Transfer*, Lausanne, Switzerland, 3-7 June 2012.

[8] Cioncolini, A., Thome, J.R., (2013). Liquid film circumferential asymmetry prediction in horizontal annular two-phase flow, *Int. J.*

Multiphase Flow, 51, pp. 44-54.

[9] Costa-Patry, E., Olivier, J., Nichita, B., Michel, B., Thome, J.R., (2011a). Two-phase flow of refrigerants in 85μm-wide multi-microchannels, Part I: pressure drop. *Int. J. Heat Fluid Flow*, Vol. 32, pp. 451-463.

[10] Costa-Patry E., Olivier, J., Michel, B., Thome, J.R., (2011b). Two-phase flow of refrigerant in 85 μm-wide multi-microchannels: Part II: heat transfer with 35 local heaters. *Int. J. Heat Fluid Flow*, Vol. 32, pp. 464–476.

[11] Szczukiewicz, S., Borhani, N., Thome, J.R., (2012a). Two-phase flow boiling in a single layer of future high-performance 3D stacked computer chips. In *13th IEEE Intersociety Conference on Thermal and Thermomechanical Phenomena in Electronic Systems*.

[12] Szczukiewicz, S., Borhani, N., Thome, J.R., (2012b). Two-phase heat transfer and high-speed visualization of refrigerant flows in 100 x 100 μm^2 silicon multi-microchannels. In *ECI 8th International Conference on Boiling and Condensation Heat Transfer*, Lausanne, Switzerland, 3-7 June 2012.

4th Micro and Nano Flows Conference
UCL, London, UK, 7-10 September 2014

Advances in Hybrid Molecular/Continuum Methods forMicro and Nano Flows

Matthew K. BORG [1], Duncan A. LOCKERBY [2], Jason M. REESE [3,*]

* Corresponding author: Tel.: ++44 (0)131 651 7081; Email: jason.reese@ed.ac.uk
1 Department of Mechanical & Aerospace Engineering, University of Strathclyde, Glasgow, UK
2 School of Engineering, University of Warwick, Coventry, UK
3 School of Engineering, University of Edinburgh, Edinburgh, UK

Keywords: Hybrid Methods, Micro Flows, Nano Flows, Molecular Dynamics, Scale Separation

We discuss our new methods for improving the efficiency of hybrid molecular/continuum models of multiscale flows, in particular at the micro and nano scales. We focus on producing general solutions to the problems associated with simulating flow regions that are typically either a) scale-separated in space and time, or b) non-scale-separated. Identifying the Heterogeneous Multiscale Method (HMM) [1] as more appropriate for most practical flow situations than conventional domain decomposition, we first present a method to make the HMM more effective for multiscale flows of arbitrary time-scale separation. Our method has an adaptability that enables the most desirable aspects of existing schemes to be applied only in the appropriate conditions, as well as a leapfrog coupling between the 'macro' and 'micro' components of the hybrid model to improve numerical accuracy over a standard simultaneous approach [2]. The test case demonstrator for this method is a micro-jet actuator for aerodynamic drag reduction applications. In this case we combine a kinetic treatment in a small flow region where rarefaction is important, with a simple continuum-conservation model in the much larger actuating domain. Our new time-stepping method consistently demonstrates as good as, or better, performance than existing schemes.

We then discuss a spatial coupling method in which the individual molecular solvers are not coupled with the continuum grid at nodes (i.e. point-wise coupling), but instead coupling occurs over distributed heterogeneous fields (i.e. field-wise coupling) [3]. This generalizes HMM to flows with arbitrarily-varying degrees of spatial scale separation (e.g. the flow from a large reservoir into a nano-channel). As the position of molecular elements does not need to be collocated with nodes of the continuum grid, the resolution of the microscopic correction can be adjusted independently of the resolution of the continuum model. This in turn means the computational cost and accuracy of the molecular correction can be independently controlled and optimised. The test case we demonstrate this method on is the Poiseuille (nano)flow of both Newtonian (Lennard-Jones) and non-Newtonian (FENE) fluids, which finds application in nanoscale filtration of contaminated liquids, such as seawater. Our multiscale method converges very quickly (within 3–4 iterations) and is an order of magnitude more computationally efficient than a full-scale Molecular Dynamics simulation.

References

[1] W. E, B. Engquist, X.T. Li, W.Q. Ren, E. Vanden-Eijnden, D.B. Hash and H.A. Hassan, "Heterogeneous multiscale methods: A review," *Communications in Computational Physics*, vol. 2, no. 3, pp. 367-450, 2007.

[2] D.A. Lockerby, C.A. Duque-Daza, M.K. Borg and J.M. Reese, "Time-step coupling for hybrid simulations of multiscale flows," *Journal of Computational Physics*, vol. 237, pp. 344-365, 2013

[3] M. K. Borg, D. A. Lockerby, and J. M. Reese, "Fluid simulations with atomistic resolution: a hybrid multiscale method with field-wise coupling," *Journal of Computational Physics*, vol. 255, pp. 149-165, 2013.

4th Micro and Nano Flows Conference
UCL, London, UK, 7-10 September 2014

Optical Sensing of miRNA Activity in Cells

Zdravka MEDAROVA [1,*]

* Corresponding author: Tel.: ++1 617/ 643-4889; Fax: ++1 617/ 726-7422; Email: zmedarova@mgh.harvard.edu
1 Molecular Imaging Laboratory, Radiology Department, Massachusetts General Hospital, Harvard Medical School, Charlestown, MA-02129, USA

Keywords: Intracellular flow, Fluorescence, miRNA, cleavable oligonucleotides

We have developed a technology for the profiling of miRNA expression in intact cells. The approach is based on sensor oligonucleotides, which upon entering the cell, bind specific miRNA targets, are cleaved as a result of this binding, and produce a fluorescent signal that is proportional to the abundance of the miRNA target.

Specifically, the sensor oligonucleotides are completely complementary to a target miRNA species, are non-stabilized around the seed region (the region cleaved by the miRNA-RISC), and are labeled with a fluorescent dye and a quencher at their 5'- and 3'- end respectively. Upon entering the cell, these oligonucleotides engage the target miRNA by complementary base pairing. This leads to recruitment of the RNA induced silencing complex (RISC) to the duplex. The complex cleaves the sensor oligonucleotide and the miRNA is free to "catalyze" subsequent clevage reactions. The cleavage of the sensor oligo leads to separation between the dye and the quencher, and a resultant fluorescent enhancement that can be measured.

We have demonstrated the feasibility of this method for the sensing of the pro-metastatic miRNA-10b in cell-free extracts and intact cells using human and murine breast adenocarcinoma cell lines.

The miRNA epigenome represents a fundamental molecular regulator of metastasis. Consequently, developing tools to understand metastatic changes at the miRNA level can lead to the mapping out of a comprehensive and systematic atlas of cancer progression. The described technology is potentially transformative because it addresses this important issue. Furthermore, the technology has broad implications and can be utilized in any model system or clinical scenario to answer questions related to microRNA function. Specifically, the technology can help distinguish, assess, and/or monitor cancer stages and progression; aid the elucidation of basic mechanisms underlying cancer initiation and progression; facilitate early cancer detection and/or cancer risk assessment; and facilitate/accelerate the process of drug discovery.

4th Micro and Nano Flows Conference
UCL, London, UK, 7-10 September 2014

New look into medicine and biology with thermoacoustic and optoacoustic tomography

Vasilis NTZIACHRISTOS [1,2*]

* Corresponding author: Tel.: ++49 (0)89 3187 3852 ; Fax: ++49 (0)89 3187 3008; Email: v.ntziachristos@tum.de
1 Chair for Biological Imaging, Technische Universität München, Germany
2 Institute of Biological and Medical Imaging, Helmholtz Zentrum München, Germany

Keywords: thermoacoustic tomography, optoacoustic tomography

Optical imaging is unequivocally the most versatile and widely used visualization modality in the life sciences. Yet it is significantly limited by photon scattering, which complicates imaging beyond a few hundred microns. For the past few years however there has been an emergence of powerful new imaging methods that can offer high resolution imaging beyond the penetration limits of microscopic methods. These methods can prove essential in cancer research. Of particular importance is the development of multi-spectral opto-acoustic tomography (MSOT) that brings unprecedented optical imaging performance in visualizing anatomical, physiological and molecular imaging biomarkers. Some of the attractive features of the method are the ability to offer 10-100 microns resolution through several millimetres to centimetres of tissue and real-time imaging. In parallel we have now achieved the clinical translation of targeted fluorescent probes, which opens new ways in the interventional detection of cancer in surgical and endoscopy optical molecular imaging. This talk describes current progress with methods and applications for in-vivo optical, opto-acoustic and thermoacoustic imaging in cancer and outlines how new opto-acoustic and fluorescence imaging concepts are necessary for accurate and quantitative molecular investigations in tissues.

4th Micro and Nano Flows Conference
UCL, London, UK, 7-10 September 2014

Optical assessment of gel-like mechanical and structural properties of surface layers: single particle tracking and molecular rotors

Alex MARKI [1,*], Axel R. PRIES [1,2]

* Corresponding author: Tel.: ++49 30 450 528 501; Fax: ++49 30 450 528 920; Email: axel.pries@charite.de
1 Institute of Physiology, Charité Medicine University, Germany
2 Center for Cardiovascular Research, Charité Medicine University, Germany

Keywords: Surface layer, Microrheology, Fluorescent microscopy

Thin gel-like layers form at many surfaces of natural or artificial origin. Important properties of such layers include thickness, viscosity and density. Here we discuss two optical approaches which allow assessment of these properties with high resolution.

The first approach relies on centroid calculation and defocus imaging based 3D tracking of fluorescent tracer particles, which is based on standard fluorescent microscopy and allows a precision of particle detection in the range of 10nm. The size of the particle and its surface charge and polarity will determine the particle invasion into the layer. Thus simultaneous application of different colored beads with different size and properties can reveal the thickness and nature of the layer. Via tracking the thermal vibration of particles invading the layer the bulk viscosity of the layer can be calculated.

The second approach uses “molecular rotor” fluorophores (MR). Due to their molecular structure, the MR’s fluorescence quantum yield increases as their internal rotation is hampered by e.g. high viscosity of the embedding medium. The MRs are several orders of magnitude smaller than the structural (macro) molecules of a gel-like layer and therefore the MRs are not necessarily directly sensitive toward the bulk viscosity of the layer. In contrast, the MRs internal rotation will be attenuated by the MRs interaction with the structural elements of the layer or the solvent included in it. Depending on their molecular structure MRs exhibit different sensitivity to the mechanical properties of the large macromolecules or the solvent in a layer. Thus, they may be used to assess the microdomain’s viscosity or density in a surface layer. Using a ratiometric imaging approach, they can be used for continuous measurements in very different experimental settings.

4th Micro and Nano Flows Conference
UCL, London, UK, 7-10 September 2014

Towards the identification of spatially resolved mechanical properties in tissues and materials: State of the art, current challenges and opportunities in the field of flow measurements

Pablo D. RUIZ

Tel.: ++44 (0)1509227660 Email: p.d.ruiz@lboro.ac.uk
Wolfson School of Mechanical and Manufacturing Engineering
Loughborough University, Loughborough, LE11 3TU, UK

Keywords: depth-resolved displacements, volume strain, identification

Our ability to predict the mechanical behaviour of materials, components and even tissues and organs is only as good as the knowledge we have about their internal structure, the spatial distribution of their properties, and the boundary conditions that constrain and drive their deformation. This talk will present state of the art advances in the measurement of internal structure and 3D deformation fields in engineering materials and tissues, and their use to identify 'spatially dependent' mechanical properties with a combination of novel optical coherence tomography systems and inversion algorithms.

Neutron diffraction, X-ray tomography, Magnetic Resonance Imaging and Optical Coherence Tomography are all examples of techniques with the ability to map 3-D strain in the bulk of solid materials. They differ in spatial resolution, strain resolution, and type of materials that can be studied. This work is focused on optical methods and different approaches will be presented, including recent developments in phase contrast wavelength scanning interferometry and a combination of optical coherence tomography and digital volume correlation to estimate elastic properties of synthetic phantoms and porcine corneas [1-3].

Inversion algorithms based on finite elements and the Virtual Fields Method (VFM) are used to extract mechanical properties from the knowledge of the applied loads, geometry and measured deformation fields. The VFM is based on the principle of virtual work and retrieves the constitutive parameters by utilizing full-field deformation measurements [4]. This method is more effective than Finite Element Updating in terms of computation time since for the latter an FE model needs to be created and updated iteratively. The VFM has been applied successfully to the identification of constitutive parameters for linear elastic materials such as composites, elasto-plasticity for metals as well as hyper-elasticity for soft and biological materials such as artery walls.

The measurement of 3-D displacement and strain using phase contrast OCT faces a number of challenges, including: 1) dispersion, i.e. variation of refractive index with wavelength, which impairs the depth resolution; 2) refraction effects, which lead to spurious strains and require refraction compensation to re-map the internal structure in a regular grid from which strain can be evaluated from displacements; 3) 3-D phase unwrapping, i.e. the process of finding the right multiple of 2π in the wrapped phase distributions obtained with phase-contrast techniques. This is a difficult problem in 3-D as phase singularity loops, which are common in experimental data, lead to phase unwrapping errors that propagate through the data volume; 4) the extension of the Virtual Fields Method to 3-D; the study of its applicability to identification and the effect of noise in the measured displacements. Also, there are interesting approaches that are emerging to study the 2-D spatial distribution of modulus in the case of known and unknown boundary conditions [5].

Current efforts into extending these OCT methods into single shot techniques have the potential of expanding the range of applications to study dynamic events such as micro-flows in engineering and biological systems in which scattering particles are transported in a flow (e.g. tribology, microfluidic devices, cell migration, multi-phase flows, etc). Proof of principle systems are currently limited to a spatial resolution of ~40×40×40 independent measurements. Temporal resolution depends on light source power and sensitivity of the 2-D photodetector array used, but can be expected to range between a few tens to a few hundreds of volumes per second.

References

[1] S. Chakraborty and P.D. Ruiz, Measurement of all orthogonal components of displacement in the volume of scattering materials using wavelength scanning interferometry. JOSA A, 2012. 29(9): p. 1776-1785.

[2] J. Fu, F. Pierron, and P.D. Ruiz, Elastic stiffness characterization using 3-D full-field deformation fields obtained with optical coherence tomography and digital volume correlation. Journal of Biomedical Optics, 2013. (under review).

[3] J. Fu, P.D. Ruiz, and F. Pierron. Correction of refraction induced distortion in optical coherence tomography corneal reconstructions for volume deformation measurements, in Photomechanics 2013. 2013. Montpellier, France.

[4] F. Pierron and M. Grédiac, The virtual fields method, Springer, New York (2012).

[5] A.T.T. Nguyen, et al. Fast Fourier virtual fields method for determination of modulus distributions from full-field optical strain data, in Fringe 2013: 7th International Workshop on Advanced Optical Imaging and Metrology. 2013. Nürtingen, Germany: Springer-Verlag Berlin Heidelberg 2014.

4th Micro and Nano Flows Conference
UCL, London, UK, 7-10 September 2014

Monolithic optofluidic chips: from optical manipulation of single cells to quantum sensing of fluids

Roberto OSELLAME[1,*]

* Corresponding author: Tel.: ++39-02-2399-6075; Fax: ++39-02-2399-6126; Email: roberto.osellame@polimi.it
1 Istituto di Fotonica e Nanotecnologie (IFN) – CNR, Dipartimento di Fisica - Politecnico di Milano, Italy

Keywords: Microfluidics, Optofluidic devices, Ultrafine resolution, Biological fluids

The frontier of optical measurements in microfluidic chips is striving to overcome the current resolution limits. In this talk two different aspects of ultrafine optical measurements will be discussed, targeting different biomedical applications. In cell analysis, ultrafine measurements means single cells resolution, which allows one to unravel the biological complexity hidden in nominally homogeneous populations. In concentration measurements of proteins in fluids, ultrafine measurements means extracting the maximum amount of information from each photon interacting with the fluid, by exploiting quantum states of light. Taking advantage of the versatility of femtosecond laser micromachining, monolithic optofluidic devices are produced, which combine optical waveguides and microfluidic channels. Biologically relevant examples of both single cell manipulation and quantum sensing of fluids will be presented and perspectives of further integration of functionalities discussed.

4th Micro and Nano Flows Conference
UCL, London, UK, 7-10 September 2014

Plasmonic droplets for high throughput sensing

Joshua B. EDEL [1,*]

* Corresponding author: Tel.: ++44 (0) 20 7594 3704; Email: joshua.edel@imperial.ac.uk
1 Department of Chemistry, Imperial College, UK

Keywords: plasmonics, self-assembly, surface enhanced Raman spectroscopy

In this talk I will present a simple, fast, and inexpensive method for characterizing adsorption and desorption of metallic gold nanoparticles at a liquid-liquid interface within micronscale droplets. These interfaces provide an ideal platform for the formation of two-dimensional monolayers of nanoparticles, as they form spontaneously, cannot be broken, and are defect-correcting, acting as 2D 'nanoparticle traps'. Such two-dimensional self-assembled nanoparticle arrays have a vast range of potential applications in displays, catalysis, plasmonic rulers, optoelectronics, sensors and detectors. As an example, I will show that this system can be used for trace analyte detection using Surface enhanced Raman spectroscopy, high level purification, fine-tuning of plasmonic properties, and for the creation of ultrahigh density aqueous solutions.

4th Micro and Nano Flows Conference
UCL, London, UK, 7-10 September 2014

Optical coherence tomography measurements of biological fluid flows with picolitre spatial localiztion

Stephen J. MATCHER [1,*]

* Corresponding author: Tel.: ++44 (0)114 225994; Fax: ++44 (0) 114 225945; Email: S.J.Matcher@sheffield.ac.uk
1 Dept of Materials Science & Engineering, University of Sheffield, UK

Keywords: Microcirculation, optical coherence tomography, speckle, phase-sensitive interferometry, rheology

Interest in studying the human and animal microcirculation has burgeoned in recent years. In part this has been driven by recent advances in volumetric microscopy modalities, which allow the study of the 3-D morphology of the microcirculation without the limitations of 2-D intra-vital microscopy. In this talk I will highlight results from my lab and others which show the power of optical coherence tomography (OCT) to image the normal and pathological microcirculation with picolitre voxel sizes. Both phase-resolved and speckle-variance methods are employed to characterize complex rheological flows both in-vitro and in-vivo.

1 Optical coherence tomography

Optical coherence tomography is an optical analogue of ultrasound imaging, with limited depth penetration into biological tissues (< 2mm) but offering high spatial resolution (picolitre voxels) and high voxel acquisition rates (up to 1 Gigavoxel per second). First generation time-domain OCT (TD-OCT) was superceded in 2003 by Fourier domain OCT (FD-OCT), bringing a 100-fold improvement in acquisition speed with no SNR penalty. OCT combines readily with Doppler velocimetry to provide 3-D flow mapping with excellent spatial, temporal and velocity resolution.

2 Doppler OCT and Doppler amplitude OCT

First generation time-domain OCT can be given velocity sensitivity by processing the low-coherence interferogram using joint time-frequency techniques such as the short-time Fourier Transform (STFT). We used this technique to study the rheology of whole blood in capillary vessels and demonstrated measurements of non-parabolic flow profiles characteristic of biphasic flows. Measuring the amplitude as well as the centre frequency within an STFT window allows mapping of the local concentration of moving scatterers. We used this to demonstrate the phenomenon of red-blood cell “tubular pinch” aggregation at high shear rates in whole blood.

3 Phase-resolved DOCT

STFT analysis leads to an undesirable trade-off between velocity resolution and spatial resolution. This can be overcome by moving to phase-resolved measurements, with the only disadvantage being aliasing at high flow speeds. This can be overcome using high A-scan acquisition rates and/or the method of synthetic phase. The technique can be readily adapted to FD-OCT. We used phase-resolved TD-OCT to demonstrate oscillatory flow dynamics described by Womersley theory in a highly scattering liquid and used phase-resolved FD-OCT to image blood flow in-vivo in the cerebral tissue of small animals. The technique has been very successfully applied to animal and human retinal blood flow imaging, and has great potential in studying neurovascular coupling in the brain, the response of the tumour microcirculation to therapeutic interventions and the presence of non-melanoma and melanoma epithelial cancer.

4 Speckle-variance and correlation mapping OCT

A limitation of phase-resolved FD-OCT is its sensitivity to motion artefacts. The high B-scan acquisition rates of FD-OCT systems makes dynamic speckle imaging a viable proposal. Speckle-variance OCT is less sensitive to motion artefacts than phase-resolved OCT but lacks quantification of flow velocity. The long acquisition times of speckle-variance imaging can be reduced by correlation-mapping, where the statistics are accumulated over a kernel in the image rather than a pixel time-series.

We used correlation-mapping OCT to detect the presence of the superficial blood vessels in the human nailfold. Such microangiography applied clinically could offer new ways to detect skin and oral cancer, with improved specificity due to the rejection of confounding influences such as inflammation.

5 Conclusions

High-speed volumetric imaging of the microcirculation is now a reality. Further improvements in acquisition speeds can be expected due to advances in swept-laser light sources and the promise of wafer-scale fabrication of electrically-pumped VCSEL lasers could drive down costs by orders of magnitude. Novel contrast mechanisms based on photothermal and photoacoustic interactions promise to supplement flow information with oxygenation information, providing a complete description of tissue oxygen transport at the capillary level. New clinical insights are promised by these advances.

4th Micro and Nano Flows Conference
UCL, London, UK, 7-10 September 2014

Imaging Flows Using CMOS Sensors

Stephen P MORGAN [1,*], Diwei HE [1], Sun SHEN [1], Barrie R HAYES-GILL [1]

* Corresponding author: Tel.: ++44 (0)115 951 5570 Email: steve.morgan@nottingham.ac.uk
1 Electrical Systems and Optics Research Division, Faculty of Engineering, University of Nottingham, UK

Keywords: Laser Doppler flowmetry, CMOS image sensors, blood flow

Laser Doppler flowmetry is a well-established tool for imaging flows. It has been used as a clinical tool for measuring microcirculation in superficial tissue for applications including studies of allergic reactions, burn depth assessment, skin cancer diagnosis, assessment of skin diseases and investigating the effects of transdermal drug delivery. Imaging is often performed by scanning a single laser beam over an area of interest to build up an image point by point, however, the acquisition time is relatively long due to the necessary mechanical scanning. For example a typical commercially available system can take up to 5 min to obtain a 256 × 256 image. Line scanners utilizing a 64 × 1 photodetector array can provide 64 × 64 pixel images in 4 s. An alternative technique is Laser Speckle Contrast Analysis (LASCA), in which a full name CCD camera is employed to acquire speckle images and a block of pixels is used to calculate the speckle contrast. The measured speckle contrast is proportional to the velocity of the moving blood cells. Although LASCA provides a cost effective method for real-time blood flow imaging the measurement results are exposure time dependent and the spatial averaging performed across a sub-array (often 5 × 5 or 7 × 7 pixels) results in a reduction in spatial resolution.

In recent years with the development of high frame rate CMOS technology and fast signal processors such as field programmable gate arrays (FPGAs), an implementation of full field laser Doppler flowmetry based on a commercial CMOS image sensor coupled with a digital signal processor has been demonstrated. The Doppler signal detected by the sensor at each pixel is multiplexed, digitized and then transferred off chip for signal processing. The advantage of this system over the scanning laser Doppler imaging system is that the frame rate of the system is increased due to the absence of moving scanning components. We have developed such a system which has allowed a direct comparison of laser speckle and laser Doppler imaging to be carried out in which the detected light is processed in real time on an FPGA using both processing algorithms.

Custom made cameras with on-chip processing can also be fabricated using CMOS technology [1]. A custom made camera design offers several advantages over commercial cameras as the specifications can be tailored to the signals of interest. For laser Doppler blood flowmetry, the pixel size, current to voltage conversion gain and number of digitization bits can be designed to best match those of typical signals. Appropriate anti-aliasing filters can also be added at the pixel level. Integration of the pixel front-end with on-chip processing enables each pixel to be sampled at a minimum rate of 40 kHz with a low data readout rate required, as the output is a processed flow image rather than a series of raw data images. In CMOS custom made designs there are considerable design constraints in terms of the silicon area of the processing electronics and the ratio between the areas of the pixel level electronics to that of the photo-detectors (fill factor). The circuits used in the discrete electronics systems cannot simply be replicated on-chip as the relatively low frequencies used in LDBF means that on-chip component sizes are commensurately often large. Therefore moving from discrete electronics at a single point to a fully integrated sensor array is a challenging task and design optimizations and compromises need to be made. The system design and results from flow phantoms and blood flow will be presented.

Reference

[1] He et al, Laser Doppler Blood Flow Imaging Using a CMOS Imaging Sensor with On-Chip Signal Processing, Sensors 13(9):12632-12647, 2013

4th Micro and Nano Flows Conference
UCL, London, UK, 7-10 September 2014

Continuous and Simultaneous Measurement of Micro Multiphase Flow Using confocal Micro-Particle Image Velocimetry (Micro-PIV)

Marie Oshima[1*], Masamichi Oishi[2]

* Corresponding author: Tel.: +81 (0)3 5452 6205; Fax: +81 (0)3 5452 6205; Email: marie@iis.u-tokyo.ac.jp
1: Interfaculty Initiative in Information Studies/Institute of Industrial Science, The University of Tokyo, Japan
2: Institute of Industrial Science, The University of Tokyo, Japan

Keywords: Confocal Micro-PIV, Micro Droplet, CIP Method

This paper presents a "Multicolor Confocal Micro Particle Image Velocimetry (Micro-PIV)" technique to visualize and measure dynamic behavior of each phase of micro multiphase flow separately and simultaneously. The technique is applied to two types of micro two -phase flow. The first case is to investigate a mechanism of microdroplet formation at a micro T-shaped junction. The measurement data are compared to the numerical simulation using CIP method. The second case is to investigate the tank-tread motion of red blood cell induced by the surrounding plasma flow.

1 Introduction

Microfluidic devices can perform various kinds of complicated fluidic and chemical operations such as mixing on small chips that can range in a size from a few millimeters to a few centimeters (Auroux, et al, 2002). The devices usually handle more than two different materials, i.e., a "multiphase flow", for example, solid-liquid multiphase flow for a blood analysis (Shevkoplyas, et al 2005) or liquid-liquid multiphase flow for micro droplets used in a drug delivery system. In order to clarify the phenomenon of micro multiphase flow inside these devices, it is necessary to measure the flow field or movement of each phase simultaneously.

In order to visualize and measure multiphase flow in a micro channels, the authors have been developing a multicolour confocal micro-PIV system (Kinoshita, et al, 2006, Oishi, et al, 2011,2012). Since confocal micro-PIV can provide clear PIV images with a very this measurement depth, the three-dimensional velocity field can be obtained by calculating an out of plane velocity from the continuity equation. The paper presents the measurement technique of confocal micro-PIV as well as its applications.

2 Multicolor confocal micro-PIV system

The multicolour confocal micro-PIV system is developed based on a conventional confocal micro-PIV system (Oishi, et al, 2011,2012). To measure two different phases simultaneously and separately, the system has an extra set of laser and camera in addition to one set in the conventional system as well as a multi-wavelength separation unit. Two different types of illumination laser beams are combined using a dichroic mirror in a laser combiner. The lasers illuminate the target, and scattered lights from the target return through a confocal scanner. Multi-wavelength emitted lights are then separated at the separation unit and are recorded by two high-speed cameras.

The range of the velocity is determined by the rotational speed of the confocal scanner. Since the tank-tread motion of red blood cells is induced by the velocity of their surrounding plasma larger flow than that of the confocal scanner, a translational stage has been added to the present multicolor confocal micro-PIV system.

3 Results

The drop formation in a T-shaped junction has been measured by the present multi-confocal micro-PIV system. Three components of the velocity are obtained for both internal flow of the droplet and its surrounding flow. Droplet formation is varied depending on a capillary number, which is represented by the ration between the shear force and surface tension. When the capillary number becomes small, the droplet is in the stage of squeezing such that its shape becomes a relatively large barrel. On the other hand, when the capillary number becomes larger than 0.1, it is in the stage of dripping such that its shape becomes small and round. The details of flow features of both phases are examined by comparing to the numerical simulation using the CIP method under the same flow condition.

The translational micro-PIV is applied to measure a motion of a red blood cell in a micro channel. The tank-treading motion of RBCs and the corresponding movement of the surrounding flow structure are measured simultaneously and quantitatively. The relationship between the tank-treading frequency and the shear rate of the surrounding flow is on the same order as in Fischer's report (1978).

References

Auroux P A, Iossifidis D, Reyes D R, and Manz A 2002 *Anal. Chem.* **74** 2637-2652

Fischer T M, St¨ohr-Liesen M and Schmid-Sch¨onbein H 1978 *Science,* **202** 894–6

Kinoshita, H., Kaneda, S., Fujii, T., Oshima, M., 2006 *Lab on a Chip*, **7** 338-346

Oishi, M., Kinoshita, H., Fujii, T., Oshima, M. 2011 *Meas. Sci. Tech.*, **22**, doi:10.1088/0957-0233/22/10/105401

Oishi, M., Utsubo, K., Kinoshita, H., Fujii, T., Oshima, M., 201 2 *Meas. Sci. Tech.*, **23,** doi:10.1088/0957-33/23/3/035301¥¥

Shevkoplyas S S, Yoshida T, Munn L L, and Bitensky M W 2005 *Anal. Chem.* **33** 933-937

Tice J D, Song H, Lyon A D, and Ismagilov R F 2003 *Langmuir* **19** 9127-9133

4th Micro and Nano Flows Conference
UCL, London, UK, 7-10 September 2014

Optical Coherence Tomography – Variations on a Theme

Justin A. T. HALLS [1], Nikita FOMIN [2,*], Clive A. GREATED[3], Carola S. KÖNIG [1], Michael COLLINS[4]

* Corresponding author: Tel.: +375 172 84 13 53; Fax: +375 172 92 25 13; Email fomin@hmti.ac.by
1 Brunel Institute for Bioengineering, Brunel University, UK
2 Heat & Mass Institute, Belarus Academy of Sciences, Minsk, 220072, Belarus
3 School of Physics and Astronomy, University of Edinburgh, Edinburgh EH9 3JZ, UK
4 School of Engineering and Design, Brunel University, UK

Keywords: Optical Coherence Tomography, Optical Imaging, Interferometric Imaging

1 Abstract

Optical Coherence Tomography (OCT) has developed extensively over the last 23 years. This paper reviews some of the imaging techniques based on OCT with particular reference to the trade-offs between lateral and axial resolution, working distance, imaging depth, acquisition speed (enabling real time observation and 3D imaging), imaged area/volume, contrast enhancement – including velocity measurement, and system complexity – including detectors, light sources and the optical path.

Time domain OCT was the original system[1] and required a simple detector, a depth scanning mirror and a short duration pulsed laser light source. Resolution was good but multiple samples were required for each A-scan which made acquisition slow. The development of spectral domain or Fourier domain (SD-OCT), and subsequently swept source (SS-OCT) methods greatly enhanced acquisition speeds. This provided a much better patient experience for retinopathy as well as enabling the possibility of real time 3D imaging. Intra-vascular OCT could also compete with intra vascular ultra-sound (IVUS) by providing both higher resolution and faster draw back times combined with the advantages of a smaller fibre-optic catheter minimizing vessel occlusion.

Various techniques have been introduced to improve image acquisition times, including the use of spatial coherence, alone or in conjunction with temporal coherence, in order to allow simultaneous sampling across multiple sites. Spectral Encoded Endoscopy (SEE) also provides sampling from multiple lateral sites within a single sample sweep, but each location only uses a part of the total bandwidth thus reducing axial resolution. Interleaved OCT on the other hand can sample from several locations simultaneously while employing almost the full bandwidth at each location by using a more complex multi-band demultiplexer (MBDX)[2].

Ultimate resolution is essentially diffraction limited laterally, and source bandwidth limited axially. In practice it is often necessary to work with low numerical aperture optical systems, such as in retinal imaging, and typical lateral resolution is around 15µm, axial resolution around 5µm. A number of high resolution OCT scanners are also available which can give an axial resolution down to around 3µm, but it is debatable whether the increased resolution actually enhances the diagnostic ability. Some improvement in lateral resolution may be achieved through the use of sources with low spatial coherence, or through virtually structured detection (VSD)[3].

OCT may be combined with other detection modalities in order to overcome some of the inherent limitations. Basic contrast enhancement can be provided through the use of polarization sensitive OCT or Doppler OCT. More advanced processes may use magnetomotive nano-particles in a modulated magnetic field for Magneto-Motive OCT[4]. Photo-acoustic microscopy (PAM) has similar penetration and resolution to OCT, but observes optical absorption rather than scattering. By using a transparent Fabry-Perot interferometer as a detector OCT can be implemented coaxially providing a complementary image. Doppler OCT can be implemented in several different ways – phase resolved Doppler (PR-DOCT), resonant Doppler flow imaging, joint spectral and time domain imaging, optical micro-angiography (OMAG) or single pass volumetric bidirectional blood flow imaging (SPFT).

Choice of light source is crucial to good OCT performance. Time domain OCT was dependent on the use of femto-second pulsed lasers. The introduction of SD-OCT and SS-OCT allowed the widespread use of super-luminescent diodes (SLD) sources with longer lifetimes and far lower cost. SLDs are readily available at wavelengths of 800nm with a bandwidth of 30nm, or at wavelengths of 1300nm providing axial resolutions down to 3µm. For ultra-high resolution systems the use of photonic crystal fibres in conjunction with sub-15fs Ti:sapphire lasers has enabled resolutions down to 0.9µm in air and 0,6µm in biological tissue. It remains to be seen whether recent developments in attosecond pulsed lasers[6] will enable resolution limits to be pushed even further.

The majority of applications of OCT are biomedical, especially ophthalmology, endoscopy and intravascular imaging. However, some industrial applications are emerging particularly for non-destructive testing and quality control, such as in the production of MEMS devices[5], or the non-destructive detection of sub-surface strain fields in injected moulded polymer parts[6].

2 References

1 Huang D, et al. (1991) Optical Coherence Tomography. Science 254:1178-1181
2 Lee HY, Sudkamp H, Marvdashti T, Ellerbee K. (2013) Interleaved Optical Coherence Tomography. Optics Express 21(22).
3 Wang B, Lu R, Zhang Q, Yao X. (2013) Breaking Diffraction Limit of Lateral Resolution in Optical Coherence Tomography. Quant. Imaging Med. Surg. 3(5):243-248
4 John R, Rezaelpoor R, Adies S, et al. (2010) In vivo Magnetomotive Optical Molecular Imaging Using Targeted Magnetic Nanoprobes. Proc. Nat. Acad. Sci. USA 107(18):8085-8090
5 Merken P, Vandersmissen R, Yurtsever G.. (2011) Optical Coherence Tomography: OCT Supports Industrial Nondestructive Depth Analysis. Laser Focus World 1 Aug 2011
6 Villeneuve D. (2009) Attosecond Light Sources. La Physique au Canada 65(1):63-66
7 http://www.recendt.at/517_ENG_HTML.php

4th Micro and Nano Flows Conference
UCL, London, UK, 7-10 September 2014

Particle self-diffusiophoresis near solid walls and interfaces

Darren CROWDY

Tel.: ++44 (0)2075 948587; Fax: ++44 (0)2075 948517; Email: d.crowdy@imperial.ac.uk
Department of Mathematics, Imperial College London, UK

Keywords: Low-Reynolds number swimmers, self-diffusiophoresis, Janus particles

The motion of small self-propelling low-Reynolds-number swimmers or colloidal particles driven by "micromotors" moving in the vicinity of no-slip walls and/or free interfaces will be studied by theoretical methods. The topic is of current interest in understanding the dynamics of self-diffusiophoretic particles where it is the differential production of chemicals over a particle surface (e.g. that of a two-faced Janus particle) that breaks symmetry and leads to a net translation/rotation of the particle. We show that in simple model systems at zero Reynolds and Peclet numbers much analytical progress can be made giving insights into the dynamics.

4th Micro and Nano Flows Conference
UCL, London, UK, 7-10 September 2014

Stretching of a capillary bridge featuring a particle-laden interface

Lorenzo BOTTO

Tel.: ++44 (0) 20 7882 7503; Fax: ++44 (0) 20 7882 3390; Email: l.botto@qmul.ac.uk
School of Engineering and Materials Science, Queen Mary University, UK

Keywords: Particle-laden flows, two-phase flows, interfaces with adsorbed solid particles

Due to the interest in replacing surfactants with colloidal particles, research on the response to deformation of fluid interfaces with adsorbed solid particles has recently gained considerable momentum. Depending on the ratio of repulsive to attractive forces, two-dimensional particle suspensions can either be stable, or form percolating networks whose microstructure depends sensitively on particle shape and surface charge. These two situations can give rise to markedly different responses.

In this talk we consider a slender axisymmetric particle-laden fluid thread, pulled at one end by a circular plate moving at specified velocity; this canonical problem is of relevance to extensional rheometry, microfluidic drop generation, and drop/bubble breakup in complex flows. In the spirit of classical two-phase flow equations, we treat the particle and fluid phases as interpenetrating media, by solving the coupled continuity and momentum equations for the particle phase, together with the corresponding transport equations for the fluid, in the thin-thread approximation. To get insights into how the stretching of the thread affects the motion of the particles, we employ a one-way-coupling approximation, in which the dynamical influence of the particles on the bulk fluid is neglected. We investigate the time-dependent particle distribution under three cases: stable suspension, dilute aggregated suspension forming a percolating network, and suspension subject to gravity. The results highlight the importance of closing the particle drag force in terms of a relevant particle-fluid velocity “slip”, and the need to account for the hysteresis of the interfacial particle pressure, to predict the time-dependent particle concentration along the thread.

4th Micro and Nano Flows Conference
UCL, London, UK, 7-10 September 2014

Macroscopic effects of microscopic roughness in suspensions

Helen WILSON [1,*], Robert H. DAVIS [2]

* Corresponding author: Tel.: ++44 (0) 20 7679 1302; Fax: ++44 (0) 20 7383 5519; Email: helen.wilson@ucl.ac.uk
1: Department of Mathematics, University College London, UK
2: Department of Chemical and Biological Engineering, University of Colorado, USA

Keywords: Suspension dynamics, microscopic surface roughness, contact effects

Two perfectly smooth spheres moving in a viscous fluid, under the action of finite forces, can never come into contact. But experiments suggest that a heavy sphere dropped past a fixed or neutrally-buoyant sphere in a highly viscous medium does undergo some sort of irreversible interaction as it passes close to the second sphere. One hypothesis is that microscopic surface roughness has caused the two particles to make physical contact.

We investigate the effect such a contact model would have on the properties of the suspension overall.

The rheology of the suspension depends, of course, on the solid volume fraction, c. When c is small we can calculate the leading-order effect of contact, which is to modify the viscosity and introduce two normal stress differences at order c^2. The values of these stresses (and indeed the viscosity) depend on the far-field flow (which is assumed to be linear) and also on the particle distribution: we present results for shear and straining flows and for two- and three-dimensional arrangements of particles. Finally, for more realistic values of c, we use Stokesian Dynamics to extend the above results for shearing flow.

The key result is that contact can reduce the viscosity of the suspension and induce a negative first normal stress difference, at least at moderately low concentrations; we will also look at the regions of parameter space where this broad-brush description does not apply.

4th Micro and Nano Flows Conference
UCL, London, UK, 7-10 September 2014

Fluctuating force-coupling method for interacting colloids

Eric KEAVENEY

Tel.: ++44 (0)2075 942780; Fax: ++44 (0)2075 948517; Email: d.keaveny@imperial.ac.uk
Department of Mathematics, Imperial College London, UK

Keywords: Colloidal suspensions, force-coupling method, simulation of suspensions

Brownian motion plays an important role in the dynamics of colloidal suspensions. It affects rheological properties, influences the self-assembly of structures, and regulates particle transport. While including Brownian motion in simulations is necessary to reproduce and study these effects, it is computationally intensive due to the configuration dependent statistics of the particles' random motion. I will discuss recent work that speeds up this calculation for the force-coupling method (FCM), a regularized multipole approach to simulating suspensions at large-scale. I will show that by forcing the surrounding fluid with a configuration independent, white-noise stress, fluctuating FCM yields the correct particle random motion, even when higher-order terms, such as the stresslets, are included in the multipole expansion. I will present the results from several simulations demonstrating the effectiveness of this approach for modern problems in colloidal science and discuss extensions of fluctuating FCM to dense suspensions.

4th Micro and Nano Flows Conference
UCL, London, UK, 7-10 September 2014

Dynamic unbinding transitions and deposition patterns in dragged meniscus problems

Uwe THIELE

Tel.: ++44 (0)1509 22 3186; Fax: ++44 (0)1509 22 3969; Email: U.Thiele@lboro.ac.uk
Department of Mathematical Sciences, Loughborough University, UK

Keywords: Dragged meniscus problems, dynamic line deposition, local and global bifurcations

We study the transfer of a film or patterned deposit onto a flat plate that is extracted from a bath of pure liquid or solution/suspension. After reviewing selected recent experiments we first address the case of a pure non-volatile liquid. Employing a long-wave hydrodynamic model, we analyse steady-state meniscus profiles as the plate velocity is changed. A number of qualitatively different bifurcation diagrams is discussed and it is argued that they show dynamic equivalents of known equilibrium unbinding transitions (namely of emptying and wetting transitions). We show in passing that the change from a monotonic to a snaking emptying transition is caused by the existence of infinitely many heteroclinic orbits close to a heteroclinic chain in an appropriate 3d phase space [1].

Next, we discuss a gradient dynamics formulation that allows us to systematically extend the one-component model used above into thermodynamically consistent two-component models [2] as used, e.g., by Friedrich and coworkers to describe the formation of line patterns during the Langmuir-Blodgett transfer of a surfactant layer from a bath onto a moving plate [3]. Recently, we developed a reduced Cahn-Hilliard-type model to analyse the bifurcation structure of this deposition process [4]. We sketch this rather involved structure and discuss how the time-periodic solutions related to line deposition emerge through various local and global bifurcations.

[1] M. Galvagno, D. Tseluiko and U. Thiele, http://arxiv.org/abs/1307.4618
[2] U. Thiele, A. J. Archer and M. Plapp, Phys. Fluids 24, 102107 (2012).
[3] M. H. Kopf, S. V. Gurevich, R. Friedrich, and L. F. Chi, Langmuir 26, 10444-10447 (2010).
[4] M. H. Kopf, S. V. Gurevich, R. Friedrich and U. Thiele, New J. Phys. 14, 023016 (2012).

4th Micro and Nano Flows Conference
UCL, London, UK, 7-10 September 2014

Asymptotic analysis of evaporating droplets

Nikos SAVVA

Tel.: ++44 (0) 29 208 75116; Fax: ++44 (0) 29 208 74199; Email: SavvaN@cf.ac.uk
School of Mathematics, Cardiff University, UK

Keywords: Evaporating droplets, contact line dynamics, lubrication theory

We consider the dynamics of an axisymmetric, partially-wetting droplet of a volatile liquid in its vapour, which is supported on a smooth superheated substrate. In this process, we assume that the liquid properties remain unchanged and invoke a one-sided, lubrication-type model for the evolution of the droplet thickness that accounts for the effects of evaporation, capillarity, gravity and slip. By asymptotically matching the flow near the contact line region and the bulk of the droplet, we obtain a set of coupled evolution equations for the droplet radius and volume. The validity of the matching procedure is verified by numerical experiments, performing also a parametric study to elucidate how the droplet dynamics is influenced by the aforementioned effects.

4th Micro and Nano Flows Conference
UCL, London, UK, 7-10 September 2014

Dielectrophoretic Manipulation of Particles and Lymphocytes Using Rail-type Electrodes

Kazuya TATSUMI[1,2*], Haruka OKUI[1], Koki KAWANO[1], Kazuyoshi NAKABE[1,2]

* Corresponding author: Tel.: ++81 (0)75 3833606; Fax: ++81 (0)75 3833608; Email: tatsumi@me.kyoto-u.ac.jp
1 Department of Mechanical Engineering and Science, Kyoto University, JAPAN
2 Advanced Research Institute of Fluid Science and Engineering, Kyoto University, JAPAN

Keywords: Micro Flow, Dielectrophoretic Force, Sorting, Manipulation, Micro-particles and Cells

1 Introduction

The technologies for manipulating and sorting cells and microparticles in the microchannel flow have been studied intensively in the last decade. Those using DEP force has been one of the promising tools because it can produce a driving force to the particles or cells without changing or modifying them or the fluid properties. Although many types of electrodes and channels have been proposed in other studies, substantial issues remain to be solved for satisfying the demands of the applications, such as accuracy, sorting rate, response and applicability under various conditions. One such problem is because the DEP force, F_{DEP}, is mainly produced by the electric field gradient, it decays markedly with the distance from the electrode. Other problems are the fact that in many cases, a negative F_{DEP}, namely a repulsion force against the electrode works on the particle or cell, and that the distance between the particles flowing in the channel are random and not aligned. It is, therefore, difficult to precisely control the particle position. In order to overcome these problems, an electrode patterns, which are not only effective but also fundamental and versatile, is developed in this study.

The Schematic of the electrode patterns are shown in Fig. 1. The manipulation and sorting device consists of the ladder-type electrode, the flip-type electrode and the oblique rail-type electrode regions. These electrodes are attached to the channel bottom wall, and the top wall is an electrode connected to the ground. The ladder-type will produce F_{DEP} which work on the particles to make them align not only at the centerline but also in equal spacing. The flip-type operating as a gate electro will lift the particle when necessary and exclude it from the electrode region. The remaining particles will be guided along the oblique rail-type electrodes and can be collected.

1 Numerical Results

Numerical simulation for particle and lymphocyte motions in the microchannel was carried out to aid the designing of the effective shape of the electrode, and to estimate the sorting performance. Fig. 2(a) shows the distribution of the streamwise velocity against time in the lymphocyte case. Among the three models we have tested, the force density model agrees well with the experiment. Further computation was carried out using this model to investigate the influences of the electrode shape, width and pitches.

2 Experimental Results

Micro-device was fabricated using Pt electrode patterned glasses and

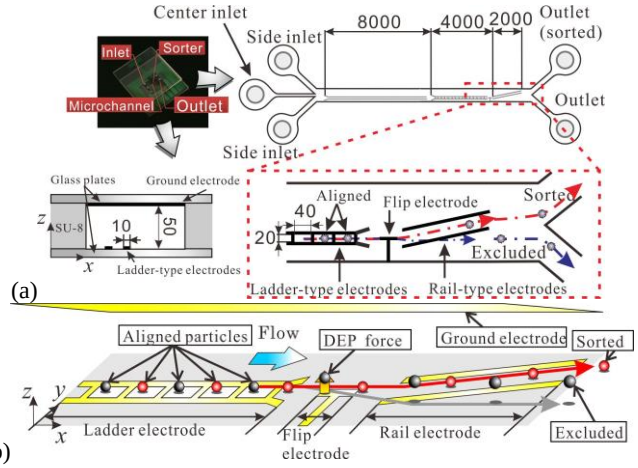

Fig. 1 (a) Schematics of the microchannel, electrodes and particle motions in the present micro-device, and (b) the concept of the alignment and sorting of the present device.

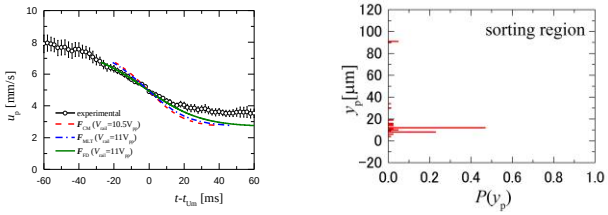

(a) Velocity of the lymphocytes (b) Sorting accuracy

Fig. 2 (a) Calculation of lymphocyte motions in microchannel and the verification of the models, and (b) probability density distributions of y_p at the outlet of the sorting region.

SU-8 (Micro Chem Co.). The voltage of 10MHz to generate DEP force was oscillated with periods of low frequency additionally in order to align the particles in the streamwise direction. The particles supplied from the upstream by the sheath flow are aligned by the ladder-type electrodes. The flip-type electrodes were activated at certain periods to sort several specific particles from others. Fig. 2(b) depicts the probability density distributions of the particle spanwise position y_p at the outlet of the sorting region. Two peaks are clearly observed in the figure at y_p =10μm and 90μm, the positions of which are for those of excluded and collected ones. By applying the rail-type and ladder-type electrodes, the accuracy of the particle position was 5%, which enabled the precise timing adjustment for sorting the particles. Detail of the performance and characteristics of the sorting technique will be discussed in the full paper.